Evaluation of the immunogenicity of a promising vaccine regimen to identify immune correlates of protection



Nawamin Pinpathomrat

Wolfson College

University of Oxford

A thesis submitted for the degree of

Doctor of Philosophy

Trinity 2018

Word count: ~33,000

Evaluation of the immunogenicity of a promising vaccine regimen to identify immune correlates of protection

Nawamin Pinpathomrat, Wolfson college

Thesis submitted for the degree of Doctor of Philosophy, Trinity Term 2018

Abstract

A vaccine against tuberculosis (TB), a disease resulting after infection with *Mycobacterium tuberculosis* (*M.tb*), is urgently needed to prevent more than a million deaths per year. Bacillus Calmette–Guérin (BCG) is the only available vaccine against TB but its efficacy is variable throughout the world. A promising vaccination regimen composed of BCG prime, followed by vaccination with a chimpanzee adenoviral vector (ChAdOx1) and a modified vaccinia Ankara virus (MVA), both expressing Ag85A, was identified in our laboratory. This regimen significantly improved BCG efficacy in animal studies. Antibody, effector and memory T cell responses induced by BCG-ChAdOx1.85A-MVA85A (B-C-M), were evaluated, to identify immune correlates of protection. This regimen induced Ag85A-specific IgG and IgA responses as well as cytokine responses in $CD4^+$ and $CD8^+$ T cells, both in the systemic and pulmonary system. To discriminate lymphocytes in the vasculature from lymphocytes in the lung parenchyma, a fluorochrome-conjugated antibody was injected intravascularly before harvesting the lungs. Lung parenchymal Ag85A-specific memory $CD4^+$ T cells that were $CXCR3^+$ $KLRG1^-$, significantly increased in B-C-M immunised mice compared to BCG alone at 4, 8 and 20 weeks post vaccination but the cell number decreased at the latter time point. These memory cells associated with protection against *M.tb* challenge, which was observed at 4 and 8 weeks but not when mice were challenged 20 weeks post vaccination. These putative T cells may have an important role against *M.tb* infection and could be a target for designing a protective vaccine. In parallel, six novel *M.tb* antigens were selected and expressed individually in a ChAdOx1 vector. The immunogenicity and protective efficacy of these vaccines were evaluated. Three antigens were not immunogenic when expressed in viral vectors and DNA. The immunogenic antigens induced cytokine production but failed to confer protection when delivered alone or with B-C-M regimen.

Acknowledgements

I have probably been the most smiley DPhil student in the Jenner, if not in the world. I am very lucky to get this project, with which I am absolutely in love, and to have an amazing supervision from Professor Helen McShane. Her kindness and guidance throughout my DPhil made me feel incredibly grateful. Thank you for giving me the opportunity to pursue my dream and for helping to make it come true. I could not have finished this project without Dr Elena Stylianou. Thanks for patiently teaching me all the techniques and being a perfect example of a genius and funny scientist. Not only being my supervisor, she is also my lovely friend and understanding sister. One of the reasons that I want to come to work every day is because of incredible colleagues in the TB group. Thanks very much Naomi and Janet for making early morning experiments a perfect time for chocolate brioche and “spicy chats”. Thanks Rachel Tanner, Rachel Kandt and Iman for your help and advice. I am very thankful to all the dedicated staff in the Jenner and FGF.

It is a real fortune to have such a supportive family. Thank you for unconditional love and endless support since the first day I was born, the day I decided to do medicine, the day I wanted to come to the UK, the day I came out gay, the day I applied for MasterChef and every day until now.

Contents

Chapter 1. Introduction 1

1.1 Tuberculosis 2

1.2 Immune responses to tuberculosis 4

1.3 Vaccination against TB 6

1.4 Viral vector vaccines 8

1.5 Animal models 9

1.6 Memory T cells 12

1.7 Antibodies 15

1.8 New *M.tb* antigens 18

1.9 Aims of this thesis 20

Chapter 2. Materials and Methods 21

2.1 Materials 22

2.1.1 Chemicals 22

2.1.2 Reagents and kits 22

2.1.3 Instruments 22

2.1.4 Consumables 23

2.1.5 Software 23

2.1.6 Mice 23

2.1.7 Vaccines 24

2.1.8 Novel Mycobacterial antigens 24

2.2 Methods 25

2.2.1 Insertion of *M.tb* antigens in viral vectors 25

2.2.2 Evaluation of vaccine protective efficacy 26

2.2.3 Evaluation of vaccine immunogenicity 27

Chapter 3. Immunogenicity and protective efficacy following B-C-M regimen . 35

3.1 Introduction 36

3.2 Results 39

3.2.1 T cell responses induced by B-C-M regimen in the lungs and spleen . 39

3.2.2 Antibody responses induced by B-C-M regimen in the airways and circulation 60

3.2.3 Evaluation of the durability of protection provided by the B-C-M regimen 65

3.3 Discussion 71

Chapter 4. Development of resident memory T cells in the pulmonary system following B-C-M regimen 78

4.1 Introduction 79

4.2 Results 83

4.2.1 Optimisation of intravascular staining technique 83

4.2.2 Resident memory T cells in the lung compartments 4 weeks post B-C-M vaccination 91

4.2.3 Resident memory T cells in lung compartments 8 weeks post B-C-M vaccination 106

4.2.4 Resident memory T cells in lung compartments 20 weeks post B-C-M vaccination 115

4.2.5 Lung parenchymal $CD4^+$ T cells induced by B-C-M vaccination as correlates of protection 123

4.2.6 Functions of the lung parenchymal T cells induced by B-C-M vaccination 125

4.3 Discussion 141

Chapter 5. Novel Mycobacterium tuberculosis antigens 146

5.1 Introduction 147

5.2 Results 153

5.2.1 Viral vector vaccines expressing novel *M.tb* antigens 153

5.2.2 Immunogenicity of the new viral vectors 157

5.2.3 Immune responses induced by the new antigens in the spleens of BCG vaccinated mice 161

5.2.4 Immunogenicity of DNA vaccines expressing non-immunogenic antigens 164

5.2.5 Protective efficacy of viral vector vaccines expressing the most immunogenic antigens 166

5.3 Discussion 172

Chapter 6. Conclusion and future work 177

Chapter 7. Appendix 185

7.1 Antibodies used for flow cytometry 186

7.2 Gating strategies 190

Bibliography 194

List of figures

Figure 3-1 Timeline of B-C-M vaccination and control groups.. 40

Figure 3-2 $CD4^+$ T cell cytokine responses in the lungs and spleen of naïve and vaccinated mice. 42

Figure 3-3 $CD8^+$ T cell cytokine responses in lungs and spleen of naïve and vaccinated mice. 44

Figure 3-4 Timeline of C-M vaccination and control groups. 45

Figure 3-5 $CD4^+$ T cell cytokine responses in lungs and spleen of naïve and vaccinated mice. 47

Figure 3-6 $CD8^+$ T cell cytokine responses in lungs and spleen of naïve and vaccinated mice. 49

Figure 3-7 Perforin and granzyme B detected using high concentration of fluorochrome-conjugated anti-mouse antibodies..... 51

Figure 3-8 Granzyme B detected using different concentration of fluorochrome-conjugated anti-human antibodies. 53

Figure 3-9 Intracellular staining using a combination of anti-human granzyme B and anti-CD107a. 55

Figure 3-10 Cytotoxic $CD8^+$ T cell responses in lungs of naïve and vaccinated mice measured with high concentration of antibodies.. 57

Figure 3-11 Granzyme B producing $CD8^+$ T cells following B-C-M vaccination measured with anti-human granzyme B. 59

Figure 3-12 Timeline of B-C-M vaccination and control groups for antibody studies. 60

Figure 3-13 Total IgG responses induced by B-C-M vaccination in the circulation..... 62

Figure 3-14 IgA responses induced by B-C-M vaccination in the airways. 64
Figure 3-15 Timeline of B-C-M vaccination and *M.tb* challenge..... 66
Figure 3-16 Protective efficacy of B-C-M, 8 weeks post vaccination in the lungs and spleen of naïve and vaccinated mice. 68
Figure 3-17 Protective efficacy of B-C-M, 20 weeks post vaccination in lungs and spleen of naïve and vaccinated mice. 70
Figure 4-1 Titration of time between intravenous injection and euthanasia 85
Figure 4-2 Titration of intravascular stain concentration. 87
Figure 4-3 Intravenous staining in the lungs, airways and blood. 88
Figure 4-4 Lung parenchymal T cells in the lungs of B-C-M immunised mice and naïve mice 90
Figure 4-5 Timeline of B-C-M vaccination and control groups. 92
Figure 4-6 Ag85A-specific parenchymal CXCR3^{+} KLRG1^{-} CD4^{+} T cells in the lungs of naïve and vaccinated mice 4 weeks post vaccination. 94
Figure 4-7 Ag85A-specific parenchymal CD4^{+} T cells expressing memory phenotypes in the lungs of naïve and vaccinated mice at 4 weeks post vaccination..... 95
Figure 4-8 Ag85A-specific vascular CX3CR1^{+} KLRG1^{+} CD4^{+} T cells in the lungs of naïve and vaccinated mice 4 weeks post vaccination. 96
Figure 4-9 Ag85A-specific CD4^{+} T cells expressing resident memory markers in the airways of naïve and vaccinated mice at 4 weeks post vaccination 98
Figure 4-10 Ag85A-specific parenchymal CXCR3^{+} KLRG1^{-} CD8^{+} T cells in the lungs of naïve and vaccinated mice at 4 weeks post vaccination. 100
Figure 4-11 Ag85A-specific parenchymal CD8^{+} T cells expressing memory phenotypes in the lungs of naïve and vaccinated mice at 4 weeks post vaccination..... 102

Figure 4-12 Ag85A-specific vascular CX3CR1^{+} KLRG1^{+} CD8^{+} T cells in the lungs of naïve and vaccinated mice 4 weeks post vaccination 103
Figure 4-13 Ag85A-specific CD8^{+} T cells expressing resident memory markers in the airways of naïve and vaccinated mice at 4 post vaccination. 105
Figure 4-14 Ag85A-specific parenchymal CD4^{+} T cells expressing memory phenotypes in the lungs of naïve and vaccinated mice at 8 weeks post vaccination..... 107
Figure 4-15 Ag85A-specific vascular CX3CR1^{+} KLRG1^{+} CD4^{+} T cells in the lungs of naïve and vaccinated mice 8 weeks post vaccination. 108
Figure 4-16 Ag85A-specific CD4^{+} T cells expressing resident memory markers in the airways of naïve and vaccinated mice at 8 weeks post vaccination 109
Figure 4-17 Ag85A-specific parenchymal CD8^{+} T cells expressing memory phenotypes in the lungs of naïve and vaccinated mice at 8 weeks post vaccination..... 111
Figure 4-18 Ag85A-specific vascular CX3CR1^{+} KLRG1^{+} CD8^{+} T cells in the lungs of naïve and vaccinated mice 8 weeks post vaccination 113
Figure 4-19 Ag85A-specific CD8^{+} T cells expressing resident memory markers in the airways of naïve and vaccinated mice at 8 post vaccination. 114
Figure 4-20 Ag85A-specific parenchymal CD4^{+} T cells expressing resident memory phenotypes in the lungs of naïve and vaccinated mice at 20 post vaccination..... 116
Figure 4-21 Ag85A-specific vascular CX3CR1^{+} KLRG1^{+} CD4^{+} T cells in the lungs of naïve and vaccinated mice 20 weeks post vaccination 117
Figure 4-22 Ag85A-specific CD4^{+} T cells expressing resident memory markers in the airways of naïve and vaccinated mice at 20 weeks post vaccination.. 118
Figure 4-23 Ag85A-specific parenchymal CD8^{+} T cells expressing memory phenotypes in the lungs of naïve and vaccinated mice at 20 weeks post vaccination..... 120

Figure 4-24 Ag85A-specific CX3CR1^{+} KLRG1^{+} CD8^{+} T cells in the lung vasculature of naïve and vaccinated mice 20 weeks post vaccination. 121
Figure 4-25 Ag85A-specific CD8^{+} T cells expressing resident memory markers in the airways of naïve and vaccinated mice at 20 post vaccination. 122
Figure 4-26 Antigen-specific lung-parenchymal CXCR3^{+} KLRG1^{-} CD4^{+} T cells induced by B-C-M vaccination as correlates of protection.. 124
Figure 4-27 Ag85A-specific cytokine producing parenchymal CD4^{+} T cells expressed CXCR3^{+} KLRG1^{-} in the lungs of naïve and vaccinated mice at 4 weeks post vaccination 127
Figure 4-28 Ag85A-specific parenchymal CD8^{+} T cells in the lungs of naïve and vaccinated mice at 4 weeks post vaccination.. 129
Figure 4-28 PPD-specific parenchymal CD4^{+} T cells and CD8^{+} T cells in the lungs of naïve and vaccinated mice at 4 weeks post vaccination.. 131
Figure 4-29 Purification of Ag85A-specific lung parenchymal and intravascular CD4^{+} T cells from B-C-M donor mice before transferring to naïve recipients. 134
Figure 4-30 Timeline of adoptive transfer experiment from B-C-Mid donors to naïve recipients before *M.tb* challenge..... 136
Figure 4-31 Purity of adoptively transferred cells from B-C-M donors to naïve recipients. 137
Figure 4-32 Viability of the sorted cells from B-C-M donors pre-adoptive transfer and at the adoptive transfer. 138
Figure 4-33 Protection against aerosol *M.tb* challenge in naïve mice receiving antigen specific lung parenchymal CD4^{+} T cells adoptively transferred from B-C-Mid immunised mice 140

Figure 5-1 Cloning steps for the construction of ChAdOx1 expressing the new antigens. 154
Figure 5-2 Cloning steps for the construction of MVA expressing the new antigens. 156
Figure 5-3 Timeline of ChAdOx1 immunisation expressing new antigens..... 157
Figure 5-4 Immunogenicity of ChAdOx1 expressing new antigens.. 158
Figure 5-5 Timeline of with MVA expressing new antigens..... 159
Figure 5-6 Immunogenicity of MVA expressing new antigens 160
Figure 5-7 Timeline of BCG vaccination for testing the new antigens..... 161
Figure 5-8 Immunogenicity of the new antigens in BCG vaccinated mice..... 163
Figure 5-9 Timeline of DNA vaccination 164
Figure 5-10 Immunogenicity of DNA vaccines..... 165
Figure 5-11 Evaluation of the protective efficacy of ChAdOx1 expressing novel antigens in lungs and spleens of naïve and vaccinated mice. 167
Figure 5-12 Timeline of B-C-M expressing new antigen vaccination and *M.tb* challenge..... 169
Figure 5-13 Protective efficacy of B-C-M expressing novel antigens in lungs and spleens of naïve and vaccinated mice 171
Figure 7-1 Gating strategy for the identification of T cells producing IFN-γ, TNF-α, granzyme B and perforin 190
Figure 7-2 Gating strategy for the identification of lung-parenchymal $CD4^+$ T cells expressing resident memory and lung-homing markers..... 191
Figure 7-3 Gating strategy for the identification of lung-parenchymal $CD8^+$ T cells expressing resident memory and lung-homing markers. 192

Figure 7-4 Gating strategy for the identification of cytokine producing lung-parenchymal T cells expressing lung-homing markers 193

List of tables

Table 2-1. Composition of complete media 28

Table 2-2. Composition of digestion media 29

Table 2-3. Composition of ACK buffer 29

Table 5-1 Novel *M.tb* antigens and their functions 149

Table 7-1 Flow cytometry antibodies for effector panel 186

Table 7-2 Flow cytometry antibodies for lung-parenchymal $CD4^+$ T_{RM} panel 187

Table 7-3 Flow cytometry antibodies for lung-parenchymal $CD8^+$ T_{RM} panel 188

Table 7-4 Flow cytometry antibodies for effector lung parenchymal panel 189

List of abbreviations

A

Ab	antibody
ACK	Ammonium-Chloride-Potassium
AF	Alexa Flour
Ag85A	antigen 85A
Ags	antigens
AIDS	acquired immune deficiency syndrome
APC	allophycocyanin
ATPase	adenosine triphosphatase

B

BAL	bronchoalveolar lavage
BCG	Bacillus Calmette–Guérin
bp	base pair
BSA	bovine serum albumin
BV	Brilliant Violet

C

CCR	CC-chemokine receptor
CD	cluster of differentiation
CFU	colony-forming units
ChAd	chimpanzee adenovirus

CMV	cytomegalovirus
CO2	carbon dioxide
CT	computed tomography
CXCR	CXC-chemokine receptor
Cy	cyanine
D	
DMEM	Dulbecco's modified Eagle medium
DNA	deoxyribonucleic acid
DNase	deoxyribonuclease
E	
E.coli	*Escherichia coli*
EDTA	ethylenediaminetetraacetic acid
ELISA	enzyme linked immunosorbent assay
ELISPot	enzyme-linked immunospot
ESAT-6	early secretory antigenic target 6
F	
FACS	fluorescent-activated cell sorting
FBS	foetal bovine serum
FMO	fluorescence minus one
G	
g	gram
g	gravity

GTPase	guanosine triphosphatase
H	
HIV	human immunodeficiency virus
I	
i.d.	intradermal
i.m.	intramuscular
i.n.	intranasal
ICS	Intracellular staining
IFN-γ	Interferon gamma
ifu	infectious units
Ig	immunoglobulin
IL	interleukin
iNOS	inducible nitric oxide synthase
IV	intravenous
K	
kbp	kilo-base pair
kDa	kilodalton
$KHCO_3$	potassium bicarbonate
L	
L	litre
LN	lymph node

M

M	molar
M.bovis	*Mycobacterium bovis*
M.smegmatis	*Mycobacterium smegmatis*
M.tb	*Mycobacterium tuberculosis*
mAB	monoclonal antibody
MDR-TB	multidrug-resistant TB
MHC	major histocompatibility complex
min	minute
ml	millilitre
mM	millimolar
MPTR	major polymorphic tandem repeats
MRI	magnetic resonance imaging
MVA	modified Vaccinia virus Ankara

N

Na_2EDTA	disodium EDTA
NH_4CL	ammonium chloride
NHP	non-human primates
NK	natural killer
NO	nitric oxide

O

OD	optical density

P

PBS	phosphate buffered saline
PE	proline-glutamate
PE	R-phycoerythrin
PerCP	peridinin chlorophyll protein
pfu	plaque forming units
PGRS	polymorphic GC-rich sequences
PPD	purified protein derivative
PPD-T	purified protein derivative of *M.tb*
PPE	proline-proline-glutamate
psig	pounds per square inch gauge

R

RNA	ribonucleic acid
RR-TB	rifampicin- resistant TB
RSV	respiratory syncytial virus

S

SCID	severe combined immunodeficiency
SFU	spot forming units

T

T_{CM}	central memory T cell
T_{EM}	effector memory T cell
Tet	tetramer

Th	T helper
TNF	tumor necrosis factor
TNF-α	tumor necrosis factor alpha
T_{RM}	resident memory T cell
U	
UK	United Kingdom
USA	United States of America
V	
VSV	vesicularstomatitis virus
W	
WHO	World Health Organization
X	
XDR-TB	extensively drug-resistant TB
µg	microgram
µg	microlitre
µM	micromolar

Chapter 1. Introduction

1.1 **Tuberculosis**

Tuberculosis (TB) is a global health issue, resulting from infection with *Mycobacterium tuberculosis* (*M.tb*). In 2016, the world health organization (WHO) reported 10.4 million new TB cases and 1.7 million deaths [1]. This makes TB the most deadly disease among all infectious diseases and one of the top 5 causes of death in low-middle-income countries [2]. A quarter of the world's population are infected with *M.tb,* amounting to approximately 1.7 billion people [3]. The endemic areas are sub-Saharan Africa, particularly Southern Africa and tropical countries [1]. However, the burden of the disease is expanding worldwide due to increased immigration. Thus, the TB epidemic remains a global problem.

Since 1990, TB research has been active in attempts to find new tools to control this epidemic. The two main approaches of TB elimination are anti-tuberculosis drug discovery and vaccine development [1, 4]. Through programmes like STOP TB, TB research has been greatly developed in the past few years [5]. We now have a better understanding of the pathogenesis of TB, more than a dozen candidate vaccines in clinical trials and two novel effective anti-tuberculosis drugs that are now licensed [6, 7, 8]. WHO has set an ambitious target to greatly reduce the mortality and incidence of TB [8]. The strategy aims to end the global TB epidemic, with targets to decrease TB deaths by 95 % and to drop new cases by 90 % between 2015 and 2035 [8]. There are several obstacles that may delay this goal. First, a clearer understanding of the pathogenesis of the disease is needed. The immune responses to TB and vaccines vary in different populations [9]. Therefore, it is difficult to make a universal vaccine to cover every region in the world. Additionally, co-infection of *M.tb* with human

immunodeficiency virus (HIV) is common. HIV infects and destroys human $CD4^+$ T cells, resulting in an immunocompromised status called Acquired Immune Deficiency Syndrome (AIDS) [10]. This patient group is prone to TB disease and has a higher mortality rate, with 75 % of HIV deaths associated with TB in 2016 [1, 10].

The standard regimen of TB treatment consists of 4 anti-tuberculosis drugs and requires at least 6 months for completion [11, 12]. Multidrug-resistant TB (MDR-TB) is TB that does not respond to at least isoniazid and rifampicin. Globally, around 150,000 cases of multidrug-resistant TB and rifampicin- resistant TB (MDR/RR-TB) were notified in 2016 [1]. The global burden of MDR-TB has recently increased to more than 20% annually. According to the WHO, approximately half of all patients treated for MDR-TB achieved a successful outcome [1]. It is becoming increasingly difficult to treat MDR-TB. Drug resistant strains of *M.tb* require 1-2 years to complete the treatment regimens [11]. Unfortunately, the extended duration of treatment and non-compliance due to adverse drugs effects result in extensively drug-resistant TB (XDR-TB) which is a form of MDR-TB with additional resistance to more anti-TB drugs [1]. In 2016, ~8000 patients in 72 countries were identified with XDR-TB [1] and the treatment success rate is 30% [1]. The death rate of XDR-TB is almost double compared to MDR-TB, increasing from 16% to 28% [13].

Bacillus Calmette–Guérin (BCG), first used in the 1920s, remains the only licensed vaccine for preventing TB. However, the efficacy of BCG is highly variable against pulmonary TB in adults [14]. Despite high coverage of BCG vaccination, the slow decline in TB incidence globally highlights the need for a much more effective vaccine that provides protection against all forms of TB in all age groups [1].

1.2 **Immune responses to tuberculosis**

There are no clear immunological biomarkers that correlate with protection against TB. The identification of such correlate/s would greatly facilitate TB vaccine development. We do however understand some aspects of host immunity that are essential for protection. As a result, detailed immunogenicity studies are used as a screening tool to select vaccine candidates to the next stage of vaccine trials as well as the use of animal models to test vaccine efficacy.

It is widely acknowledged that $CD4^+$ T cells are essential for protection against *M.tb.* There is a robust correlation between risk of TB disease and HIV infection. Reduction of the $CD4^+$ T cell count in HIV-infected patients results in an increased risk of developing active TB disease [15, 16, 17]. T helper1 (Th1) cell-mediated immune responses play an important role in protection against *M.tb*, as shown by several studies in humans and mice [18, 19, 20]. In particular, IFN-γ has been shown to be critical for the control of *M.tb* infection. Mice lacking the IFN-γ gene have increased susceptibility to *M.tb* infection [21, 22]. IFN-γ helps to activate macrophages to phagocytise and kill intracellular mycobacteria by inducing phagosomal maturation, autophagy, inducible nitric oxide synthase (iNOS), IFN-γ-inducible GTPases and vitamin-D [23, 24, 25, 26, 27, 28]. In humans, IFN-γ deficiencies result in a higher susceptibility to TB [29]. Furthermore, IFN-γ-secreting BCG-specific $CD4^+$ T cells correlated with a reduced risk of TB disease in BCG vaccinated infants [30]. Taken together, $CD4^+$ T cells secreting IFN-γ activate macrophages in order to kill intracellular *M.tb.* This cell population may be an ideal target for the vaccine development to enhance immune response against TB. Interestingly, $CD4^+$ T cells secreting *M.tb*-specific IFN-γ are intact in active TB patients

[31]. That means even though IFN-γ produced by $CD4^+$ T cells is necessary for controlling *M.tb* infection, it is not sufficient to prevent active TB disease. From several vaccine studies in mice and humans, *M.tb*-specific Th1 cells fail to show the prediction of protective immunity [32, 33, 34, 35, 36] and do not correlate with protection against *M.tb* infection [32, 33, 35, 36, 37, 38].

Studies looking into the pathogenesis of TB highlight the complexity of *M.tb* infection. In murine models, it has been shown in several studies that tumor necrosis factor alpha (TNF-α), interleukin-2 (IL-2) or interleukin-6 (IL-6) knockout mice, which can still produce IFN-γ, cannot tolerate *M.tb* infection [39, 40, 41, 42]. By neutralising TNF-α *in vivo* or knocking out the TNF receptor gene, mice rapidly succumbed to *M.tb* infection [39]. In humans, treatment with TNF-α antibody in Crohn's disease and rheumatoid arthritis has been observed to reactivate latent *M.tb* infection [43].

The importance of both $CD4^+$ and $CD8^+$ T cells in *M.tb* protection has been shown by a large number of studies [44, 45, 46]. Reducing $CD4^+$ T cell count in HIV-infected patients results in increasing risk of developing active TB disease [15, 16, 17]. There are no similar human associations related to $CD8^+$ T cells. It is clear that *M.tb* infection induces $CD8^+$ T cells and these cells can be cytokine producing and cytotoxic in humans [47, 48]. Rhesus macaques depleted of $CD8^+$ T cells were no longer protected by BCG vaccination after challenge with high dose *M.tb* [44]. Knockout mice lacking $CD8^+$ T cells were found to be more susceptible to *M.tb* infection [49]. Depletion of $CD8^+$ T cells in the chronic *M.tb* infection resulted in increased bacterial colony-forming units (CFU), suggesting they are essential for long-term control of infection in mice [50]. $CD8^+$ T cells can also recognise *M.tb* infected non-phagocytic cells such as epithelial cells. That means $CD8^+$

T cells can kill a wider range of cell populations [51]. They can also produce cytotoxic cytokines to lyse infected cells using Fas-Fas ligands [47, 48].

As far as innate immune responses are concerned, innate immune cells such as macrophages and natural killer (NK) cells are considered to have a significant role in protective immunity. The bactericidal activity of macrophages in T cell-independent manner has been observed in a great deal of *in vitro* and *in vivo* experiments [52, 53, 54, 55]. In the early phase of *M.tb* infection, NK cells produce IFN-γ non-specifically before the development of adaptive immunity [56, 57, 58].

1.3 **Vaccination against TB**

Development of novel vaccines and development of novel drugs are two important ways to control the TB epidemic. The combination and duration of the therapeutic drug regimens are crucial to minimise side effects and drug interactions between antibiotics [11]. Considering cost effectiveness, the development of anti-TB drugs seems to be inferior compared to vaccination development [59]. Mathematical modelling predicts an increase in MDR-TB and XDR-TB in high-burden countries in the forth-coming decades [60]. Thus, the leading cost-effective intervention against TB is vaccination. Reaching the WHO End TB Strategy targets will require a new vaccine that is effective in adults as well as in latently infected *M.tb* patients [1]. Vaccines also offer the best chance to contain the accelerating spread of drug resistant tuberculosis [1].

BCG provides some protection against severe forms of paediatric TB but has highly variable protective efficacy in adults against pulmonary TB, which is the most common form of TB [14]. A recent meta-analysis shows a vast variation in the efficacy of BCG in

humans, ranging from 0% to 80% [61]. Boosting with a second BCG vaccination is widely considered not to result in improved protection [62]. However, in a recent clinical trial where the endpoint was initial and sustained QuantiFERON conversion as a measure of *M.tb* infection, the BCG revaccination surprisingly showed significant protection against *M.tb* infection [63]. However, a new effective and consistent TB vaccine is still urgently required.

The development of TB vaccines started in 1990, seven decades after BCG was introduced [64]. Fourteen vaccine candidates are currently being evaluated in clinical trials: three in Phase I, eight in Phase II and three in Phase III [65]. Vaccine development approaches are divided into two main strategies: boosting BCG with subunit vaccines expressing mycobacterial antigens [66] or replacing BCG with attenuated live mycobacteria. MTBVAC is a live strain of *M.tb*, attenuated via the deletions of *phoP* and *fadD26* genes. The primary target is neonates as a BCG replacement candidate; the secondary target is adolescents and adults as a booster vaccine [67]. Another example of live attenuated vaccines is VPM1002. It was also successfully tested in phase II trial in healthy South Africa newborns and being assessing the safety and immunogenicity of the vaccine in HIV-exposed and unexposed neonates [68].

Subunit vaccines are aimed to boost BCG and are designed to express one or more mycobacterial antigens. Antigens can be delivered as deoxyribonucleic acid (DNA) vaccines, proteins in adjuvants or expressed by recombinant viral vectors [69, 70].

In a series of non-human primate (NHP) experiments, it has been observed that mucosal or intravenous vaccination with whole cell mycobacterial vaccines provides better protection than parenteral vaccination [71, 72, 73]. These novel routes of

immunisation induce strong Th17 cells [74], resident memory T cells [75] and effector T cells [72].

1.4 **Viral vector vaccines**

Viral vectors are a novel approach to strongly induce adaptive immune responses, delivering immunodominant antigens into the cytoplasm of host cells. [76, 77]. The antigens are processed by ribosomes and expressed on major histocompatibility complex (MHC) Class I and Class II, inducing potent T cell responses [77, 78, 79]. Viral-vectored subunit vaccines have the potential to activate innate immunity and avoid the need for adjuvants. A modified Vaccinia virus Ankara (MVA) has been the leading viral vector vaccine to enter clinical trials [80, 81, 82]. Other viruses such as adenovirus type 35 (Ad35), Sendai virus, lentivirus, vesicularstomatitis virus (VSV), chimpanzee adenovirus and cytomegalovirus (CMV) have also been used as subunit vaccines [83, 84, 85, 86, 87, 88, 89, 90, 91]. CMV vector is able to express multiple *M.tb* antigens and the manufacturing of this vector is attractive for TB vaccine development because it offers sustained antigen expression and long-term immunity [83]. Therefore, the use of replication deficient viruses is much more favourable to construct vaccines. In a recent study, a CMV-based vaccine provided 47% of sterile protection in rhesus macaques against *M.tb* challenge [92]. However, there are some regulatory concerns on giving a replicating CMV vector to humans [93].

MVA expressing the Ag85A antigen from *M.tb*, (MVA85A) was the first prophylactic TB vaccine candidate to be evaluated in a phase 2b efficacy trial [82, 94]. This study showed the vaccine was safe but unable to improve the efficacy of BCG [95]. From the negative result of this well-designed trial, novel insights into immune responses that

correlate with protection have been evaluated [30]. Consequently, a novel replication-deficient chimpanzee adenovirus viral vector was developed expressing the same antigen (ChAdOx1.85A), to be used in combination with MVA85A [84]. While MVA85A mainly induces $CD4^+$ T cell responses [96], ChAdOx1.85A induces potent $CD8^+$ T cell immunity [97, 98]. In mice, boosting an intradermal BCG prime with intranasally administered ChAdOx1.85A, followed by an intradermal or intranasal boost with MVA85A, was the most protective regimen of all combinations tested, and significantly better than BCG alone [98]. Without a BCG prime, ChAdOx1.85A followed by MVA85A was not protective [98]. The immunogenicity of this protective regimen needs to be evaluated, aiming to identify immune correlates of protection in animal models. ChAdOx1 vector is a recombinant E1 E3-deleted chimpanzee adenovirus vector [84]. Cellular immunogenicity of the replication deficient virus is comparable to other vectors including ChAd63, the first simian adenovirus vector to enter clinical trials in humans [84]. Virus neutralizing antibodies against the ChAdOx1 vector in human serum samples are low compared to other chimpanzee adenoviruses [84]. ChAdOx1 vectors have been used to construct vaccines against several infectious diseases and the safety of vaccines have been shown in clinical trials [78, 99, 100, 101].

1.5 **Animal models**

Infecting people with *M.tb* is unethical and therefore animal models are a necessary requirement for developing TB vaccines. A clinical trial takes 5-10 years to complete and uses an enormous amount of funding [63, 95]. Animal models are important as they not only allow the assessment of vaccine efficacy but allow the in-depth analysis of immune responses and the identification of immune correlates of protection. Safety

is a further factor which can be determined in animal studies prior to human clinical trials. Animal studies are a crucial tool for screening new vaccines before proceeding to the challenge experiment, which costly and require a very well-equipped facility to be able to carry out the experiment [102].

There are several animal models that have been used in the development of TB vaccines. Three common models are mice, guinea pigs and non-human primates (NHPs). The murine model is the most widely used in pre-clinical vaccine research because it is easy to handle and perform procedures and the most cost effective among other models [103, 104]. Mice can be genetically modified and also can be used in large number increasing statistical power [22, 104, 105, 106]. However, it is less translational because immune responses in mice are different to humans [104]. For example, some T cell makers, such as CD1 and granulomatous formation of TB disease [103, 104, 107]. In mice, CD1 lipid presentation and T cell recognition has been widely studied on CD1d. However, humans possess three additional CD1 molecules: CD1a, CD1b and CD1c, referred to as the Group 1 CD1s [107]. The lack of an appropriate murine molecule to probe the function of these molecules, despite their crucial role in human immunity, is an impairment [107]. It has been shown in several studies that IFN-γ and TNF-α are crucial for a protective immune response in genetically modified murine models [21, 39, 108]. These findings have since been confirmed in human studies, validating the similarities of human and murine immune responses to *M.tb* infection [43, 109]. The protective ability of $CD4^+$ T cells has been observed in both mouse and human studies [15, 16, 17, 18, 19, 20]. Particular strains of mice such as DBA/2J and C57Bl/6J have a similar susceptibility to *M.tb* infection to humans and show pulmonary lesions similar to TB

pathogenesis found in human disease [110, 111, 112]. This model could potentially be a powerful tool to dissect the pathogenesis of TB disease, leading to a better strategy of vaccine design and development.

Animal models allow researchers to carry out some advanced techniques that are impossible to perform in humans. There is a limitation of sample collection in TB research performed in humans. Peripheral blood and bronco-alveolar lavage (BAL) fluid are two main samples collected by phlebotomy and bronchoscopy respectively. Bronchoscopy is an invasive procedure to collect respiratory fluid, cells or even tissues, as biopsies has been previously performed in respiratory syncytial virus (RSV) patients [113]. Injection of an intravascular stain in mice, which cannot be performed in humans, allows scientists to truly identify tissue-resident cells in the lung parenchyma [114, 115, 116, 117, 118, 119]. Moreover, this model is feasible to study the function of particular cell types by adoptively transfering an interesting cell population from donor mice to recipient mice [106, 114, 120].

Guinea pigs are also used to test the vaccine efficacy. Even though the immune responses are closer to humans compared to mice, it is difficult to improve upon BCG due to the high level of BCG efficacy in this model [69, 102, 121]. There are also limited tools available for immunological analysis in guinea pigs, although these are now improving. NHPs are the most translational model physically and immunologically. Promising efficacy should be demonstrated in this animal model before a vaccine candidate can progress to clinical trials [122, 123]. However, there are high costs associated with this animal model [102, 124]. To analyse the disease outcome in NHPs, costly imaging procedures such as computed tomography (CT) and magnetic resonance imaging

(MRI) are used to visualise the pathology [124]. As a result, studies in NHPs are typically performed once a vaccine candidate has shown promise in the mouse and guinea pig models.

1.6 **Memory T cells**

The hallmark of adaptive immunity is the development of memory immune responses. An adaptive immune response is established after infection or immunisation. This is the classic principle of vaccinology, to create long-lived memory cells, which are specific to their cognate antigen. The memory cells robustly enhance cell mediated responses against their specific primed antigens. Memory responses happen rapidly and efficiently compared to innate immunity, providing optimal control of pre-exposed diseases [125, 126].

Even though $CD4^+$ T cells are known to play a key role in the control of *M.tb* infection, the knowledge of memory $CD4^+$ T cells is much less than for memory $CD8^+$ T cells. The understanding of memory T cells started in the field of acute viral studies where memory $CD8^+$ T cells overpower the responses of memory $CD4^+$ T cells [127, 128, 129]. Until recently, the lack of effective MHC class II tetramers to identify antigen-specific $CD4^+$ T cells by fluorescence-activated cell sorting (FACS) technique made it more difficult to phenotypically evaluate the specificity of memory $CD4^+$ T cells [130].

The subsets of memory T cells have been defined using their phenotype, location and production of effector cytokines. Two distinct memory T cell populations have been proposed since 1999. They are classified by effector function, proliferation and location [131]. Located in the lymphoid organs, central memory T cells (T_{CM}) express CC-

chemokine receptor type 7 (CCR7) and CD62L on their surface and secrete IL-2. In contrast, effector memory T cells (T_{EM}) produce abundant effector cytokines but have no expression of CCR7 and CD62L, allowing them to recirculate between vasculature and peripheral tissues [131].

Tissue resident memory T cells (T_{RM}), originally identified in a skin lesion from a patient with herpes simplex virus, have been recently characterised and named after their ability to stay in non-lymphoid tissues and their lack of re-recirculation in the vasculature [132]. This cell type has been observed in other organs such as small intestinal mucosa, brain tissue and lung parenchyma [114, 133, 134]. The intravascular staining technique has been recently introduced to discriminate T_{RM} cells from the other cells, which are circulating in the vascular compartment [114, 115, 116, 117, 118, 119]. Lung T_{RM} cells are permanently located at the infection site and rapidly counteract *M.tb* infection in the lungs and attract other immune cells to infected sites [114, 117, 133, 135, 136].

A mouse parabiosis model was used to reveal the presence of $CD4^+$ T_{RM} in the lungs of influenza-infected mice, migrating to the lungs during the infection [114]. These cells provided better protection compared to splenic memory cells. Sakai *et al.* introduced the intravascular staining technique to discriminate lung parenchymal $CD4^+$ T cells from intravascular cells after *M.tb* infection [106]. From this study, the lung parenchymal cells provided significantly better protection compared to intravascular $CD4^+$ T cells, as demonstrated by adoptively transferring these cells to lymphocytopenic recipient mice. However, lung parenchymal cells produced lower levels of IFN-γ than the lung vasculature cells, suggesting that location rather than effector function of these cells

is the crucial factor in protective immunity. Interestingly, TB-specific $CD4^+$ T cells in the lung parenchyma homed back to the lungs of infected recipients after adoptively transfer, showing the lung parenchymal T_{RM} cells are loyal to the origin [106].

The main target of vaccines is the induction of memory T cells such as effector memory T cells (T_{EM}) and resident memory T cells (T_{RM}) [137]. These cell populations are induced to high levels after challenge with acute respiratory viruses, facilitating viral clearance and protection against infectious viral diseases [138, 139]. In *M.tb* infection and BCG vaccination, T_{EM} (expressing high CD44 and low CD62L) are enhanced in the lungs [140]. T_{RM} are located in barrier surfaces of peripheral tissues and provide a mucosal defence [141]. The expression of CD69 is crucial to retain these cells in the peripheral tissues [142]. In a murine model, $CD4^+$ T_{RM} cells express CD11a, whereas $CD8^+$ T_{RM} present CD103 in the lungs [114, 117]. $CD4^+$ T_{RM} cells have high expression of CD69 and CD11a following influenza infection. The viral-specific T_{RM} cells are compartmentalised in both the murine and human airways [117]. The efficacy of $CD8^+$ T_{RM} against *M.tb* has been demonstrated using cell depletion and adoptive transfer methods [45, 143, 144]. Recently lung homing markers have been introduced to discriminate lung parenchymal and intravascular memory T cells. The later T cell population expresses high levels of CX3C-chemokine receptor 1 (CX3CR1), which is also known as the fractalkine receptor, and killer cell lectin like receptor G1 (KLRG1), which has frequently been used as a marker of cellular differentiation [106, 136]. The expression of KLRG1 is decreased when the effector cells home back to the lungs and become resident memory cells. The absence of KLRG1, together with the expression of CXC-chemokine receptor 3 (CXCR3), which is a chemokine receptor that is highly expressed on effector T cells and plays an

important role in T cell trafficking and function, is used to phenotypically identify memory T cells in the lung parenchyma [106]. This population are enhanced after vaccination or *M.tb* infection [106]. Woodworth *et al.* have shown that $CXCR3^+$ $KLRG1^-$ $CD4^+$ T cells were localised in the lung vasculature and were associated with protective immunity [145]. In this study, vaccination also enhanced $KLRG1^-$ $CD4^+$ T cells in the vasculature and they were able to specifically home back to the lungs [145].

In humans, it is very difficult to study the protective function of T_{RM} cells. These cells can be found in the lung and are able to respond to a common respiratory pathogen such as influenza virus [146]. In the lungs of *M.tb* latently infected patients, antigen-specific memory T cells are found in the BAL samples [147]. Administering with purified protein derivative of *M.tb* (PPD-T) determined the recruitment of $CD4^+$ T cells, homing back into the lungs of latently *M.tb* infected individuals [148]. This study suggests mucosal immunity may contribute to protective immunity against human *M.tb* infection. However, the mechanism of their protective contribution remains unclear and needs to be studied further.

1.7 **Antibodies**

Cell-mediated immunity has been well established to play an important role against *M.tb* infection, both in animal models and humans [98, 117, 145]. However, the role of antibodies in TB disease remains unclear with some studies emphasising a protective and some other studies revealing a harmful role. Antibodies demonstrate a predominant correlation with protective immunity in other diseases and are relatively easy to induce by vaccination [149]. Thus, if protective, an antibody approach could potentially be a novel strategy for TB vaccine design.

It has been suggested that not only antibodies fail to provide protection, but they may do harm by causing immunological pathology in active disease [150]. To determine the function of anti-mycobacterial antibodies, serum therapy studies have been conducted in mouse models, showing both protective and non-protective effects [151]. Immunoglobulin deficient mice with normal B-cell counts are more susceptible to *M.tb* infection [152]. The transfusion of serum from naive mice did not reverse susceptibility. Blocking of IL-10 signalling resulted in reversal of susceptibility in the spleens and lungs of the mice, suggesting that the immune response were mediated by IL-10 producing B-cells rather than antibodies [152]. In contrast to these findings, after high dose of *M.tb* challenge, B-cell deficient mice developed neutrophilia which was recovered by serum transfusion from *M.tb* infected mice, suggesting *M.tb*-specific antibodies may contribute to protection [153].

Antibody subclasses may also be a factor in contradicting role of antibodies in protection during *M.tb* infection, due to their variable roles in interacting with other immune cells [154]. Immunoglobulin G1 (IgG1) and immunoglobulin G3 (IgG3) are the common human antibody subclasses against TB [155]. IgG1 was able to enhance the production of TNF-α from monocytes in TB patients [156]. In new, recurrent and chronic *M.tb* infected patients, IgG1 and IgG3 were also found to be elevated [157]. Immunoglobulin A (IgA) knockout mice had a higher bacterial CFU numbers in the lungs compared to control mice after *M.tb* challenge where the production of antigen-specific IgG and Immunoglobulin M (IgM) are still intact [158]. Recently, higher titres of Ag85A-specific IgG have been shown to be associated with reduced risk of developing active disease in infants [30].

In vaccine studies, vaccines composed of *M.tb* surface membrane proteins enhance antibody production as well as poly-functional $CD4^+$ cells, resulting in superior protection to BCG in mouse models [159, 160]. Reljic *et al.* have constructed a novel TB vaccine coating *M.tb* antigens onto the surface of inert bacterial spores [161]. Intranasal vaccination of the vaccine enhanced antibody and multifunctional T cell responses, resulting in a significant reduction of bacterial loads in the lungs and spleens following *M.tb* challenge [161]. Using antigen-coated nanoparticles delivered mucosally also induced humoral and cellular immune response and provided protection against *M.tb* infection [162]. Aerosol immunisation of Adhu5Ag85A induced T cell responses as well as Ag85A specific-IgG and IgA in the BAL fluid [163]. Mucosal vaccination of Adhu5Ag85A provided protection in B cell–depleted mice to a similar extent as in B cell–competent mice [164]. Adoptive transfer of B cells purified from naive mice to B cell–deficient mice vaccinated with Adhu5Ag85A did not enhance anti-TB protection [164]. Moreover, T cells induced by mucosal vaccination were able to enhance protection in severe combined immunodeficiency (SCID) mice, and the transfer of vaccine-primed B cells alongside T cells did not further enhance such protection, suggesting that B cells have no role in protective immunity against *M.tb* [164]. This study emphasises the need of identifying dominant epitopes that stimulate functional antibodies against *M.tb.* In rhesus macaques, aerosolised BCG vaccination induces PPD-IgG in the circulation and T cell responses in the airways and provided superior protection compared to intradermal BCG [71]. For vaccine design, it is encouraging that mucosal vaccination can induce antibody responses systemically and locally which may help to improve protective immunity by opsonising *M.tb*.

1.8 **New *M.tb* antigens**

Sequencing of the genome of M.tb resulted in the discovery of around 4000 genes [165], which led to an effort to identify protective antigens for vaccine research and development [166]. A key challenge to subunit vaccine development is the selection of promising antigens to be used in subunit vaccines. The limited understanding of the function of the antigens and their expression together with the lack of immune correlates of protection contributes to the challenges in vaccine design [167, 168].

There are several ways to identify immunogenic mycobacterial antigens for inclusion in subunit vaccine candidates. Mass spectrometry was introduced to identify protein structures [169, 170]. The immunoproteomic approach has been previously performed in a number of mycobacterium species, including *Mycobacterium smegmatis (M.smegmatis)* [171], *Mycobacterium vaccae* [172] and *M.tb* [173]. This method revealed a great deal of immunogenic proteins, which may be used as candidate antigens. Combining this approach with an immunological approach may reveal more promising antigens. Lewinsohn *et al.* identified a number of immunodominant $CD8^+$ T cell antigens which were well recognised by active TB patients and *M.tb* latently infected individuals [174]. Stylianou *et al.* then confirmed the immunogenicity of these antigens in *M.tb* infected mice [121]. Immunodominant antigens are enriched in the cell wall and secretome of *M.tb* [175]. Immunogenic activities of these cell wall and secreted proteins have been investigated in mice, and they have been demonstrated to conferr protection against *M.tb* infection [176, 177]. For example, the Esx protein family has been previously reported as potential T cell antigens in humans and a number of subunit vaccine candidates are using them as components [176, 177]. A fusion protein vaccine

combining 5 Esx family proteins enhanced strong cytokine and T cell responses and conferred better levels of protection than Ag85A and PPE18 against intravenous BCG challenge [176].

The sequencing of the mycobacterial genome revealed a large family of proteins. Proline-glutamate (PE)/proline-proline-glutamate (PPE) family members have a conserved structure and repeat motifs [178, 179, 180]. They are relatively underrepresented among the immunodominant peptide pools [174]. This could be a potential source of mycobacterial antigenic variation and host immune evasion [180]. Several of the members induce strong $CD4^+$ T cell responses, resulting in superior protection compared with unvaccinated mice [181]. Members of this family have also been shown to elicit $CD8^+$ T cell responses in humans [182]. TB Vaccines composed in part of PPE genes are already in clinical studies. M72 vaccine contains PPE 18 also known as Mtb39a which has been reported to comprise potential T-cell epitopes [183, 184]. In phase 2 trail, M72 with adjuvant AS01E was immunogenic in *M.tb* infected adults previously or currently treated but the high local reactogenicity was observed in adults undergoing TB treatment [185]. PPE 42 was used to construct a TB vaccine called ID93 [186]. In phase 1 trail, the vaccine induced antigen-specific $CD4^+$ T cell and humoral responses in BCG-immunised, *M.tb*-infected individuals and showed an acceptable safety profile [187]. Taken together, immunogenic proteins from this family could potentially be promising candidates for vaccine construction.

A ChAdOx boost-MVA prime regimen has been shown to synergistically stimulate T cell responses and provide promising protection [81, 99, 188]. In an attempt to further improve the protective efficacy of the BCG-ChAdOx1.85A-MVA85A vaccination

regimen, novel *M.tb* antigens have been identified that could be used in combination with Ag85A antigen. I selected six mycobacterial antigens that were well recognised by active TB patients and *M.tb* latently infected individuals [174] as well as by *M.tb* infected mice [121]. All antigens selected belong to the PE/PPE family, which have a potential to be a candidate for prophylaxis TB vaccines and also can be used as post-exposure vaccines delivered using the viral vectors.

1.9 **Aims of this thesis**

The overall objective of this research project is to evaluate the immunogenicity induced by the protective B-C-M regimen in depth, focusing on the characterisation of memory T cells in an attempt to identify immune correlates of protection against *M.tb* infection. The specific aims are;

- Evaluate the immunogenicity of the BCG-ChAdOx1.85A-MVA85A vaccine regimen, focusing on memory T cell responses
- Identify immune correlates of protection by comparing immune responses induced by the protective B-C-M regimen to responses induces by non-protective regimes
- Improve the efficacy of B-C-M by designing and evaluating viral vector vaccines expressing novel Mycobacterial antigens

Chapter 2. Materials and Methods

2.1 Materials

2.1.1 Chemicals

Chemical	Supplier
Ethanol	VWR, Leicestershire, UK
PBS tablets	Sigma-Aldrich, Dorset, UK
Tween 20	Sigma-Aldrich, Dorset, UK

2.1.2 Reagents and kits

Reagents and kits	Supplier
Aqua fixable dye	Invitrogen, Paisley, UK
OneComp eBeads	Invitrogen, Paisley, UK
BD CompBeads	BD Bioscience, Oxford, UK
BD Cytofix™	BD Bioscience, Oxford, UK
Collagenase D	Sigma-Aldrich, Dorset, UK
Desoxyribonuclease I (DNase)	Sigma-Aldrich, Dorset, UK
Alkaline Phosphatase conjugate substrate kit	BioRad, CA, USA

2.1.3 Instruments

Instruments	Supplier
BD LSRII	BD Bioscience, NJ, USA
gentleMACS dissociator	Miltenyi Biotec, Surrey, UK
CASY counter	Roche, Basel, Switzerland

2.1.4 Consumables

Consumables	Supplier
ELISA MaxiSorp™ plates	Thermo Scientific, Wilmington, DE, USA
MultiScreen-IP Filter plates	Millipore, Hertfordshire, UK
Cell strainers Nylon	BD Bioscience, Oxford, UK
CryoTube™ Vials	Thermo Scientific, Wilmington, DE, USA
CK28-R tubes	Stretton Scientific, Derbyshire, UK
gentleMACS™ tubes	Miltenyi Biotec, Surrey, UK
EASYstrainer™ Cell sieve (40µm and 100µm)	Greiner Bio-One, Stonehouse, UK
Modified 7H11 agar plates (BPU0104)	Animal and Plant Health Agency, UK

2.1.5 Software

Software	Supplier
GraphPad Prism version 7	GraphPad software, CA, USA
FlowJo version 10	Tree Star, Ashland, OR, USA
Gen5 Software	BioTek, Swindon, UK
AID ELISpot Software	AID-diagnostika, Germany

2.1.6 Mice

Six to eight-week-old female BALB/c mice and C57BL/6 were purchased from Envigo (Cambridgeshire, UK) and CB6F1 mice were purchased from Charles River (Kent, UK). Mice were housed in the Functional Genomics Facility in the Wellcome Trust Centre

for Human Genetics, University of Oxford. All animal experiments were approved and licensed by the UK Home Office under license 30/2889 and P9804B4F1.

2.1.7 Vaccines

Bacillus Calmette–Guérin (BCG) Pasteur was cultured in-house in 7H9 Broth (BD, UK) with 10 % Middlebrook ADC Enrichment and 0.05 % Tween-80 until mid-log phase. BCG was spun down and resuspended in PBS before storing at -80°C.

Replication-deficient chimpanzee adenovirus vector (ChAdOx1) [84, 100] and modified vaccinia Ankara (MVA) [189] expressing antigen Ag85A were constructed in-house by the Vector Core Facility at the Jenner Institute.

2.1.8 Novel Mycobacterial antigens

Antigens were selected from a list of mycobacterial antigens, identified by Lewinsohn D. (Oregon Health and Science University, USA) to be recognised by active TB patients and *M.tb* latently infected individuals [174]. Recognition of these antigens, by lungs and spleen cells from *M.tb* infected C57BL/6 and BALB/c mice, was confirmed later [121]. Based on the results from the above experiments, six antigens were selected. These are PE-PGRS50 (Rv3345c), PE-PGRS23 (1243c), CtpF (Rv 1997), IrtA (Rv1348), PPE68 (Rv3873) and PE9 (Rv1088).

2.2 Methods

2.2.1 Insertion of *M.tb* antigens in viral vectors

The peptide sequences of the six antigens were sent to GeneArt (Thermo Fisher Scientific, Manchester, UK) for gene synthesis. The antigen DNA was cloned into a gateway entry vector using Acc65I and Not I restriction enzymes and then recombined into a E1-E3 deleted ChAdOx1 destination plasmid (Life Technologies Ltd, UK). The DNA plasmids were transformed into Steller Competent cells (Clontech, CA, USA) or NEB 5-alpha Competent *E. coli* (High Efficiency) (New England Biolabs, MA, USA) according to the manufacturer's protocol. To confirm insertion of the antigens at the different cloning steps, plasmid constructs were sent for sequencing (Source BioScience, UK). The vector encoded each antigen under the control of human cytomegalovirus immediate early promoter and expressed in frame with a signal peptide from the human tissue plasminogen activator for increased immunogenicity [80].

For the construction of MVA expressing antigens, the DNA fragment was cloned into a gateway entry vector (p1990) with the same methods as described above. To confirm insertion of the fragment, the plasmid was digested with Acc65I and XhoI. MVA vector was digested with Acc65I and XhoI and dephosphorylated. The entry vector containing the antigen was combined with digested MVA vector and sent off for virus preparation. Correct antigen sequence was confirmed at every cloning step.

2.2.2 Evaluation of vaccine protective efficacy

2.2.2.1 *M.tb* challenge

Aerosol challenge with *M.tb* was conducted using a Biaera AeroMP®-controlled nebuliser (Biaera technologies, Hagertown, USA) contained in a biosafety level 3 TCOL isolator (Total containment Oxford Ltd.) Mice were loaded in nose-only restainers and exposed to aerosolised bacteria. *M.tb* Erdman K01 (TMC107) (BEI resources; Manassas, USA) was prepared at $1x10^6$ CFU/ml and loaded in the nebuliser. The machine was programmed to run for 10 min followed by a 5-minute purge at airflow 10 L/min and pressure 20 pounds per square inch gauge (psig). The infectious dose was 50-100 CFU per animal, verified 24 hours after the challenge using two mice per experiment.

2.2.2.2 Colony forming unit (CFU) determination

To measure bacterial CFU in the organs of *M.tb* infected mice, lungs and spleen were harvested into CK28-R tubes containing 2.8 mm ceramic beads (Stretton Scientific, Derbyshire, UK), filled with 1 ml of PBS. The samples were homogenised twice using a Precellys 24 (Stretton Scientific, Derbyshire, UK) for 20 seconds at 5500 revolutions per minute (rpm). Homogenised specimens were serially diluted in PBS and plated in duplicate on Modified 7H11 agar plates (Animal and Plant Health Agency, UK). The colony count was obtained after a 5-week incubation at 37°C.

2.2.3 Evaluation of vaccine immunogenicity

2.2.3.1 Immunisations

Immunisations were performed under inhalational anaesthesia using isoflurane (Sigma). BCG was intradermally (i.d.) administered at a dose of $4x10^5$ colony forming units (CFU) at the ears of mice (25 µl on each side). Mice were vaccinated with $5x10^6$ plaque forming units (pfu) of MVA via the i.d or i.n. route. ChAdOx1 was delivered intranasally (i.n.) at a dose of $1x10^8$ infectious units (ifu) in a final volume of 50 µl.

2.2.3.2 Collection of organs and cell extraction

I. Brochoalveolar lavage (BAL)

The mice were sacrificed using cervical dislocation. BAL was recovered by three successive lung lavages with 1 ml of 10 mM Ethylenediaminetetraacetic acid (EDTA) (Sigma-Aldrich) in PBS. All samples were spun at 600 x *g* for 5 min and the cell pellet was resuspended in complete media (Table 2-1). To obtain the total cell number, the cells were diluted in CASYton and counted using CASY counter (Roche, Switzerland), range 5.5 – 10.8 µm. The remaining BAL cells were stained for flow cytometry analysis.

Table 2-1. Composition of complete media

Reagent	Concentration	Supplier
Dulbecco's Modified Eagle Medium (DMEM)		Sigma-Aldrich, Dorset, UK
Foetal Bovine sSerum (FBS)	10%	Sigma-Aldrich, Dorset, UK
L-glutamine (100x)	2 mM	Sigma-Aldrich, Dorset, UK
Penicillin-Streptomycin (100x)	100 U/ml	Sigma-Aldrich, Dorset, UK

ll. **Lungs**

To perfuse the lungs, 5 ml of PBS was injected into the right ventricle of the heart. For the intravascular staining technique, no lung perfusion was performed. Lungs were dissected and transferred into a C-tube (Miltenyi Biotec) containing 5 ml of the digestion media (Table 2-2). A gentleMACS dissociator (Miltenyi Biotec) was used to homogenise the lungs according to the manufacturer's programme (lung_02). The homogenised lungs were incubated in a shaking incubator at 37 °C for 1 hour. The content was poured through a 100 µm cell strainer (Greiner Bio-One) into a 50 ml tube. Chilled complete media (Table 2-1) was added through the sieve for the end volume of 30 ml. The samples were spun for 8 min, 300 x *g* at 4 °C. After the spinning, the cells were treated with 5 ml of ACK buffer (Table 2-3) for 5 min following the addition of 10 ml complete media and filtered using a 40 µm cell strainer (Greiner Bio-One). The suspension was filled up to 30 ml and centrifuged as above. The cell pellet was resuspended in 500 µl of complete media. The cells were counted using CASY counter to determine total cell numbers.

Table 2-2. Composition of digestion media

Reagent	Concentration	Supplier
Complete media		
DNase	3 mg/ml	Sigma-Aldrich, Dorset, UK
Collagenase D	7 mg/ml	Sigma-Aldrich, Dorset, UK

Table 2-3. Composition of ACK buffer

Reagent	Concentration	Supplier
NH_4CL	0.15 M	Sigma-Aldrich, Dorset, UK
$KHCO_3$	1 mM	Sigma-Aldrich, Dorset, UK
Na_2EDTA	0.1 mM	Sigma-Aldrich, Dorset, UK
Distilled water		

III. **Spleen**

The spleen was removed and kept in PBS before processing. To obtain the cell suspension, the spleen was crushed using a syringe plunger and suspended in PBS before passing through a 70 µm cell strainer into a new 50 ml tube. PBS was topped up to the end volume of 30 ml through the sieve. The homogenised spleen was centrifuged for 5 min, 600 x *g* at 4 °C. The cell pellet was treated with 5 ml of ACK buffer (Table 2-3) for 5 min, adding 25 ml of PBS to stop the lysis then centrifuged as above. The cells were resuspended in 5 ml of complete media (Table 2-1) and counted using CASY counter.

IV. **Serum**

Blood was collected from the right cervical vein of naïve and vaccinated mice and stored at 4 °C overnight. Blood was spun at 2000 x *g* for 10 min at 4 °C. Serum was collected and stored in -80 °C for antibody analysis.

2.2.3.3 Flow cytometry analysis

I. **Intravascular staining**

BALB/c mice were pre-heated at 37 °C in a heat box for 10 min. 2.5 µg of FITC-conjugated anti-CD45.2 (BD Biosciences) was injected intravenously into the tail of the mice in a volume of 100 µl. One minute after the injection, mice were sacrificed, and the lungs were collected. Lungs were placed in a C-tube (Miltenyi Biotec) containing 10ml of the digestion media (Table 2-2). A gentleMACS dissociator was used to homogenise the lungs according to the manufacturer's protocol. The homogenised lungs were topped up with 10 ml of complete media (Table 2-1Table 2-2) to dilute antibody concentration. The protocol for lung processing was then applied as per 2.2.3.2II to obtain a single cell suspension.

II. **Cell surface staining and tetramer staining**

$2x10^6$ lung cells and spleen cells as well as all BAL cells were stained per sample/stimulation. Cells were washed with PBS and centrifuged at 600 x *g* at 4 °C. To identify antigen-specific $CD4^+$ and $CD8^+$ T cells, 50 µl of Ag85A-specific tetramer mixture diluted 1:100 in PBS (Class II: I-E(d) *M.tb* Ag85A 165-178 LPGWLQANRHVKPT, Class I: H-2L(d) *M.tb* Ag85B 110-118 MPVGGQSSF) (NIH Tetramer Core Facility, USA) was added for 25 min at 4 °C. Cells were washed twice with PBS and surface staining was performed. Cells were initially stained with 10 µl of live/dead Aqua fixable dye

(1:1000 in PBS; Invitrogen) for 10 min followed by 30 min incubation with 40 µl of fluorochrome-conjugated surface antibodies (Appendix 7.1) and anti-mouse CD16/CD32 receptor antibody (1:200, eBioscience) diluted in 2 % Bovine Serum Albumin (BSA) (Sigma-Aldrich) in PBS (FACS buffer). The stained cells were washed and fixed with 100 µl of 1 % Paraformaldehyde, for 10 min at room temperature (RT), spun and resuspended in FACS buffer for running on an LSRII flow cytometer (BD Bioscience). The acquired data were analysed using FlowJo version 10 (Tree Star, USA).

III. **Intracellular staining**

To detect cytokine producing T cells, $2x10^6$ lung cells were stimulated with 2 µg/ml of Ag85A 66 peptide pool (15mers overlapping by 10 amino acids) or purified protein derivative of *M.tb* (PPD-T), or complete media (Table 2-1) as an unstimulated control at 37 °C and 5% CO_2. After 2 hours, GolgiPlug (1:1000, BD Bioscience) was added for further 4 hours. The stimulated cells were stored at 4 °C for staining the next day. Cell surface staining was performed as described in 2.2.3.3II. After the surface staining, the cells were fixed and permeabilised using CytoFix (BD Biosciences) as per the manufacturer's protocol. Cells were stained with 50 µl of fluorochrome conjugated antibodies (Appendix Table 7-1 and Table 7-4) and Fc block in diluted CytoPerm buffer (BD Biosciences) for 1 hour at 4 °C. Cells were washed with CytoPerm buffer then washed with FACS buffer before resuspending in FACS buffer. All samples were run and analysed as above.

2.2.3.4 Enzyme-linked immunospot (ELISpot)

MultiScreen-IP Filter plates (Millipore) were coated with 50 µl of anti-mouse IFN-γ mAb (Mabtech) diluted coating solution (0.05 M carbonate-bicarbonate buffer

capsule (Sigma-Aldrich) in 100 ml deionised water) and stored at 4 °C overnight. The coating solution was discarded, and the plates were blocked with 100 µl of complete media for a minimum of 1 hour at 37 °C. Spleens were harvested and processed as described in 2.2.3.2III. After washing the plates 6 times with PBS, the splenocytes were plated at 50 µl at different dilutions. 50 µl of complete media or diluted antigen (final concentration of 2 µg/ml) were added to each well to 100 µl final volume. The plates were incubated for 18-20 hours at 37 °C in a humidified incubator. After incubation, the plates were washed and then incubated with 50 µl/well of biotinilyated goat anti-mouse IgG diluted 1:1000 in PBS for 2 hours at RT. The plates were washed before adding 50 µl of streptavidin-alkaline phosphatase (Mabtech) diluted 1:1000 in PBS and incubated for 1 hour at RT. The plates were washed and developed with 100 µl of developing buffer (alkaline phosphatase conjugate substrate kit, BioRad) at RT until spots could be adequately visualised. The reaction was stopped by washing the plates under running tap water. The plated were left to dry and spots were counted using AID ELISpot reader (AID-diagnostika).

2.2.3.5 Enzyme-linked Immunosorbent Assay (ELISA)

Enzyme-linked immunosorbent assay (ELISA) was used to measure Ag85A and PPD specific antibodies in BAL fluid and serum. Maxisorp 96-well plates (ThermoFisher Scientific) were coated with 50 µl of diluted recombinant 85A (r85A) (2 µg/ml for detecting IgG, 10 µg/ml for detecting IgA) or PPD-T (6.67 µg/ml) in PBS incubated overnight at RT. The plates were washed 6 times with PBS/Tween-20 (Sigma-Aldrich) and blocked with 200 µl of 2.5 % BSA (Sigma-Aldrich) in PBS for 1 hour at RT. After blocking, the plates were washed with the same method. Serum samples were

prepared at an initial dilution of 1:50 whereas BAL samples were plated neat. Serial dilutions were done in 0.1 % BSA/PBS/Tween or PBS/Tween for serum and BAL respectively. Fifty µl of the samples were incubated for 2 hours at RT. After washing with PBS/Tween-20, 50 µl of alkaline phosphatase conjugated anti-IgG (1:5000) or anti-IgA (1:1000) (Sigma-Aldrich) diluted in PBS/Tween was added and incubated for 1 hour at RT. The plates were washed before addition of 100 µl development buffer (1 mg/ml of 4-nitrophenylphosphate tablet (Sigma-Aldrich)) diluted in diethanolamine buffer (ThermoFisher Scientific). The reaction was developed at RT and optical density (OD) was read at 405 nm (Gen5 software) using a spectrophotometer (BioTeK Microplate Reader). Mean optical density of duplicate blank wells were subtracted from mean OD of test samples to obtain adjusted OD. Serum from naïve mice was used as negative control. Previously determined high responders were used as positive control.

2.2.3.6 Adoptive transfer

Donor mice were injected intravascularly with anti-CD45.2 1 min prior to euthanasia as described in 2.2.3.3I. The lungs were harvested and processed to obtain a single cell suspension. The MHC class II tetramer staining was performed as described above. Tetramer positive, CD45+/- cells were sorted using a MoFlo® (Beckman Coulter) with Summit software (Cytomation, Inc.) into complete media supplemented with 40% FBS. Fluorescence-activated cell sorting (FACS) was performed by Dr Andrew Worth (Jenner Institute, Oxford UK). The sorted cells were washed and spun at 800 x *g* for 8 min. Approximately 5000 cells were resuspended in 100 µl of PBS for intravenous transfer into recipient mice. Mice were warmed in a heat box before the injection was

conducted on the lateral tail vein. Animals were challenged with *M.tb* 24 hours after adoptive transfer.

2.2.3.7 Statistical analysis

Statistical analyses were performed using GraphPad Prism 7 software (GraphPad Software Inc.). To determine the statistical significance, Mann Whitney test was used to compare two groups while, Kruskal-Wallis followed by Dunn's multiple comparisons test was performed when analysing multiple groups. Values of $p \leq 0.05$ were considered as statistically significant. *p≤0.05, **p≤0.01, ***p≤0.001, ****p≤0.0001.

Chapter 3. Immunogenicity and protective efficacy following B-C-M regimen

3.1 **Introduction**

A vaccination regimen composed of a prime with BCG followed by a boost with ChAdOx1.85A, and a further boost by MVA85A (B-C-M), was shown to provide superior protection to BCG alone [98]. Stylianou *et al*. has reported that 4 weeks after the last vaccination, only B-C-M was protective against *M.tb* infection, but not B-C, with M delivered either intranasally (i.n) or intradermally (i.d.) [98]. Based on these findings it was decided to investigate whether there was any correlation between the protective efficacy of the B-C-M regimen and its immunogenicity.

Th1 cell-mediated immune responses play an important role in protection against *M.tb*, as shown by several studies in humans and mice [18, 19, 20]. In particular, IFN-γ has been shown to be critical for the control of *M.tb* infection. Mice lacking the IFN-γ gene have increased susceptibility to *M.tb* infection [21, 22]. In humans, IFN-γ deficiencies result in a higher susceptibility to BCG and TB [29]. Furthermore, IFN-γ-secreting BCG-specific $CD4^+$ T cells correlated with a reduced risk of TB disease in BCG vaccinated infants [30]. TNF-α is also important for controlling *M.tb* infection [39, 40, 41, 42, 43]. By neutralising TNF-α *in vivo* or knocking out the TNF receptor gene, mice rapidly succumbed to *M.tb* infection [39]. TNF-α antibody treatment in patients with inflammatory diseases has been observed to reactivate latent *M.tb* infection [43].

The importance of both $CD4^+$ and $CD8^+$ T cells in *M.tb* protection has been shown by a large number of studies [44, 45, 46]. In murine models, $CD4^+$ T cells have been shown to play an important role in this protective mechanism [18, 19, 20]. A lower $CD4^+$ T cell count in HIV-infected patients results in an increased risk of developing active TB disease [15,

[16, 17]. There are no similar human associations related to $CD8^+$ T cells. It is clear that *M.tb* infection induces $CD8^+$ T cells and these cells can be cytokine producing and cytotoxic in humans [47, 48]. $CD8^+$ T cells depleted macaques were no longer protected by BCG vaccination after infected with high dose *M.tb* [44]. In mice, lacking $CD8^+$ T cells was found to increase susceptibility to *M.tb* infection [49]. Depletion of $CD8^+$ T cells resulted in increased bacterial CFU in the chronic *M.tb* infection stage, suggesting they are essential for long-term control of infection in mice [50].

$CD8^+$ T cells from the lungs of *M.tb*-infected animals have been shown to produce perforin and lyse infected macrophages [190]. Interestingly, perforin knockout mice were not more susceptible to *M.tb* infection [191]. Adoptive transfer of $CD8^+$ T cells isolated from perforin-deficient mice did not protect recipient mice from *M.tb* infection [45]. In humans, $CD8^+$ T cells have also been shown to lyse *M.tb* infected macrophages and killed intracellular bacilli [192]. However, detecting perforin production *in vivo* has been challenging due the higher production of effector cytokines compared to perforin during *M.tb* infection [193].

Serine proteases such as granzymes produced by $CD8^+$ T cells are stored in granules and delivered across the immunologic synapse via perforin [194]. Mice lacking granzyme B did not appear more susceptible to *M.tb* infection [191]. $CD8^+$ T cells from latently infected individuals had a higher expression of Granzyme B compared to active TB patients [195]. The lack of granulysin expression in mice makes it difficult to assess the full potential of this T cell subset in protection against tuberculosis in this model [196].

Unlike T cells, whose importance in *M.tb* control is well established, the role of antibodies is less clear. Serum therapy studies have been conducted in mouse models

with inconsistent results [151]. Absence of both B cells and immunoglobulin did not compromise protection against *M.tb* infection in mice [152]. In contrast, serum transfusion from *M.tb* infected mice could recover neutrophilia which occurred after high dose challenge of *M.tb* in B cell deficient mice, suggesting *M.tb*-specific antibodies may contribute to protection [153]. IgA knockout mice have higher bacterial CFU numbers in the lungs compared to control mice after *M.tb* challenge [158]. A more recent study in infants showed that higher titres of Ag85A-specific IgG were associated with reduced risk of developing active disease [30]. The above data support the idea that antibody responses should also be investigated when evaluating novel vaccines against TB.

The aims of this chapter were;

1. To identify immune responses that correlate with the protective efficacy of the B-C-M vaccination regimen. To achieve this, immune responses that have been previously shown to have a role in protection were investigated. These include, Th1 effector, cytolytic and antibody responses.
2. To study the durability of protection provided by the B-C-M regimen. The protective efficacy of the vaccine regimen was examined at 8 weeks and 20 weeks post vaccination.

3.2 **Results**

3.2.1 T cell responses induced by B-C-M regimen in the lungs and spleen

A vaccination regimen composed of a prime with intradermal BCG (B) followed by a boost with intranasal ChAdOx1.85A (C), and a further boost by intradermal MVA85A (B-C-Mid) four weeks later, was shown to provide superior protection compared to BCG alone [98]. In contrast, ChAdOx1.85A alone failed to improve BCG efficacy indicating that MVA85A is necessary for protection.

In order to identify immune correlates of protection, the immune responses of B-C-M vaccinated mice were compared to responses induced by the less protective controls (B and B-C) (Figure 3-1). Four weeks post ChAdOx1 vaccination, some mice were sacrificed to study the immune responses just before the MVA85A boost (B-C4). B-C4 was included in the published efficacy study so this regimen would directly compare to the protection finding. Eight weeks post ChAdOx1 vaccination (B-C8) control was also included as an exact replicate of B-C-M regimen but without MVA boost. This group would reveal the effect of MVA85A on the B-C-M regimen. Lung and spleen cells from vaccinated mice were stimulated *ex-vivo* with purified protein derivative from *M.tb* (PPD-T) and antigen 85A (Ag85A) and then intracellularly stained for IFN-γ and TNF-α using effector panel (Appendix Table 7-1). PPD-specific cytokine-producing cells represent immune responses induced mainly by BCG, Ag85A stimulation reveals the effector cells that are induced specifically by Ag85A found in BCG, ChAdOx1.85A and MVA85A.

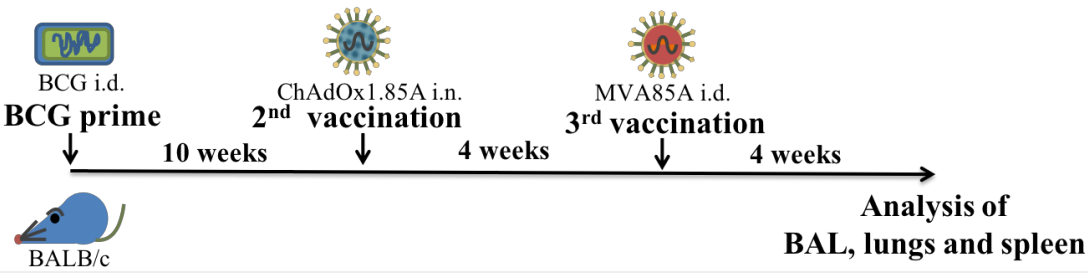

NA:	No vaccination----------18wks----------->Harvest
B:	BCG----------18wks ----------->Harvest
B-C8:	BCG----10wks-----> ChAdOx1.85A----------8wks----------->Harvest
B-C4:	BCG----------10 wks---------->ChAdOx1.85A---4wks--->Harvest
B-C-Mid:	BCG----10wks-----> ChAdOx1.85A--4wks--->MVA85A---------4wks--->Harvest

Figure 3-1 Timeline of B-C-M vaccination and control groups. BALB/c mice were vaccinated intradermally (i.d.) with $4x10^5$ CFU of BCG Pasteur (B) and boosted 10 weeks later with $1x10^8$ ifu of ChAdOx1.85A (C) intranasally (i.n.). Four weeks after ChAdOx1.85A vaccination, some mice received a further boost of intradermal MVA (Mid) at a dose of $5x10^6$ pfu. Murine samples were harvested at 4 weeks after the last vaccination in B-C-Mid and B-C4 groups, at 8 weeks post ChAdOx1 vaccination in B-C8 group.

3.2.1.1 B-C-M regimen induces effector cytokine production in the lungs and spleen of vaccinated mice

I. **Measuring $CD4^+$ cytokine production in the lungs and spleen of B-C-M vaccinated and control mice**

The percentage of $CD4^+$ T cells producing cytokines was higher in the B-C-M group compared to B-C8 and B-C4 in the lungs (Figure 3-2 A and B) and spleen (Figure 3-2 C and D) but the differences were not statistically significant. Unlike the control groups, vaccination with B-C-M significantly increased the percentage of Ag85A-specific IFN-γ producing $CD4^+$ T cells in the lungs ($p=0.0218$) (Figure 3-2 A) and IFN-γ and TNF-α in the spleen, compared to the BCG group ($p=0.0287$ and 0.0076 respectively) (Figure 3-2 C and D). Stimulation with Ag85A and PPD resulted in comparable responses but the magnitude of responses was higher with PPD stimulation. With PPD stimulation, there was a trend for higher cytokine production in the BCG group compared to the groups that received the additional boosting with ChAdOx1.85A (Figure 3-2 A-D). Cytokine production was higher in the lungs of B-C-Mid vaccinated mice compared to BCG alone, but the differences were not statistically significant (Figure 3-2 A and B). In the spleen, An MVA85A boost maintained the PPD-specific IFN-γ and TNF-α production, showing comparable levels of responses between B-C-Mid and BCG groups (Figure 3-2 C and D).

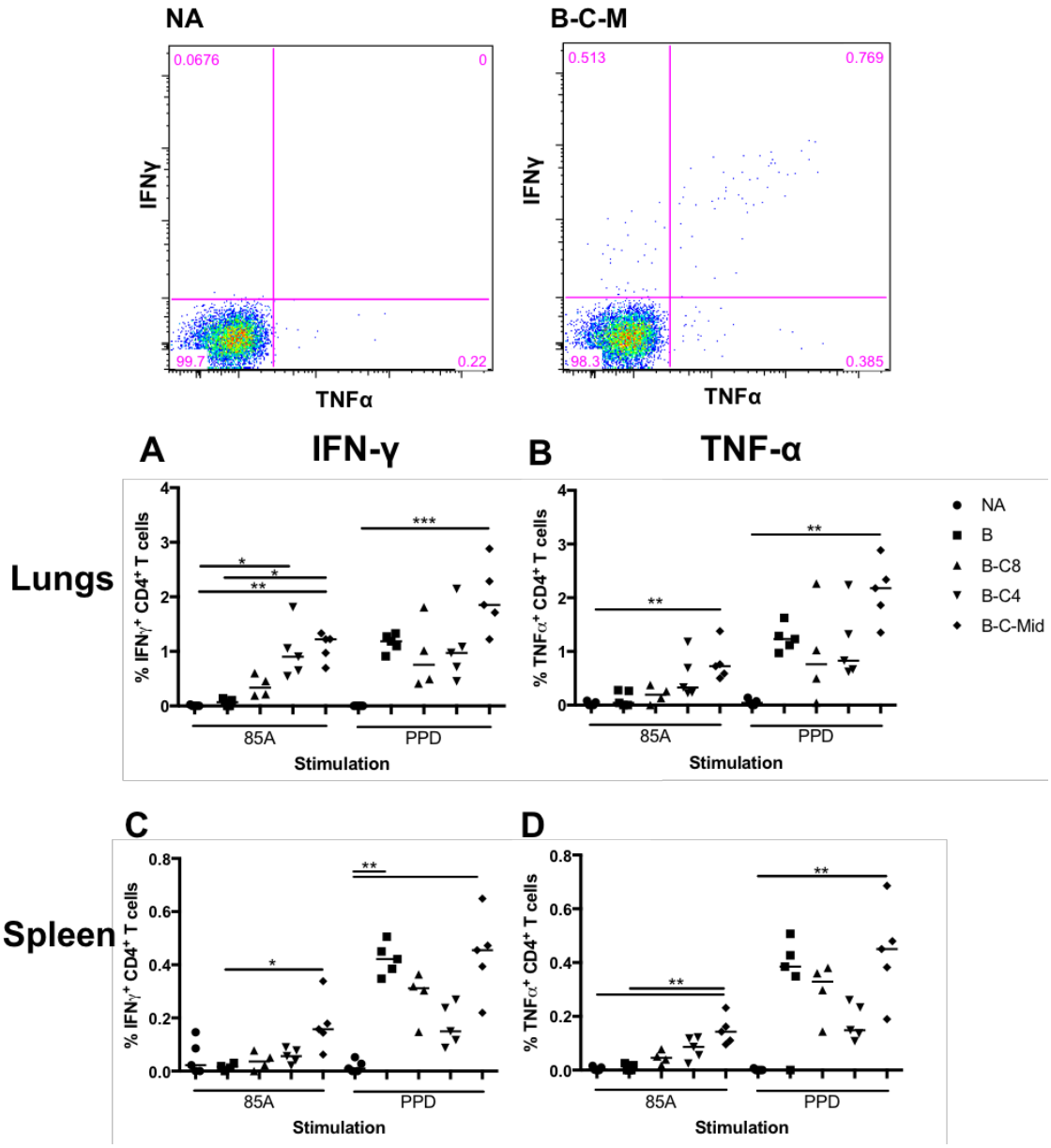

Figure 3-2 CD4⁺ T cell cytokine responses in the lungs and spleen of naïve and vaccinated mice. Lung and spleens cells were stimulated *ex-vivo* with Ag85A peptide pool (85A) and purified protein derivative from *M.tb* (PPD). Representative flow plots show cytokine-producing CD4⁺ T cells in the lungs of naïve (NA) (Left panel) and B-C-M (Right panel) group. (A) Percentage of IFN-γ⁺ and (B) TNF-α⁺ CD4⁺ T cells in lungs and spleens (C) and (D) respectively. The experiment was repeated twice with similar results. Each symbol represents one animal and the line is the median of each group (n=4-5 mice). Statistical significance was determined using Kruskal-Wallis test with Dunn's multiple comparisons test. *p≤0.05; **p≤0.01; ***p≤0.001.

II. Measuring $CD8^+$ cytokine production in the lungs and spleen of B-C-M vaccinated and control mice

IFN-γ and TNF-α producing $CD8^+$ T cells were also detected in the lungs and spleen of vaccinated mice (Figure 3-3 A-D). In the lungs of B-C4 and B-C-Mid immunised mice, one third of $CD8^+$ T cells produced IFN-γ after Ag85A stimulation (Figure 3-3 A) and more than half of this population were double positive cells, secreting also TNF-α (Figure 3-3 representative flow plots). Four weeks after the last vaccination, effector cytokines were comparable in the lungs of B-C4 and B-C-Mid immunised mice (Figure 3-3 A and B). Without MVA85A boost, ChAdOx1.85A failed to maintain the effector responses at 8 weeks post vaccination showing a reduction of cytokine producing $CD8^+$ T cells in both organs of B-C8 mice compared to B-C-Mid immunised mice (Figure 3-3 A-D). A significant increase in IFN-γ and TNF-α producing $CD8^+$ T cells was observed in the lungs of B-C-Mid vaccinated compared with BCG alone vaccinated mice ($p=0.0218$ and 0.0131 respectively) as well as in the spleen ($p=0.0024$ and 0.0009 respectively) (Figure 3-3 A-D). Effector cytokines were undetectable in $CD8^+$ T cells stimulated with PPD (Figure 3-3 A-D).

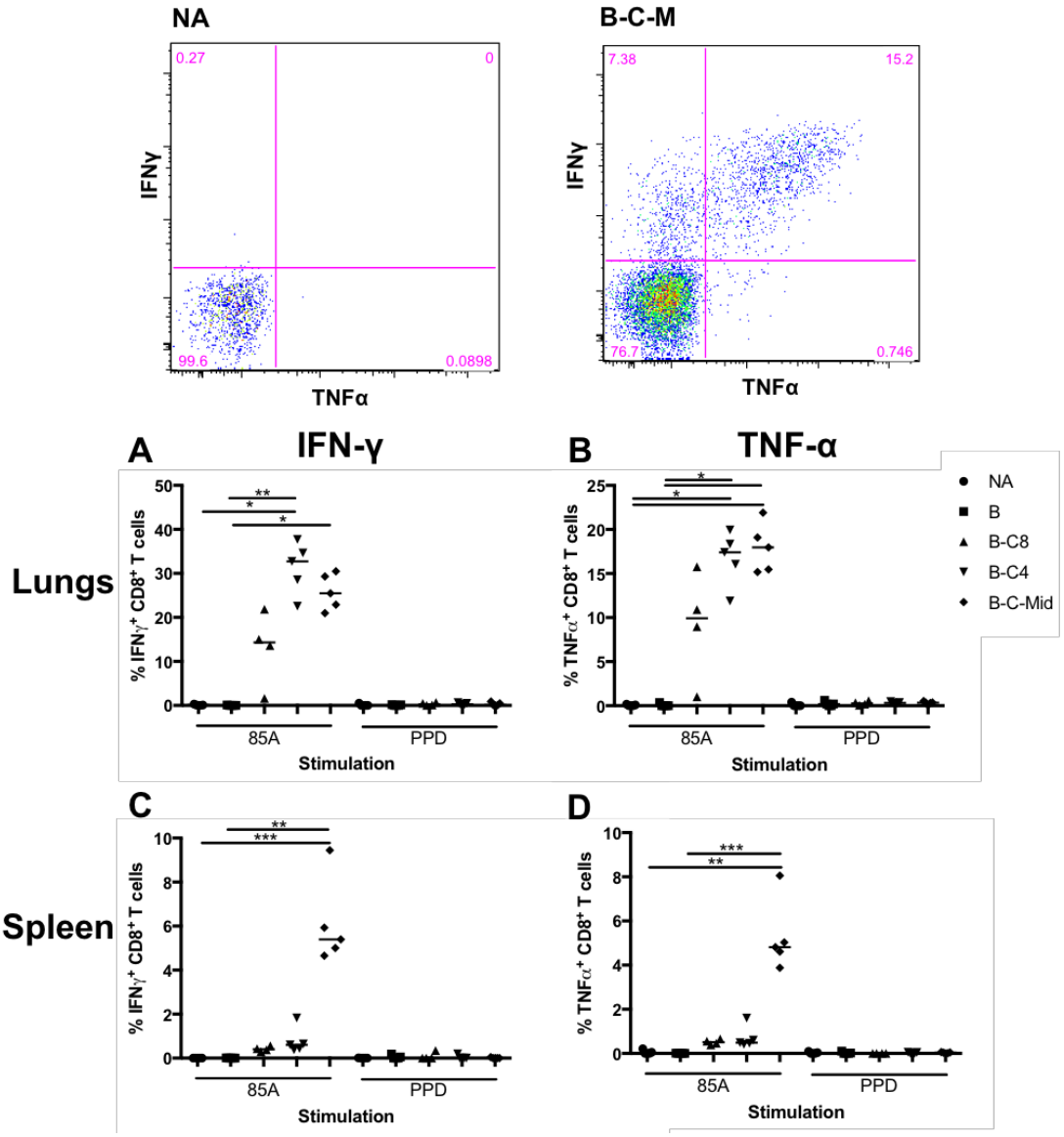

Figure 3-3 CD8⁺ T cell cytokine responses in lungs and spleen of naïve and vaccinated mice. Representative flow plots show cytokine-producing CD8⁺ T cells in the lungs of naïve (NA) (Left panel) and B-C-M (Right panel) groups. (A) Percentage of IFN-γ⁺ and (B) TNF-α⁺ CD8⁺ T cells in lungs and spleens (C) and (D) respectively. The experiment was repeated twice with similar results. Each symbol represents one animal and the line is the median of each group (n=4-5 mice). Statistical significance was determined using Kruskal-Wallis test with Dunn's multiple comparisons test. *, p≤0.05; **, p≤0.01; ***, p≤0.001.

3.2.1.2 Effector cytokine responses induced by C-M regimen in the lungs and spleen

Mice vaccinated with C-M were not protected against *M.tb* challenge, suggesting that BCG priming is necessary for the protective efficacy of the B-C-M regimen [98]. In order to investigate the effect of BCG to the B-C-Mid regimen a similar experiment was set up as above but without a BCG prime (Figure 3-4).

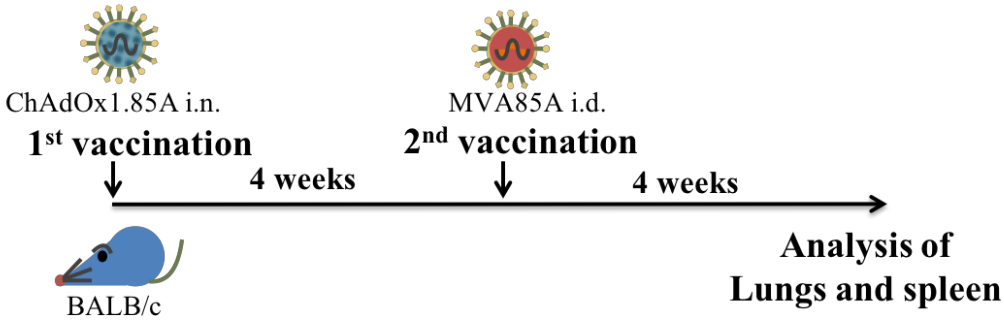

NA:	No vaccination----------8wks---------->Harvest
C8:	ChAdOx1.85A----------8wks---------->Harvest
C4:	ChAdOx1.85A----4wks---->Harvest
C-M:	ChAdOx1.85A---4wks--->MVA85A---------4wks---->Harvest

Figure 3-4 Timeline of C-M vaccination and control groups. A replicate experiment was performed but without BCG priming in order to investigate the effect of BCG to the regimen. Mice were vaccinated with ChAOx1.85A i.n. Four weeks post vaccination, some mice were boosted with MVA85A i.d. (C-M). Some mice did not receive an MVA85A boost and were sacrificed at 4 weeks (C4) and 8 weeks (C8) post vaccination later together with C-M group.

I. Measuring $CD4^+$ cytokine production in the lungs and spleen of C-M vaccinated and control mice

Vaccination with C-M significantly increased the percentage of Ag85A-specific IFN-γ and TNF-α producing $CD4^+$ T cells in the lungs compared to the naïve group (p=0.0035 and 0.0016 respectively) (Figure 3-5 A and B). Four weeks after ChAdOx1.85A immunisation (C4), a significant increase of Ag85A-specific IFN-γ producing $CD4^+$ T cells was observed in the lungs of C4 mice compared to naïve group (NA) (p=0.0104) (Figure 3-5 A). Ag85A-specific TNF-α producing $CD4^+$ T cells were also higher in C4 mice compared to unvaccinated mice, but the difference was not statistically significant (p=0.0548) (Figure 3-5 B).

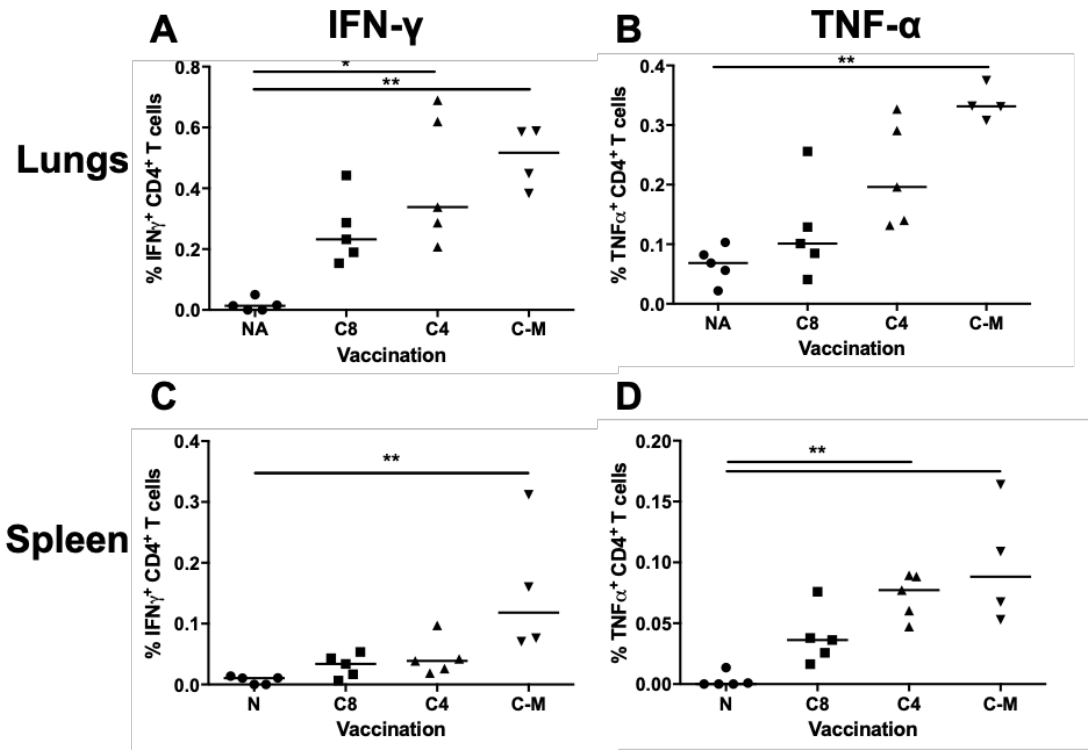

Figure 3-5 CD4$^+$ T cell cytokine responses in lungs and spleen of naïve and vaccinated mice. Lung cells were stimulated with Ag85A peptide. (A) Percentage of IFN-γ$^+$ and (B) TNF-α$^+$ CD4$^+$ T cells in lungs. (C) Percentage of IFN-γ$^+$ and (D) TNF-α$^+$ CD4$^+$ T cells in spleen. The experiment was repeated twice with similar results. Each symbol represents one animal and the line is the median of each group (n=4-5 mice). Statistical significance was determined using Kruskal-Wallis test with Dunn's multiple comparisons test. *, p≤0.05; **, p≤0.01.

II. Measuring $CD8^+$ cytokine production in the lungs and spleen of C-M vaccinated and control mice

IFN-γ and TNF-α producing $CD8^+$ T cells were significantly increased in the lungs of C4 mice compared to unvaccinated mice (p=0.0007 and 0.0024 respectively) (Figure 3-6 A and B). However, an MVA85A boost failed to further improve effector $CD8^+$ T cell responses in the lungs compared to ChAdOx1.85A alone (C8 and C4) (Figure 3-6 A and B). Without the MVA vaccination, the responses were comparable in the lung of C8 mice compared to other vaccinated groups (Figure 3-6 A and B).

In the spleen, ChAdOx1.85A vaccination induced very low $CD8^+$ effector cytokine production in the lungs and spleen at 4 weeks (C4) and 8 weeks (C8) post vaccination (Figure 3-6 C and D). TNF-α producing $CD8^+$ T cells were significantly increased in the spleen of C4 vaccinated mice compared to naïve controls (p=0.0339) (Figure 3-6 C and D). The levels of IFN-γ and TNF-α production were significantly increased after MVA85A boost in the spleen of C-M mice compared to naïve mice (p=0.0057 and 0.0004 respectively) (Figure 3-6 C and D).

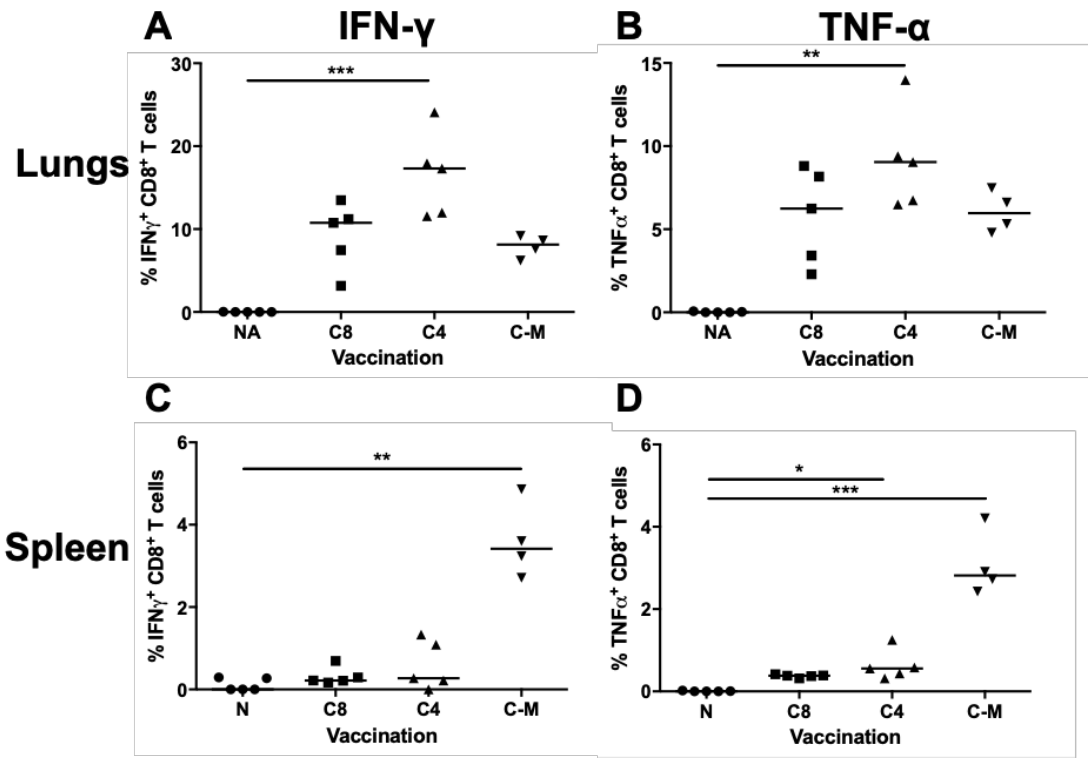

Figure 3-6 CD8$^+$ T cell cytokine responses in lungs and spleen of naïve and vaccinated mice. Lung cells were stimulated with Ag85A peptide. (A) Percentage of IFN-γ$^+$ and (B) TNF-α$^+$ CD8$^+$ T cells in lungs. (C) Percentage of IFN-γ$^+$ and (D) TNF-α$^+$ CD8$^+$ T cells in spleen. The experiment was repeated twice with similar results. Each symbol represents one animal and the line is the median of each group (n=4-5 mice). Statistical significance was determined using Kruskal-Wallis test with Dunn's multiple comparisons test. *, p≤0.05; **, p≤0.01; ***, p≤0.001.

3.2.1.3 Cytotoxic cytokine production induced by vaccination

I. Optimising conditions for staining perforin and granzyme B intracellularly

Detection of cytotoxic cytokines *in vivo* is difficult due to the low level of expression of these cytokines compared to the production of effector cytokines [193]. Thus, optimisation of perforin and granzyme B staining was performed to identify the optimal detection conditions for these cytokines.

a. Detection of cytotoxic cytokines using high concentrations of antibodies

To detect the production of granzyme B and perforin, naïve spleens were harvested and processed in single cell suspension. Splenocytes were stimulated with anti-CD3 and anti-CD28 for 6 hours before surfacely stained with CD3 and CD8. PE-Cy7 conjugated anti-mouse granzyme B and PE conjugated anti-mouse perforin were used at dilutions of 1:10 and 1:20 to intracellularly stain for the cytokines.

There were no responses detected in either Fluorescence Minus One (FMO) control (Figure 3-7 Top and Bottom Left plots). Using 1:10 dilution of anti-granzyme B, 17 % of granzyme B producing $CD8^+$ T cells were observed in the stimulated splenocytes (Figure 3-7 Top Middle plot). The percentage decreased to 5 % when a lower concentration of antibody was used, (1:20) (Figure 3-7 Top Right plot). Approximately 6% of $CD8^+$ T cells secreting perforin were detected when a 1:10 dilution of anti-perforin antibody was used (Figure 3-7 Bottom Middle plot). The response was almost undetectable when the dilution of antibody was decreased to 1:20 (Figure 3-7 Bottom Right plot).

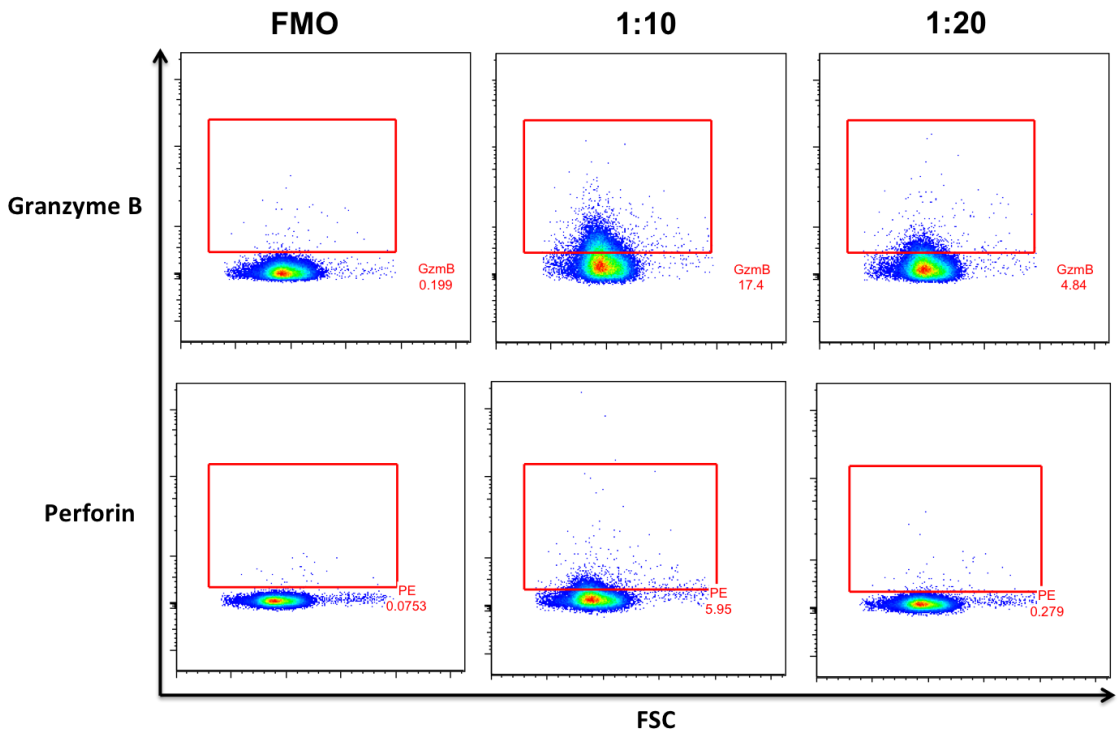

Figure 3-7 Perforin and granzyme B detected using high concentration of fluorochrome-conjugated anti-mouse antibodies. Spleens were harvested from naïve BALB/c mice. Splenocytes were stimulated with anti-CD3 and anti-CD28 for 6 hours. The stimulated cells were surface stained with CD3 and CD8 before intracellularly stained with fluorochrome-conjugated anti-mouse granzyme B and perforin. 1:10 (Left) and 1:20 (Right) dilutions of the antibodies were used for the intracellular staining. Granzyme B (Top) and perforin (Bottom) were measured using flow cytometry and gated on CD3, CD8 and the cytokines. FMOs were included as a negative gating control.

b. Detection of Granzyme B using anti-human antibody

Low responses of granzyme B production were detected using the anti-mouse antibody. The anti-human granzyme B antibody has been shown to cross-react with mouse granzyme B [197]. Loebbermann *et al.* used fluorochrome-conjugated anti-human granzyme B to stain lung cells from RSV infected mice with/without re-stimulation and obtained high responses [198]. There was no report in using anti-human perforin to stain murine cells. Therefore, perforin was not tested using the anti-human antibody.

To examine the cross-reactivity of anti-human granzyme B in mice, lungs were collected from BCG-ChAdOx1.85A vaccinated mice. The lung cells were stimulated with Ag85A for 6 hours and then surface stained for T cell markers. Anti-human granzyme B was used to intracellularly stain the cells at different concentrations and was not added in an FMO control.

No responses were detected in the FMO control (Figure 3-8 Top Left plot). At 1:50 dilution, 38 % of granzyme B producing $CD8^+$ T cells were observed in the lungs of the vaccinated mice (Figure 3-8 Top Middle plot). The responses decreased in a dilution dependent manner from 26 % in 1:100 dilution to 7 % in 1:400 dilution (Figure 3-8 Top Right and Bottom plots). Thus, 1:50 dilution of the fluorochrome-conjugated anti-human granzyme B was selected for optimal measurement of granzyme B.

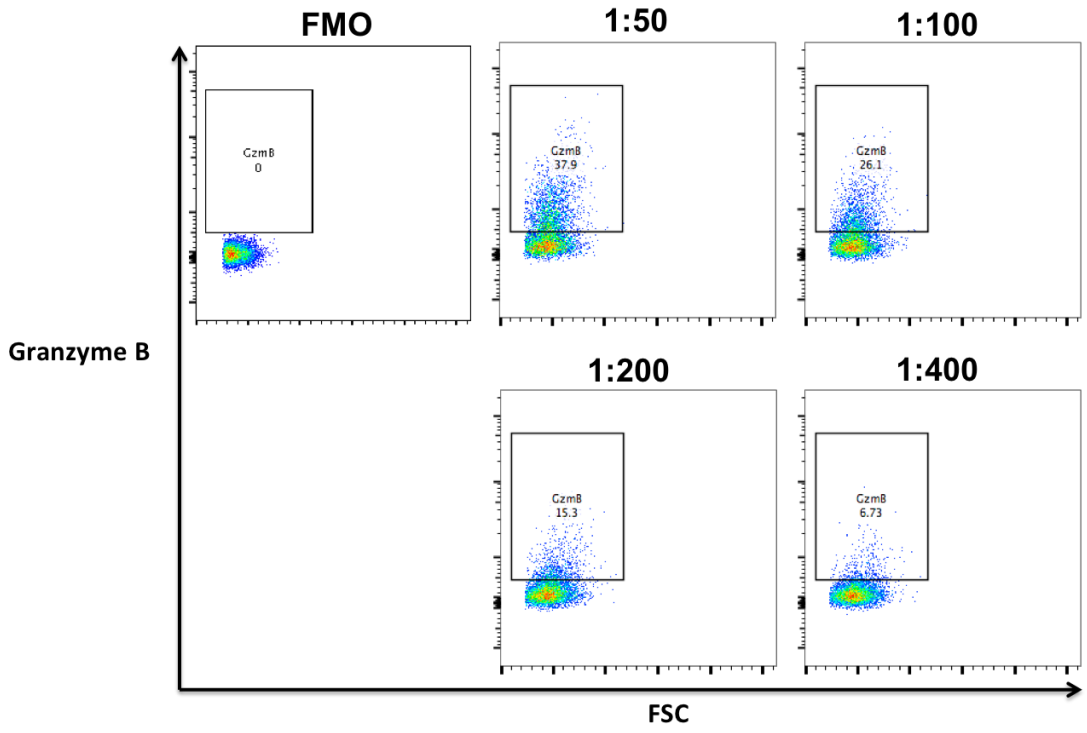

Figure 3-8 Granzyme B detected using different concentration of fluorochrome-conjugated anti-human antibodies. BALB/c mice were vaccinated with intradermal BCG and boosted with intranasal ChAdOx1.85A 10 weeks post BCG prime. Lungs were harvested and processed to obtain single cell suspension. Lung cells were stimulated with Ag85A peptide for 6 hours. The stimulated cells were surfacely stained with live/dead, CD3 and CD8 before intracellularly stained with fluorochrome-conjugated anti-human granzyme B. 1:50, 1:100, 1:200 and 1:400 dilutions of the antibody were tested and analysed using flow cryometry, gated on CD3, CD8 and granzyme B. The anti-human granzyme B was not added to a sample to be used as an FMO.

II. Combination of Granzyme B and CD107a intracellular staining

CD107 is characterised as a marker of cytotoxic T cells [199]. Several studies have combined CD107a with granzyme to analyse cytotoxic cytokine production to increase the specificity of the staining [198, 199, 200, 201].

To examine the cross-reactivity of anti-human granzyme B in mice, lungs were collected from BCG-ChAdOx1.85A vaccinated mice and naïve mice. The lung cells were stimulated with Ag85A and/or incubated together with fluorochrome-conjugated anti-mouse CD107a for 6 hours to obtain optimal staining. The stimulating antigen and antibodies were not added in the unstimulated samples. The cells were stained with surface T cell markers and fluorochrome conjugated anti-human granzyme B.

There was a very low background response in naïve sample incubated with media (Figure 3-9 Top Left plot). Without Ag85A stimulation, 42 % of granzyme B production from $CD8^+$ T cells were observed in BCG-ChAdOx1.85A samples (Figure 3-9 Top Right plot). The response was slightly decreased after stimulation with Ag85A (Figure 3-9 Middle and Bottom Right). 30 % of the granzyme B producing $CD8^+$ T cells also expressed CD107a (Figure 3-9 Bottom Right). Combining CD107a with the intracellular staining for granzyme B did not increase the detection or the specificity of granzyme B production (Figure 3-9 Middle and Bottom Right). Thus, I have decided that inclusion of CD107a staining was unnecessary for future experiments.

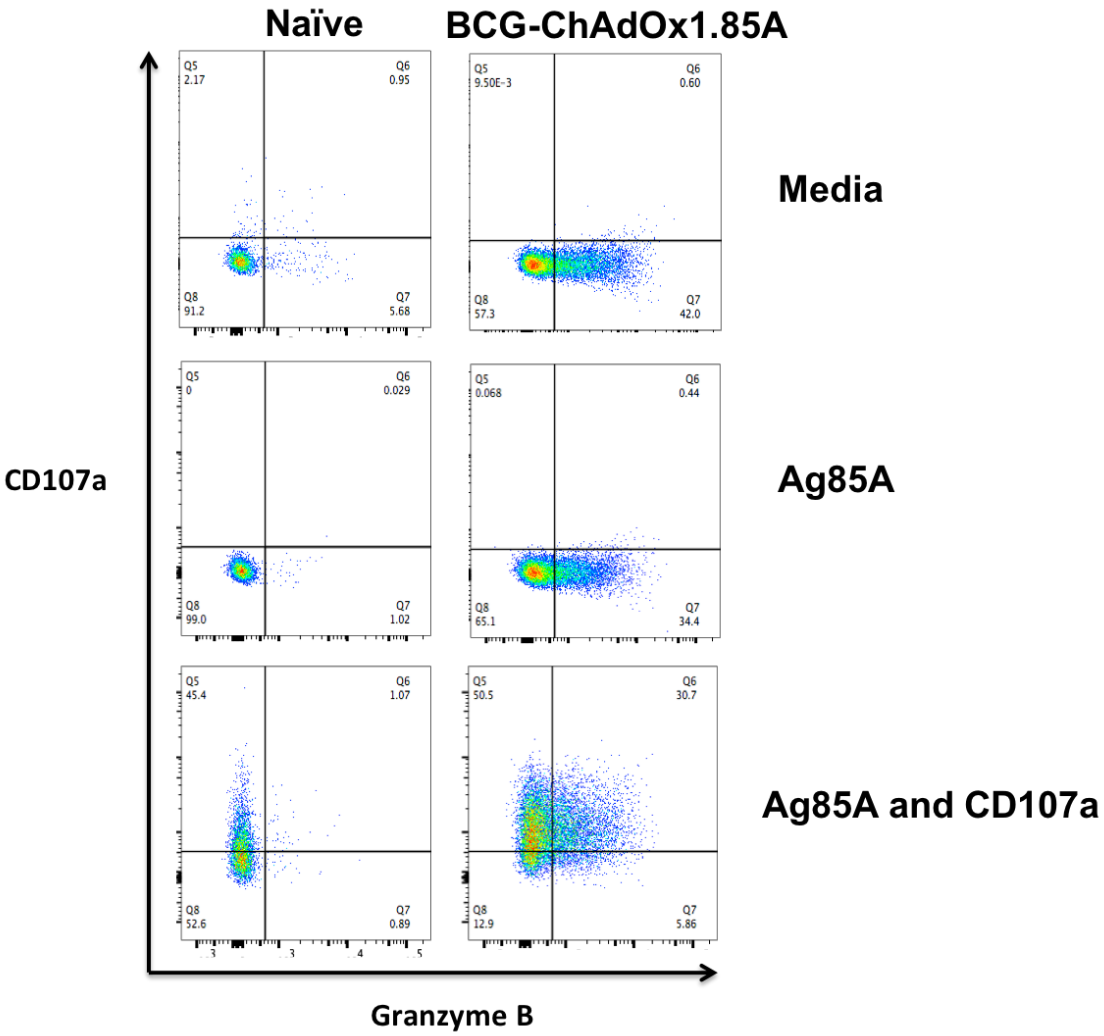

Figure 3-9 Intracellular staining using a combination of anti-human granzyme B and anti-CD107a. BALB/c mice were vaccinated with intradermal BCG and boosted with intranasal ChAdOx1.85A 10 weeks post BCG prime. Lungs form naïve and vaccinated mice were harvested and processed to obtain single cell suspension. Lung cells were stimulated with Ag85A peptide for 6 hours. Fluorochrome-conjugated anti-CD107a was incubated with the cells during the stimulation. The stimulated cells were surfacely stained with live/dead, CD3 and CD8 before intracellularly stained with fluorochrome-conjugated anti-human granzyme B. The stained cells were analysed using flow cryometry, gated on CD3, CD8, CD107a and granzyme B.

III. Measuring $CD8^+$ cytokine cytotoxic production in the lungs and spleen of B-C-M vaccinated and control mice

Cytotoxic cytokine producing $CD8^+$ T cells were observed after viral and *M.tb* infection in several studies [45, 47, 191, 197, 198]. In this chapter, BCG vaccination failed to induce perforin and granzyme B production compared to naïve controls (Figure 3-10 A and B). ChAdOx1.85A boost significantly enhanced Ag85A-specific perforin producing $CD8^+$ T cells in the lungs at 4 weeks post vaccination (B-C4) compared to BCG alone ($p=0.0045$) but the response was not significant at 8 weeks post vaccination (B-C8) (Figure 3-10 A). MVA85A could not increase the responses further, showing comparable responses in the lungs of B-C-Mid with the B-C8 and B-C4 groups (Figure 3-10 A). The PPD-specific responses were low compared to Ag85A stimulation. BCG also failed to improve PPD-specific perforin producing $CD8^+$ T cells but they were increased at 4 weeks post ChAdOx1.85A boost compared to naïve mice (Figure 3-10 A).

Stimulation with Ag85A induced granzyme B responses in the lungs of BCG vaccinated mice (Figure 3-10 B). The responses were significantly enhanced after 4 weeks of ChAdOx1.85A intranasal boost (B-C4) compared to BCG alone ($p=0.0339$) (Figure 3-10 B). At 8 weeks post ChAdOx1.85A boost, the response was lower compared to 4 weeks post B-C vaccination but boosting B-C4 mice with MVA85A intradermally could maintain granzyme B production. Ag85A-specific granzyme B secreting $CD8^+$ T cells in the lungs of B-C-Mid mice were comparable with the B-C4 group but significantly increased compared with naïve animals ($p=0.0084$) (Figure 3-10 B). In PPD stimulation, BCG failed to enhance granzyme B production. Low responses were detected in B-C4

and B-C-Mid vaccinated groups but the responses were not significant compared to BCG and naïve controls (Figure 3-10 B).

Very low production of perforin and granzyme B was observed in the spleen (data not shown).

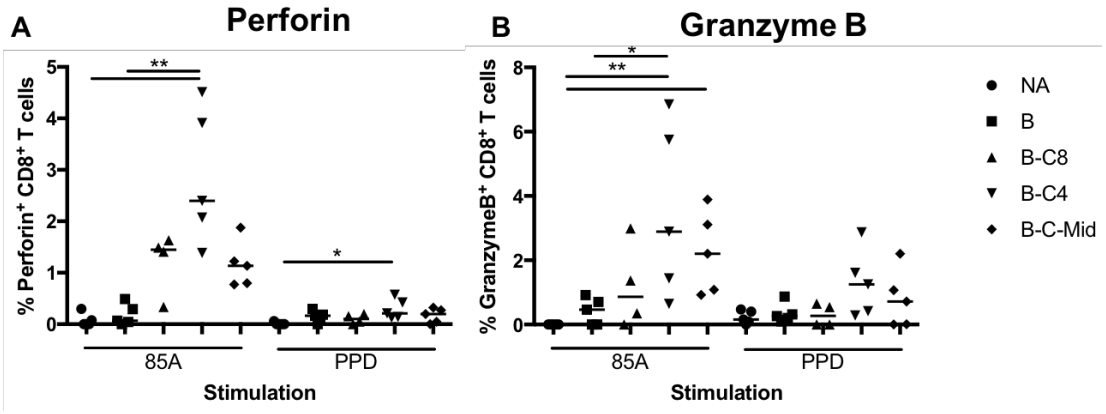

Figure 3-10 Cytotoxic CD8$^+$ T cell responses in lungs of naïve and vaccinated mice measured with high concentration of antibodies. BALB/c mice were vaccinated as shown in Figure 3-1. Lungs were harvested and processed into a single cell suspension. Lung cells were stimulated with Ag85A peptide. Percentage of lung CD8$^+$ T cells expressing perforin (A) and granzyme B (B). The experiment was repeated twice with similar results. Each symbol represents one animal and the line is the median of each group (n=4-5 mice). Statistical significance was determined using Kruskal-Wallis test with Dunn's multiple comparisons test. *, p≤0.05; **, p≤0.01.

A separate experiment was set up investigate granzyme B production using the anti-human granzyme B antibody, previously shown to provide superior staining compared to the mouse antibody. Although the experimental setting was similar to the published B-C-M study [98], responses were measured 8 weeks, rather than at 4 weeks post vaccination as shown in Figure 3-12. This was due to difficulties in granzyme B staining and therefore the harvest timepoint was delayed. The efficacy of B-C-M, 8 weeks post vaccination is shown at the end of this chapter (Figure 3-16).

BCG vaccination did not induce granzyme B production in $CD8^+$ T cells. Boosting with ChAdOx1.85A, significantly increased granzyme B-producing $CD8^+$ T cells in the lung of B-C vaccinated mice compared to naïve mice (p=0.0230) (Figure 3-11 A). MVA85A failed to further enhance the cytokine production, resulting in comparable responses between B-C, B-C-Mid and B-C-Min groups (Figure 3-11 A). B-C-Mid and B-C-Min provided significant expansion of the granzyme B producing $CD8^+$ T cells compared to naïve mice (p=0667 and p=0.0004 respectively) (Figure 3-11 A). B-C-Min mice had better granzyme B production compared to BCG alone (p=0.00095) (Figure 3-11 A).

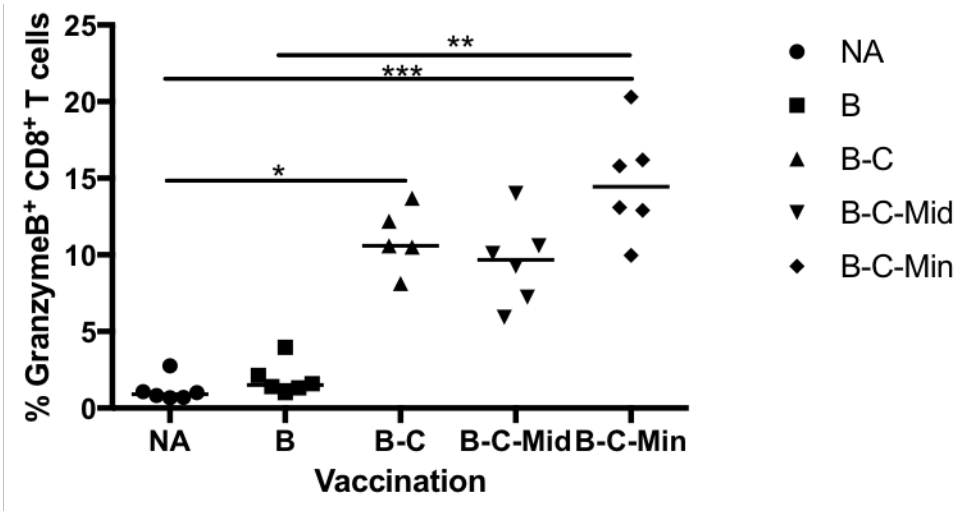

Figure 3-11 Granzyme B producing CD8$^+$ T cells following B-C-M vaccination measured with anti-human granzyme B. BALB/c mice were vaccinated intradermally (i.d.) with 4x10^5 CFU of BCG Pasteur (B) and boosted 10 weeks later with 1x10^8 ifu of ChAdOx1.85A (B), intranasally (i.n.). Four weeks after ChAdOx1.85A vaccination, intradermal (Mid) or intranasal (Min) boost of MVA85A was administered at a dose of 5x10^6 pfu. Lungs were harvested 8 weeks after the last vaccination and processed to obtain a single cell suspension. Cells were surface stained with live/dead, CD3 and CD8 before intracellularly stained with fluorochrome-conjugated anti-human granzyme B. The stained cells were analysed using flow cryometry, gated on CD3, CD8 and granzyme B.

3.2.2 Antibody responses induced by B-C-M regimen in the airways and circulation

Antibodies may contribute to protection against *M.tb,* particularly when induced mucosally [71, 164]. The B-C-Min regimen, where MVA85A was delivered intranasally, is also protective against *M.tb* challenge, although not more so than the B-C-Mid regimen [98]. To investigate whether antibody responses correlate with protection, a similar experiment to the effector T cell study reported above was conducted but the B-C-Min regimen was included to study the local immunity induced by intranasal MVA vaccination (Figure 3-12). The B-C8 group was excluded from this study due to the large number of animals required for this experiment.

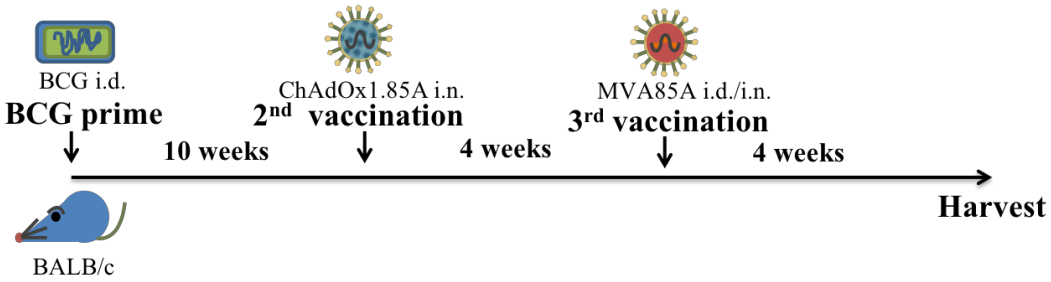

NA:	No vaccination----------18wks----------->Harvest
B:	BCG----------18wks ----------->Harvest
B-C:	BCG----------10wks----------->ChAdOx1.85A-----4wks---->Harvest
B-C-Mid:	BCG----10wks-----> ChAdOx1.85A--4wks--->MVA85Aid---------4wks---->Harvest
B-C-Min:	BCG----10wks-----> ChAdOx1.85A--4wks--->MVA85Ain---------4wks---->Harvest

Figure 3-12 Timeline of B-C-M vaccination and control groups for antibody studies. BALB/c were vaccinated intradermally with BCG (B), followed by intranasal vaccination with ChAOx1.85A (C). MVA85A was delivered either via the intradermal (Mid) or intranasal (Min) route. Differences in antibody responses were evaluated in BAL fluid and serum of vaccinated mice and control groups, at 4 weeks post last vaccination.

3.2.2.1 Antigen-specific IgG responses in the circulation of B-C-M vaccinated and control mice

In the serum of B-C-Mid and B-C-Min vaccinated mice, there was a significantly higher level of Ag85A-specific total IgG compared to the BCG control (p=0.0023 and 0.0042 respectively) (Figure 3-13 A and C). IgG responses were also higher in the serum of B-C immunised mice compared to BCG mice, but the difference was not statistically significant (Figure 3-13 A and C). Boosting with i.d. or i.n. MVA85A failed to enhance the IgG responses, resulting in a comparable level in the serum of B-C, B-C-Mid and (B-C-Min) groups (Figure 3-13 C). There were no detectable Ag85A-specific IgG in the serum of BCG immunised mice (Figure 3-13 A and C).

PPD-specific IgG was observed in the serum of all immunised groups that received BCG (Figure 3-13 B). Boosting BCG with the viral vector vaccines did not enhance these responses (Figure 3-13 D). These PPD-specific IgG responses were not statistically significant compared to unvaccinated group, which had a high background (Figure 3-13 D).

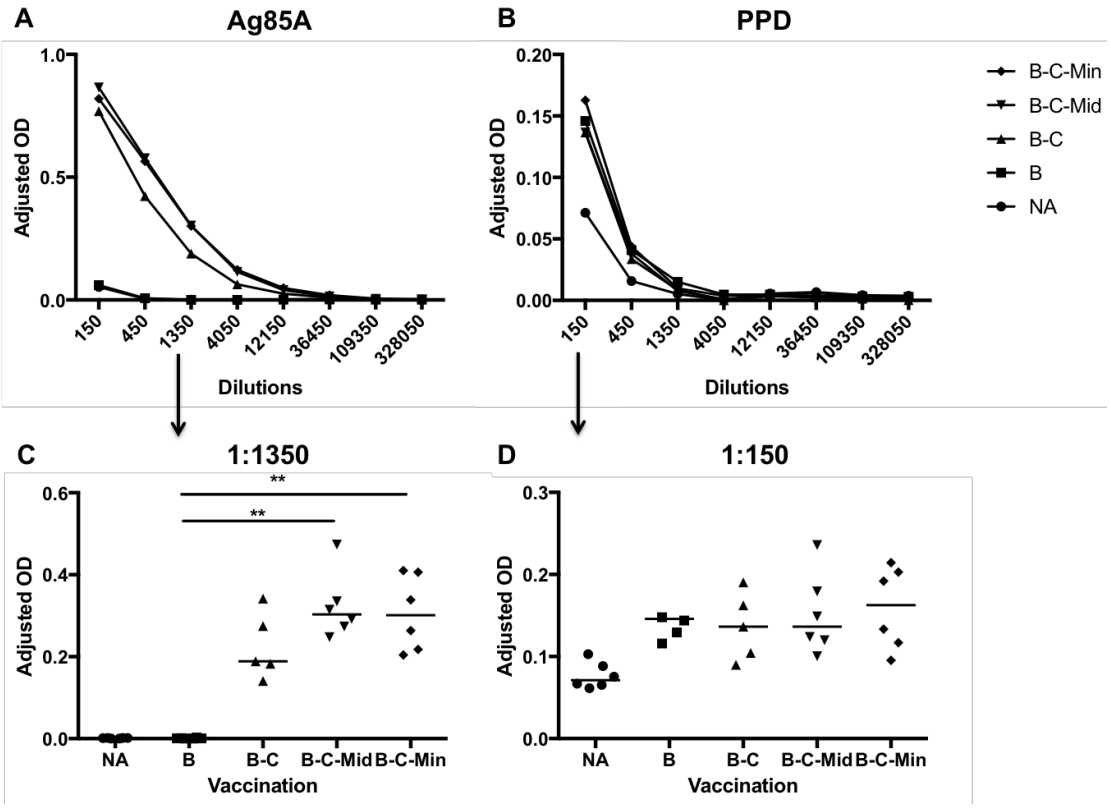

Figure 3-13 Total IgG responses induced by B-C-M vaccination in the circulation. Mice were vaccinated as shown in Figure 3-12. Blood samples were collected and spun to obtain the serum. (A) Ag85A-specific total IgG and (B) PPD-specific total IgG in serum were measured using ELISA. The top two graphs are presented as serial dilutions. (C) 1:1350 dilution was selected to represent Ag85A-specific total IgG while 1:150 dilution was used for PPD-specific total IgG. Each symbol represents one animal and the line is the median of each group (n=4-6 mice). Statistical significance was determined using Kruskal-Wallis test with Dunn's multiple comparisons test. ** p≤0.01.

3.2.2.2 Antigen-specific IgA responses in the airways of B-C-M vaccinated and control mice

In the airways, a significant increase in Ag85A-specific IgA production was observed in B-C and B-C-Min immunised mice compared to BCG mice (p= 0.0117 and 0.0015 respectively) (Figure 3-14 A and C). An intradermal boost with MVA85A failed to maintain Ag85A-specific IgA secretions, resulting in a trend for lower antibodies in the airways of B-C-Mid compared to B-C-Min immunised mice (Figure 3-14 C). No Ag85A-specific IgA was detected in the BAL fluid of BCG vaccinated mice (Figure 3-14 C). Higher levels of PPD-specific IgA were detected in the airways of B-C-Min vaccinated mice compared to the other groups (Figure 3-14 B and D). B-C-Min mice had significantly higher IgA compared to BCG vaccinated mice (Figure 3-14 D) (p=0.0004). There was no detectable IgA, even when the undiluted serum samples of BCG vaccinated mice were analysed (Figure 3-14 D).

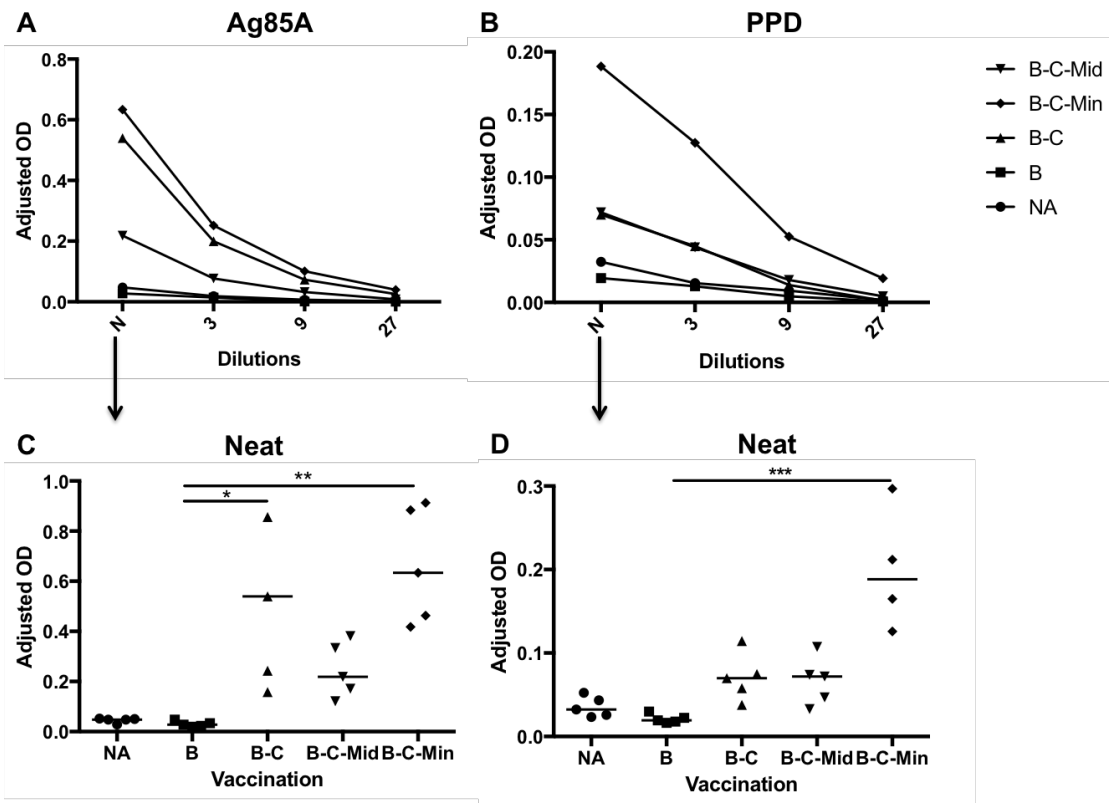

Figure 3-14 IgA responses induced by B-C-M vaccination in the airways. BAL samples were collected and spun to obtain the BAL supernatant. (A) Ag85A-specific IgA and (B) PPD-specific IgA were measured using ELISA. The top two graphs are presented as serial dilutions. Bottom two graphs are (C) Ag85A-specific IgA and (D) PPD-specific IgA in neat (N) samples. Each symbol represents one animal and the line is the median of each group (n=4-6 mice). Statistical significance was determined using Kruskal-Wallis test with Dunn's multiple comparisons test. *, p≤0.05; **, p≤0.01; ***, p≤0.001.

3.2.3 Evaluation of the durability of protection provided by the B-C-M regimen

The B-C-M vaccination regimen was shown to provide superior protection to BCG at 4 weeks post vaccination. To investigate the durability of this protection, mice were vaccinated and challenged as shown in Figure 3-15. Animals were challenged with 50-100 CFU of aerosol *M.tb* Erdman at 8 and 20 weeks post vaccination. Four weeks after the challenge, lungs were removed and analysed to obtain bacterial CFU counts.

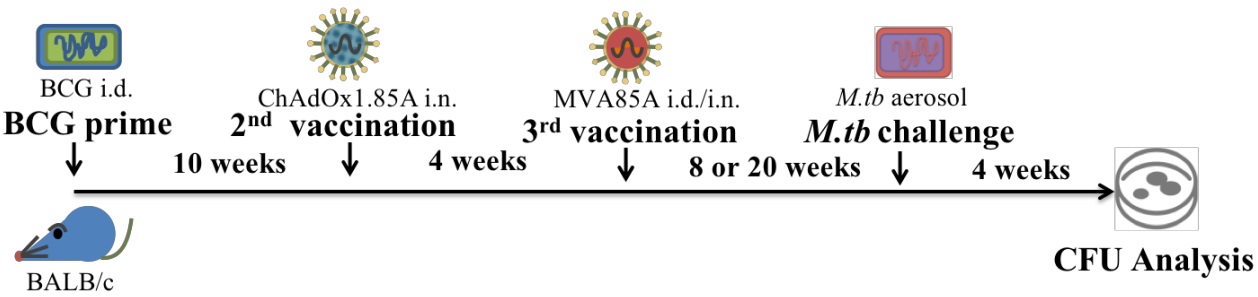

NA:	No vaccination----------22 or 34wks----------*M.tb*--->Harvest
B:	BCG---------- ----------22 or 34wks ----------*M.tb*--->Harvest
B-C:	BCG---10wks---> ChAdOx1.85A----------12 or 24wks---*M.tb*--->Harvest
B-C-Mid:	BCG---10wks---> ChAdOx1.85A--4wks-->MVA85Aid---8 or 20wks---*M.tb*--->Harvest
B-C-Min:	BCG---10wks---> ChAdOx1.85A--4wks-->MVA85Ain---8 or 20wks---*M.tb*--->Harvest

Figure 3-15 Timeline of B-C-M vaccination and *M.tb* challenge. BALB/c mice were vaccinated intradermally (i.d.) with $4x10^5$ CFU of BCG Pasteur (B) and boosted 10 weeks later with $1x10^8$ ifu of ChAdOx1.85A (B), intranasally (i.n.). Four weeks after ChAdOx1.vaccination, intradermal (Mid) or intranasal (Min) boost of MVA85A was administered at a dose of $5x10^6$ pfu. Animals were challenged with 50-100 CFU of aerosol *M.tb* Erdman, 8 or 20 weeks after the last vaccination. Four weeks after challenge, lungs and spleen were harvested for CFU enumeration.

3.2.3.1 Protection against aerosol *M.tb* challenge in mice 8 weeks after B-C-M vaccination

At 8 weeks post vaccination, BCG vaccinated mice had a significantly lower lung CFU compared to unvaccinated mice (p=0.0059) (Figure 3-16 A). ChAdOx1.85A (B-C) failed to further improve protection. A further boost with i.d. MVA85A (B-C-Mid) resulted in significant improvement compared to the BCG control group (p=0.0447) (Figure 3-16 A). In B-C-Min vaccinated mice, there was also a decrease in CFU compared to the BCG group, with the difference almost approaching statistical significance (p=0.0513) (Figure 3-16 A).

In the spleen, BCG was still significantly protective compared to naïve mice (p=0.0006) (Figure 3-16 B). ChAdOx1.85A did not enhance the protection compared to BCG alone (Figure 3-16 B). Unlike in the lungs, intradermal and intranasal MVA85A failed to further improve BCG protection in the spleen (Figure 3-16 B).

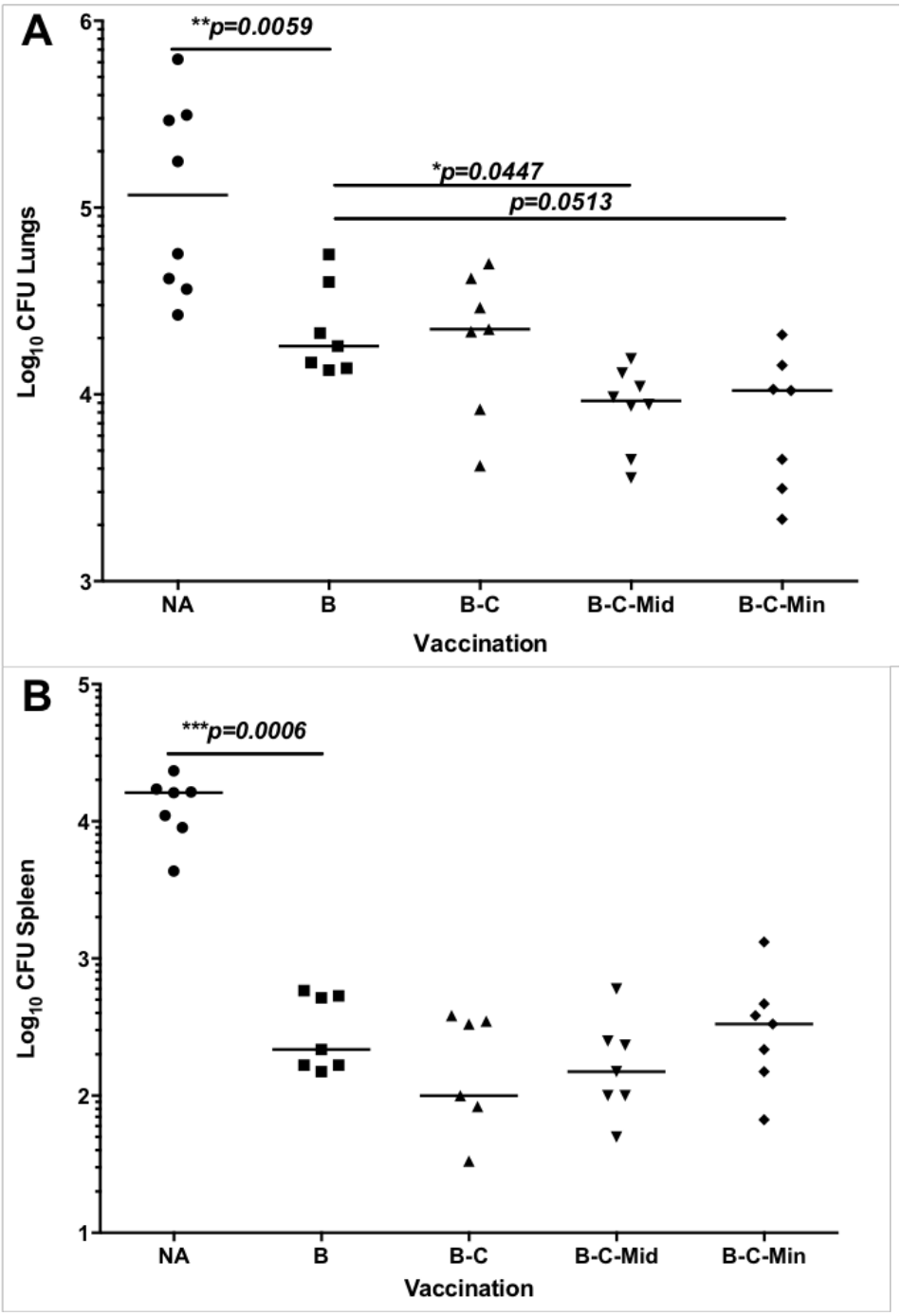

Figure 3-16 Protective efficacy of B-C-M, 8 weeks post vaccination in the lungs and spleen of naïve and vaccinated mice. BALB/c mice were immunised as per Figure 3-15. *M.tb* challenge was performed 8 weeks post vaccination. Lungs (A) and spleen (B) were analysed for bacterial colony enumeration. Each symbol represents one animal and the line is the median of each group (n=6-8 mice). Statistical significance was determined using Kruskal-Wallis test with Dunn's multiple comparisons test. *, p≤0.05; **, p≤0.01; ***, p≤0.001.

3.2.3.2 Protection against aerosol *M.tb* challenge in mice 20 weeks after B-C-M vaccination

20 weeks post-immunisation, BCG was still protective in the lungs (p=0.0004) (Figure 3-17 A). B-C, B-C-Mid and B-C-Min all provided some degree of protection but were not significantly better when compared to BCG alone (Figure 3-17 A).

Similar results were observed in the spleen, in that BCG significantly reduced bacterial CFU compared to naïve mice (p=0.0003) (Figure 3-17 B). B-C, B-C-Mid and B-C-Min provided comparable protection with BCG vaccination (Figure 3-17 B).

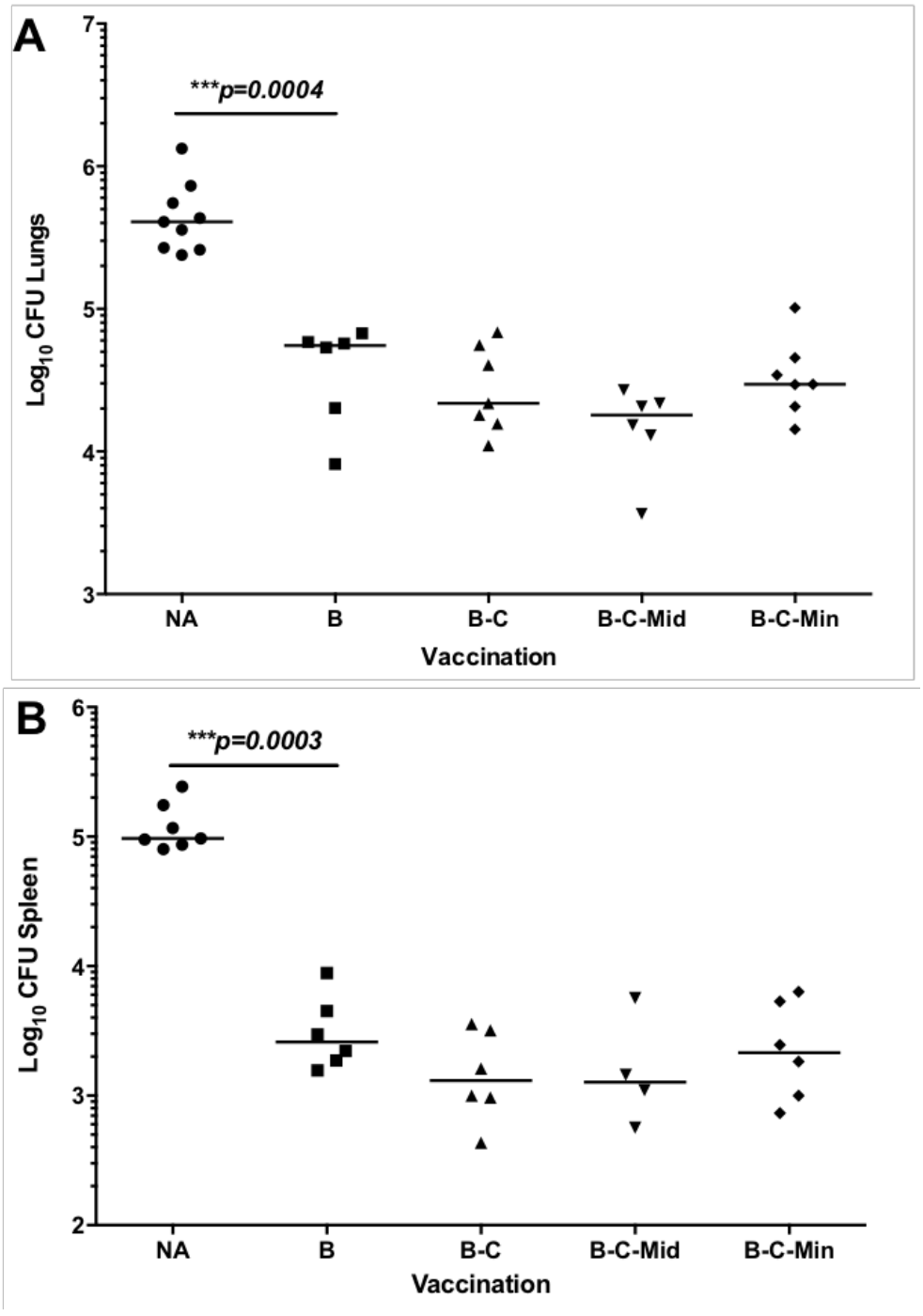

Figure 3-17 Protective efficacy of B-C-M, 20 weeks post vaccination in lungs and spleen of naïve and vaccinated mice. BALB/c mice were vaccinated as per Figure 3-15. *M.tb* challenge was performed 20 weeks post vaccination. Lungs (A) and spleen (B) were harvested for CFU enumeration. Each symbol represents one animal and the line is the median of each group (n=4-9 mice). Statistical significance was determined using Kruskal-Wallis test with Dunn's multiple comparisons test. ***, p≤0.001.

3.3 **Discussion**

One of the aims of the work presented in this chapter was to identify immune responses that correlate with the protective efficacy of the BCG-ChAdOx1.85A-MVA85A regimen. Finding a definite correlation could be a key success to vaccine development as it would help to predict vaccine efficacy against *M.tb* infection, saving time and costs involved in vaccine research and development. In this chapter, immune responses induced by vaccination regimens that have been previously associated with *M.tb* protection were analysed.

IFN-γ and TNF-α play an important role in protection against TB in both human and murine models. The induction of IFN-γ and TNF-α is a necessary requirement for vaccine candidates. Viral vector and protein subunit vaccines have been shown to induce IFN-γ and TNF-α releasing $CD4^+$ and $CD8^+$ T cells [91, 121, 202]. Unlike B-C, the B-C-M regimen significantly improved protection afforded by BCG alone [98]. To identify immune responses that correlate with protection, an effector T cell flow panel was developed to study IFN-γ and TNF-α responses (Figure 3-1) (Appendix Table 7-1). Cytokine-producing $CD4^+$ and $CD8^+$ T cells were significantly increased in the lungs and spleen of B-C-M mice compared to BCG and BC8 control groups (Figure 3-2 and Figure 3-3). These data are in agreement with previously published immunogenicity data using this regimen [98]. Consistent with a recent study, boosting BCG with ChAdOx1 expressing PPE15, a novel protective antigen, enhanced effector cytokine responses [121]. ChAdOx1 expressing Ag85A or PPE15 both were able to induce high responses of IFN-γ and TNF-α production [98, 121]. The cytokine production induced by BCG-ChAdOx1.85A may provide a component of a protective response. However, only BCG-

ChAdOx1.PPE15, but not BCG-ChAdOx1.85A improved BCG protection [98, 121]. This may be because PPE15 was more immunogenic compared to Ag85A, boosting both $CD4^+$ and $CD8^+$ T cells primed by BCG. Perhaps this is because ChAdOx1.85A boosted mainly $CD8^+$ responses and the MVA85A boost was required to help to enhance $CD4^+$ responses in order to obtain better BCG protection [82, 84, 99]. In BCG primed mice, boosting with the recombinant viral vaccine vesicular stomatitis virus (VSV)-846 elicited T cell mediated immune responses, showing a significant increase in IFN-γ production of $CD4^+$ T cells and consequently improving BCG protection at six weeks post VSV boost [85]. This is consistent with our finding that heterologous boosting with the viral vector vaccines enhanced cytokine production and improved BCG protective efficacy. Mucosal vaccination with Sendi virus (SeV85AB) provided greater induction of $CD8^+$ $cytokine^+$ effector T cells, including IFN-γ, TNF-α and IL-2, compared to BCG immunised mice [89]. Boosting BCG with SeV85AB, resulted in an improved BCG protection against *M.tb* challenge [89].This result confirms that BCG prime-viral vector boost regimens have been shown to be consistently protective in TB vaccine studies.

A replicate experiment was set up to assess the effect of a BCG prime to the regimen (Figure 3-4). Interestingly, while effector cytokine producing $CD8^+$ T cells were increased in the lungs of the B-C-Mid, compared to B-C8 group, (Figure 3-3 A and B), the responses were comparable between C-M and C8 (Figure 3-6 A and B). This finding suggests that in the absence of a BCG prime, MVA85A fails to enhance cytokine secreting $CD8^+$ T cells in the lungs. This could be explained by MVA85A boosting T cell responses already primed by BCG, and that BCG alone is a poor inducer of $CD8^+$ T cells. A similar finding has been reported showing a very weak response of $CD8^+$ T cells

induced by MVA85A in humans [203]. This could be due to the inability to induce strong $CD8^+$ responses but consistently induced $CD4^+$ responses of MVA85A [95, 204]. Modest antigen-specific $CD4^+$ T cells were observed in the circulation of BCG vaccinated infants boosted with intradermal MVA85A [95]. Mucosal delivery of MVA85A in BCG vaccinated adults also enhanced airway antigen-specific $CD4^+$ T cells compared to the intradermal group [204]. Therefore, combining MVA with ChAdOx1, which induces strong CD8 responses, may both enhance immune response and improve protection [84, 100]. The combination of chimpanzee adenovirus-MVA immunisation has been shown to immunogenic and protective against infectious diseases in clinical trials, inducing high $CD8^+$ and $CD4^+$ T cells responses [77, 78, 205, 206].

In *M.tb* infection, the impairments of perforin and granzyme B production have been reported in several studies in both humans and mice [195, 207, 208, 209], suggesting that the cytotoxic cytokines do not play a key role in controlling *M.tb* infection and the bacteria might use this as an immune evasion to compromise host immune responses. However, a few studies have shown the killing and protective functions of perforin in mice [45, 190]. Thus, the knowledge on cytotoxic cytokine responses in TB vaccines are still unclear and required further evaluations. Interestingly, perforin and granzyme B containing $CD8^+$ T cells were enhanced after boosting BCG with ChAdOx1.85A (Figure 3-10). In agreement, granzyme B production of cytotoxic T cells was observed after influenza vaccination in older adults [210]. However, no data has been reported on cytotoxic cytokine production in a TB vaccine research field. Chan *et al.* have observed perforin granules, but not granzyme B, in the effector $CD8^+$ T lymphocytes of CMV-seropositive rhesus macaques [201]. A CMV-based TB vaccine showed protection against

M.tb infection in rhesus macaques [92]. Taken together, CMV vector vaccine expressing *M.tb* antigens provided protection could result in part from the induction of perforin, which is consistent with our finding that perforin production was increased after B-C and B-C-M vaccination. However, the lack of the granzyme B secretion in macaques could not be directly compared with mice but the cytotoxic activity of granzyme B may be compensated with perforin cytotoxicity and overpowered from effector cytokines. However, the perforin and granzyme B responses observed in B-C and B-C-M groups were comparable, meaning MVA85A could not improve the cytotoxic cytokine production further (Figure 3-10). Therefore, these responses were not a correlate of protection in mice.

Antibodies may have a potential role in protection against *M.tb,* particularly when induced mucosally [71, 150, 159, 160, 164]. B-C-Mid and B-C-Min were both included in the antibody studies in order to further discriminate mucosal versus systemic responses induced by MVA85A (Figure 3-12). Intranasal ChAdOx1.85A vaccination induced Ag85A-specfic IgG responses which were improved after either Mid or Min boost (Figure 3-13 A and C). In RSV vaccines, an intranasal prime with PabAd3 followed by an intramuscular boost with MVA increased antigen-specific IgG titre in the serum of CD1 mice compared to mice received both vaccines systemically [211]. These results suggest that MVA may improve specific IgG responses in the circulation of adenovirus primed mice, when the adeno-prime is delivered mucosally. In Lentiviral vector expressing Ag85A-E6, the immunised mice had higher levels of antigen-specific IgG in the serum compared with the serum of BCG vaccinated mice [90]. In BCG primed mice, intranasal vaccination of *M.tb* antigen-coated bacterial spores or antigen-coated

nanoparticles enhanced antigen-specific IgG responses in the sera and IgA responses in the BAL, resulting in a reduction of bacterial CFU following *M.tb* challenge [161, 162]. In the later study, BCG alone failed to induce the antibody production in the circulation and the airways [162], which is consistent with our finding that BCG induces very low Ag85A-specific IgG responses despite high PPD-specific IgG (Figure 3-13 B and D). PPD extracted from *M.tb* contained more than 695 unique peptides [212]. Among 256 different proteins of *M.tb* PPD, 80 were shared with *Mycobacterium bovis (M.bovis)* PPD which would reflect BCG specific responses [212]. That could explain why we observed strong PPD-specific antibody responses in BCG vaccinated samples but not Ag85A-specific antibodies in the circulation (Figure 3-13). Interestingly, only mucosal MVA vaccination maintained the secretion of Ag85A-specifc IgA in the airways (Figure 3-14 A and C). Intranasal MVA in B-C-Min regimen not only sustained Ag85A-specific IgA secretion, but also improved the production of PPD-specific IgA further from BCG alone (Figure 3-14 A-D). This result confirms that mucosal vaccination enhance antibody responses in the airways against *M.tb* as has been reported previously in murine and NHP studies [71, 72, 164].

In conclusion, the protective regimen, B-C-Mid, is able to induce strong $CD4^+$ and $CD8^+$ T cell responses which have been previously shown to be associated with protection. The regimen enhanced the production of effector and cytotoxic cytokines as well as antibody responses both in the lungs and systemic. However, B-C4 which does not improve BCG protection elicited similar responses to B-C-Mid. That means although these immune responses play a substantial role in conferring protection against *M.tb,* they do not directly corelate with the protection observed by the B-C-M regimen.

The longevity of the protective efficacy of B-C-M was investigated at 8 and 20 weeks post immunisation. Protection provided by the B-C-M regimen was superior over BCG alone, 8 weeks post vaccination. This vaccine regimen was still protective at 20 weeks post vaccination but was not statistically significantly better compared to BCG alone (Figure 3-16 and Figure 3-17). *M.tb* challenge in both experiments was conducted using the same protocol and same dilution of bacteria given into the mice. However, the studies were performed separately, resulting in the level of infection in the 20-week experiment being half a log higher in the lungs of naïve controls (log_{10} 6 CFU) compared to the 8-week experiment (log_{10} 5.5 CFU). This could explain the loss of protection observed at 20-week timepoint because higher bacterial infection could minimise the chance to see the differences between the vaccine regimens [213, 214].

Previous studies have reported that BCG was recovered from the lungs of vaccinated mice, more than two months after intratracheal immunisation [215]. The protective effect of BCG was still observed at 10 months post vaccination [216]. Consistent with our finding that the protection of BCG was still observed at 8 week and 20 weeks after vaccination (Figure 3-16 and Figure 3-17). Mainly memory $CD4^+$ T cells were primed by BCG and remained in the circulation and in the airways [217]. ChAdOx1.85A initiated potent both $CD4^+$ and $CD8^+$ immune responses [84, 98]. Even though effector cytokines and antibody production were enhanced after the boost, this did not result in an improvement of protection. Interestingly, a second boost with i.d. or i.n. MVA85A provided superior protection in the B-C-M mice compared to BCG alone at 4 and 8 weeks post immunisation. Unlike BCG, the ChAdOx1 and MVA viruses do not persist in mouse lungs as they are replication deficient [82, 84]. In cotton rats, MVA could not be

detected in lungs five days after intranasal vaccination [218]. However, the immunogenicity of MVA expressing Ag85A has been observed in animals and humans to enhances long term Th1 responses [82]. MVA could boost T cell responses primed by BCG-ChAdOx1 further, inducing the memory cells to remain staying in pulmonary and circulatory systems. The loss of protection may be explained by a reduction of vaccine immunogenicity. This data leads to the aims of next chapter to examine immune responses induced by B-C-M regimen at 4, 8 and 20 weeks post vaccination and identify immune correlates of protection.

Chapter 4. Development of resident memory T cells in the pulmonary system following B-C-M regimen

4.1 **Introduction**

Memory immune responses are the hallmark of adaptive immunity. Vaccines are able to induce long-lived memory cell repertoires, which are specific to their cognate antigen/s. Memory immunity responds rapidly and effectively compared to innate immunity, providing optimal control of pre-exposed diseases [125, 126].

Even though $CD4^+$ T cells are recognised to play an important role in the control of *M.tb* infection, much less is known about memory $CD4^+$ T cells, unlike memory $CD8^+$ T cells. The understanding of memory T cells was established in the field of acute viral studies where memory $CD8^+$ T cells overpower the responses of memory $CD4^+$ T cells [127, 128, 129]. Until recently, the lack of effective MHC class II tetramers made the phenotypic evaluation of the specificity of memory $CD4^+$ T cells more difficult [130].

Two distinct memory T cell populations have been proposed since 1999. They were classified by effector function, proliferation and location [131]. Located in the lymphoid organs, central memory T cells (T_{CM}) express CD62L on their surface. In contrast, effector memory T cells (T_{EM}) produce abundant effector cytokines but have no expression of CD62L, allowing them to recirculate between the vasculature and peripheral tissues [131].

A new population of memory cells has been recently characterised. These cells are named tissue resident memory T cells (T_{RM}), after their ability to stay in non-lymphoid tissues and the lack of re-recirculation in the vasculature [132]. This cell type has been observed in several organs such as the small intestinal mucosa, brain tissue and lung parenchyma [114, 133, 134]. Lung T_{RM} have been shown to be permanently located at the

infection site and rapidly counteract *M.tb* infection. By secreting some cytokines and chemokines, these resident cells can recruit other immune cells to help against the infection [114, 117, 133, 135, 136].

The main target of vaccines is the induction of memory T cell subsets such as effector memory T cells (T_{EM}) and resident memory T cells (T_{RM}) [137]. In *M.tb* infection and BCG vaccination, T_{EM} (expressing high CD44 and low CD62L) are enhanced in the lungs [140]. T_{RM} are located in barrier surfaces of peripheral tissues and provide a mucosal defence [141]. The expression of CD69 is crucial to retain T_{RM} cells in the peripheral tissues [142]. In mice, $CD4^+$ T_{RM} cells express CD11a, whereas $CD8^+$ T_{RM} cells present CD103 in the lungs [114, 117]. Mucosal vaccination of BCG enhances $CD8^+$ T_{RM} cells expressing CD69 and CD103 [75]. The efficacy of $CD8^+$ T_{RM} against *M.tb* has been determined using cell depletion and adoptive transfer approaches [45, 143, 144].

Recently lung homing markers have been introduced to further discriminate lung parenchymal and intravascular memory T cells. The later T cell population expresses high levels of CX3CR1 and KLRG1 [106, 136]. The expression of KLRG1 is decreased when the effector cells home back to the lungs and become resident memory cells. The absent of KLRG1 together with CXCR3 expression are used to phenotypically identify memory T cells in the lung parenchyma [106]. This population of cells is enhanced after vaccination or *M.tb* infection and has the ability to migrate rapidly back into the parenchyma [106, 145]. Woodworth *et al.* have showed that $CXCR3^+$ $KLRG1^-$ $CD4^+$ T cells induced by a subunit TB vaccine candidate were localised in the lung-vasculature, which may be classified as a circulating population and capable of specifically homing back to the lungs [145]. Lindenstrom *et al.* have shown that IL-2 producing $KLRG1^-$ $CD4^+$

T cells were induced in the draining lymph nodes following a BCG prime-subunit vaccine boost regimen [219]. This population was able to produce effector cytokines and proliferate after *M.tb* challenge at 2-years post vaccination, suggesting the development of central memory T cells which provide long term responses at the site of infection. Jeyanathan *et al.* have performed experiments using an adenovirus-vectored vaccine in BALB/c mice. The authors have identified that the expression of CXCR3 in circulating T cells is crucial for the cells to enter into the lung parenchyma and airways [220]. Perdomo *et al.* have observed that $CD4^+$ and $CD8^+$ T cells in the airways of mucosal BCG vaccinated mice express CXCR3 and display resident memory phenotypes [75]. These airway cells confer protection against *M.tb* when mucosally transferred.

To date in the field of TB vaccines, an adoptive transfer of antigen-specific lung-parenchymal $CD4^+$ T cells has not been done before. Adoptive transfer of antigen-specific lung-vascular $CD4^+$ T cells induced by a subunit vaccine has been conducted by Woodworth *et al.* but the transfer of the lung-parenchymal cells is not reported [145]. This study shows that the lung-vascular cells migrate to the lung-parenchyma, but the protective function against *M.tb* infection is not assessed. Perdomo *et al.* have transferred airway-resident memory $CD4^+$ and $CD8^+$ T cells induced by mucosal BCG vaccination to naïve mice [75]. The airway cells provided protection against *M.tb* infection after mucosal transfer. Adoptive transfer of lung-parenchymal cells was not performed in this study.

The aims of this chapter were;

1. To optimise the intravascular staining technique in order to allow for clear discrimination between lung-vascular and lung-parenchymal populations.
2. To investigate the immunogenicity of the B-C-M regimen focusing on memory T cells to identify immune correlates of protection. To phenotypically characterise these cell populations, intravascular staining techniques were included to identify lung parenchymal T cells expressing memory markers.
3. If the immune correlates of protection are identified, the effector function as well as the protective function would be evaluated by intracellular cytokine staining and adoptive transfer of the relevant cell population.

4.2 **Results**

4.2.1 Optimisation of intravascular staining technique

The discrimination between lung-vascular and lung-parenchymal cells is important to truly identify resident memory cells. A T cell subset localised in the lung tissue and known as T_{RM} may play a critical role in protecting against *M.tb* infection. Lung perfusion is the conventional technique used to remove blood from the lungs. However, the perfusion cannot totally eliminate lung-vascular cells and has been reported to disrupt the structure of the lungs [115]. Recently, an intravascular staining technique has been introduced to clearly separate these two populations [115]. A fluorochrome conjugated antibody is injected intravenously. The antibody travels in the circulation, staining intravascular cells, but cannot access the tissue outside the vessels. Intravascular cells are positively stained with the antibodies, while parenchymal compartment is spared from the staining, resulting in a negative stained population. Two separated populations are obtained after flow cytometric analysis.

The intravascular staining has been widely used to identify lung-tissue resident T cells [106, 115, 117, 120, 121, 145, 217, 221]. To obtain a clear separation between populations and make the protocol reproducible, optimisation experiments were performed to titrate the concentration of the antibody as well as the interval between injection and euthanasia. Lung, BAL and blood samples were collected to prove that the antibody was confined to the lung vasculature but not in the lung parenchymal tissue and the airways.

Lung-parenchymal T cells have been shown to be enhanced after *M.tb* infection [106] and vaccination [121, 145]. A group of mice immunised with B-C-Mid was included as a positive control to validate the technique compared with naïve animals in order to observe differences between these two groups before taking this protocol forward for the remainder of the project.

4.2.1.1 Titration of time between intravenous injection and euthanasia

Woodworth *et al.* has published data on circulating $CD4^+$ T cells induced by subunit vaccines [145]. In this scientific paper, FITC-conjugated anti-CD45.2 (BD Biosciences) was used for intravascular staining at a dose of 2.5 μg per mouse, 3 minutes prior to lung harvest in CB6F1 mice. Therefore, this protocol was adopted for the optimisation.

To optimise the intravascular technique, FITC-conjugated anti-CD45.2, a common lymphocyte marker, was selected. 2.5 μg of the antibody in a volume of 100 μl was injected intravenously in the tail of BALB/c mice. The mice were sacrificed at 1 minute, 3 minutes and 10 minutes after the injection.

The impact of time-length between intravascular injection and sacrifice was compared. At 1-minute post injection, two separated populations were obtained when analysed with flow cytometry. The positive and negative events started merging after 3 minutes and the separation was lost at 10 minutes post injection. Thus, 1 minute was chosen as it showed optimal separation of positively and negatively stained lymphocytes (Figure 4-1).

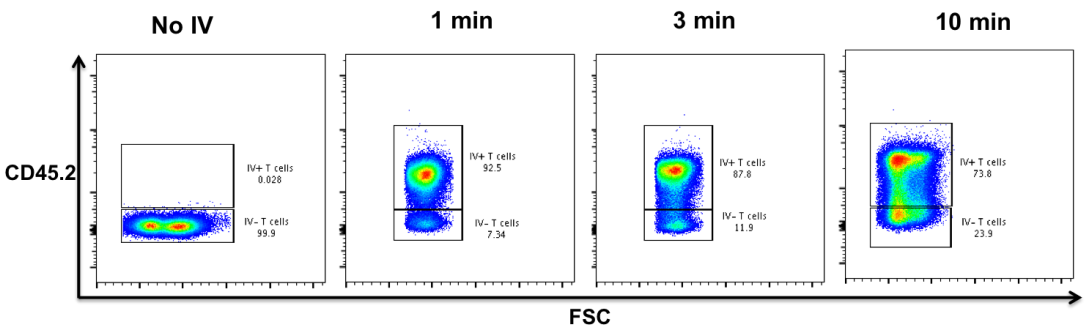

Figure 4-1 Titration of time between intravenous injection and euthanasia. Naïve BALB/c mice were injected intravenously with anti-CD45.2-FITC. A negative control did not receive the injection (No IV). After the injection for 1 minute, 3 minutes and 10 minutes, lung samples were harvested to discriminate lung-parenchymal and lung-vascular lymphocytes.

4.2.1.2 Titration of antibody concentration

In the timing optimisation in 4.2.1.1, anti-CD45.2-FITC was used in a preparation of 100 μl of 25 μg/ml. The optimal discrimination was obtained but the quantity of the antibody could have been used at a lower concentration. The Intravascular staining technique has been performed in our group using PE-conjugated anti-CD45 (eBioscience), 100 μl per animal in a concentration of 6 μg/ml, in BALB/c mice [217]. Concentration of antibody injected was tested of 1 μg/ml, 2 μg/ml, 4 μg/ml, 6 μg/ml and 25 25 μg/ml to find an appropriate concentration for the intravascular staining.

In the negative control, there was no separation observed (Figure 4-2 Top Left). No distinct positive population was detected up to 6 μg/ml concentration (Figure 4-2 Bottom Middle). 25 μg/ml was selected as it consistently provided optimal discrimination between the two populations (Figure 4-2 Bottom Right).

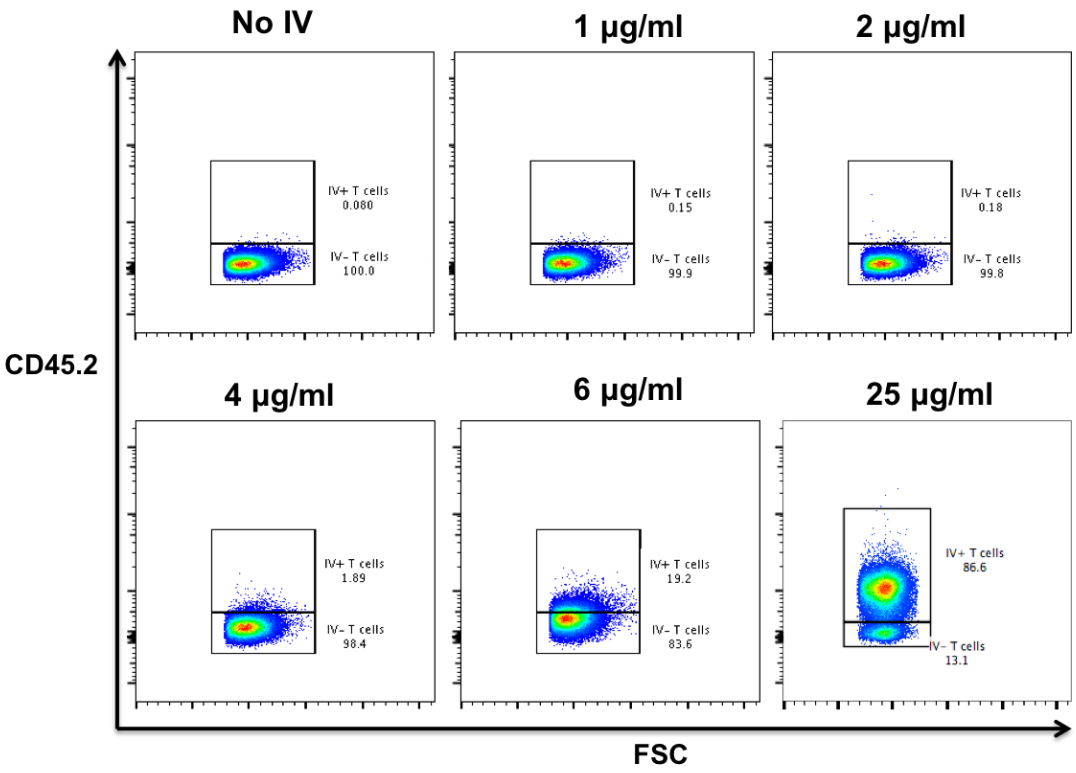

Figure 4-2 Titration of intravascular stain concentration. Naïve BALB/c mice were injected intravenously with anti-CD45.2-FITC before euthanasia to identify lung-parenchymal and lung-vascular lymphocytes. Represent flow plots are shown at each concentration.

4.2.1.3 Validation of intravascular staining technique

I. **Proof of concept of intravascular staining technique**

To validate the intravascular staining procedure, naïve BALB/c mice were injected intravenously with 100 µl of 25 µg/ml of anti-CD45.2-FITC. One minute after the injection, blood, BAL and lung samples were collected and processed. The cells were stained for CD3 and CD8 and analysed using flow cytometry (Figure 4-3). In the blood, all $CD8^+$ T cells stained positive for CD45.2 (Figure 4-3 Right). $CD8^+$ T cells in the BAL samples were all negatively stained for CD45.2 (Figure 4-3 Middle). In the lungs, two thirds of $CD8^+$ lymphocytes were positively stained with CD45.2 whereas, the rest of the $CD8^+$ lymphocytes were spare from intravascular staining, showing a negative population in the flow plot (Figure 4-3 Left).

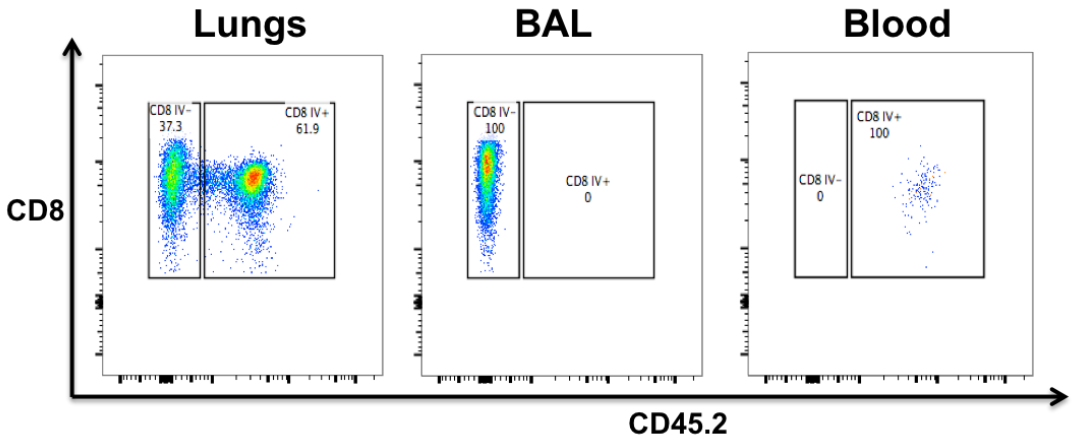

Figure 4-3 Intravenous staining in the lungs, airways and blood. BALB/c mice were immunised with $1x10^8$ ifu of ChAdOx1.85A intranasally. Two weeks post vaccination, lung, BAL and blood samples were collected at 1 minute after an intravenous injection of CD45.2 conjugated with FITC. The samples were processed and stained with CD3, CD4 and CD8. Representative flow plots show the intravenous population (IV+) and lung parenchymal population (IV-) in the lungs (Left flow plot), airways (Middle flow plot) and blood (Right flow plot) of the vaccinated mice.

II. Discrimination of lung-intravascular and lung-parenchymal lymphocytes using intravascular staining technique in B-C-M vaccinated mice and naïve controls.

Previous studies have shown that lung parenchymal lymphocytes were increased in the lung compartment of *M.tb* infected mice compared to naïve mice [106]. To observe this, B-C-Mid was used as a positive control in this optimisation because it was shown in the previous chapter to induce strong immune responses. BALB/c mice were vaccinated with B-C-Mid regimen and some unvaccinated mice were used as naïve controls. Four weeks post vaccination, the intravascular staining was performed, and the lung samples were harvested. The lung cells were stained with CD3, CD4 and CD8 and gated against CD45.2 to determine the proportion of intravascular lymphocytes and lung parenchymal lymphocytes (Figure 4-4).

After vaccination the mice with B-C-Mid, lung parenchymal $CD4^+$ T cells were increased 5 times more in B-C-Mid mice than naïve mice from 2 % to 10 % (Figure 4-4 A and B). One third of the percentage of intravascular $CD4^+$ T cell in the lungs of vaccinated mice were decreased compared to naïve mice (Figure 4-4 A and B). Lung parenchymal $CD8^+$ T cells were also enhanced in B-C-Mid mice compared to naïve mice, increasing the percentage of this cell population from 1 % to 6 % (Figure 4-4 C and D). The percentage of $CD8^+$ T cells in the lung vasculature of B-C-Mid vaccinated was comparable with the naïve group (Figure 4-4 C and D).

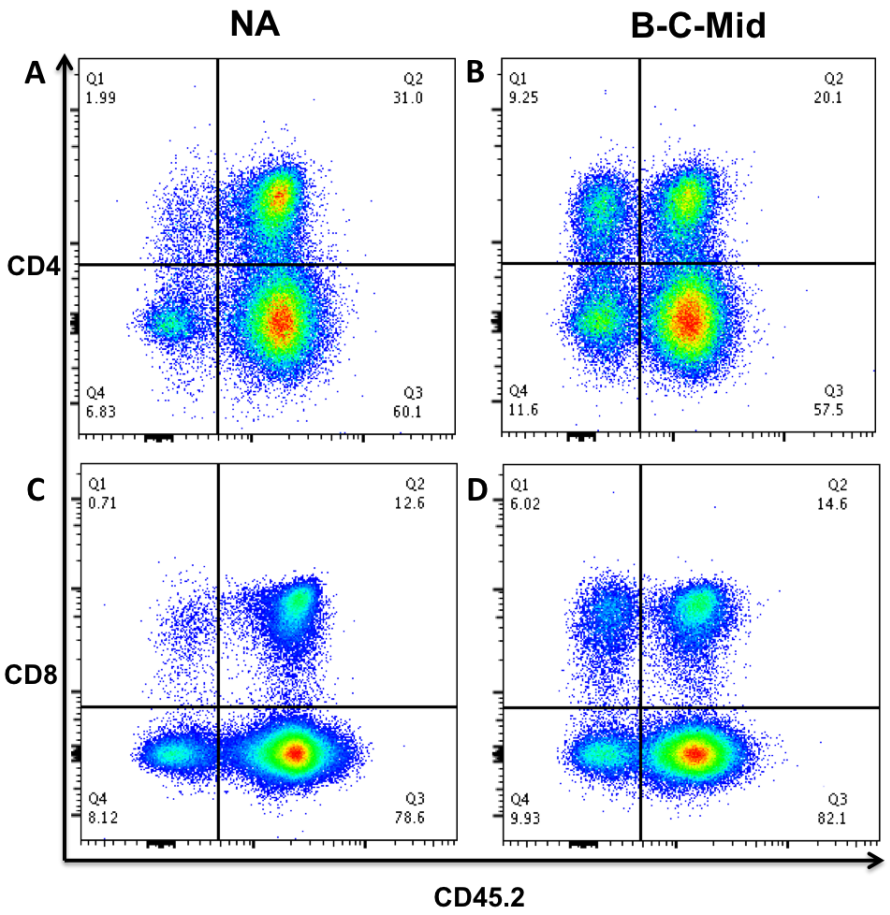

Figure 4-4 Lung parenchymal T cells in the lungs of B-C-M immunised mice and naïve mice. BALB/c mice were immunised with B-C-Mid regimen. Four weeks post vaccination, lung samples were harvested at 1 minute after an intravenous injection of CD45.2 conjugated with FITC. The tissues were processed and stained with CD3, CD4 and CD8. Representative flow plots show $CD4^+$ T cells (A and B) and $CD8^+$ T cells (C and D) in the lungs of naïve (NA) mice (A and C) and B-C-Mid vaccinated mice (B and D). In the flow plots, lung parenchymal populations (Q1 and Q4) and intravenous populations (Q2 and Q3) were gated.

4.2.2 Resident memory T cells in the lung compartments 4 weeks post B-C-M vaccination

In the previous chapter, I have shown that neither effector memory T cells (T_{EM}) producing IFN-γ and TNF-α, nor antibody responses in the airways and the circulation inducted by B-C-Mid regimen directly correlated with the protective efficacy of the B-C-M regimen. This could be because the responses observed came from both intravascular and parenchymal cells. Consistent with literatures [75, 121, 145, 217], lung parenchymal cells were enhanced after vaccination compared to naïve animals. Intravascular staining method has been optimised in section 4.2.1. This technique could be a useful tool to reveal immune responses specifically in lung-parenchymal compartment as well as intravascular compartment, identifying immune correlates of protection.

In this chapter, memory T cell responses were evaluated further focusing on resident memory T cell (T_{RM}) markers and lung homing markers at 4, 8 and 20 weeks post vaccination to identify immune correlates of protection. As shown at the end of Chapter 3, B-C-Mid and B-C-Min were still protective against *M.tb* challenge at 8 weeks after vaccination but the protection was no longer significant at the 20 week post-infection timepoint compared to BCG alone. A cell population that has the similar kinetic change in all timepoints could associate with protection.

To investigate the location of the $CD4^+$ and $CD8^+$ T cells induced by our vaccine regimen, as well as to characterise them in detail, mice were vaccinated as per the schedule in Figure 4-5. Intravascular staining was performed 1 minute before sacrificing. Lung and BAL samples were collected from vaccinated mice and controls.

Tetramer staining and surface staining were performed using fluorochrome-conjugated antibodies. Flow cytometry panels (Appendix Table 7-2 and Table 7-3) were designed to classify memory $CD4^+$ T cells and $CD8^+$ T cells at 4, 8 and 20 weeks post immunisation.

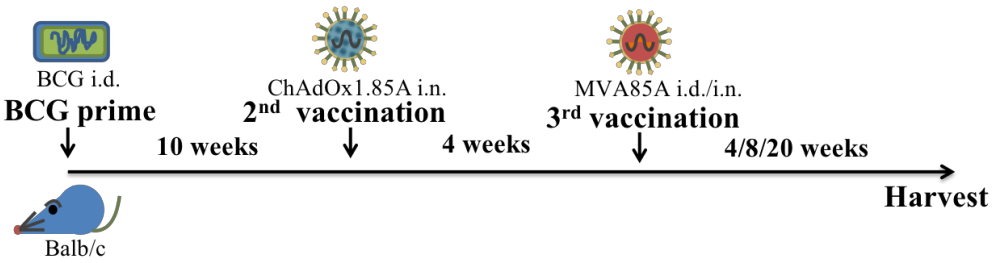

NA:	No vaccination----------18/22/34wks----------->Harvest
B:	BCG----------18/22/34wks ----------->Harvest
B-C:	BCG----------10wks----------->ChAdOx1.85A---4/8/20wks--->Harvest
B-C-Mid:	BCG----10wks-----> ChAdOx1.85A--4wks--->MVA85Aid------4/8/20wks---->Harvest
B-C-Min:	BCG----10wks-----> ChAdOx1.85A--4wks--->MVA85Ain------4/8/20wks---->Harvest

Figure 4-5 Timeline of B-C-M vaccination and control groups. BALB/c mice were vaccinated intradermally (i.d.) with $4x10^5$ CFU of BCG Pasteur (B) and boosted 10 weeks later with $1x10^8$ ifu of ChAdOx1.85A (C) intranasally (i.n.). Four weeks after ChAdOx1.85A vaccination, MVA85A was delivered either via the intradermal (Mid) or intranasal (Min) route in a dose of $5x10^6$ pfu. Samples were harvested at 4, 8 and 20 weeks after the last vaccination in B-C-Mid/in and B-C groups. The naïve (NA) and BCG (B) controls were sacrificed at 18, 22 and 34 weeks post vaccination respectively.

4.2.2.1 $CD4^+$ T cells responses in different lung compartments 4 weeks following B-C-M vaccination

I. **$CD4^+$ T cells responses in the lung parenchyma 4 weeks following B-C-M vaccination**

Recently, lung homing markers were introduced to identify lung parenchymal and intravascular memory T cells [116]. This population of cells are enhanced after vaccination or *M.tb* infection and have been shown to associate with protective immunity [106, 145].

Four weeks post vaccination, 2 % of lung parenchymal (IV-) $CD4^+$ T cells were antigen Ag85A-specific as detected with MHC-class II tetramer staining (Figure 4-6 B). Ag85A-specific $CXCR3^+$ $KLRG1^-$ $CD4^+$ T cells were detected after boosting BCG with intranasal ChAdOx1.85A (B-C) (Figure 4-6 A Left flow plot). An additional boost of intradermal or intranasal MVA85A doubled the percentage of this cell population compared to B-C (Figure 4-6 A). The percentage of Ag85A-specific $CXCR3^+$ $KLRG1^-$ $CD4^+$ T cells in the lung parenchyma of B-C-Mid immunised mice was significantly increased compared to BCG vaccinated mice (p=0.0027) (Figure 4-6 C). There was a trend for expansion of the lung parenchymal cells in the B-C-Min group compared to BCG controls (Figure 4-6 C). The total cell number of Ag85A-specific lung parenchymal $CXCR3^+$ $KLRG1^-$ $CD4^+$ T cells followed the same pattern with the percentages (Figure 4-6 C and Figure 4-7 A). Both B-C-Mid and B-C-Min groups had a significantly higher number of cells compared to BCG controls (p=0.0002 and p=0.0344 respectively) (Figure 4-7 A).

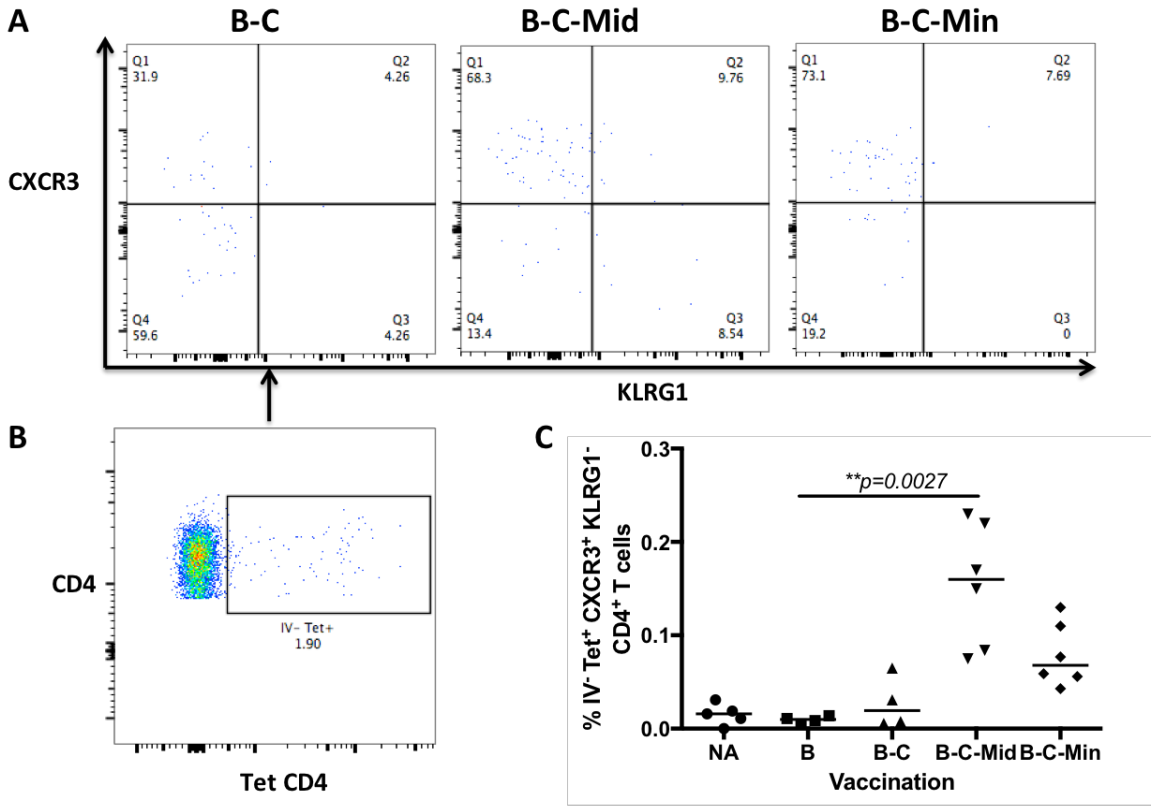

Figure 4-6 Ag85A-specific parenchymal CXCR3$^+$ KLRG1$^-$ CD4$^+$ T cells in the lungs of naïve and vaccinated mice 4 weeks post vaccination. Mice were vaccinated as shown in Figure 4-5 and lungs were harvested 4 weeks post vaccination. Fluorochrome-conjugated CD45.2 was injected intravenously 1 minute before sacrificing. Lung cells were assessed using surface staining and tetramer staining. (A) Representative flow plots show Ag85A-specific parenchymal CD4$^+$ T cells expressing CXCR3 and/or KLRG1 in the lungs of B-C (Left), B-C-Mid (Middle) and B-C-Min (Right) groups. (B) A representative flow plot shows Ag85A-specific CD4$^+$ T cells in the lungs of B-C-Mid immunised mice. (C) Percentage of Ag85A-specific lung parenchymal CXCR3$^+$ KLRG1$^-$ CD4$^+$ T cells. Each symbol represents one animal and the line is the median of each group (n=4-6 mice). Statistical significance was determined using Kruskal-Wallis test with Dunn's multiple comparisons test. ** p≤0.01.

Resident memory T cell markers (CD44, CD62L, CD69 and CD11a) were also included in this study to further characterise the memory and lung homing phenotype of lung parenchymal cells.

Ag85A-specific lung parenchymal $CD4^+$ T cells expressing $CD44^{hi}$ $CD62L^{low}$ $CD69^+$ $CD11a^+$ (characteristic of resident memory cells) were significantly increased in B-C-Mid mice compared to BCG animals (p=0.0005) and approached significance in the B-C-Min group (p=0.0525) (Figure 4-7 B).

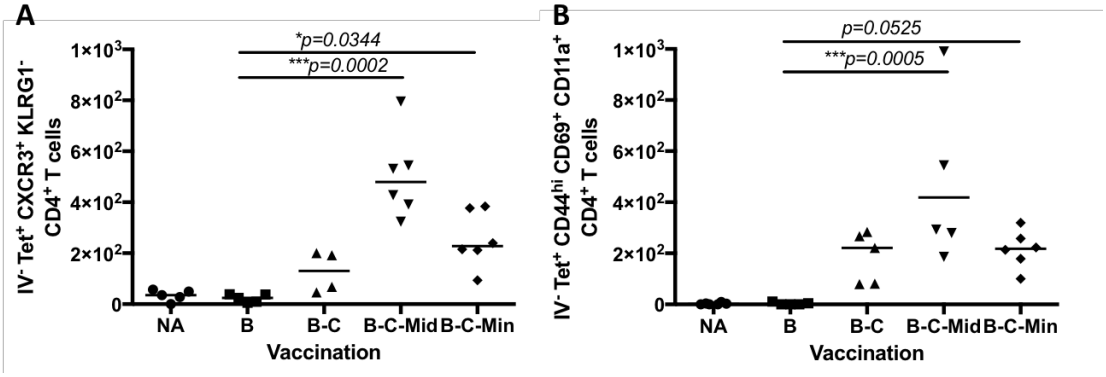

Figure 4-7 Ag85A-specific parenchymal $CD4^+$ T cells expressing memory phenotypes in the lungs of naïve and vaccinated mice at 4 weeks post vaccination. Mice were immunised as shown in Figure 4-5. Four weeks post vaccination, fluorochrome-conjugated CD45.2 was injected intravenously before sacrificing. Lung cells were assessed using surface staining and tetramer staining. (A) Total cell number of Ag85A-specific lung parenchymal $CXCR3^+$ $KLRG1^-$ $CD4^+$ T cells at 4 weeks post vaccination. (B) Total cell number of Ag85A-specific lung parenchymal $CD44^{hi}$ $CD69^+$ $CD11a^+$ $CD4^+$ T cells at 4 weeks post vaccination. Each symbol represents one animal and the line is the median of each group (n=4-6 mice). Statistical significance was determined using Kruskal-Wallis test with Dunn's multiple comparisons test. *, p≤0.05; ***, p≤0.001.

II. CD4$^+$ T cells responses in the lung vasculature 4 weeks following B-C-M vaccination

Intravascular lymphocytes are phenotypically identified by the expression of CX3CR1 and KLRG1 [106, 222]. Unlike CXCR3$^+$ KLRG1$^-$ T lymphocytes, CX3CR1$^+$ KLRG1$^+$ T cells are retained in the lung vasculature and contribute less to the control of infection compared to lung parenchymal T cells [106].

In the lung vasculature, Ag85A-specific CX3CR1$^+$ KLRG1$^+$ T cells were enhanced after BCG vaccination compared to naïve mice, but the data was not statistically significant (Figure 4-8). ChAdOX1.85A and MVA85A boost failed to increase the expansion of this population further (Figure 4-8).

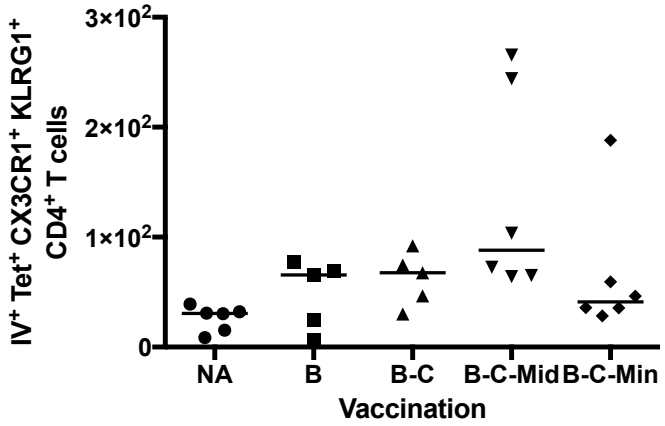

Figure 4-8 Ag85A-specific vascular CX3CR1$^+$ KLRG1$^+$ CD4$^+$ T cells in the lungs of naïve and vaccinated mice 4 weeks post vaccination. Mice were immunised as shown in Figure 4-5. Four weeks post vaccination, fluorochrome-conjugated CD45.2 was injected intravenously before sacrificing. Lung cells were assessed using surface staining and tetramer staining. Total cell number of Ag85A-specific lung parenchymal CX3CR1$^+$ KLRG1$^+$ CD4$^+$ T cells at 4 weeks post vaccination is presented. Each symbol represents one animal and the line is the median of each group (n=5-6 mice). No statistical significance was observed using Kruskal-Wallis test with Dunn's multiple comparisons test.

III. **$CD4^+$ T cells responses in the airways 4 weeks following B-C-M vaccination**

Mucosal immunity is currently of interest in TB vaccine development. MVA85A has been delivered to humans via aerosol and found to be safe and highly immunogenic [204]. In mice, mucosally delivered BCG enhances T cells responses in the airways and improves protection compared to subcutaneous route [75]. As shown in the previous chapter and in the literature, boosting BCG prime-ChAdOx1.85A vaccinated mice with MVA85A intranasally (B-C-Min) is also protective against aerosol *M.tb* challenge [98]. Thus, BAL samples were assessed to observe resident memory phenotypes of the airway cells.

Airway T_{RM} cells are increased after mucosal vaccination with BCG compared to systemic routes and shown to confer protection against *M.tb* challenge [75]. Intradermal BCG did not enhance Ag85A-specific $CD4^+$ T cells expressing $CD44^{hi}$ $CD62L^{low}$ $CD69^+$ $CD11a^+$ in the airways of the vaccinated animals compared to naïve controls (Figure 4-9). This cell population was slightly increased after BCG was boosted with ChAdOx1.85A intranasally (Figure 4-9). A further boost with intradermal MVA85A significantly increased the T_{RM} cells in the airways of B-C-Mid mice compared to BCG alone ($p=0.005$) (Figure 4-9). In B-C-Min mice, an intranasal boost with MVA85A failed to enhance this memory subset in the airway compared to BCG controls (Figure 4-9).

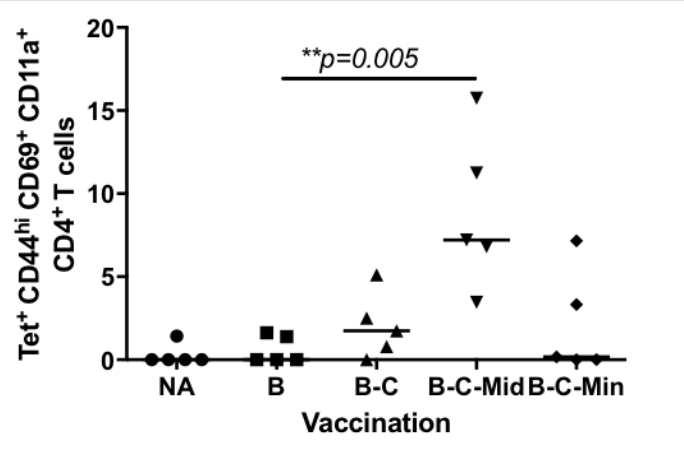

Figure 4-9 Ag85A-specific CD4$^+$ T cells expressing resident memory markers in the airways of naïve and vaccinated mice at 4 weeks post vaccination. Mice were immunised as shown in Figure 4-5. Fluorochrome-conjugated CD45.2 was injected intravenously before sacrificing. BAL samples were assessed using surface staining and tetramer staining. Total cell number of Ag85A-specific CD44^{hi} CD69$^+$ CD11a$^+$ CD4$^+$ T cells in the airways of vaccinated mice and naïve mice at 4 weeks post vaccination are presented. Each symbol represents one animal and the line is the median of each group (n=4-6 mice). Statistical significance was determined using Kruskal-Wallis test with Dunn's multiple comparisons test. **, p≤0.01.

4.2.2.2 $CD8^+$ T cells responses in different lung compartments 4 weeks following B-C-M vaccination

I. **$CD8^+$ T cells responses in the lung parenchyma 4 weeks following B-C-M vaccination**

The importance of $CD8^+$ T_{RM} in protection against *M.tb* infection has been previously shown in cell depletion and adoptive transfer studies [45, 143, 144]. Thus, $CD8^+$ T cell responses in the lung parenchyma were investigated (Figure 4-10). BCG failed to induce Ag85A-specific $CD8^+$ T cells (Figure 4-10 C). After BCG was boosted with intranasal ChAdOx1.85A, around 20 % of lung parenchymal $CD8^+$ T cells were positively stained with the MHC-I tetramer (Figure 4-10 B). More than 60 % of these cells in the lungs of B-C mice had a $CXCR3^+$ $KLRG1^-$ phenotype (Figure 4-10 A Left flow plot) and the percentage of this phenotype in $CD8^+$ T cells was significantly increased compared to BCG-vaccinated mice (Figure 4-10 C) ($p=0.0296$). After a boost with intradermal or intranasal MVA, this cell population was enhanced in the lungs of B-C-Mid and B-C-Min vaccinated mice compared to BCG mice (Figure 4-10 A). Ag85A-specific $CXCR3^+$ $KLRG1^-$ $CD8^+$ T cells in the lung parenchyma of B-C-Min mice were significantly increased compared to BCG controls ($p=0.0008$) (Figure 4-10 C). The percentage of this cell population was also increased in B-C-Mid mice compared to BCG mice, but the data was not statistically significant (Figure 4-10 C).

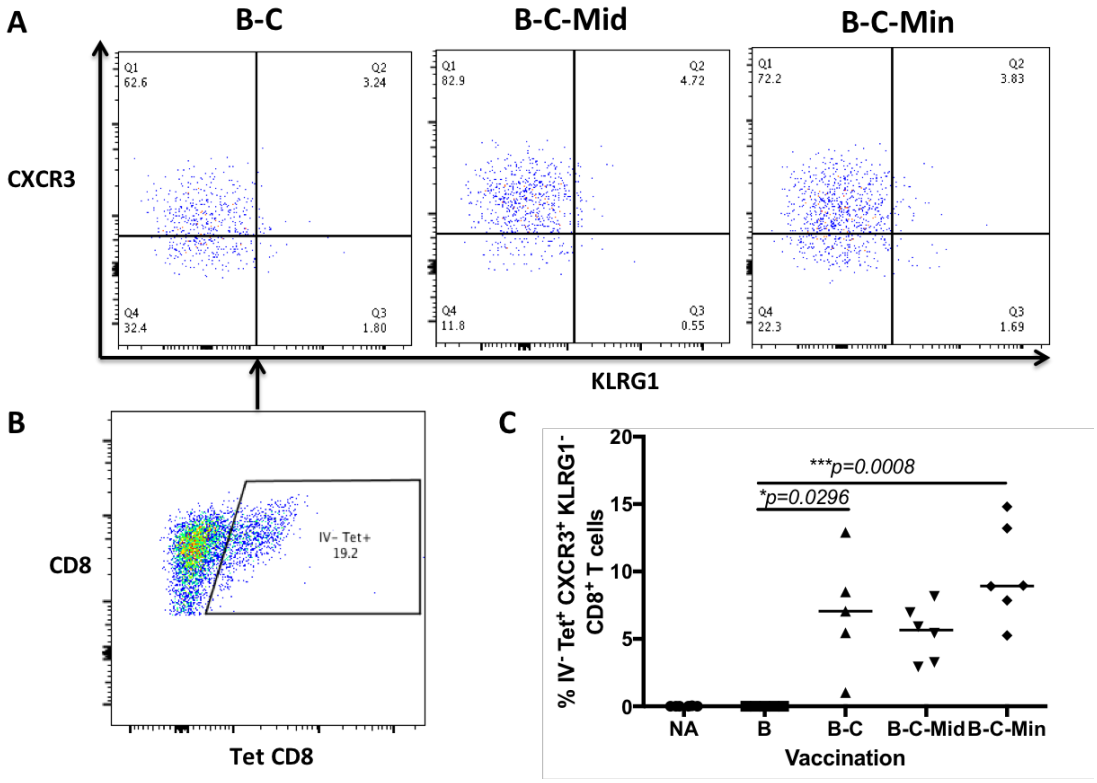

Figure 4-10 Ag85A-specific parenchymal CXCR3$^+$ KLRG1$^-$ CD8$^+$ T cells in the lungs of naïve and vaccinated mice at 4 weeks post vaccination. Mice were vaccinated as shown in Figure 4-5. and analysed at 4 weeks post vaccination. Fluorochrome-conjugated CD45.2 was injected intravenously 1 minute before sacrificing. Lung cells were assessed using surface staining and tetramer staining. (A) Representative flow plots show Ag85A-specific parenchymal CD4$^+$ T cells expressing CXCR3 and KLRG1 in the lungs of B-C (Left), B-C-Mid (Middle) and B-C-Min (Right) groups. (B) A representative flow plot shows Ag85A-specific CD8$^+$ T cells in the lungs of B-C-Mid immunised mice. (C) Percentage of Ag85A-specific lung parenchymal CXCR3$^+$ and KLRG1$^-$ CD8$^+$ T cells. Each symbol represents one animal and the line is the median of each group (n=4-6 mice). Statistical significance was determined using Kruskal-Wallis test with Dunn's multiple comparisons test. *, p≤0.05; ***, p≤0.001.

MVA85A boost did not further enhance the $CD8^+$ T cells responses compared to B-C regimen (Figure 4-10 C and Figure 4-11 A). Presented as total cell numbers, both B-C-Mid and B-C-Min significantly enhanced Ag85A-specific lung parenchymal $CXCR3^+$ $KLRG1^-$ $CD8^+$ T cells compared to the BCG alone group (p=0.0135 and p=0.0079 respectively) (Figure 4-11 A). This cell type was also increased in the lungs of B-C mice compared to BCG vaccinated mice, but the difference was no longer significant (Figure 4-11 A).

In mice, $CD4^+$ T_{RM} cells express CD11a, whereas $CD8^+$ T_{RM} present CD103 in the lungs [114, 117]. By boosting BCG with intranasal ChAdOx1.85A, a significant increase in Ag85A-specific lung parenchymal $CD44^{hi}$ $CD62L^{low}$ $CD69^+$ $CD103^+$ $CD8^+$ T cells was observed in the B-C group compared to BCG alone (Figure 4-11 B). B-C-Mid and B-C-Min groups did not further improve this cell population compared to the B-C group. (Figure 4-11 B). Both B-C-Mid/in were also not significantly better compared to BCG when correcting for multiple comparisons (p=0.0808 and 0.0520 respectively) (Figure 4-11 B).

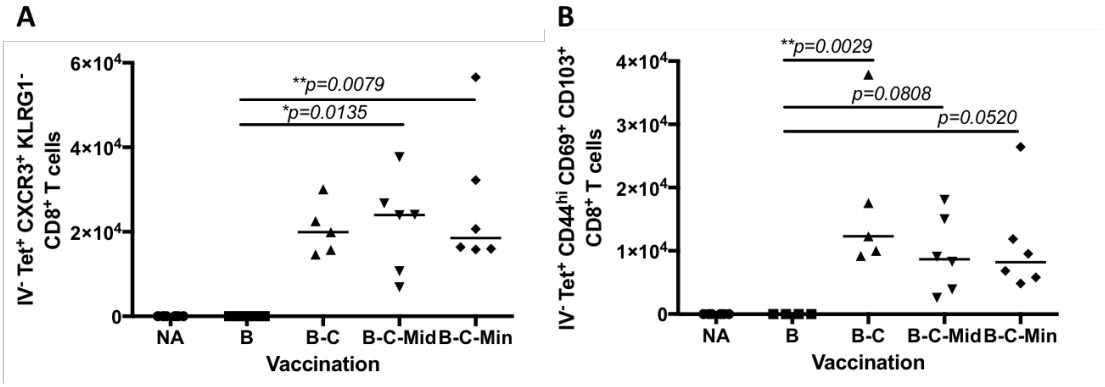

Figure 4-11 Ag85A-specific parenchymal CD8$^+$ T cells expressing memory phenotypes in the lungs of naïve and vaccinated mice at 4 weeks post vaccination. Mice were immunised as shown in Figure 4-5 and analysed at 4 weeks post vaccination. Fluorochrome-conjugated CD45.2 was injected intravenously before sacrificing. Lung cells were assessed using surface staining and tetramer staining. (A) Total cell number of Ag85A-specific lung parenchymal CXCR3$^+$ KLRG1$^-$ CD8$^+$ T cells and (B) total cell number of Ag85A-specific lung parenchymal CD44^{hi} CD69$^+$ CD103$^+$ CD8$^+$ T cells. Each symbol represents one animal and the line is the median of each group (n=4-6 mice). Statistical significance was determined using Kruskal-Wallis test with Dunn's multiple comparisons test. *p≤0.05; **, p≤0.01.

II. CD8⁺ T cells responses in the lung vasculature 4 weeks following B-C-M vaccination

Intravascular CD8⁺ T cells are expanded after *M.tb* infection and vaccination [75, 106]. In this work, BCG alone and BCG prime-ChAdOx1.85A boost failed to induce Ag85A-specific CX3CR1⁺ KLRG1⁺ CD8⁺ T cells in the lung vasculature of the vaccinated mice (Figure 4-12). Boosting B-C with MVA85A intradermally and intranasally, the intravascular cells were significantly increased in the B-C-Mid and B-C-Min vaccinated mice compared to BCG controls ($p<0.0001$ and $p=0.0292$ respectively). The magnitude was much higher in the B-C-Mid group compared to the B-C-Min group but the difference was not statistically significant (Figure 4-12).

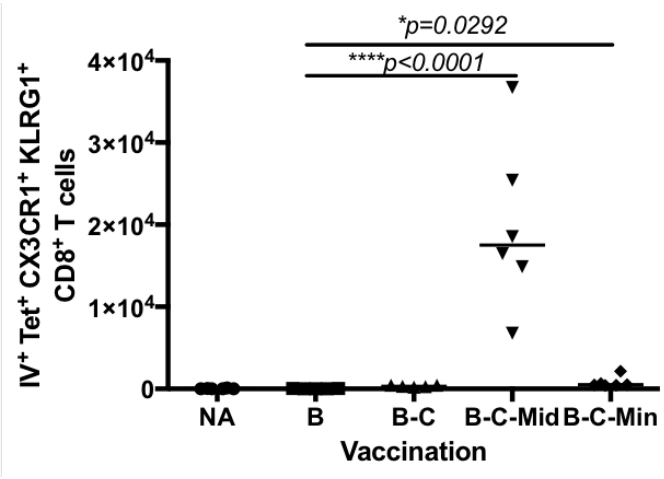

Figure 4-12 Ag85A-specific vascular CX3CR1⁺ KLRG1⁺ CD8⁺ T cells in the lungs of naïve and vaccinated mice 4 weeks post vaccination. Mice were immunised as shown in Figure 4-5. Four weeks post vaccination, fluorochrome-conjugated CD45.2 was injected intravenously before sacrificing. Lung cells were assessed using surface staining and tetramer staining. Total cell number of Ag85A-specific lung parenchymal CX3CR1⁺ KLRG1⁺ CD8⁺ T cells at 4 weeks post vaccination is presented. Each symbol represents one animal and the line is the median of each group (n=5-6 mice). Statistical significance was determined using Kruskal-Wallis test with Dunn's multiple comparisons test. *, p≤0.05; ****, p≤0.0001.

III. **$CD8^+$ T cells responses in the airways 4 weeks following B-C-M vaccination**

Airway-resident memory $CD8^+$ cells expressing prototypical T_{RM} markers are increased after mucosal vaccination of BCG and protective against *M.tb* infection [75]. BAL cells were collected from vaccinated and naïve mice and analysed for T_{RM} phenotypes. Intradermal BCG did not enhance Ag85A-specific $CD8^+$ T cells expressing $CD44^{hi}$ $CD62L^{low}$ $CD69^+$ $CD103^+$ in the airways of BCG vaccinated animals compared to naïve controls (Figure 4-13). This cell population was significantly expanded after BCG was boosted with ChAdOx1.85A compared to BCG alone (p=0.0129) (Figure 4-13). MVA85A boost did not enhance the responses further from the expansion obtained from B-C vaccination (Figure 4-13). The airway-resident memory $CD8^+$ cells were increased in the B-C-Mid and B-C-Min groups compared to BCG alone, and the difference was statically significant when the vaccine boost was delivered intradermally (p=0.0077) but not intranasally (Figure 4-13).

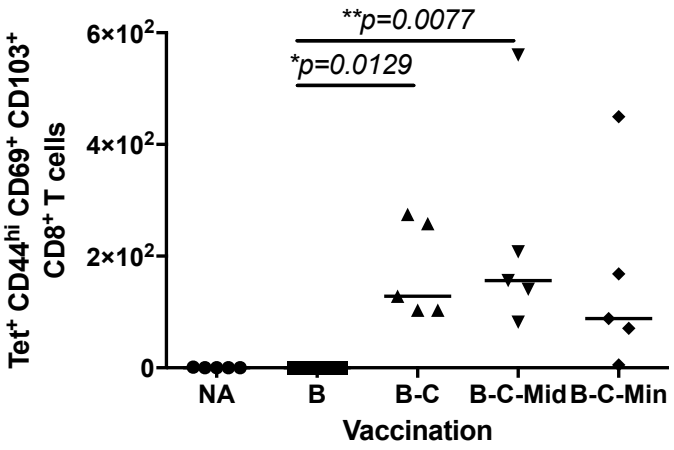

Figure 4-13 Ag85A-specific CD8$^+$ T cells expressing resident memory markers in the airways of naïve and vaccinated mice at 4 post vaccination. Mice were immunised as shown in Figure 4-5. Fluorochrome-conjugated CD45.2 was injected intravenously before sacrificing. BAL samples were assessed using surface staining and tetramer staining. Total cell number of Ag85A-specific CD44^{hi} CD69$^+$ CD103$^+$ CD8$^+$ T cells in the airways of vaccinated mice and naïve mice at 4 weeks post vaccination. Each symbol represents one animal and the line is the median of each group (n=4-6 mice). Statistical significance was determined using Kruskal-Wallis test with Dunn's multiple comparisons test. *p≤0.05; **, p≤0.01.

4.2.3 Resident memory T cells in lung compartments 8 weeks post B-C-M vaccination

In the previous section 4.2.2, the memory T cell responses were studied, showing the expansion of lung parenchymal T cells 4 weeks following B-C-M vaccination. B-C-M regime was also protective at 8 weeks after the last immunisation. Vaccinated mice and controls were analysed in this section to observe memory T cell responses at the 8-week timepoint (Figure 4-5), identifying cell population that could correlate with protection.

4.2.3.1 $CD4^+$ T cells responses in different lung compartments 8 weeks following B-C-M vaccination

I. **$CD4^+$ T cells responses in the lung parenchyma 8 weeks following B-C-M vaccination**

Eight weeks post vaccination, lung homing and resident memory markers showed an almost identical pattern (Figure 4-14 A and B). Ag85A-specific $CXCR3^+$ and $KLRG1^-$ $CD4^+$ T cells were significantly increased in the lung parenchyma of B-C-Mid and B-C-Min mice compared to BCG immunised mice (p=0.0170 and p=0.0103 respectively) (Figure 4-14 A). The lung parenchymal $CD4^+$ T cells expressing $CD44^{hi}$ $CD69^+$ $CD11a^+$ were significantly enhanced in the B-C-Mid and B-C-Min groups compared to the BCG controls (p=0.0103 and p=0.0428 respectively) (Figure 4-14 B).

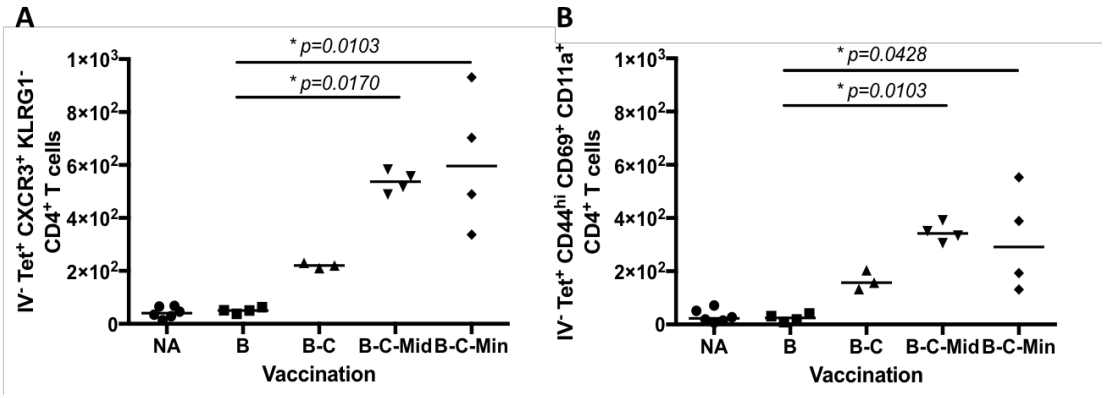

Figure 4-14 Ag85A-specific parenchymal CD4$^+$ T cells expressing memory phenotypes in the lungs of naïve and vaccinated mice at 8 weeks post vaccination. Mice were immunised as shown in Figure 4-5. Eight weeks post vaccination, fluorochrome-conjugated CD45.2 was injected intravenously before sacrificing. Lung cells were assessed using surface staining and tetramer staining. (A) Total cell number of Ag85A-specific lung parenchymal CXCR3$^+$ KLRG1$^-$ CD4$^+$ T cells at 8 weeks post vaccination. (B) Total cell number of Ag85A-specific lung parenchymal CD44^{hi} CD69$^+$ CD11a$^+$ CD4$^+$ T cells at 8 weeks post vaccination. Each symbol represents one animal and the line is the median of each group (n=3-6 mice). Statistical significance was determined using Kruskal-Wallis test with Dunn's multiple comparisons test. *p≤0.05.

II. CD4$^+$ T cells responses in the lung vasculature 8 weeks following B-C-M vaccination

At 8 weeks, the overall responses of intravascular CD4$^+$ T cells in the lungs of vaccinated and naïve mice were low. Naïve controls had a high background which made it difficult to interpret the result. However, there is a trend for higher Ag85A-specific CX3CR1$^+$ KLRG1$^+$ CD4$^+$ T cells in the lung vasculature of B-C-Mid immunised mice compared to naïve mice (Figure 4-15).

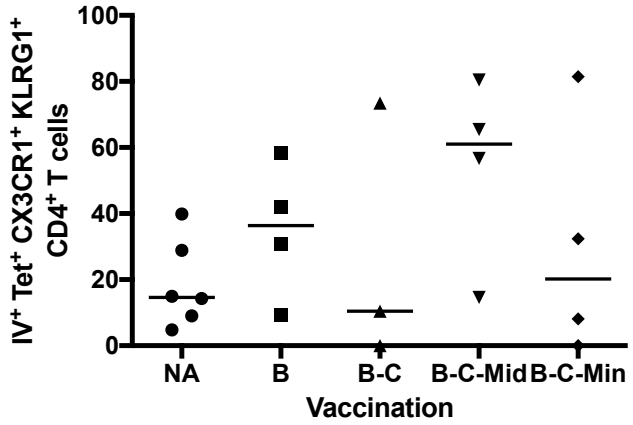

Figure 4-15 Ag85A-specific vascular CX3CR1$^+$ KLRG1$^+$ CD4$^+$ T cells in the lungs of naïve and vaccinated mice 8 weeks post vaccination. Mice were immunised as shown in Figure 4-5. Eight weeks post vaccination, fluorochrome-conjugated CD45.2 was injected intravenously before sacrificing. Lung cells were assessed using surface staining and tetramer staining. Total cell number of Ag85A-specific lung parenchymal CX3CR1$^+$ KLRG1$^+$ CD4$^+$ T cells at 8 weeks post vaccination is presented. Each symbol represents one animal and the line is the median of each group (n=5-6 mice). No statistical significance was observed using Kruskal-Wallis test with Dunn's multiple comparisons test.

III. CD4$^+$ T cells responses in the airways 8 weeks following B-C-M vaccination

In the airways, Ag85A-specific resident memory CD4$^+$ T cells expressing CD44, CD69 and CD11a were significantly increased after boosted BCG prime mice with ChAdOx1.85A compared to BCG alone (p=0.0182) (Figure 4-16). The memory cells were not expanded further after an additional boost with MVA85A by either the intradermal or intranasal routes (Figure 4-16).

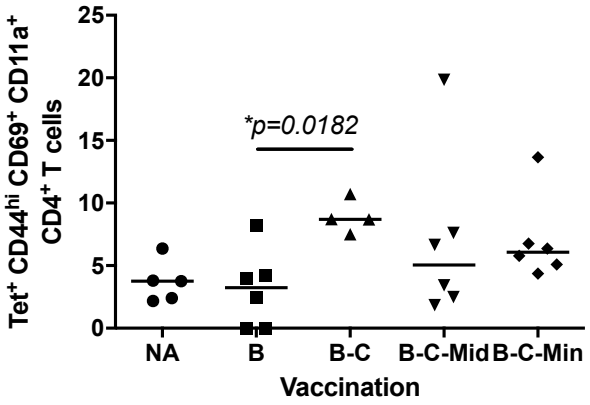

Figure 4-16 Ag85A-specific CD4$^+$ T cells expressing resident memory markers in the airways of naïve and vaccinated mice at 8 weeks post vaccination. Mice were immunised as shown in Figure 4-5. Fluorochrome-conjugated CD45.2 was injected intravenously before sacrificing. BAL samples were assessed using surface staining and tetramer staining. Total cell number of Ag85A-specific CD44^{hi} CD69$^+$ CD11a$^+$ CD4$^+$ T cells in the airways of vaccinated mice and naïve mice at 8 weeks post vaccination. Each symbol represents one animal and the line is the median of each group (n=4-6 mice). Statistical significance was determined using Kruskal-Wallis test with Dunn's multiple comparisons test. *p≤0.05.

4.2.3.2 $CD8^+$ T cells responses in different lung compartments 8 weeks following B-C-M vaccination

I. **$CD8^+$ T cells responses in in the lung parenchyma 8 weeks following B-C-M vaccination**

At 8 weeks post vaccination, both memory phenotypes of the memory $CD8^+$ T cells in the lung parenchyma were enhanced after BCG was boosted with ChAdOx1.85A compared to BCG alone but the difference was not significant (Figure 4-17 A and B). After MVA85A boosting, Ag85A-specific lung parenchymal $CXCR3^+$ and $KLRG1^-$ $CD8^+$ T cells were significantly increased in the lungs of B-C-Mid and B-C-Min mice compared to BCG immunised mice (p=0.0170 and p=0.0342 respectively) (Figure 4-17 A). The antigen-specific lung parenchymal $CD8^+$ T cells expressed $CD44^{hi}$ $CD69^+$ $CD11a^+$ were significantly increased in the B-C-Mid compared to the BCG controls (p=0.0079) and the difference was approaching statistical significance in B-C-Min groups compared to the BCG group (p=0.0802) (Figure 4-17 B).

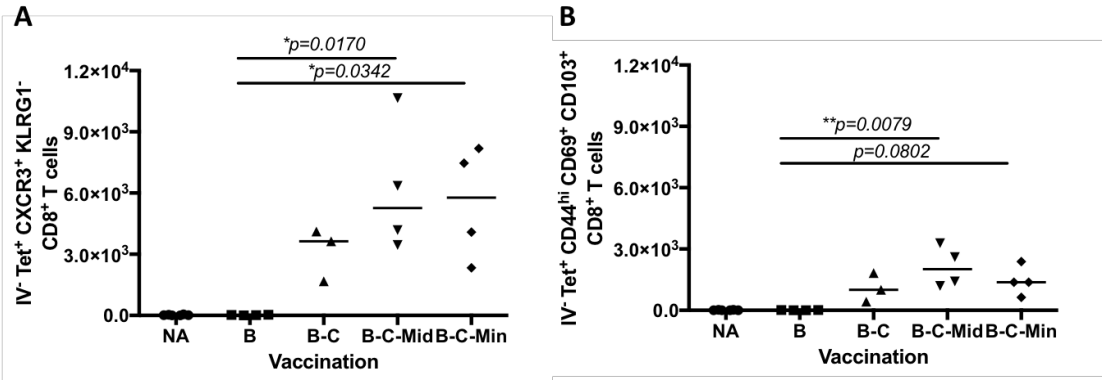

Figure 4-17 Ag85A-specific parenchymal CD8$^+$ T cells expressing memory phenotypes in the lungs of naïve and vaccinated mice at 8 weeks post vaccination. Mice were immunised as shown in Figure 4-5. Eight weeks post vaccination, fluorochrome-conjugated CD45.2 was injected intravenously before sacrificing. Lung cells were assessed using surface staining and tetramer staining. (A) Total cell number of Ag85A-specific lung parenchymal CXCR3$^+$ KLRG1$^-$ CD8$^+$ T cells at 8 weeks post vaccination. (B) Total cell number of Ag85A-specific lung parenchymal CD44^{hi} CD69$^+$ CD103$^+$ CD8$^+$ T cells at 8 weeks post vaccination. Each symbol represents one animal and the line is the median of each group (n=3-5 mice). Statistical significance was determined using Kruskal-Wallis test with Dunn's multiple comparisons test. *p≤0.05; **, p≤0.01.

II. $CD8^+$ T cells responses in the lung vasculature 8 weeks following B-C-M vaccination

In the lung vasculature, Ag85A-specific $CD8^+$ T cells expressed CX3CR1 and KLRG1 were not expanded after BCG vaccination, even after a further boost with ChAdOx1.85A. The intravascular cells were boosted with MVA85A intradermally, resulting in the significant expansion of Ag85A-specific $CX3CR1^+$ $KLRG1^+$ $CD8^+$ T cells in the lung vasculature of B-C-Mid vaccinated mice compared to B-C immunised mice ($p=0.0093$) (Figure 4-18). The enhancement of this cell population was also significant in B-C-Mid immunised mice compared to BCG controls ($p=0.0241$) (Figure 4-18). The $CD8^+$ T lymphocytes were also observed in the lung vasculature of B-C-Min immunised animals, but the difference was not statistically significant when compared with BCG controls (Figure 4-18).

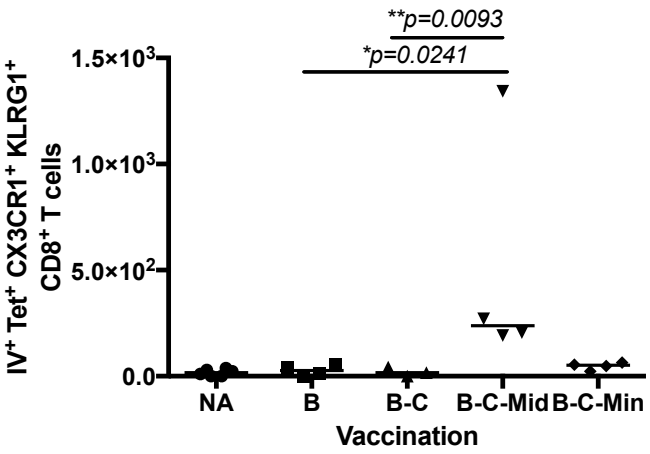

Figure 4-18 Ag85A-specific vascular CX3CR1$^+$ KLRG1$^+$ CD8$^+$ T cells in the lungs of naïve and vaccinated mice 8 weeks post vaccination. Mice were immunised as shown in Figure 4-5. Eight weeks post vaccination, fluorochrome-conjugated CD45.2 was injected intravenously before sacrificing. Lung cells were assessed using surface staining and tetramer staining. Total cell number of Ag85A-specific lung parenchymal CX3CR1$^+$ KLRG1$^+$ CD8$^+$ T cells at 8 weeks post vaccination is presented. Each symbol represents one animal and the line is the median of each group (n=3-6 mice). Statistical significance was determined using Kruskal-Wallis test with Dunn's multiple comparisons test. *, p≤0.05; **, p≤0.01.

III. CD8$^+$ T cells responses in the airways 8 weeks following B-C-M vaccination

In the airways, resident memory CD8$^+$ T cells expressed T_{RM} phenotypes (CD44^{hi} CD62L^{low} CD69$^+$ CD103$^+$) were significantly enhanced after boosted BCG vaccinated mice with intranasal ChAdOx1.85A compared to BCG alone (p=0.0007) (Figure 4-19). After MVA85A boosting, these resident memory cells were not expanded further but significantly increased in the airways of B-C-Mid and B-C-Min vaccinated mice compared to BCG immunised mice (p=0.0358 and p=0.0242 respectively) (Figure 4-19).

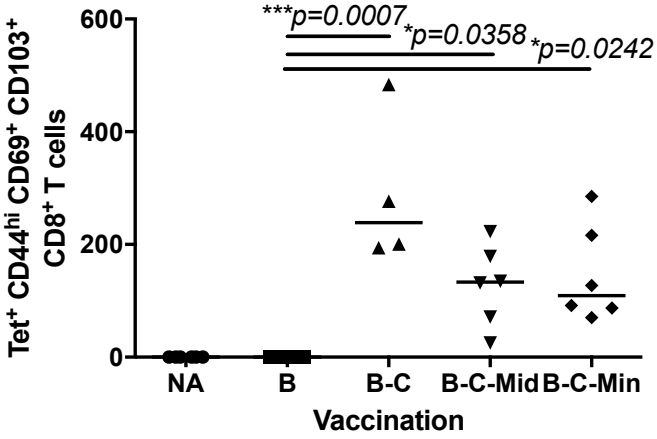

Figure 4-19 Ag85A-specific CD8$^+$ T cells expressing resident memory markers in the airways of naïve and vaccinated mice at 8 post vaccination. Mice were immunised as shown in Figure 4-5. Fluorochrome-conjugated CD45.2 was injected intravenously before sacrificing. BAL samples were assessed using surface staining and tetramer staining. Total cell number of Ag85A-specific CD44^{hi} CD69$^+$ CD103$^+$ CD8$^+$ T cells in the airways of vaccinated mice and naïve mice at 8 weeks post vaccination. Each symbol represents one animal and the line is the median of each group (n=4-6 mice). Statistical significance was determined using Kruskal-Wallis test with Dunn's multiple comparisons test. *p≤0.05; ***, p≤0.001.

4.2.4 Resident memory T cells in lung compartments 20 weeks post B-C-M vaccination

Resident memory T cell responses in the lungs at 4 weeks and 8 weeks post vaccination have been described in section 4.2.2 and section 4.2.3 respectively. At 20 weeks following B-C-M vaccination, the protective efficacy of the vaccine regimen declined, and the statistical significance of the results was lost. Mice were vaccinated as shown in Figure 4-5 and analysed at 20 weeks after B-C-M regimen completed. Memory T cells responses in the lung compartments induced by B-C-M vaccination would be described in this section.

4.2.4.1 $CD4^+$ T cells responses in different lung compartments 20 weeks following B-C-M vaccination

I. **$CD4^+$ T cells responses in the lung parenchyma 20 weeks following B-C-M vaccination**

At 20 weeks post vaccination, Ag85A-specific lung parenchymal $CD4^+$ T cells expressing $CXCR3^+$ $KLRG1^-$ or expressing $CD44^{hi}$ $CD69^+$ $CD11a^+$ were observed after BCG vaccinated mice were boosted with ChAdOx1.85A (Figure 4-20 A and B). Boosting B-C with MVA85A, the Ag85A-specific lung parenchymal $CXCR3^+$ $KLRG1^-$ $CD4^+$ T cells were enhanced in the lungs of B-C-Mid and B-C-Min groups but only the data of the latter group was approaching statistical significance when compared with the B-C group ($p=0.0595$) (Figure 4-20 A). No improvement after the MVA boost was observed when analysed for the T_{RM} phenotype (Figure 4-20 B). Compared B-C-Mid and B-C-Min with BCG controls, both groups significantly enhanced the lung parenchymal $CD4^+$ T cell responses expressing $CXCR3^+$ $KLRG1^-$ ($p=0.0068$ and $p=0.0026$ respectively) (Figure

4-20 A), as well as expressing CD44^{hi} CD69^{+} CD11a^{+} (p=0.0063 and p=0.0043 respectively) (Figure 4-20 B).

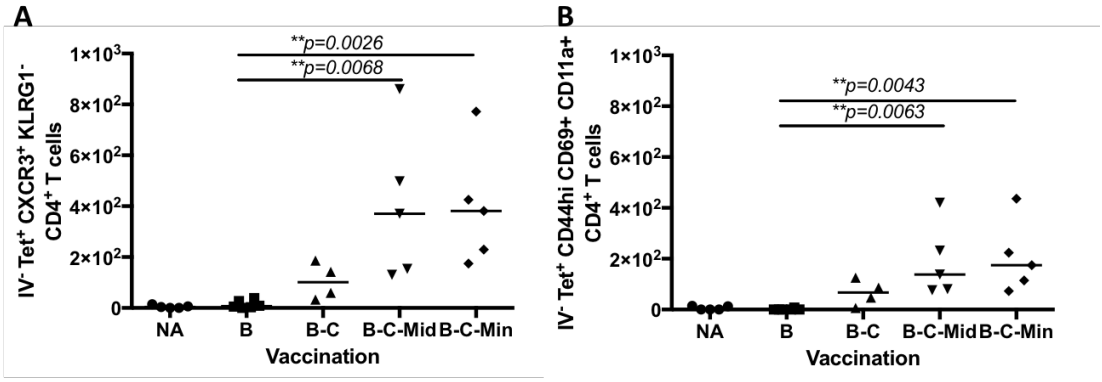

Figure 4-20 Ag85A-specific parenchymal CD4^{+} T cells expressing resident memory phenotypes in the lungs of naïve and vaccinated mice at 20 post vaccination. Mice were immunised as shown in Figure 4-5. 20 weeks post vaccination, fluorochrome-conjugated CD45.2 was injected intravenously before sacrificing. Lung cells were assessed using surface staining and tetramer staining. (A) Total cell number of Ag85A-specific lung parenchymal CXCR3^{+} KLRG1^{-} CD4^{+} T cells at 20 weeks post vaccination. (B) Total cell number of Ag85A-specific lung parenchymal CD44^{hi} CD69^{+} CD11a^{+} CD4^{+} T cells at 20 weeks post vaccination. Each symbol represents one animal and the line is the median of each group (n=4-6 mice). Statistical significance was determined using Kruskal-Wallis test with Dunn's multiple comparisons test. **, p≤0.01.

II. CD4$^+$ T cells responses in the lung vasculature 20 weeks following B-C-M vaccination

In the intravascular compartment of the lungs, the overall responses of Ag85A-specific CD4$^+$ T cells were very low with some background observed in naïve control mice. Ag85A-specific CX3CR1$^+$ KLRG1$^+$ CD4$^+$ T cells were comparable in the lung vasculature of all the vaccinated groups tested (Figure 4-21). A very weak signal for higher expansion of the intravascular T cells was detected in the lungs of B-C-Mid immunised mice compared to naïve mice (Figure 4-21).

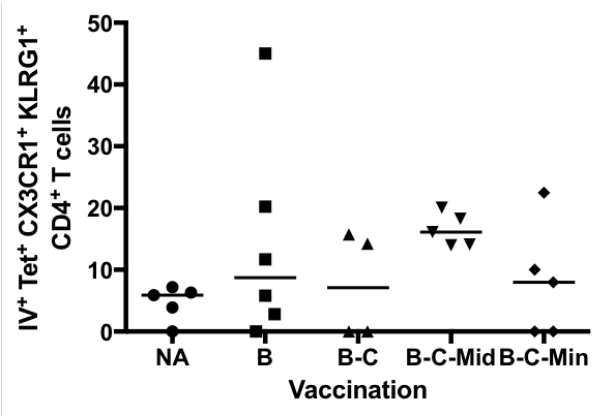

Figure 4-21 Ag85A-specific vascular CX3CR1$^+$ KLRG1$^+$ CD4$^+$ T cells in the lungs of naïve and vaccinated mice 20 weeks post vaccination. Mice were immunised as shown in Figure 4-5. 20 weeks post vaccination, fluorochrome-conjugated CD45.2 was injected intravenously before sacrificing. Lung cells were assessed using surface staining and tetramer staining. Total cell number of Ag85A-specific lung parenchymal CX3CR1$^+$ KLRG1$^+$ CD4$^+$ T cells at 20 weeks post vaccination is presented. Each symbol represents one animal and the line is the median of each group (n=5-6 mice). No statistically significant differences were observed using Kruskal-Wallis test with Dunn's multiple comparisons test.

III. CD4$^+$ T cells responses in the airways 20 weeks following B-C-M vaccination

BAL samples were also analysed at 20 weeks post immunisation. A low number of Ag85A-specific CD44^{hi} CD69$^+$ CD11a$^+$ CD4$^+$ T cells was detected in the airways of BCG immunised mice (Figure 4-22). Boosting BCG with ChAdOx1.85A and/or MVA85A did not enhance the CD4$^+$ T_{RM} in the airways, resulting in no differences were observed when compared to BCG alone (Figure 4-22).

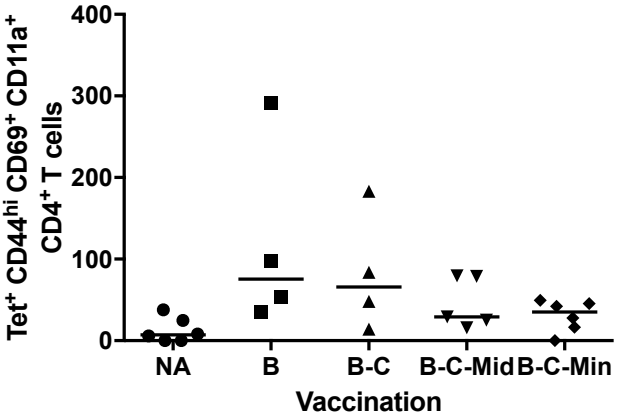

Figure 4-22 Ag85A-specific CD4$^+$ T cells expressing resident memory markers in the airways of naïve and vaccinated mice at 20 weeks post vaccination. Mice were immunised as shown in Figure 4-5. Fluorochrome-conjugated CD45.2 was injected intravenously before sacrificing. BAL samples were assessed using surface staining and tetramer staining. Total cell number of Ag85A-specific CD44^{hi} CD69$^+$ CD11a$^+$ CD4$^+$ T cells in the airways of vaccinated mice and naïve mice at 20 weeks post vaccination. Each symbol represents one animal and the line is the median of each group (n=4-6 mice). No statistical significance was observed using Kruskal-Wallis test with Dunn's multiple comparisons test.

4.2.4.2 $CD8^+$ T cells responses 20 weeks in different lung compartments following B-C-M vaccination

I. **$CD8^+$ T cells responses in the lung parenchyma 20 weeks following B-C-M vaccination**

20 week-post vaccination, Ag85A-specific lung parenchymal $CXCR3^+$ $KLRG1^-$ $CD8^+$ T cells were enhanced after BCG was boosted with ChAdOx1.85A compared to BCG alone (Figure 4-23 A). There were trends for higher responses after MVA boosting on top of B-C vaccination, but the differences were not statistically significant (Figure 4-23 A). In B-C-Mid and B-C-Min mice, Ag85A-specific lung parenchymal $CD8^+$ T cells expressed the protective lung homing markers were significantly increased compared to BCG vaccinated mice (p=0.0058 and p=0.0022 respectively) (Figure 4-23 A). Expressed resident memory markers were also significantly expanded compared to the BCG alone group (p=0.0038 and p=0.0068 respectively) (Figure 4-23 B). A similar pattern of the responses was observed between two memory phenotypes, but the amplitude of lung-homing markers was higher compared to the T_{RM} markers (Figure 4-23 A and B).

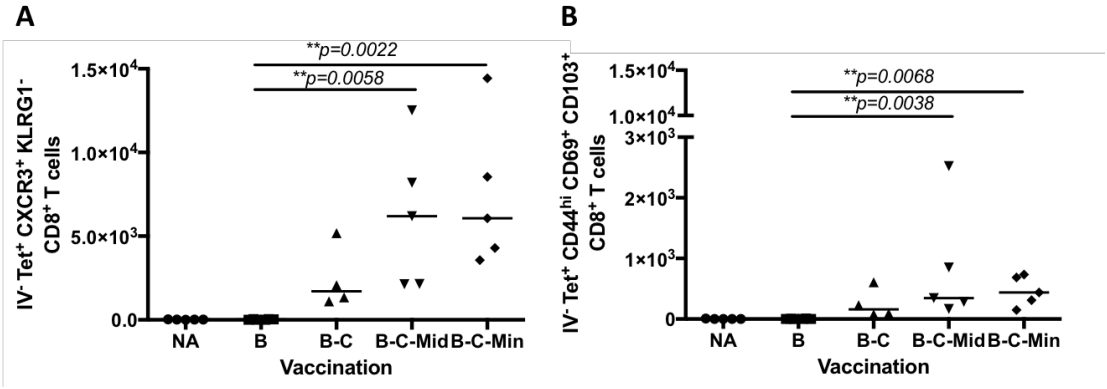

Figure 4-23 Ag85A-specific parenchymal CD8$^+$ T cells expressing memory phenotypes in the lungs of naïve and vaccinated mice at 20 weeks post vaccination. Mice were immunised as shown in Figure 4-5. 20 weeks post vaccination, fluorochrome-conjugated CD45.2 was injected intravenously before sacrificing. Lung cells were assessed using surface staining and tetramer staining. (A) Total cell number of Ag85A-specific lung parenchymal CXCR3$^+$ KLRG1$^-$ CD8$^+$ T cells at 20 weeks post vaccination. (B) Total cell number of Ag85A-specific lung parenchymal CD44^{hi} CD69$^+$ CD103$^+$ CD8$^+$ T cells at 20 weeks post vaccination. Each symbol represents one animal and the line is the median of each group (n=3-4 mice). Statistical significance was determined using Kruskal-Wallis test with Dunn's multiple comparisons test. **, p≤0.01.

II. CD8$^+$ T cells responses in the lung vasculature 20 weeks following B-C-M vaccination

The lung-vascular CD8$^+$ T cells were analysed at 20 week-timepoint. ChAdOx1.85A could not enhance Ag85A-specific CX3CR1$^+$ KLRG1$^-$ CD8$^+$ T cells after boosting BCG primed mice (Figure 4-24). The intravascular cells were significantly increased after boosted with intradermal MVA85A in the lung of B-C-Mid vaccinated mice compared to B-C and BCG groups (p=0.0032 and p=0.0058) (Figure 4-24). In lung vasculature of B-C-Min, the responses were also enhanced but the differences were not statistically significant when compared to B-C and BCG immunised mice (Figure 4-24).

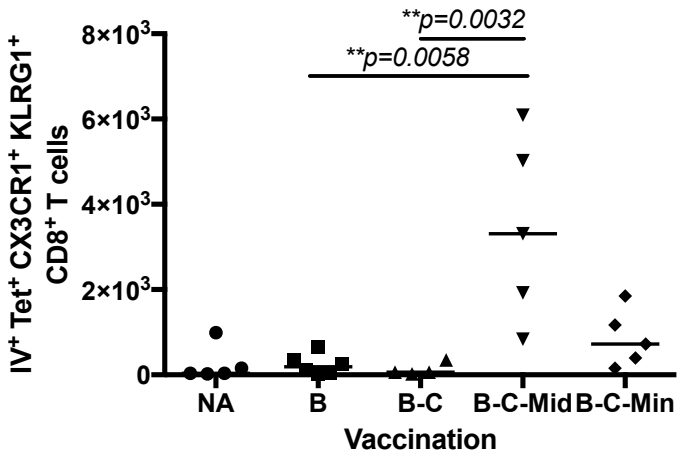

Figure 4-24 Ag85A-specific CX3CR1$^+$ KLRG1$^+$ CD8$^+$ T cells in the lung vasculature of naïve and vaccinated mice 20 weeks post vaccination. Mice were immunised as shown in Figure 4-5. 20 weeks post vaccination, fluorochrome-conjugated CD45.2 was injected intravenously before sacrificing. Lung cells were assessed using surface staining and tetramer staining. Total cell number of Ag85A-specific lung parenchymal CX3CR1$^+$ KLRG1$^+$ CD8$^+$ T cells at 20 weeks post vaccination is presented. Each symbol represents one animal and the line is the median of each group (n=4-6 mice). Statistical significance was determined using Kruskal-Wallis test with Dunn's multiple comparisons test. **, p≤0.01.

III. CD8$^+$ T cells responses in the airways 20 weeks following B-C-M vaccination

Mucosal responses were also observed at 20 weeks after the vaccination completed. BCG failed to induce Ag85A-specific CD44^{hi} CD69$^+$ CD103$^+$ CD8$^+$ T cells in the airway of the immunised mice but the responses were improved when boosted with ChAdOx1.85A (Figure 4-25). Boosting B-C with MVA85A did not enhance the expansion of the airway-T_{RM} but the quantities of the cells were significantly increased in the airways of B-C-Mid and B-C-Min vaccinated mice compared to BCG alone (p=0.0023 and p=0.0039) (Figure 4-25).

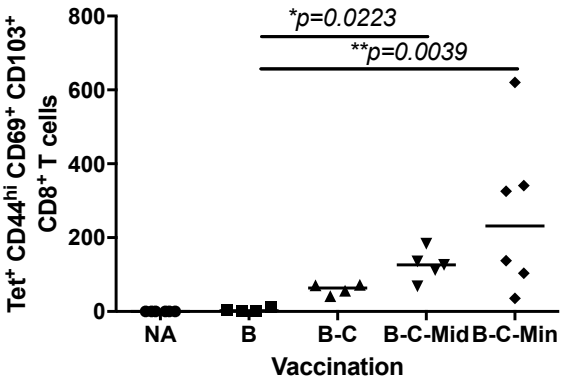

Figure 4-25 Ag85A-specific CD8$^+$ T cells expressing resident memory markers in the airways of naïve and vaccinated mice at 20 post vaccination. Mice were immunised as shown in Figure 4-5. Fluorochrome-conjugated CD45.2 was injected intravenously before sacrificing. BAL samples were assessed using surface staining and tetramer staining. Total cell number of Ag85A-specific CD44^{hi} CD69$^+$ CD103$^+$ CD8$^+$ T cells in the airways of vaccinated mice and naïve mice at 20 weeks post vaccination. Each symbol represents one animal and the line is the median of each group (n=4-6 mice). Statistical significance was determined using Kruskal-Wallis test with Dunn's multiple comparisons test. *p≤0.05; **, p≤0.01.

4.2.5 Lung parenchymal CD4$^+$ T cells induced by B-C-M vaccination as correlates of protection

Resident memory T cell responses in the lungs at 4, 8 and 20 weeks post vaccination have been described in section 4.2.2, 4.2.3 and 4.2.4 respectively. A kinetic change of Ag85A-specific CD4$^+$ T cells expressing CXCR3$^+$ KLRG1$^-$ in the lung parenchyma of B-C-M vaccinated mice was observed to associate with protective efficacy provided by the vaccine regimen. The results from all three timepoints were presented to visibly compare immunogenicity and protectivity induced by B-C-M regimen.

The numbers of the lung parenchymal cells in the lungs of B-C-Mid and B-C-Min vaccinated mice were declined at 20 weeks post vaccination compared to the 8-week timepoint from 500-600 cells to 400 cells when gated on the protective lung-homing phenotype. At 4 weeks post vaccination, the cell number of the lung-parenchymal CD4$^+$ T cells in B-C-Min group was slightly lower than B-C-Mid group (around 300 cells), resulting in loss of protection against *M.tb* infection. The results suggest that Ag85A-specific lung parenchymal CXCR3$^+$ KLRG1$^-$ CD4$^+$ T cells may associate with protection and the number of the memory cells could be crucial to control *M.tb* infection (Figure 4-27).

There was a limitation when interpreting the cell number between the timepoints. The analysis was performed separately for each individual timepoints. It was not possible to analyse all three timepoints at the same time. In theory, the data cannot be directly compared between experiments. However, the cell number for all samples was determined after processing and back calculated into the total cell number of CD4$^+$ T cells in the lungs. The numbers of live cells and CD4$^+$ T cells were comparable

between the three individual experiments. Therefore, the cell number could be compared to observe the expansion of the cell quantity throughout the timepoints.

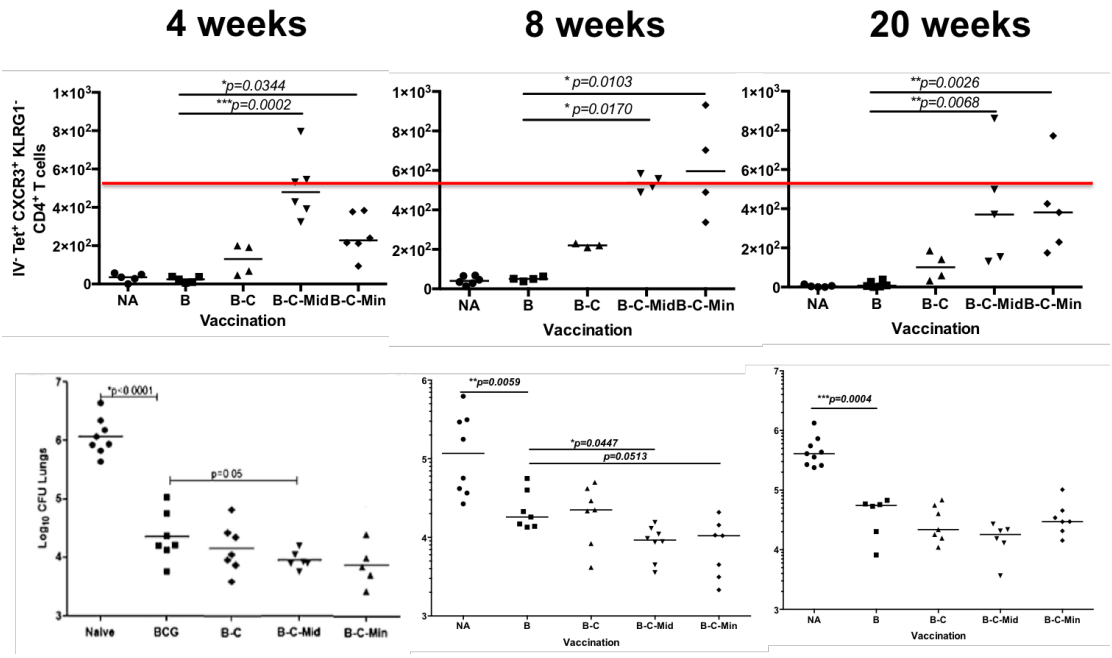

Figure 4-26 Antigen-specific lung-parenchymal CXCR3$^+$ KLRG1$^-$ CD4$^+$ T cells induced by B-C-M vaccination as correlates of protection. The protective efficacy of B-C-M regimen against *M.tb* challenge was assessed at 4, 8 and 20 week post immunisation. Protection was significantly greater than BCG alone at 4 and 8 weeks but not at 20 weeks post vaccination. T cell responses were analysed by selecting for lung parenchymal cells, Ag85A-specific CD4$^+$ T cells (Tet$^+$) and memory T cell markers; CXCR3$^+$ and KLRG1$^-$. This cell population significantly increased in B-C-M immunised mice compared to BCG mice at 4, 8 and 20 weeks post vaccination but the cell number decreased at 20 weeks post vaccination. Each symbol represents one animal and the line is the median of each group. Statistical significance was determined using Kruskal-Wallis test with Dunn's multiple comparisons test.

4.2.6 Functions of the lung parenchymal T cells induced by B-C-M vaccination

Stylianou *et al.* have shown that B-C-M vaccine is the most protective regimen among all the vaccine combinations tested and provides better control of *M.tb* infection in mice at 4 week post vaccination [98]. The vaccine regimen was then examined for the durability of the protection at later timepoints, showing the protective efficacy remained at 8 weeks but did not at 20 weeks post vaccination. Memory T cells responses induced by B-C-M regimen were dissected using intravascular staining to discriminate lung-parenchymal cells and lung-intravascular cells and tetramer staining to identify antigen specific cells. Resident memory and lung-homing markers were optimised and included in the flow cytometry panels for phenotypically characterising memory T cells. As shown in sections 4.2.2, 4.2.3 and 4.2.4, lung parenchymal $CD4^+$ T cells and $CD8^+$ T cells expressing either lung-homing markers or resident memory markers were enhanced by the protective regimen at 4, 8 and 20 weeks post vaccination, suggesting these cell phenotypes could associate with protection. However, the antigen-specific resident memory $CD8^+$ T cells were expanded by B-C vaccination, which is the non-protective regimen. The B-C induced responses were comparable for the B-C-Mid and B-C-Min groups, suggesting that these $CD8^+$ T cell phenotypes could contribute some protective effects but not directly associate with protection. This leaves the antigen-specific lung parenchymal memory $CD4^+$ T cells as a lead candidate for an immune correlate of protection.

The memory phenotypes of the lung parenchymal $CD4^+$ T cells have been thoroughly characterised, but the function of these cells needed to be evaluated further. The

effector function of the lung-parenchymal T cells was assessed in this section and the protective effect tested if promising effector responses observed.

4.2.6.1 Antigen specific cytokine production of the lung parenchymal T cells induced by B-C-M vaccination

To determine effector functions of these cells, intracellular staining for effector cytokines was performed to reveal effector abilities of the lung parenchymal cells. Mice were vaccinated with B-C-M regimen as shown in Figure 4-5. Four weeks post vaccination, the lungs were harvested after 1-minute intravascular injection of fluorochrome-conjugated CD45.2. Lungs cells were stimulated *ex-vivo* with Ag85A peptide pool and PPD-T. The stimulated cells were intracellularly stained for IFN-γ and TNF-α and surface stained for lung-homing markers (Appendix Table 7-4). After staining, the cells were analysed using flow cytometry and gated on T cell markers, intracellular cytokines and protective lung homing phenotypes.

90 % of cytokine-secreting $CD4^+$ T cells, in the lungs of B-C-Min/id, were $CXCR3^+$ $KLRG1^-$ when stimulated with Ag85A (Figure 4-27 A). The cytokine producing $CXCR3^+$ $KLRG1^-$ $CD4^+$ Tells were significantly enhanced after B-C vaccination (p=0.0065) (Figure 4-27 B). B-C-Mid and B-C-Min vaccination compared to BCG alone (p=0.0040 and p=0.0409 respectively) (Figure 4-27 B).

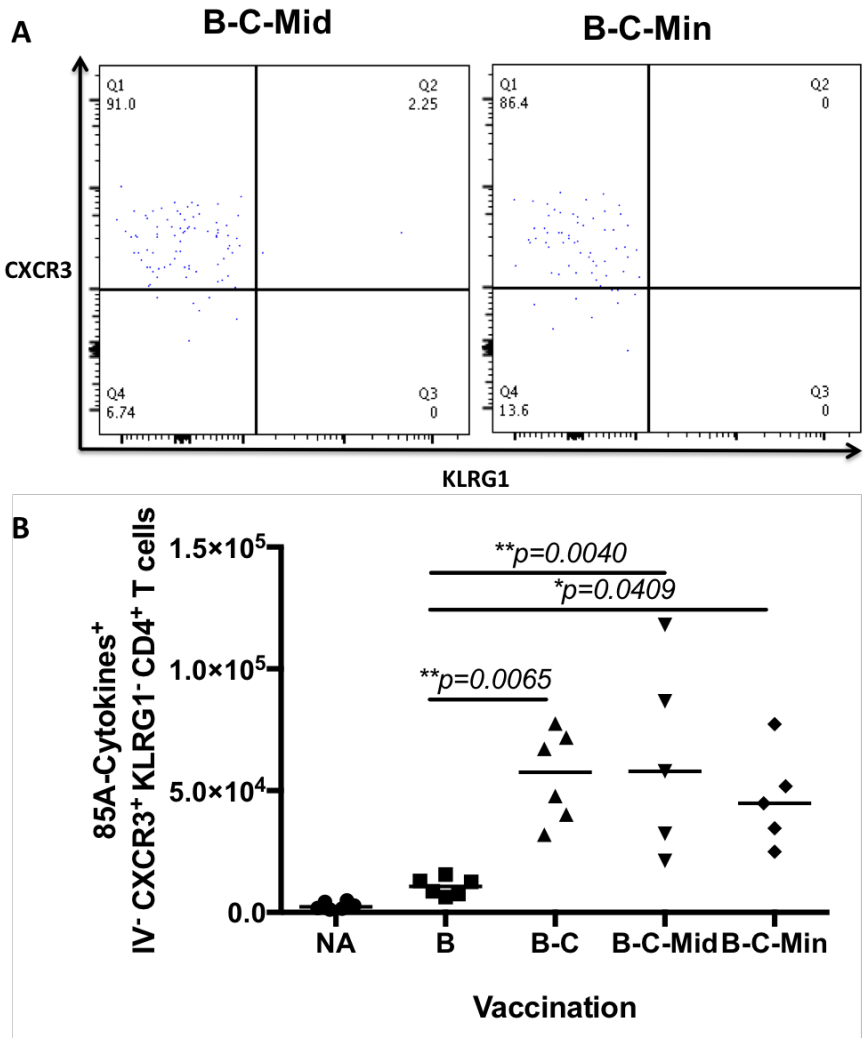

Figure 4-27 Ag85A-specific cytokine producing parenchymal CD4$^+$ T cells expressed CXCR3$^+$ KLRG1$^-$ in the lungs of naïve and vaccinated mice at 4 weeks post vaccination. Mice were vaccinated as shown in Figure 4-5 and analysed at 4 weeks post vaccination. Fluorochrome-conjugated CD45.2 was injected intravenously before sacrificing. Lungs cells were stimulated ex-vivo with Ag85A (85A) peptide pool. (A) Representative flow plots show Ag85A-specific IFN-γ and/or TNF-α producing lung parenchymal CD4$^+$ T cells expressing CXCR3$^+$ KLRG1$^-$ in B-C-Mid (Left) and B-C-Min (Right) mice. (B) Total cell number of Ag85A-specific cytokine producing lung parenchymal CXCR3$^+$ KLRG1$^-$ CD4$^+$ T cells in naïve and vaccinated mice. Each symbol represents one animal and the line is the median of each group (n=4-6 mice). Statistical significance was determined using Kruskal-Wallis test with Dunn's multiple comparisons test. *p≤0.05; **, p≤0.01.

$CD8^+$ T cell responses have also been shown to play a role in protection against *M.tb* infection [50, 75]. In the lungs of B-C-Mid vaccinated mice, 84 % of lung parenchymal $CD8^+$ T cells was $CXCR3^+$ $KLRG1^-$, while 42 % of the cell population expressed $CXCR3^+$ $KLRG1^-$ in BCG mice (Figure 4-10 A Bottom and Top Left). Among the lung parenchymal $CXCR3^+$ $KLRG1^-$ $CD8^+$ T cells in BCG immunised mice, a few of them produced Ag85A-specifc cytokines (IFN-γ and/or TNF-α) (Figure 4-28 A Top Right). On the other hand, the Ag85A-specific cytokine producing cells were detected in most of the lung parenchymal $CXCR3^+$ $KLRG1^-$ $CD8^+$ T cells in B-C-Mid vaccinated mice (Figure 4-28 A Bottom Right). This cytokine producing memory cells were significantly increased in the lung parenchyma of B-C vaccinated mice compared to BCG mice ($p=0.0005$) (Figure 4-28 B). In B-C-Mid and B-C-Min groups, the effector responses were comparable with the B-C group and increased when compared with BCG controls, but the differences were not statistically significant ($p=0.0541$ and $p=0.0708$) (Figure 4-28 B).

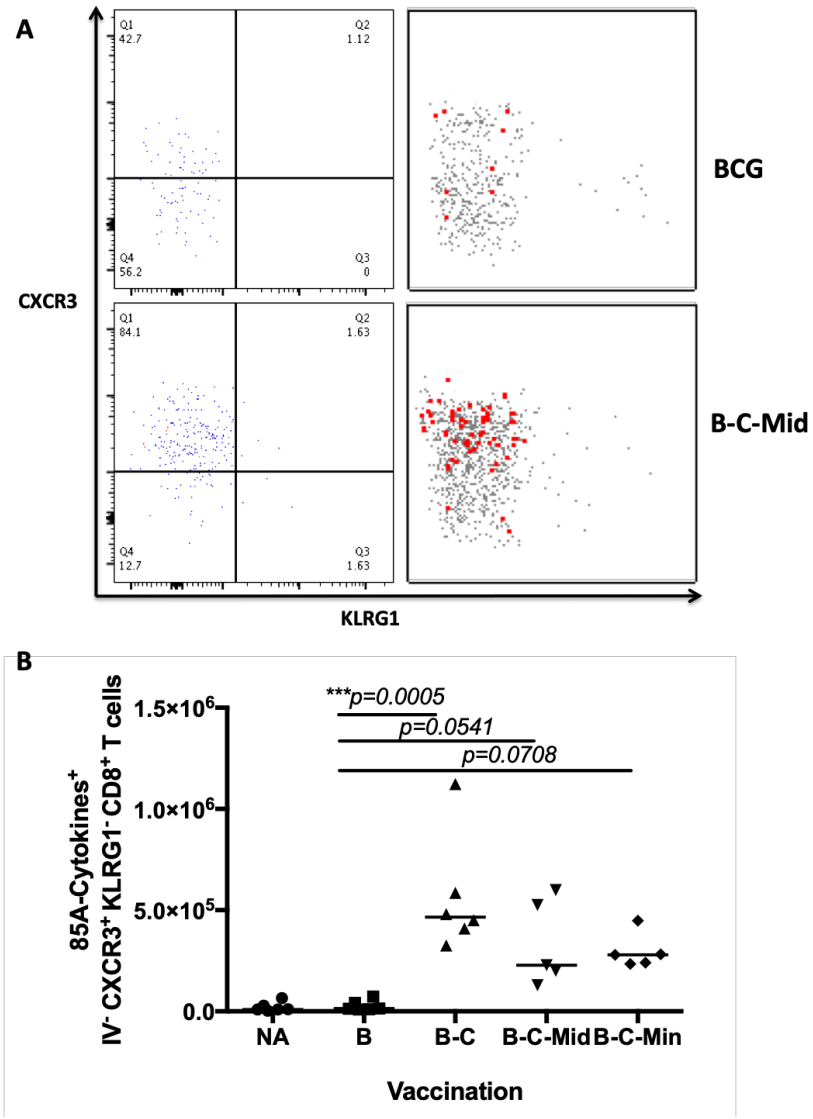

Figure 4-28 Ag85A-specific parenchymal CD8⁺ T cells in the lungs of naïve and vaccinated mice at 4 weeks post vaccination. Mice were vaccinated as shown in Figure 4-5 and analysed at 4 weeks post vaccination. Fluorochrome-conjugated CD45.2 was injected intravenously before sacrificing. Lungs cells were stimulated ex-vivo with Ag85A (85A) peptide pool. (A) Representative flow plots show Ag85A-specific IFN-γ and/or TNF-α producing lung parenchymal CD8⁺ T cells expressing CXCR3⁺ KLRG1⁻ in BCG (Top) and B-C-Mid (Bottom) mice. (A; Right flow plots) The big dots represent Ag85A-specific cytokine producing cells. (B) Total cell number of Ag85A-specific cytokine producing lung parenchymal CXCR3⁺ KLRG1⁻ CD8⁺ T cells in naïve and vaccinated groups. Each symbol represents one animal and the line is the median of each group (n=4-6 mice). Statistical significance was determined using Kruskal-Wallis test with Dunn's multiple comparisons test. ***, p≤0.001.

PPD-T was also used to stimulate the cells to observe the specific responses to *M.tb* proteins. PPD-specific cytokine producing $CXCR3^{+}$ $KLRG1^{-}$ $CD4^{+}$ T cells were significantly increased in the lung parenchyma of B-C mice compared to BCG mice (p=0.0434) (Figure 4-29 A). These cytokine-producing cells in the lung parenchyma of B-C-Mid and B-C-Min mice were comparable with the B-C group (Figure 4-29 A). B-C-Mid and B-C-Min vaccination increased the cytokine secreting cells compared to BCG mice, but the differences were not statically significant (Figure 4-29 A).

PPD-specific cytokine producing $CXCR3^{+}$ $KLRG1^{-}$ $CD8^{+}$ T cells were significantly increased in the lung parenchyma of B-C and B-C-Min mice compared to BCG mice (p=0.0116 and p=0.0018) (Figure 4-29 B). The responses provided by B-C-Mid were comparable with B-C and B-C-Min vaccination but not significantly better compared to BCG controls (p=0.0808) (Figure 4-29 B).

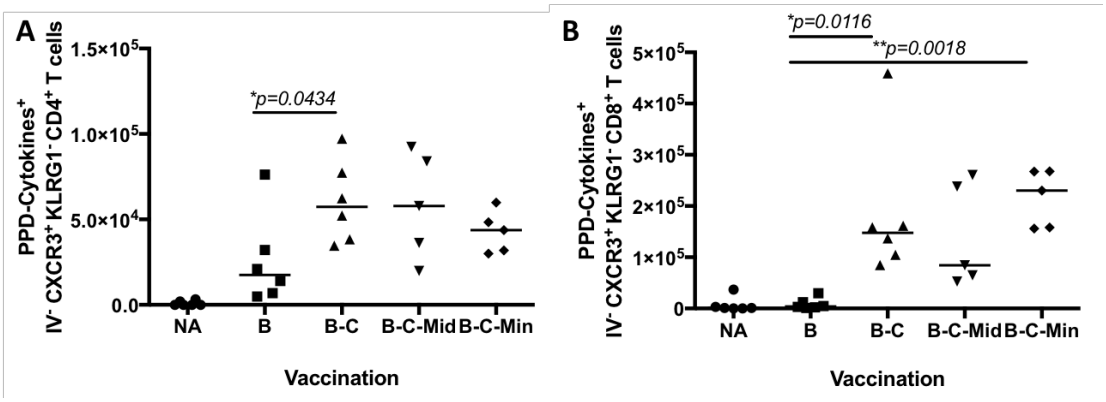

Figure 4-29 PPD-specific parenchymal CD4$^+$ T cells and CD8$^+$ T cells in the lungs of naïve and vaccinated mice at 4 weeks post vaccination. Mice were vaccinated as shown in Figure 4-5 and analysed at 4 weeks post vaccination. Fluorochrome-conjugated CD45.2 was injected intravenously before sacrificing. Lungs cells were stimulated ex-vivo with PPD-T (PPD). Total cell number of PPD-specific cytokine producing lung parenchymal CXCR3$^+$ KLRG1$^-$ CD4$^+$ T cells (A) and CD8$^+$ T cells (B) in naïve and vaccinated mice. Each symbol represents one animal and the line is the median of each group (n=4-6 mice). Statistical significance was determined using Kruskal-Wallis test with Dunn's multiple comparisons test. *p≤0.05; **, p≤0.01.

4.2.6.2 Adoptive transfer of antigen specific lung parenchymal CD4$^+$ T cells from B-C-M immunised mice

Ag85A-specific lung parenchymal T cells expressing CXCR3$^+$ KLRG1$^-$, induced by B-C-M, are associated with protection. In the previous section 4.2.6.1, the effector function of the lung parenchymal T cells expressing the protective memory phenotype were observed. This cell type was able to produce IFN-γ and TNF-α both of which have been shown to play a role in protection against TB. The protective function of this memory phenotype was then tested using an adoptive transfer approach. I decided to adoptively transfer Ag85A-specific lung parenchymal CD4$^+$ T cells (IV- Tet+) from B-C-Mid vaccinated mice into naïve recipient mice to determine the protective function of these cells against *M.tb* challenge.

l. **Optimisation of the purity of the antigen specific CD4$^+$ T cells in the lung parenchyma and lung vasculature from B-C-M immunised mice**

To my knowledge, this was the first time ever that tetramer-specific lung parenchymal CD4$^+$ T cells have been adoptively transferred to observe their protection against *M.tb* challenge. There were difficulties of performing this experiment especially sorting the antigen-specific cells. MHC class II tetramer weakly detected antigen-specific CD4$^+$ T cells, resulting in very low number of tetramer positive cells after cell sorting. Thus, optimisation of the purity of the antigen specific cells was conducted to find an optimal sorting strategy to maximise cell purity but avoid compromising cell number.

From the 1st sorting, the purity of IV- Tet+ cells was 70 %, while the purity of IV+ Tet+ cells was 31 % (Figure 4-30 Top Middle and Right). The yields of the sorted cells were around 1000-1200 cells per sample for each population. The sorting gates were then

adjusted aiming to increase the purity. The purity of IV- Tet+ cells in the 2nd sorting was 97 % (Figure 4-30 Bottom Middle). IV+ Tet+ cell purity was also increased to 68 % in the 2nd sorting (Figure 4-30 Bottom Right). The yields of the sorted cells were slightly decreased, recovering the cells from the sorting around 600-800 cells per sample for each population. Perdomo *et al*. transferred 2500 cells of T_{RM} and T_{EM} cells from the airways of the donor into naïve recipients [75] and the protection against *M.tb* challenge was observed in this study. I then aimed to transfer around 5000 cells for each IV- Tet+ and IV+ Tet+ cell populations which resulted in 8:1 ratio of B-C-Mid donors: naïve recipients.

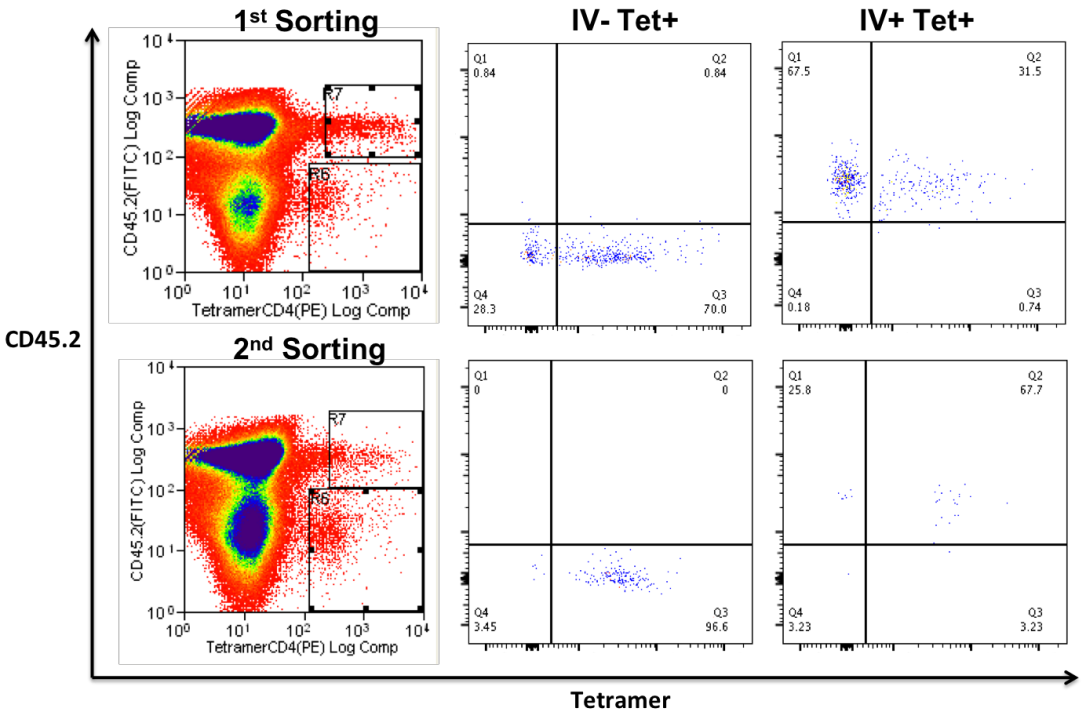

Figure 4-30 Purification of Ag85A-specific lung parenchymal and intravascular CD4$^+$ T cells from B-C-M donor mice before transferring to naïve recipients. B-C-Mid vaccinated mice were injected intravenously with fluorochrome-conjugated CD45.2 (IV) at 1 minute before the lungs were harvested. Lung cells were stained with CD4 tetramer (Tet) and positively sorted for IV- Tet+ and IV+ Tet+ cells. Test sorting was performed twice,1st sorting (Top flow plots) and 2nd sorting (Bottom flow plots). Flow plots of sorting gates (Left column). Purity flow plots of IV- Tet+ cells after sorted (Middle column). Purity flow plots of IV+ Tet+ cells after sorted (Right column).

II. Adoptive transfer of antigen-specific lung parenchymal $CD4^+$ T cells from B-C-M immunised mice into naïve mice

a. Design of adoptive transfer experiments

Adoptive transfer experiments were set up as shown in Figure 4-31. B-C-Mid donors were injected intravenously with anti-CD45.2-FITC. One minute after the injection, lungs were harvested and stained with MHC class II tetramer. The stained cells were sorted into IV- Tet+ and IV+ Tet+ populations. IV+ Tet+ cells were also transferred for comparison. Around 5000 cells (from 7-8 donors) were transferred intravenously into each of the naïve recipients. The adoptive transfer study was performed in two separate experiments, transferring the cells to 3 naïve recipients per group in each case. This was due to the limitation of the donor samples that could be processed in a day. The mice were challenged with *M.tb* one day after the transfer which has been shown to be enough time for the memory cells to migrate back to the lungs after adoptively transferred [75, 106]. Two control groups were also included in the challenge study, a group vaccinated with B-C-Mid as positive control and naïve mice used as a negative control. Lungs and spleens were harvested 4 weeks post infection for bacterial enumeration.

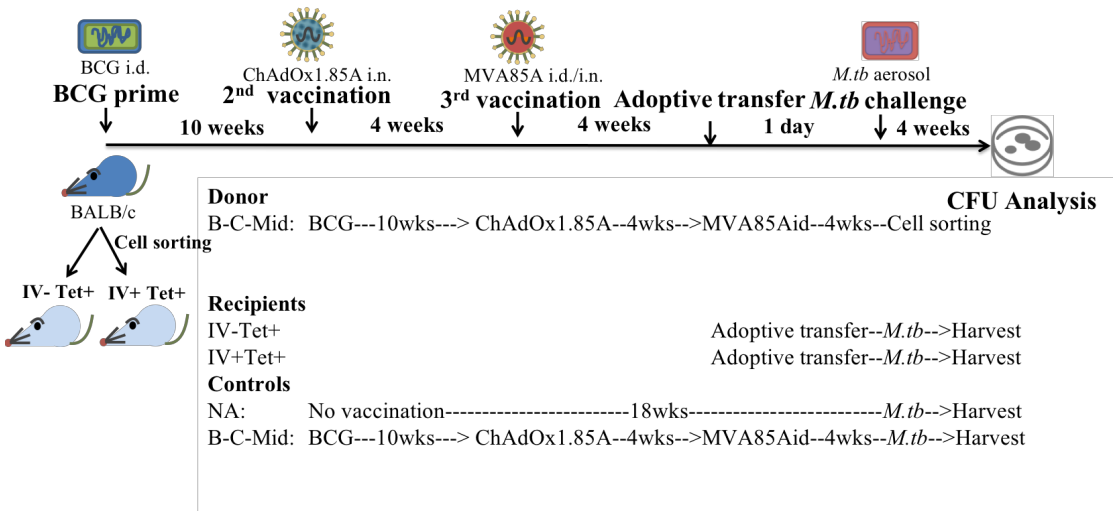

Figure 4-31 Timeline of adoptive transfer experiment from B-C-Mid donors to naïve recipients before *M.tb* challenge. BALB/c mice were vaccinated intradermally (i.d.) with $4x10^5$ CFU of BCG Pasteur (B) and boosted 10 weeks later with $1x10^8$ ifu of ChAdOx1.85A (C) intranasally (i.n.). Four weeks after ChAdOx1.85A vaccination, MVA85A was delivered intradermally (Mid) in a dose of $5x10^6$ pfu. Some of the B-C-Mid mice were used as donors and the rest were assigned as positive controls. Four weeks post vaccination, the donors were injected intravenously with fluorochrome-conjugated CD45.2 (IV) at 1 minute before the lungs were harvested. Lung cells were stained with CD4 tetramer (Tet) and positively sorted for IV- Tet+ and IV+ Tet+ cells. Around 5000 cells of each population were adoptively transferred to assigned naïve recipients. Some naïve mice were used as negative controls. The recipients and the controls were challenged with 50-100 CFU of aerosol *M.tb* Erdman 1 day after the adoptive transfer. Four weeks after challenge, lungs and spleens were harvested for CFU enumeration.

b. Purity of adoptively transferred cells

In the first transfer, the purity of IV- Tet+ cells was 70 % whereas the purity if IV+ Tet+ cells was 44 % (Figure 4-32). The purity in the second sorting was comparable with the first one, obtaining 64 % and 40 % of the purity for IV- Tet+ and IV+ Tet+ respectively (Figure 4-32).

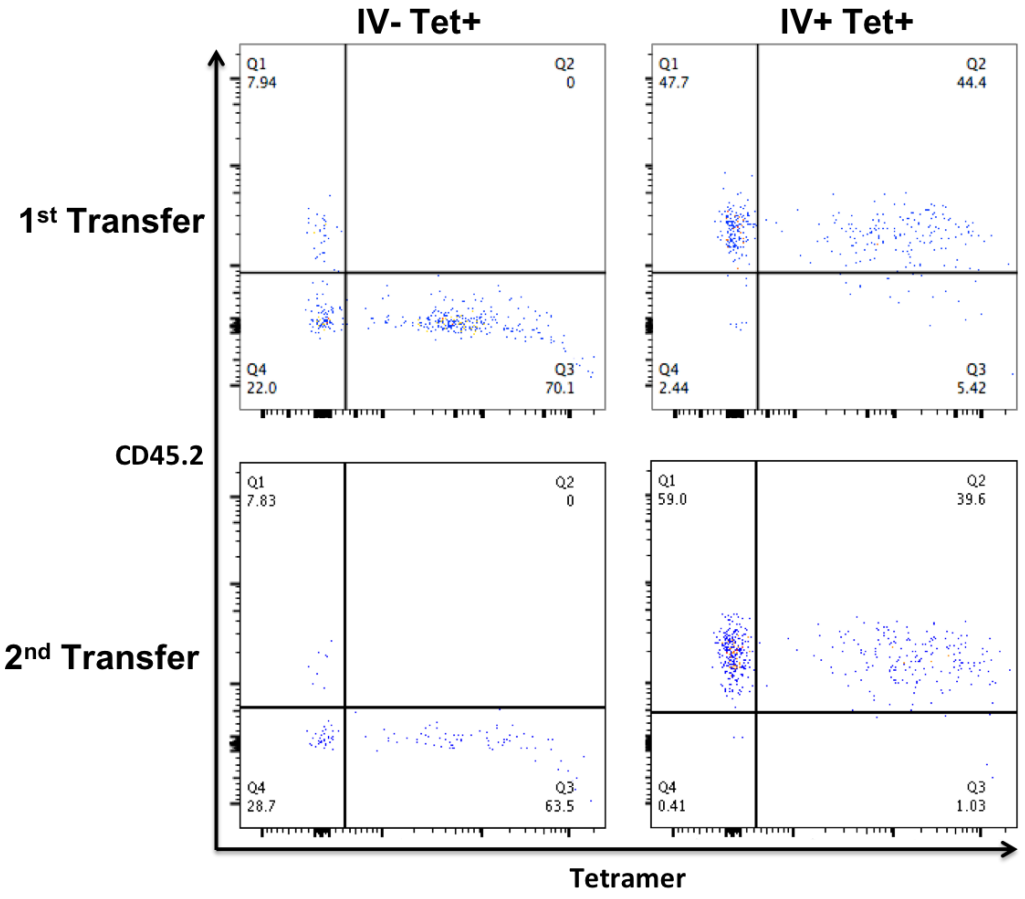

Figure 4-32 Purity of adoptively transferred cells from B-C-M donors to naïve recipients. Mice were vaccinated as shown in Figure 4-31. Four weeks post vaccination, the B-C-Mid donors were injected intravenously with fluorochrome-conjugated CD45.2 (IV) at 1 minute before the lungs were harvested. Lung cells were stained with CD4 tetramer (Tet) and positively sorted for IV- Tet+ and IV+ Tet+ cells. Adoptive transfer was performed twice, 1st transfer (Top flow plots) and 2nd transfer (Bottom flow plots). Purity flow plots of IV- Tet+ cells after sorted (Left column). Purity flow plots of IV+ Tet+ cells after sorted (Right column).

c. Viability of adoptively transferred cells pre and post transfer

The viability of the sorted cells was examined before and at the time of the adoptive transfer. Before the transfer, almost 100 % of the sorted were live after the first and the second sorting (Figure 4-33 Left column). After the cells were transferred into naïve recipients, the leftover cells were Live/Dead stained for viability testing, showing 100 % of live cells (Figure 4-33 Right column).

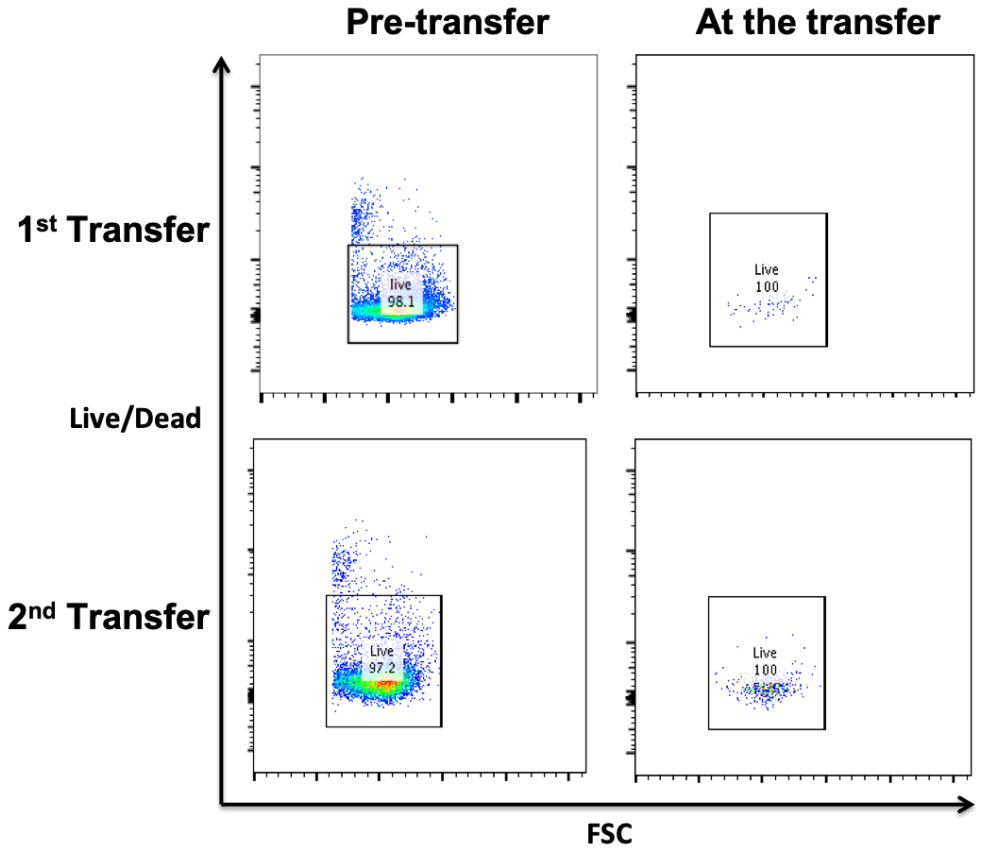

Figure 4-33 Viability of the sorted cells from B-C-M donors pre-adoptive transfer and at the adoptive transfer. Adoptive transfer was performed as shown in Figure 4-31. B-C-Mid donors were injected intravenously with fluorochrome-conjugated CD45.2 (IV) at 1 minute before the lungs were harvested. Lung cells were stained with CD4 tetramer (Tet) and positively sorted for IV- Tet+ and IV+ Tet+ cells. The cells were adoptively transferred twice, 1st transfer (Top flow plots) and 2nd transfer (Bottom flow plots). Some sorted cells were stained for Live/Dead before the transfer (Pre-transfer) and at the time of transfer (At the transfer).

III. **Protection against aerosol *M.tb* challenge in naïve mice receiving antigen specific lung parenchymal CD4$^+$ T cells adoptively transferred from B-C-M immunised mice**

In the lungs, the B-C-Mid vaccinated group had lower bacterial count compared to the naïve control group, but the difference was not statistically significant (Figure 4-34 A) (p=0.0825). There was no protection observed in the recipient mice since the bacterial counts of both IV- Tet+ and IV+ Tet+ -recipient mice were comparable to naïve mice (Figure 4-34 A). Similar results were observed in the spleen (Figure 4-34 B). B-C-Mid was protective in the spleens of vaccinated mice but it was not significantly better compared to naïve mice (Figure 4-34 B) (p=0.0631). The experiment was performed twice (Red and blue dots) with similar results in lungs and spleens (Figure 4-34 A and B).

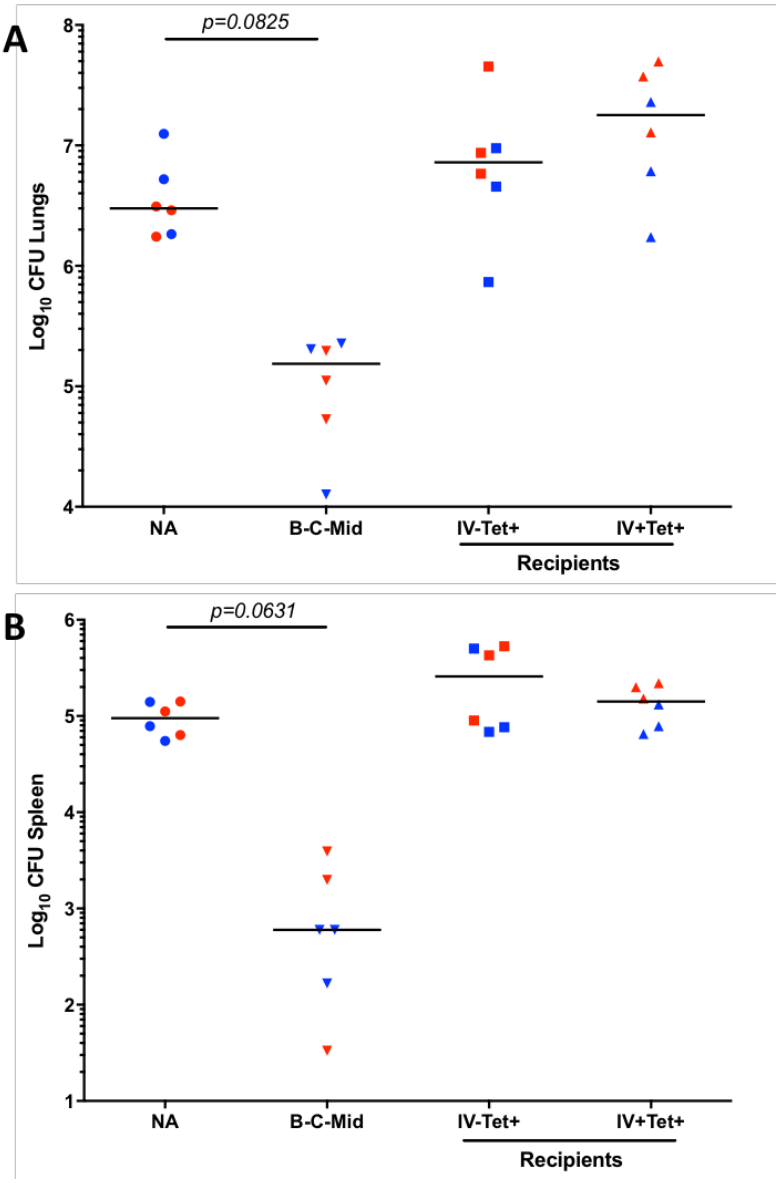

Figure 4-34 Protection against aerosol *M.tb* challenge in naïve mice receiving antigen specific lung parenchymal CD4$^+$ T cells adoptively transferred from B-C-Mid immunised mice. Adoptive transfer experiments were performed as shown in Figure 4-31. IV- Tet+ and IV+ Tet+ cells were collected from 21-24 donors and adoptively transferred to 3 recipients in each group. *M.tb* challenge was performed 1 day post adoptive transfer. Lungs (A) and spleens (B) were analysed for bacterial colonies. The experiment was performed twice with identical vaccination protocol. Red and blue symbols show the results from the two separate experiments. Each symbol represents one animal and the line is the median of each group (n=6 mice). Statistical significance was determined using Kruskal-Wallis test with Dunn's multiple comparisons test.

4.3 **Discussion**

The protection provided by B-C-M regimen 4 weeks post vaccination has been reported by our group [98]. In the previous chapter, the protective efficacy was observed at 8 weeks but not 20 weeks after the B-C-M vaccination. Without MVA boost, B-C failed to provide protection against *M.tb* at all three timepoints. Potential immune correlates of protection were then investigated in terms of T cell and antibody responses. Total IgG in the circulation and secretory IgA in the airways did not associate with protection. Effector cytokine producing T cells were increased in the lungs and spleen of mice immunised with the protective and non-protective regimes. Therefore, these cell populations were shown not to correlate with protection. In this chapter, lung-parenchymal and lung-intravascular lymphocytes were clearly identified using intravascular staining technique. Resident memory and lung-homing phenotypes were selected to characterise the memory T cell responses, identifying correlation between these memory phenotypes and the protection of B-C-M regimen.

Concerning CD8 responses, lung-homing phenotype ($CXCR3^+$ $KLRG1^-$) and resident memory phenotype ($CD44^{hi}$ $CD62L^{low}$ $CD69^+$ $CD103^+$) of Ag85A-specific lung parenchymal $CD8^+$ T cells both were increased in B-C, B-C-Mid and B-C-Min groups compared to BCG alone at 4, 8 and 20 weeks post vaccination. Consistent with recent reports, resident memory $CD8^+$ T cells were enhanced after vaccination with BCG and subunit vaccines [75, 121]. As the responses were also observed in the B-C group which was the non-protective regimen, these cells may not directly correlate with protection. However, the effector function of lung parenchymal $CXCR3^+$ $KLRG1^-$ $CD8^+$ T cells was shown in this chapter as they produced antigen-specific IFN-γ and TNF-α.

These cells might have a role in control of *M.tb* infection and contribute to protection. In a recent study, protective function of resident memory $CD8^+$ T cells has been shown using mucosal adoptive transfer of the airway-$CD8^+$ T_{RM} cells but only after the recipients had BAL removal before the transfer [75].

At 4, 8 and 20 weeks post B-C-M vaccination, Ag85A-specific $CD4^+$ T cells, displayed a $CXCR3^+$ $KLRG1^-$ phenotype, were increased in the lung-parenchyma of B-C-Mid and B-C-Min immunised mice. This lung-parenchymal cells have been found in the lungs of *M.tb* infected mice, conferring protection against the infection [106]. In systemic vaccination with a subunit vaccine, the same cell phenotype was observed in the circulation of the vaccinated mice [145]. Jeyanathan *et al.* have reported the same finding following systemic vaccination with a viral-vectored TB vaccine [220]. The pattern of the lung parenchymal cells displayed a $CD44^{hi}$ $CD69^+$ $CD11a^+$ phenotype mirrored the cell pattern presented $CXCR3^+$ and $KLRG1^-$. This resident memory phenotype of $CD4^+$ T cells was significantly increased in B-C-Mid and B-C-Min groups compared to BCG immunised mice at 4, 8 and 20 weeks post vaccination. Consistent with Perdomo *et al.,* Resident memory T cells were detected in the airways following mucosal vaccination of BCG [75].

Without MVA, B-C failed to enhance the memory $CD4^+$ T cells in the lung parenchyma of the vaccinated mice. The responses obtained from the non-protective regimen were not significantly higher compared to BCG vaccination. This result could explain the inferior protection of B-C compared to B-C-M vaccination. Unlike B-C, B-C-M regimen consistently protected against *M.tb* challenge at 4 and 8 weeks post vaccination but it was no longer protective 20 week-post immunisation. This could be

explained by the reduction of the antigen-specific lung-parenchymal $CD4^+$ T cells displaying the protective phenotype, suggesting that Ag85A-specific lung parenchymal $CXCR3^+$ $KLRG1^-$ $CD4^+$ T cells may correlate with protection.

Ag85A-specific lung-parenchymal $CXCR3^+$ $KLRG1^-$ $CD4^+$ T cells induced by B-C-M regimen may correlate with protection. Effector cytokine production of these cell was analysed to test for effector function of the cells. Ag85A-specific IFN-γ and TNF-α cytokines were detected in the lung-parenchymal $CXCR3^+$ $KLRG1^-$ CD4+ T cells induced by B-C-M regimen, suggesting these memory cells may contribute some effector responses to control *M.tb* infection. The protective function of these cells was tested using adoptive transfer.

To demonstrate potential protection provided by these antigen-specific lung parenchymal $CD4^+$ T cells, adoptive transfer experiments were performed. There was no protection observed in the lungs and spleen of naïve recipient mice receiving either the antigen-specific lung-parenchymal cells or the antigen-specific lung-vascular cells. A few studies have successfully performed adoptive transfer of lung-parenchymal $CD4^+$ T cells from *M.tb*-infected mice [106, 120]. These memory cells are shown to be able to traffic back to the lung-parenchyma in a day and confer protection against *M.tb* challenge. However, the recipients in the transfer were *M.tb*-infected mice or T cell-deficient mice. By using an infection-matched recipient, the requirement of donor cells to the lung-parenchyma may result from unspecific attracting chemokine from the inflammation not from the lung-homing capacity. In this chapter, the donor cells were then adoptively transferred to naïve recipients rather than infected mice. The naïve recipients were also immunocompetent to truly reflect the effect of the lung-

parenchymal cells. This may have made it more difficult to observe protective responses after *M.tb* challenge.

In addition to the difficulties on the existing immune responses in the lungs of the recipients, there were several technical challenges in the cell number obtained after sorting the lung cells. The lack of effective MHC class II tetramers to identify antigen specific cells greatly compromised the yield after sorting. By increasing the specificity of the sorting gate, the quantity of the tetramer positive cells was substantially decreased. The purity of sorted cells was determined to be around 70 % for IV- Tet+ cells and around 40-60 % for IV+ Tet+ cells. Perdomo *et al*. mucosally transferred 2500 cells of airway-$CD4^+$ T cells expressing a T_{RM} phenotype with the purity of 86 % into the recipient lungs, conferring protection against *M.tb* infection [75]. Even though 5000 cells of Ag85A-specific lung-parenchymal/lung-vascular cells were transferred, no protection was observed in the lungs and spleen of recipient mice. It was also difficult to keep the lung cells viable after purification. The viability of the cells after cell sorting and at the time of the transfer was assessed, showing 99-100 % of live cells.

In summary, immune correlates of protection were revealed after combining intravascular staining with tetramer and surface staining for resident memory and protective lung-homing phenotypes. This approach specifically identified lung-parenchymal cells and allow the surface markers to phenotypically characterise T cell responses induced by B-C-M vaccination. B-C-M regimen enhanced Ag85A-specific lung-parenchymal $CXCR3^+$ $KLRG1^-$ $CD4^+$ T cells further compared to BCG alone at 4, 8 and 20 weeks post vaccination. The number of these cell declined at 20 week which correlated with the loss of protection at the same timepoint. Effector function of

$CXCR3^+$ $KLRG1^-$ $CD4^+$ T cells was observed in the lung-parenchymal of B-C-M immunised mice after stimulated with Ag85A. Due to several limitations of adoptive transfer experiments, no protection was observed in the lungs and spleen of immunocompetent naïve recipients received the antigen-specific lung-parenchymal and lung-vascular $CD4^+$ T cells.

Chapter 5. Novel Mycobacterium tuberculosis antigens

5.1 **Introduction**

A key challenge to subunit vaccine development is the selection of protective antigens for inclusion into a vaccine delivery system. Sequencing of the genome of *M.tb* discovered around 4000 genes [165], which led to an effort to identify antigens that would be most suitable for vaccine research and development [166]. The limited understanding of the function of the antigens, together with the lack of immune correlates of protection, contribute to challenges in vaccine design [167, 168].

A subunit vaccine can express one or multiple mycobacterial antigens and can be delivered as DNA vaccines, proteins in adjuvants or expressed by recombinant viral vectors [69, 70].

Recombinant viral vector vaccines have been used as vaccine candidates to deliver immunodominant antigens into the cytoplasm of host cells [77, 78, 79] and have been shown to strongly induce adaptive immune responses [76, 77]. MVA85A was the first prophylactic TB vaccine candidate to be evaluated in a phase 2b efficacy trial [82, 94]. This study showed the vaccine was safe but unable to protect against TB beyond the efficacy of BCG [95]. Thus, there is a need to further improve the efficacy of this vaccine in a variety of ways. In mice, boosting BCG with intranasally administered ChAdOx1.85A, followed by an intradermal or intranasal boost with MVA85A, resulted in a significant improvement of BCG efficacy [98].

It is possible that one of the reasons that MVA85A failed to improve BCG induced protection was because this vaccine candidate only contains a single mycobacterial antigen. In an attempt to further improve the protective efficacy of the BCG-

ChAdOx1.85A-MVA85A vaccination regimen, novel *M.tb* antigens have been identified that could be used in combination with Ag85A. Multi-antigen vaccines might be a better approach to induce different immune responses and improve protection against TB [223, 224]. Moreover, this approach could increase a chance to cover a diverse human population [225]. Lewinsohn *et al.* identified a number of immunodominant $CD8^+$ T cell antigens, which were strongly recognised by active TB patients and *M.tb* latently infected individuals [174]. Stylianou *et al.* then confirmed the immunogenicity of these antigens in *M.tb* infected mice [121]. The advantage of this approach is that the antigen can be used to make both prophylactic and therapeutic vaccines. I selected six mycobacterial antigens from this list to evaluate for protective efficacy. The known functions of these antigens are shown in Table 5-1. To develop a subunit vaccine that will boost BCG, one of the most important criteria for selection was expression by BCG. All the selected antigens were expressed by BCG except PPE68. However, this antigen appeared to be promising and has been used as a vaccine candidate. Therefore, it was selected to proceed to viral vector vaccine construction [226, 227].

Table 5-1 Novel *M.tb* antigens and their functions

Antigen names	Gene numbers	Functions
PE-PGRS50	Rv3345c	• Contains calcium binding motifs, associated with immunopathogenesis of virulent *M.tb* strains [228]
PE-PGRS23	Rv1243c	• N/A
Cation transporter ATPase F (CtpF)	Rv1997	• Coding for the P-type ATPase cation transporter which is affected by hypoxia and over-expression of *M.tb* DosR regulator [229] • Used for the development of anti-tuberculosis drugs and vaccines [230]
Iron-regulated transporter A (IrtA)	Rv1348	• Involved in the iron export of *M.tb,* interfering the balance of siderophores and thus iron inside *M.tb* [231]
PPE68	Rv3873	• Absent from BCG and the attenuated strains of *M.tb* [165]. • Inducing IFN-γ production in *M.tb* infected mice [226] • Being used in TB vaccine candidates, overexpressed in BCG [226, 227]
PE9	Rv1088	• Forms a complex with PE10 to induce apoptosis of macrophages through Toll-like receptor 4 ligand [232]

PE-PGRS50 (Rv3345c) and PE-PGRS23 (Rv1243c) belong to the *M.tb* PE-PGRS multigene family which are thought to be expressed on the surface of the pathogen and to be involved in antigenic variation. PE-PGRS50 and PE-PGRS23 are novel antigens in this family. No particular function has been identified for PE-PGRS23. On the other hand, PE-PGRS50 contains a large number of calcium binding motifs which are associated with immunopathogenesis of virulent *M.tb* strains [228].

CtpF (Rv1997) is a gene coding for the P-type ATPase cation transporter of *M.tb*, which is activated under stress conditions, such as hypoxia and starvation, and is important for the survival of latent *M.tb* [229]. Anti-tuberculosis drugs and toxic substances also induce the expression of this gene [230].

The balance of iron metabolism is one of the basic survival strategies of mycobacteria. Iron-regulated transporter A (IrtA) (Rv1348) is involved in the iron export of *M. tb* [231]. Boosting immune responses using this antigen may enhance a protective effect against *M.tb*.

PPE68 (Rv3873) belongs to the PPE family of *M.tb* proteins. PPE68 protein is absent from BCG and the attenuated strains of *M.tb* [165]. It plays an important role in antigen diversity and the mechanism of immune escape. Interestingly, candidate TB vaccines have been made using this antigen by recombining with BCG [226, 227].

PE9 (Rv1088) is an important surface protein of *M.tb* from the PE family. PE9 forms a complex with PE10, inducing macrophage apoptosis through Toll-like receptor 4 ligand [232].

All antigens selected belong to the PE/PPE family (N-terminal motifs Pro–Glu (PE) or Pro–Pro–Glu (PPE)), which have a conserved structure and repeat motifs [178, 179, 180]. This could be a potential source of mycobacterial antigenic variation and host immune evasion [180]. However, most PE and PPE proteins have no known functions and their high degree of homology makes them difficult to study [179, 180, 233]. A subgroup of the PE proteins contains polymorphic GC-rich sequences (PGRS), while a subgroup of the PPE proteins contains major polymorphic tandem repeats (MPTR) [165, 178, 234]. Both these sub-groups are characterised by their GC-rich DNA sequences, having repetitive glycine-rich amino acid motifs and high molecular weight up to ~365 kilodalton (kDa) [165, 235]. Several of the members have been shown to induce strong $CD4^+$ T cell responses and conferred protection in vaccinated mice [181]. Members of this family have also been shown to elicit $CD8^+$ T cell responses in humans [182]. A recent study has reported that PPE15, which was selected using the same criteria as the six antigens I selected, provided protection against *M.tb* infection in mice when expressed in a ChAdOx1 vector [121]. Additionally, this ChAdOx1.PPE15 vaccine candidate improved BCG-induced protection in the lungs and spleens of BCG primed-ChAdOx1.PPE15 boost vaccinated mice compared with BCG alone [121]. Taken together, immunogenic proteins from this family could potentially be promising candidates for vaccine construction.

The aims of this chapter were:

1. To construct recombinant viral vector vaccines expressing novel *M.tb* antigens and evaluate their immunogenicity. To obtain the vaccines, 6 antigens were

selected and cloned into ChAdOx1 and MVA. The viral vaccines were then tested in mice for immunogenicity studies.

2. To determine the protective efficacy the new vaccines. The immunogenic vaccines were tested for protection against *M.tb* challenge with and without a BCG prime. To observe maximum protection, B-C-M regimen was used as the best protective vaccine combination.

5.2 **Results**

5.2.1 Viral vector vaccines expressing novel *M.tb* antigens

The amino acid sequence of each antigen was sent to GeneArt for the construction of DNA sequences. PE-PGRS50 is presented as a representative example of the cloning steps (Figure 5-1 A). After each cloning step, plasmid DNA was sent off for sequencing to confirm the presence of the insert and correct sequence. The PE-PGRS50 fragment (1.3 kilo base pairs (kbp)) was cloned into a gateway entry vector (p1990) (Figure 5-1 B). To confirm insertion of the fragment, the plasmid was digested with Acc65I and NotI, resulting in 4.7 kbp for the backbone plasmid and 1.3 kbp for the antigen (Figure 5-1 C). The gateway entry vector containing PE-PGRS50 was recombined with a destination vector coding for the ChAdOx1 vector; (Figure 5-1 D). The resulting plasmid was sequenced, linearised and sent off for virus preparation (Figure 5-1 E).

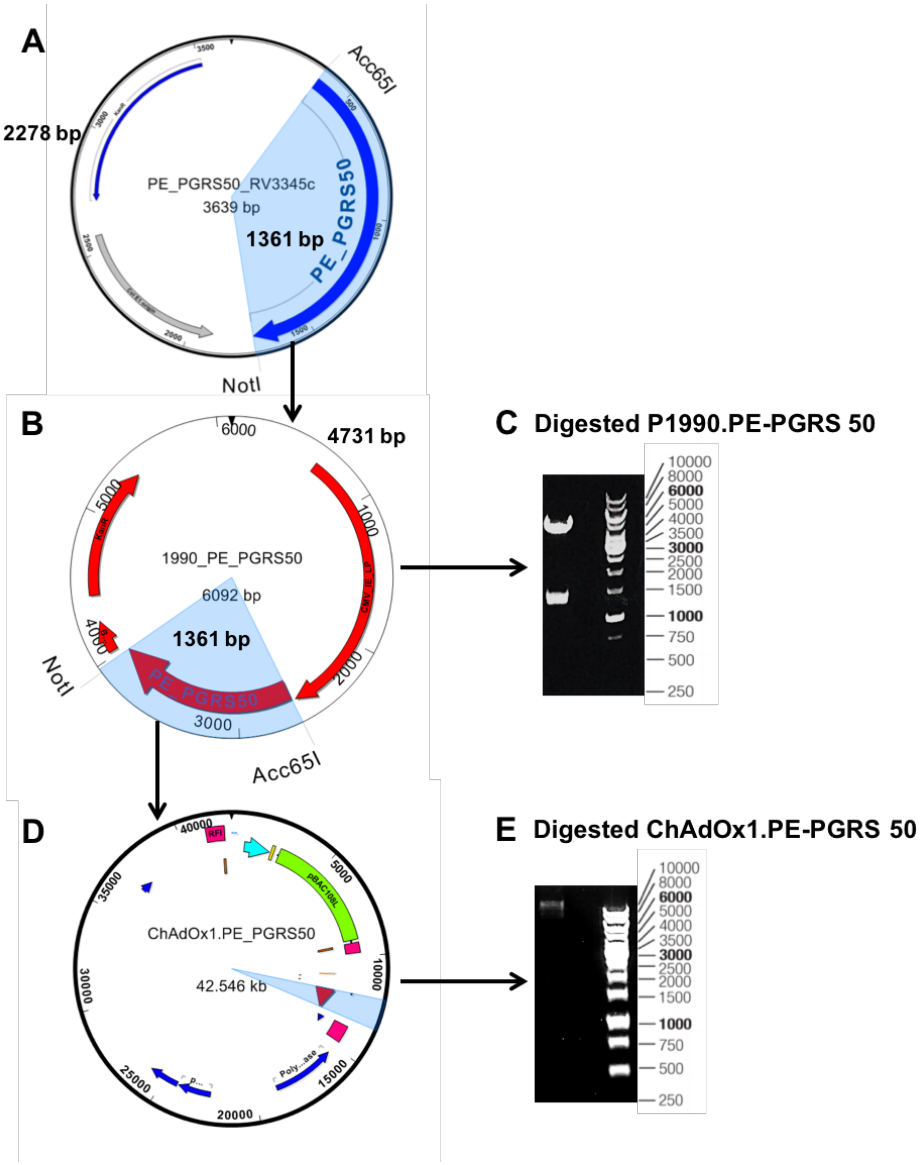

Figure 5-1 Cloning steps for the construction of ChAdOx1 expressing the new antigens. (A) The plasmid containing the mycobacterial antigen DNA sequence (PE-PGRS50) was transformed into competent cells. The DNA plasmid was then purified and digested with Acc651 and NotI to excise the antigen insert (B). The 1361 bp DNA fragment was cloned into p1990 gateway entry vector. (C) Test digestion was performed with Acc65I and NotI to confirm the presence of the correct size antigen fragment. (D) The gateway entry clone in (B) was recombined with the destination vector; ChAdOx1. (E) ChAdOx1 expressing PE-PGRS50 was linearised with PmeI. The viral vector was produced at the Vector Core Facility. The other five peptides were also cloned into ChAdOx1 using the same method.

To clone PE-PGRS50 into MVA vector, the PE-PGRS50 fragment (1.3 kbp) was cloned into a gateway entry vector (p1990) with the same methods as described above (Figure 5-2 A and B). To confirm insertion of the fragment, the plasmid was digested with Acc65I and XhoI, resulting in 4.7 kbp for the backbone plasmid and 1.3 kbp for the antigen (Figure 5-2 C). XhoI was used to digest the plasmid instead of NotI according to the digestion of the destination vector. MVA vector was digested with Acc65I and XhoI and dephosphorylated. The entry vector containing PE-PGRS50 was combined with digested MVA vector (Figure 5-2 D). The resulting plasmid was sequenced, linearised and sent off for virus preparation (Figure 5-2 E).

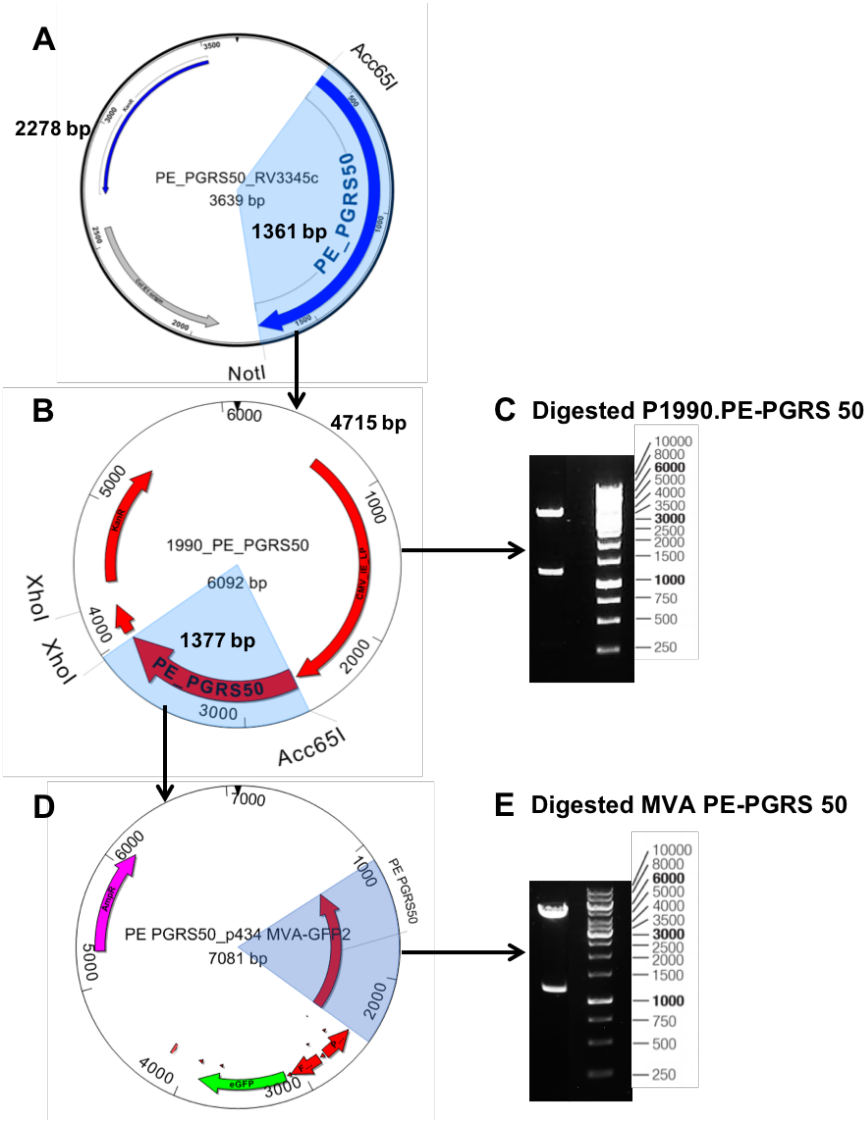

Figure 5-2 Cloning steps for the construction of MVA expressing the new antigens. (A) The plasmid containing the mycobacterial antigen DNA sequence (PE-PGRS50) was transformed into competent cells. The DNA plasmid was then purified and digested with Acc651 and NotI to excise the antigen insert (B). The 1361 bp DNA fragment was cloned into p1990 gateway entry vector. (C) Test digestion was performed with Acc65I and XhoI to confirm the presence of the correct size antigen fragment. (D) The gateway entry clone in (B) was recombined with the destination vector; MVA. (E) MVA expressing PE-PGRS50 was linearised with AatII. The viral vecor was produced at the Vector Core Facility. The other five peptides were also cloned into MVA using the same method except MVA PE-PGRS23 was linearised using XmnI.

5.2.2 Immunogenicity of the new viral vectors

To examine immune responses induced by ChAdOx1 expressing novel mycobacterial antigens, mice were immunised intradermally with the vaccines. The spleens were harvested and analysed for antigen-specific IFN-γ production two weeks post the last vaccination (Figure 5-3).



Figure 5-3 Timeline of ChAdOx1 immunisation expressing new antigens. CB6F1 mice were vaccinated with $1x10^8$ ifu intradermally (i.d.). Two-weeks post vaccination, the spleens were analysed for IFN-γ production using ELISpot.

Vaccination with ChAdOx1.85A was used as a positive control in this experiment and induced strong IFN-γ production (Figure 5-4). ChAdOx1.IrtA, ChAdOx1.PPE68 and ChAdOx1.PE9 induced a similar level of response compared to ChAdOx1.85A (Figure 5-4). ChAdOx1.IrtA was the most immunogenic of the three constructs. However, the response was not significantly better compared to ChAdOx1.85A (Figure 5-4). There was a trend to higher IFN-γ production in the spleens of ChAdOx1.IrtA vaccinated mice compared to ChAdOx1.PE PGRS50 immunised mice (p=0.0634) (Figure 5-4). A low number of IFN-γ producing cells was detected in the spleens of ChAdOx1.CtpF immunised mice (Figure 5-4). There were no responses induced by ChAdOx1 expressing PE PGRS50 and PE PGRS23 (Figure 5-4).

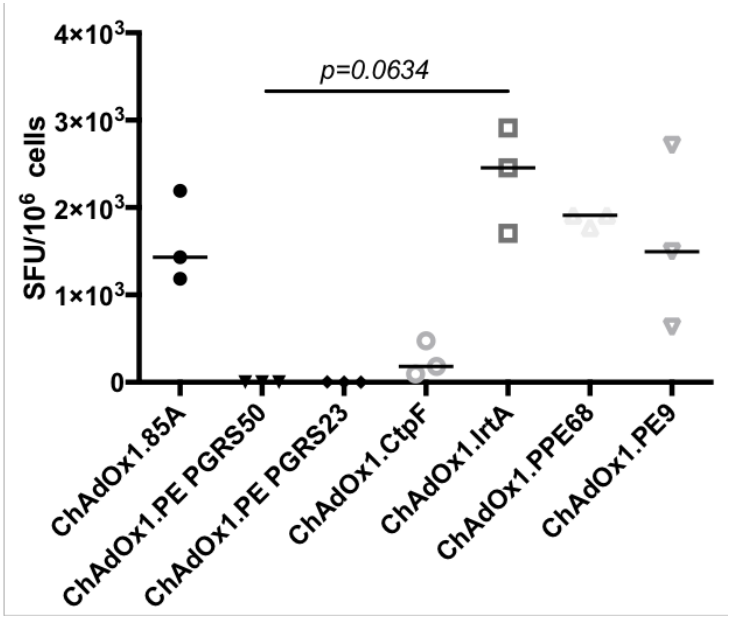

Figure 5-4 Immunogenicity of ChAdOx1 expressing new antigens. Two weeks after vaccination with ChAdOx1 expressing individual antigens, spleens from vaccinated mice were harvested. The splenocytes were stimulated with their cognate antigens for antigen-specific IFN-γ production using ELISpot and presented as spot forming units (SFU). Each symbol represents one animal and the line is the median of each group (n=3 mice). Statistical significance was determined using Kruskal-Wallis test with Dunn's multiple comparisons test.

MVA has been shown to be a good boost to ChAdOx1 and a good inducer of $CD4^+$ T cell responses [79, 96, 99], complementing the strong $CD8^+$ T cell responses induced by ChAdOx1 [97, 98]. For this reason, the same set of antigens was used to construct MVA vectors (Figure 5-2). During the viral vector production, Vector Core Facility could not produce MVA expressing PE-PGRS23. Together with the disappointing immunogenicity of ChAdOx1.PE PGRS23, this viral vector was excluded from the study. To examine the immunogenicity of the new MVA vectors, CB6F1 mice were immunised intradermally with the five MVA expressing antigens. A week after the vaccination, ELISpot was performed on spleen cells from vaccinated mice to measure IFN-γ production (Figure 5-5).



Figure 5-5 Timeline of with MVA expressing new antigens. CB6F1 mice were vaccinated with $5x10^6$ pfu intradermally (i.d.). One-week post vaccination, spleens were analysed for IFN-γ production using ELISpot.

MVA85A, used as a positive control, was immunogenic, inducing strong IFN-γ responses by splenocytes from immunised mice (Figure 5-6). MVA IrtA had the highest level of the cytokine production compared with other MVA constructs and significantly better compared to MVA PE PGRS50 (p=0.0216) (Figure 5-6). There was a trend to higher cytokine secretion in the spleen of the IrtA group compared to the CtpF group, but this did not reach statistical significance (p=0.0529) (Figure 5-6). MVA PPE68 and MVA PE9 were also immunogenic, inducing around 200 Spot Forming Units (SFU) per million splenocytes (Figure 5-6). No responses were detected from MVA PE PGRS50 and MVA CtpF groups (Figure 5-6).

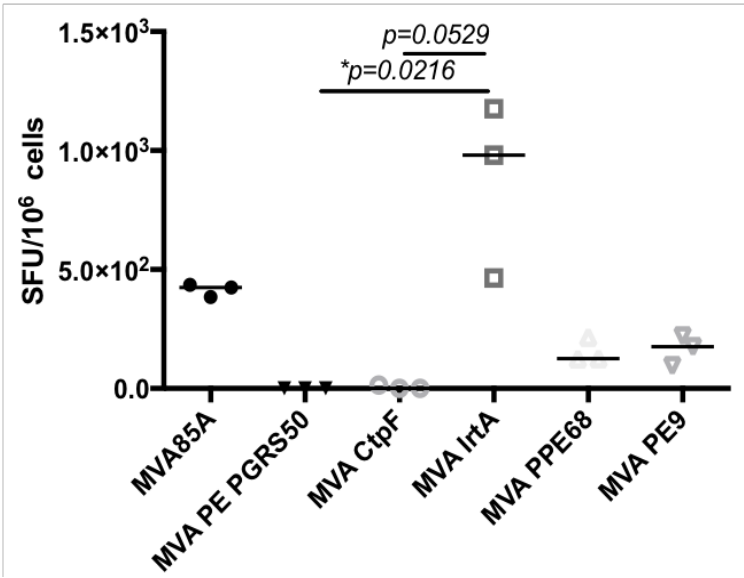

Figure 5-6 Immunogenicity of MVA expressing new antigens. A week after vaccination with MVA expressing individual antigens, spleens from vaccinated mice were harvested. Splenocytes were stimulated with their cognate antigens for antigen-specific IFN-γ production using ELISpot and presented as spot forming units (SFU). Each symbol represents one animal and the line is the median of each group (n=3 mice). Statistical significance was determined using Kruskal-Wallis test with Dunn's multiple comparisons test. *p≤0.05.

5.2.3 Immune responses induced by the new antigens in the spleens of BCG vaccinated mice

All the selected antigens were expressed by BCG except PPE68 (Table 5-1). It would be interesting to see systemic immune responses induced by these antigens in BCG vaccinated mice. To achieve this, mice were vaccinated with BCG intradermally. Four and 10 weeks post vaccination, the spleens were harvested and analysed for IFN-γ production using ELISpot assay as shown in Figure 5-7. While 4 weeks-time point would reveal the early immune responses of BCG recognising these novel antigens, the 10 weeks- time point would potentially be the optimal responses as this time point represents the peak BCG induced response [236]. Hence, this was the time point that BCG was boosted with the viral vector vaccines.

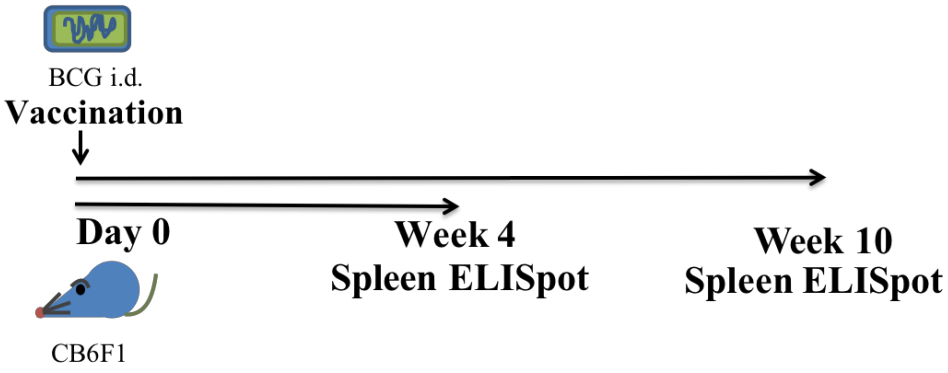

Figure 5-7 Timeline of BCG vaccination for testing the new antigens. Female CBFF1 mice were vaccinated intradermally (i.d.) with $4x10^5$ CFU of BCG Pasteur. Four and 10 weeks after vaccination, splenocytes were analysed for IFN-γ production using ELISpot assay.

PPD-T and Ag85A were used as positive controls of this study. After 18-20 hours of stimulation with PPD-T, around 600 SFU per a million splenocyte were observed at 4 weeks and 10 weeks post BCG vaccination (Figure 5-8 A and B). Ag85A was recognised in the spleens of BCG vaccinated animals at both time points at a similar level; ~200 SFU per 10^6 cells (Figure 5-8 A and B). PE9 was the strongest inducer compared with other new antigens tested at 4 weeks and 10 weeks (Figure 5-8 A and B). Ten-week post BCG vaccination, PE9 significantly increased the number of IFN-γ producing cells compared to PE-PGRS50 ($p=0.0105$) (Figure 5-8 B). There was a low level of responses observed in the spleens when stimulated with IrtA and PPE68 peptides at 4 weeks post vaccination (Figure 5-8 A), but the responses were almost undetectable at the 10 week-time point (Figure 5-8 B).

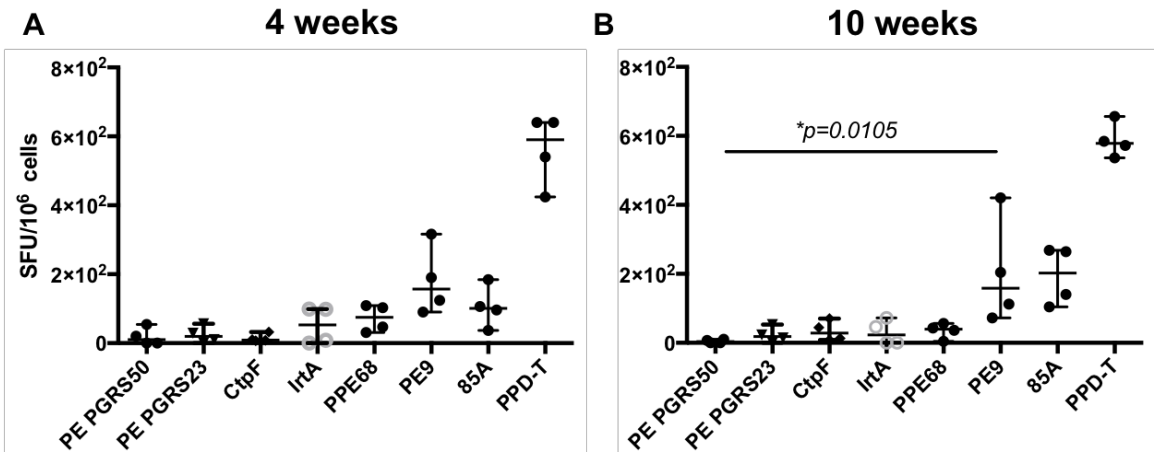

Figure 5-8 Immunogenicity of the new antigens in BCG vaccinated mice. Mice were vaccinated as shown in Figure 5-7. Four weeks (A) and 10 weeks (B) after vaccination, splenocytes were analysed for IFN-γ production using ELISpot assay. The new antigens were used to stimulate the splenocytes for 18-20 hours. PPD-T and Ag85A were included as a positive control. Antigen-specific IFN-γ production was defined as the number of spot forming units (SFU) per 10^6 splenocytes. Each symbol represents one animal and the line is the median of each group (n=4 mice). Statistical significance was determined using Kruskal-Wallis test with Dunn's multiple comparisons test. *p≤0.05.

5.2.4 Immunogenicity of DNA vaccines expressing non-immunogenic antigens

PE-PGRS50, PE-PGRS23 and CtpF induced little to no responses when expressed by the two viral vectors, ChAdOx1 and MVA (section 5.2.2). To investigate whether this was due to antigen-vector incompatibility, these antigens were administered as DNA vaccines. DNA constructs in p1990 vector were scaled up and purified using endotoxin-free kits (Figure 5-1 B). The vaccines were injected intramuscularly (i.m.) in BABL/c and C57BL/6 mice as shown in Figure 5-9. Three weeks after the last vaccination, spleens were analysed using ELISpot assay to measure antigen-specific IFN-γ production.

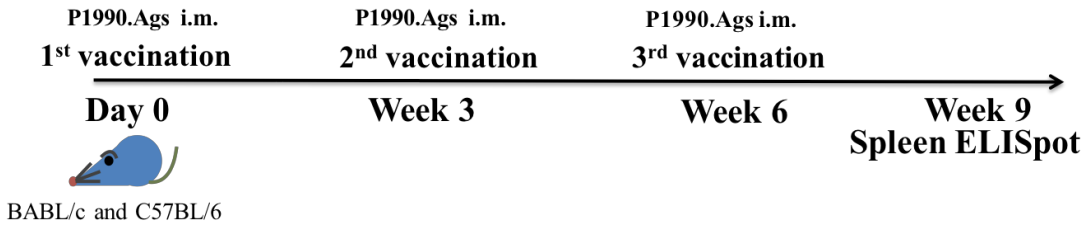

Figure 5-9 Timeline of DNA vaccination. BABL/c and C57BL/6 were vaccinated intramuscularly (i.m.) with 100 μg of DNA plasmids expressing individual antigens (P1990.Ags). Mice received three doses at three-week intervals. ELISpot was performed three weeks after the last vaccination to analyse the immunogenicity in the spleens.

Vaccination with DNA plasmid expressing Ag85A (P1990.85A), induced Ag85A-specific IFN-γ producing cells (500 SFU per 10^6 splenocytes), in both BABL/c and C57BL/6 mice (Figure 5-10). P1990.CtpF was not immunogenic, inducing very low antigen-specific IFN-γ release in both strains of mice (Figure 5-10 A and B). Vaccination with P1990 expressing either PE-PGRS50 or PE-PGRS23 resulted in low or undetectable IFN-γ responses in the spleens of vaccinated C57BL/6 and BALB/c mice (Figure 5-10 A and B). No DNA vaccines tested in these experiments were as immunogenic as P1990.85A (Figure 5-10 A and B).

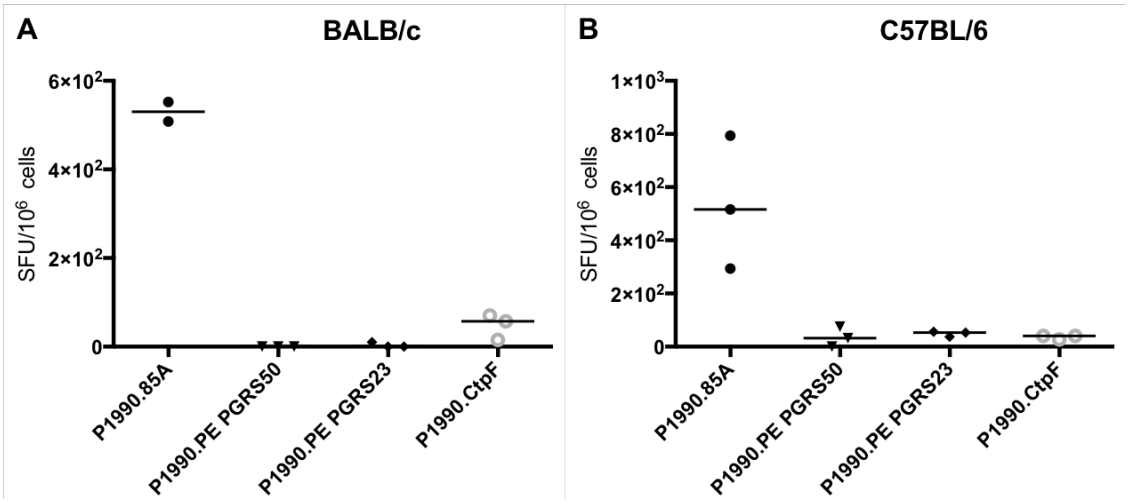

Figure 5-10 Immunogenicity of DNA vaccines. Three weeks after the last vaccination, splenocytes were analysed for IFN-γ production using ELISpot assay. P1990.85A was used as a positive control. Antigen-specific IFN-γ production was defined as the number of spot forming units (SFU) per 10^6 splenocytes from BALB/c (A) and C57BL/6 mice (B). Each symbol represents one animal and the line is the median of each group (n=2-3 mice). No statistical significance was observed between the new antigens using Kruskal-Wallis test with Dunn's multiple comparisons test.

5.2.5 Protective efficacy of viral vector vaccines expressing the most immunogenic antigens

5.2.5.1 Protective efficacy of ChAdOx1 expressing immunogenic antigens

From the ChAdOx1 immunogenicity study (Figure 5-4), CtpF, IrtA, PPE68 and PE9 antigens were immunogenic and they were therefore selected for evaluation of their protective efficacy against *M.tb* challenge. Even though ChAdOx1.CtpF induced low IFN-γ production (Figure 5-4), I decided it would be interesting to observe its performance against *M.tb* infection as a representative of the non-immunogenic antigens. CB6F1 mice were used in this challenge study because they represented responses obtained from both parental strains; BALB/c and C57BL/6. Female CB6F1 mice were vaccinated with ChAdOx1.CtpF, ChAdOx1.IrtA, ChAdOx1.PPE68 and ChAdOx1.PE9 intranasally. Intradermal BCG (B) was included as a positive control and naïve mice were used as a negative control. *M.tb* challenge was performed 4 weeks after the viral vector vaccination or 10 weeks after BCG injection. Lungs and spleens were analysed to measure bacterial CFU at 4 weeks post challenge.

BCG vaccination significantly decreased *M.tb* CFU counts both in the lungs and spleens of vaccinated animals compared with naïve mice (p=0.0023 and 0.0004 respectively) (Figure 5-11 A and B). None of the new viral vector vaccines provided protection compared to naïve mice either in lungs or spleens (Figure 5-11 A and B). BCG vaccination was the best group among the vaccines tested in this experiment (Figure 5-11 A and B).

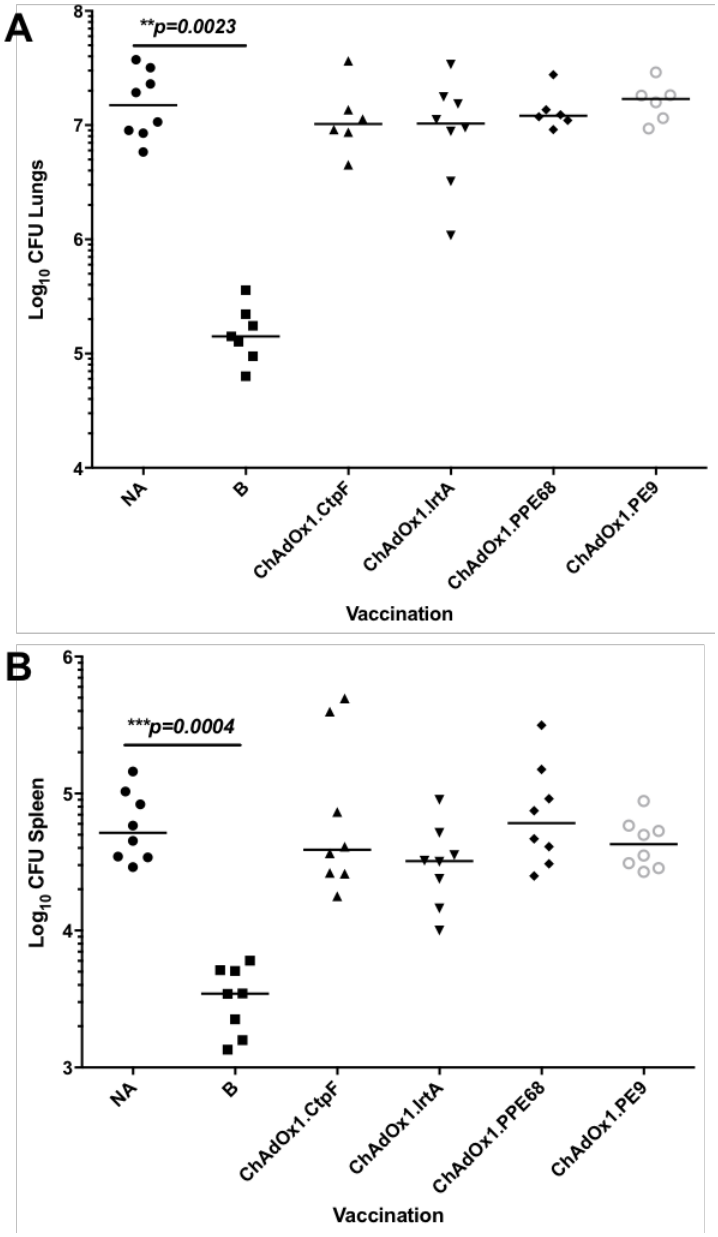

Figure 5-11 Evaluation of the protective efficacy of ChAdOx1 expressing novel antigens in lungs and spleens of naïve and vaccinated mice. CB6F1 mice were immunised with intranasal ChAdOx1 expressing either CtpF, IrtA, PPE68 and PE9. BCG vaccinated group (B) and naïve group (NA) were included as a positive and a negative control respectively. *M.tb* challenge was performed at 4 weeks post ChAdOx1 vaccination or 10 weeks post BCG. (A) Lungs and (B) spleens were analysed for bacterial enumeration. Each symbol represents one animal and the line is the median of each group (n=6-8 mice). Statistical significance was determined using Kruskal-Wallis test with Dunn's multiple comparisons test. **p≤0.01; ***p≤0.001.

5.2.5.2 Protective efficacy of B-C-M regimen expressing immunogenic antigens

The efficacy of the four novel antigens was then evaluated in our established optimal vaccination regimen, B-C-M, previously shown to improve BCG protection, using Ag85A as an antigen [98]. At this stage, CtpF was excluded from the prime-boost study due to weak immune responses induced by ChAdOx1.CtpF and the absence of IFN-γ production with MVA CtpF (Figure 5-4 and Figure 5-6).

CB6F1 mice were primed with intradermal BCG and boosted with intranasal ChAdOx1 and then received a second boost with intradermal MVA, both expressing the same antigen as shown in Figure 5-12. Aerosol *M.tb* challenge was performed 4 weeks post MVA vaccination. Lungs and spleens were harvested for CFU analysis at 4 weeks post *M.tb* infection (Figure 5-12).

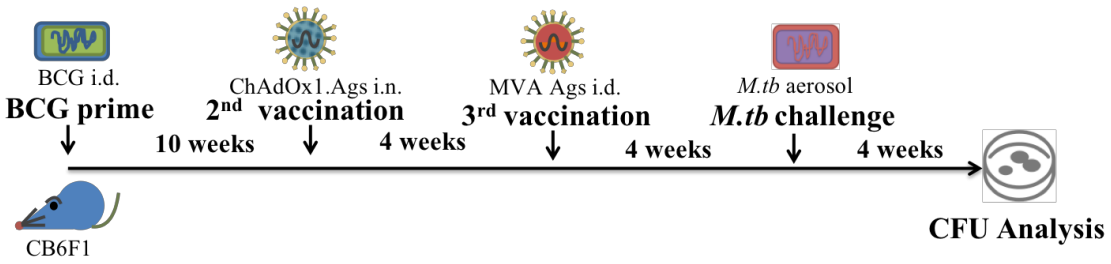

NA:	No vaccination----------18 wks----------*M.tb*--->Harvest
B:	BCG----------18 wks ----------*M.tb*--->Harvest
B-C-M IrtA:	BCG---10wks---> ChAdOx1.IrtA-----4wks-->MVA IrtA-----4 wks---*M.tb*--->Harvest
B-C-M PPE68:	BCG---10wks---> ChAdOx1.PPE68--4wks-->MVA PPE68--4 wks---*M.tb*--->Harvest
B-C-M PE9:	BCG---10wks---> ChAdOx1.PE9-----4wks-->MVA PE9-----4 wks---*M.tb*--->Harvest

Figure 5-12 Timeline of B-C-M expressing new antigen vaccination and *M.tb* challenge. CB6F1 mice were vaccinated intradermally (i.d.) with $4x10^5$ CFU of BCG Pasteur (B) and boosted 10 weeks later with $1x10^8$ ifu of ChAdOx1 (C) expressing new antigens intranasally (i.n.). Four weeks after ChAdOx1 vaccination, intradermal boost of MVA (M) was administered at a dose of $5x10^6$ pfu. Animals were challenged with 50-100 CFU of aerosol *M.tb* Erdman 4 weeks after the last vaccination. Four weeks after challenge, lungs and spleens were harvested for CFU enumeration.

BCG vaccination significantly decreased the bacterial load in the lungs and spleens of vaccinated mice compared to naïve mice ($p=0.0185$ and $p=0.0155$ respectively) (Figure 5-13 A and B). Boosting BCG with ChAdOx1 and MVA expressing IrtA, PPE68 or PE9 did not improve protection provided by BCG alone in both organs tested (Figure 5-13 A and B). The protection levels were comparable in all vaccinated groups in pulmonary and systemic compartments (Figure 5-13 A and B).

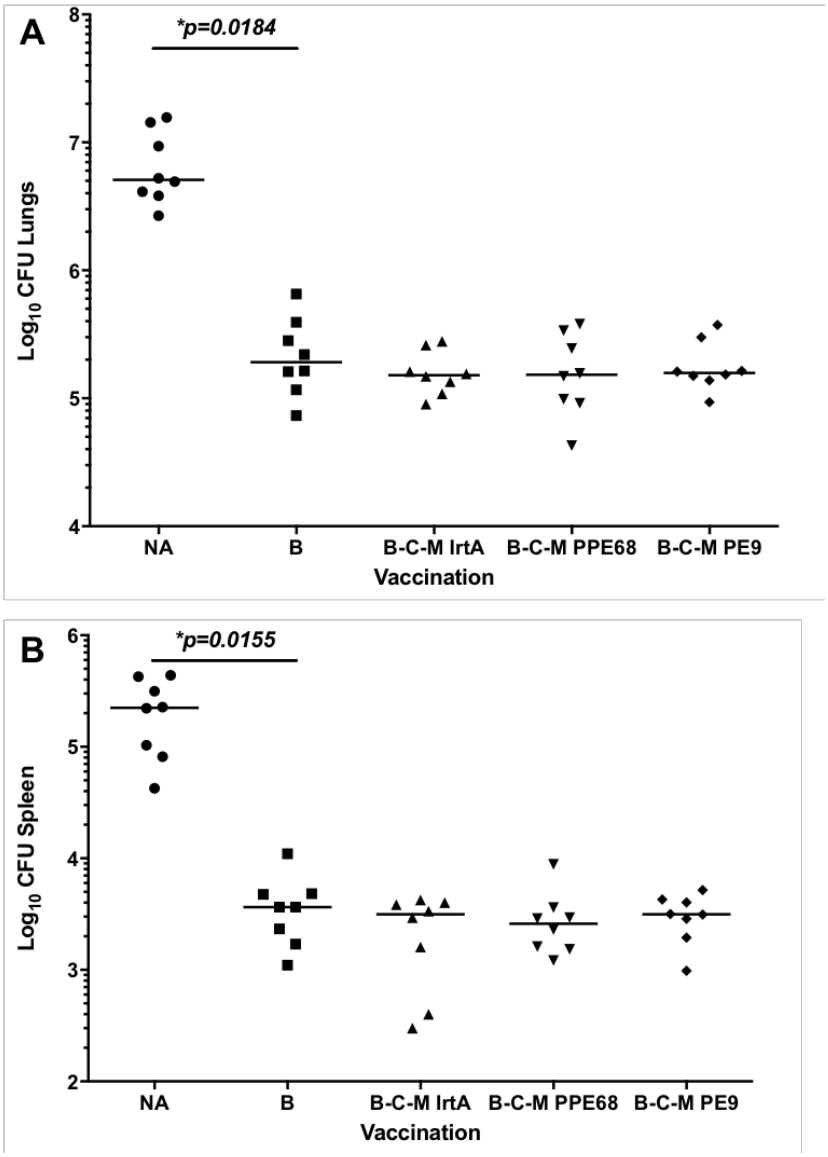

Figure 5-13 Protective efficacy of B-C-M expressing novel antigens in lungs and spleens of naïve and vaccinated mice. CB6F1 mice were immunised as in Figure 5-12. BCG vaccinated group (B) and naïve group (NA) were included as a positive and a negative control respectively. (A) Lungs and (B) spleens were analysed to measure the bacterial colonies. Each symbol represents one animal and the line is the median of each group (n=8 mice). Statistical significance was determined using Kruskal-Wallis test with Dunn's multiple comparisons test. *p≤0.05.

5.3 **Discussion**

PE-PGRS 50 (Rv3345c), PE-PGRS 23 (Rv1243c), CtpF (Rv1997), IrtA (Rv1348), PPE68 (Rv3873) and PE9 (Rv1088) are secreted during course of *M.tb* infection. All of the above antigens are well recognised by active and latently infected individuals [174] as well as by *M.tb* infected mice [121]. I investigated whether one or all of the antigens could boost immune responses and protective efficacy of a prior BCG vaccination. I initially expressed each antigen individually in ChAdOx1 and did head-to-head immunogenicity and protection experiments with and without a BCG prime.

All six novel *M.tb* antigens selected belong to the PE/PPE family. PE-PGRS proteins are the subset of this family [165]. PE-PGRS passed the antigen selection criteria by being recognised in active TB patients, *M.tb* latently infected people and *M.tb* infected mice but it failed to induce immune responses when used as a subunit vaccine (Figure 5-4, Figure 5-6 and Figure 5-10). The recognition of these antigens in humans and mice could be explained by the high antigenic variation of these proteins. PE-PGRS proteins have been shown to be differentially expressed by *M.tb* both *in vivo* [237] and *in vitro* [238, 239]. However, the regulatory mechanisms affecting *pe_pgrs* gene expression are unknown. Talarico *et al.* reported that insertions/deletions and frameshifts can be frequently observed in clinical isolates of *M.tb pe_pgrs* genes [240, 241]. Interestingly, most of the mutations occurred on the PGRS repeat sequences, suggesting that *pe_pgrs* genes may be a source of antigenic variation for *M.tb* [165].

PE-PGRS50 and PE-PGRS23 were not immunogenic when delivered by ChAdOx1 (Figure 5-4). Some possible explanations could be the large size of the proteins which

may interfere the stability of the constructs. High level of post translational modification of these proteins might be needed for stability, especially the glycosylation of the repeated motifs [242]. Unlike *M.tb*, the viral vectors might not be able to add these motifs resulting in instability of the constructed vector [242, 243]. Additionally, these antigens could be generally toxic to the viruses as the production of MVA PE PGRS23 failed.

PE-PGRS50 and PE-PGRS23 also failed to induce immune responses when administered as DNA plasmids (Figure 5-10). In a recent study, the repetitive glycine-rich motifs in PE-PGRS proteins specifically exported in *M.tb* but not in BCG due to the absence of the region of difference (RD) 5 [244]. The repetitive domains of PE-PGRS may not be expressed in viral vectors or in *E. coli* when produced as DNA plasmids. They might need Mycobacterium species to express these regions. As shown in a study using *Mycobacterium smegmatis (M. smegmatis).* Singh *et al.* inserted DNA plasmids contained PE-PGRS33, PE-PGRS26 and PE-PGRS16 individually into *M. smegmatis*. The genetically modified mycobacteria expressing different PE-PGRS proteins were tested for host immune responses both *in vitro* and *in vivo* [245]. In C57BL/6 mice, the PE-PGRS proteins enhanced NO, IL-12 and IL-10 production when expressed in *M. smegmatis* [245]. Intramuscular immunisation with these antigens as DNA vaccines showed no protection against *M.tb* challenge [245]. However, immunogenicity of the DNA vaccines was not reported in the study.

Unlike PE-PGRS, PPE proteins do not have the repetitive glycine-rich sequences. PPE18 [183], PPE14 [246] and PPE44 [247] have been shown to be protective when delivered as DNA vaccines and recombinant proteins with adjuvant. Although recombinant viral vectors

expressing PPE68 were immunogenic (Figure 5-4 and Figure 5-6), these vaccines did not provide protection against *M.tb* challenge (Figure 5-11 and Figure 5-13). PPE68 has been recognised in active TB patients and *M.tb* latently infected individuals [174] and *M.tb* infected mice [121]. However, this antigen could not induce cytokine production in the spleens of BCG vaccinated CB6F1 mice which are the cross-breed of BALB/c and C57BL/6 strains (Figure 5-8). Consistent with our finding, Demangel *et al.* have tested this antigen in C57BL/6 mice infected with *M.tb* and vaccinated with BCG and observed the same results [226]. This was suggested to be due to the lack of PPE68 expression in BCG [165]. By expressing PPE68 with BCG (PPE68-rBCG) strong Th1 immune response in mice were induced [227]. This suggests that PPE68 alone as a single antigen vaccine is not enough to induce immune responses and protect against *M.tb* infection.

Several studies have reported that PE/PPE proteins have immunomodulatory functions, such as altering host cytokine responses by interaction with Toll-like receptors or inhibition of antigen presentation [233, 234, 248]. Recently this year, our group has reported a set of protective antigens. PPE15 and PPE51 provided protection against *M.tb* challenge in the lungs of CB6F1 mice when delivered in ChAdOx1 vectors [121]. Even though all six of the antigens were selected using the same selection criteria, that did not refer to their immunogenicity and protectivity. IrtA, which involves in the iron export of *M.tb* [231], offered promising immunogenicity when expressed in ChAdOx1 as well as in MVA (Figure 5-4 and Figure 5-6). However, ChAdOx1 expressing this antigen failed to provide protection against *M.tb* infection compared to naïve controls (Figure 5-11). ChAdOx1 was developed to induce both $CD4^+$ and $CD8^+$ T cell responses and to be used in combination with MVA [84]. The ChAdOx1 primed-MVA

boosted regimen has been demonstrated to greatly enhance protective immunity [81, 99, 188]. ChAdOx1 expressing IrtA, PPE68 or PE9 could not improve BCG even with an extra boost of MVA expressing the same antigen (Figure 5-13). PE9, works as a complex with PE10 to induce apoptosis of macrophages [232], was strongly recognised in BCG vaccinated mice (Figure 5-8). Interestingly, ChAdOx1-MVA expressing this antigen did not enhance protection of BCG (Figure 5-13). Unlike the non-protective antigens, ChAdOx1.PPE15 significantly improved BCG by reducing *M.tb* colonies in lungs and spleens of BCG-ChAdOx1.PPE15 mice compared to BCG alone [121].

The *ctpF* gene en-codes for the P-type ATPase cation transporter, which is affected by hypoxia and over-expression of *M.tb* DosR regulator [229]. The large number of P-type ATPases encoded in the bacillus genome suggesting the importance of *M.tb* metal cation homeostasis [230, 249]. CtpF protein has not been used as a vaccine candidate before. This antigen was selected using the same criteria with other antigens, identified as an immunodominant target for $CD8^+$ T cells in *M.tb* infected humans [174] and recognised in *M.tb* infected mice [121]. However, the antigen induced very low immune responses when delivered using viral vectors and DNA plasmids (Figure 5-4, Figure 5-6 and Figure 5-10). A possible explanation could be the large size of the peptides. CtpF was the biggest antigen among 5 antigens tested which may result in the instability of the viral vaccine constructs and DNA plasmids.

It was difficult to predict immunogenicity and protective efficacy of the antigen when expressed as viral vector vaccines. The lack of immune correlates of protection complicates antigen/vaccine selection. An immunogenicity study does not mirror protective efficacy against *M.tb* infection but it is useful for excluding non-

immunogenic vaccines out before entering the challenge study. This suggests that the evaluation of protective efficacy is a mandatory early step for pre-clinical vaccine development.

Chapter 6. Conclusion and future work

An effective TB vaccine is urgently needed because the efficacy of BCG, the only licenced vaccine, is highly variable [1]. MVA85A, the first prophylactic vaccine evaluated in a phase 2b clinical trial, failed to further improve BCG protection [95]. Therefore, ChAdOx1.85A was constructed in our group to be used in combination with MVA85A, aiming to improve efficacy by enhancing $CD8^+$ and $CD4^+$ T cell responses against *M.tb* infection [98]. In mice, BCG-ChAdOx1.85A-MVA85A (B-C-M) regimen has consistently provided superior protection compared to BCG alone [98]. This combination is the most protective regimen so far among all the combinations tested in our laboratory. This research project examined the longevity of B-C-M protection and its immunogenicity with the aim of identifying immune responses that correlate with efficacy.

Stylianou *et al.* have shown that B-C-M is protective against *M.tb* challenge 4 weeks post vaccination [98]. The durability of protection was analysed at 8 and 20 week-timepoints in this study. At 8 weeks after vaccination, B-C-M was still protective against *M.tb* infection, significantly improving BCG efficacy. Although this regimen remained partially protective at 20 weeks, there was a decrease in the magnitude of protection, resulting in the loss of statistical significance. This could be partly due to a higher infection dose in the latter experiment (half a log different compared to the former experiment), which could result in smaller differences between the protective and control groups. Alternatively, protective immune responses induced by B-C-M might decrease over time. To investigate the later, immune responses were studied in detail at the different time points post vaccination, to observe kinetic changes over time, focusing on T cell and antibody responses.

Challenging humans with *M.tb* is not possible and *M.tb* challenge experiments in animals are costly and time consuming. The identification of immune correlates of protection would therefore make TB vaccine research and development more efficient. Cytokine producing $CD4^+$ T cells have been proposed to correlate with protection [18, 19, 20]. However, several vaccines have been shown to induce very good responses in this T cell population but failed to improve BCG efficacy [32, 95, 250]. In this study, B-C-M significantly enhanced antigen-specific IFN-γ and TNF-α producing $CD4^+$, as well as $CD8^+$ T cells, in the lungs and spleen compared to BCG alone. Perforin and granzyme B production by $CD8^+$ T cells were also observed in the lungs of B-C-M vaccinated mice. However, these responses were also induced by the non-protective B-C vaccination regimen. This suggests that whilst the cytokine secretion might play an important role in the control *M.tb* infection, it does not directly correlate with protection.

As far as antibody responses are concerned, the role of antibodies in TB is unclear showing both protective and harmful effects [150, 151, 152, 161]. IgG in the circulation and IgA in the airways of B-C-M vaccinated mice were examined. Antigen specific-antibody responses were enhanced after boosting BCG with ChAdOx1.85A. Boosting B-C with intradermal MVA85A (B-C-Mid) failed to further enhance antibody responses systemically and mucosally. On the other hand, mucosal delivery of MVA85A (B-C-Min) enhanced Ag85A specific-IgA production in the airways but not in the circulation. Mucosal vaccination has been introduced as a novel route of vaccine delivery, enhancing antibody responses both locally and systemically in mouse, NHP and human studies [71, 72, 75, 161, 162, 163, 204]. Consistent with the findings in this thesis, this

suggests that antigen-specific mucosal IgA and systemic IgG responses induced by B-C-M expressing Ag85A do not correlate with protection.

All three vaccine components of the B-C-M regimen are required for protection against *M.tb* infection, as neither B-C or B-M are protective in BALB/c mice [98]. BCG is a strong inducer of $CD4^+$ but not $CD8^+$ T cell responses [33]. ChAdOx1.85A induces good $CD8^+$ T cell responses but they were not increased when BCG was boosted with this vaccine compared to ChAdOx1.85A alone [98]. In the absence of a BCG prime, MVA85A failed to boost cytokine secreting $CD8^+$ T cells in the lungs. This suggests that MVA85A could enhance the T cell responses already primed by BCG in this regimen. MVA85A alone is a weak inducer of $CD8^+$ T cell response [95, 203, 204]. Therefore, combining MVA with ChAdOx1 enhances both $CD4^+$ and $CD8^+$ T cell responses and improves protection which agrees with data observed in several clinical trials [78, 84, 100, 205]

Lung-resident memory T cells are a target population for new TB vaccines in development. This cell type is known to remain in the lung, the most common site of infection, and provide protection against *M.tb* infection [75, 89, 106, 217, 221]. Recently, the intravascular staining technique was introduced to discriminate lung-parenchymal from vascular cells [106, 115]. This technique was adopted and optimised in our laboratory for antibody concentration and timing between antibody injection and euthanasia. Combining intravascular staining technique with tetramer and surface staining of lung-homing markers revealed a cell population that was significantly expanded after vaccination with the protective regimen. Vaccination with B-C-M significantly increased antigen-specific $CXCR3^+$ $KLRG1^-$ $CD4^+$ T cells in the lung parenchyma compared to BCG alone at 4, 8 and 20 weeks post vaccination. Unlike B-C-M, the non-

protective B-C regimen induced low responses of this cell phenotype. Interestingly, the number of these cells declined at 20 weeks post B-C-M vaccination which might help explain the reduction of B-C-M protection observed at the same timepoint. The result suggests that antigen-specific lung parenchymal $CD4^+$ T cells expressing the protective lung-homing phenotype, $CXCR3^+$ $KLRG1^-$, associate with protection. This protective cell population has been shown to expand after protective vaccination and *M.tb* infection in mouse studies [106, 121]. Systemic delivery of protective subunit vaccines, resulted in the induction of cells with this phenotype in the lung-vasculature of vaccinated mice compared to naïve controls [145, 220]. This suggests that the protective lung-homing phenotype is induced, depending on the route of vaccination. A large proportion of the lung-parenchymal $CXCR3^+$ $KLRG1^-$ T cells also expressed the T_{RM} phenotype. Resident memory $CD4^+$ T cells, $CD44^{hi}$ $62L^{low}$ $CD69^+$ $CD11a^+$, followed the same pattern of the protective lung-homing phenotype. Therefore, this cell phenotype also associates with protection. Perdomo *et al.* have observed that the same T_{RM} phenotype was enhanced after mucosal delivery of BCG and mucosal transfer of these cells provided protection against *M.tb* challenge [75].

The effector function of $CXCR3^+$ $KLRG1^-$ $CD4^+$ T cells was examined, showing that these cells are able to induce effector cytokines in the lung parenchyma of B-C-M vaccinated mice. This confirms the ability of cells with this protective phenotype to produce cytokines. In future work, it would be interesting to study the proliferative capacity of these cells by measuring Ki67 *ex vivo* [251, 252, 253].

To confirm the protective role of antigen-specific lung parenchymal CD4+ T cells, adoptive transfer was performed, and the recipient mice were then challenged with

M.tb. The IV- Tet+ cells from B-C-Mid vaccinated donor mice failed to protect naïve recipients. Around 5000 cells, collected from 8 donors, were transferred, however it is possible that more cells are required for protection. There was a difficulty in obtaining good cell purity without compromising the cell number. Future work might investigate the possibility of more donors to achieve a higher cell number, with the caveat that this will result in a less manageable experiment. In addition, protective correlates of protection are likely to be multifactorial. Circulating $CD4^+$ T cells were enhanced after systemic vaccination and were able to home back to the lungs following adoptive transfer [46, 220]. Additionally, both T_{RM} $CD8^+$ and $CD4^+$ T cells in the airways provided protection against *M.tb* infection [75]. Thus, adoptive transfer of only one cell type might not be sufficient to improve protection against *M.tb* challenge in naïve recipients. In addition, Sakai *et al.* have shown that $CXCR3^+$ $KLRG1^-$ $CD4^+$ T cells migrated back to the *M.tb*-infected lungs within 1.5 days [106]. It would be important to confirm that once adoptively transferred the lung-parenchymal cells induced by B-C-M vaccination were able to travel back to the lungs and remain viable in time before *M.tb* challenge.

The construction of viral vector vaccines was conducted in parallel to the above immunogenicity studies. Stylianou *et al.* have constructed PPE15 (Rv1039c) into a ChAdOx1 vector and observed superior protection when BCG was boosted with ChAdOx1.PPE15 [121]. PE PGRS50 (Rv3345c), PE PGRS23 (Rv 1243c), CtpF (Rv1997), IrtA (Rv1348), PPE68 (Rv3873) and PE9 (Rv1088) were selected using the same criteria as PPE15 since they were recognised by active and latently infected individuals [174] as well by *M.tb* infected mice (21). These antigens were expressed individually in

ChAdOx1, and whereas IrtA, PPE68 and PE9 were immunogenic, PE PGRS50, PE PGRS23 and CtpF were unable to induce strong immune response. The last three antigens were then administered as DNA vaccines, which also failed to induce immune responses.

ChAdOx1 expressing IrtA, PPE68 or PE9 induced strong cytokine responses however the efficacy of these vaccine candidates was not better compared to naïve mice. Furthermore, they were also unable to improve BCG protection when used to boost BCG. Unlike these antigens, PPE15 expressed by a ChAdOx1 vector was protective on its own and improved BCG protection when given as a mucosal boost [121]. These antigens were then administered in the most optimised vaccine regimen in our laboratory, B-C-M, to exclude that the lack of protection was due to antigen delivery platform used. However, ChAdOx1-MVA expressing the same antigen was also not successful in improving BCG protection. It can be concluded that these antigens are not good enough to be used in vaccines when delivered as viral vectors and DNA vaccines.

In conclusion, work presented in this thesis has examined immunogenicity of six novel mycobacterial antigens. PE-PGRS50, PE-PGRS23 and CtpF were not immunogenic when delivered as a viral vector or DNA vaccine. ChAdOx1 expressing IrtA, PPE68 or PE9 were immunogenic but failed to provide protection when delivered on its own or combined with MVA expressing the same antigen to boost BCG. This project has also identified antigen-specific $CD4^+$ T cells expressing a protective phenotype in the lung parenchyma following B-C-M vaccination. This cell population was shown to be associated with protection at 4, 8 and 20 weeks post vaccination. The effector function

of this cell population was characterised, but it was not possible to observe a protective function when adoptively transferred to naïve mice. The future work mentioned above could be performed to address these problems. The lung parenchymal $CD4^+$ T cells with the expression of protective phenotype identified in this study could be a target for new TB vaccine candidates in development.

Chapter 7. Appendix

7.1 Antibodies used for flow cytometry

Table 7-1 Flow cytometry antibodies for effector panel

Antigen	Fluorochrome	Clone	Supplier
Surface staining			
CD3	eFluor 450	14A2	eBioscience, Hatfield, UK
CD19	Brilliant Violet 510	6D5	BioLegend, CA, USA
CD4	Alexa Fluor 700	GK1.5	BioLegend, CA, USA
CD8a	APC-eFluor780	53-6.7	eBioscience, Hatfield, UK
Intracellular staining			
IFN-γ	APC	XMG1.2	eBioscience, Hatfield, UK
TNF-α	AF488	MP6-XT22	eBioscience, Hatfield, UK
Granzyme B (anti-mouse)	PE-Cy 7	NGZB	eBioscience, Hatfield, UK
Granzyme B (anti-human)	PE-CF594	GB11	BD Bioscience,Oxford, UK
Perforin	PE	eBioOMAK-D	eBioscience, Hatfield, UK

Table 7-2 Flow cytometry antibodies for lung-parenchymal CD4$^+$ T_{RM} panel

Antigen	Fluorochrome	Clone	Supplier
Intravascular staining			
CD45.2	FITC	104 (RUO)	eBioscience, Hatfield, UK
Tetramer staining			
Class II: I-E(d)	PE	NIH Tetramer Core Facility, Atlanta, USA	
Ag85A 165-178 LPGWLQANRHVKPT			
Surface staining			
CD19	Brilliant Violet 510	6D5	BioLegend, CA, USA
CD4	Alexa Fluor 700	GK1.5	BioLegend, CA, USA
CD44	Brilliant Violet 711	IM7	BioLegend, CA, USA
CD62L	APC-eFluor780	MEL-14	eBioscience, Hatfield, UK
CD69	Brilliant Violet 605	H1.2F3	BioLegend, CA, USA
CD11a	APC	M17/4	eBioscience, Hatfield, UK
KLRG1	PE-Cyanine7	2F1	eBioscience, Hatfield, UK
CXCR3	PerCP-Cyanine5.5	CXCR3-173	eBioscience, Hatfield, UK
CX3CR1	Brilliant Violet 421	SA011F11	BioLegend, CA, USA

Table 7-3 Flow cytometry antibodies for lung-parenchymal CD8$^+$ T_{RM} panel

Antigen	Fluorochrome	Clone	Supplier
Intravascular staining			
CD45.2	FITC	104 (RUO)	eBioscience, Hatfield, UK
Tetramer staining			
Class I: H-2L(d)	APC	NIH Tetramer Core Facility, Atlanta, USA	
Ag85B 110-118 MPVGGQSSF			
Surface staining			
CD19	BV510	6D5	BioLegend, CA, USA
CD8a	APC-eFluor780	53-6.7	eBioscience, Hatfield, UK
CD44	Brilliant Violet 711	IM7	BioLegend, CA, USA
CD62L	Alexa Fluor 700	MEL-14	eBioscience, Hatfield, UK
CD69	Brilliant Violet 605	H1.2F3	BioLegend, CA, USA
CD103	PerCP-Cy5.5	2E7	BioLegend, CA, USA
KLRG1	PE-Cyanine7	2F1	eBioscience, Hatfield, UK
CXCR3	PE	CXCR3-173	eBioscience, Hatfield, UK
CX3CR1	Brilliant Violet 421	SA011F11	BioLegend, CA, USA

Table 7-4 Flow cytometry antibodies for effector lung parenchymal panel

Antigen	Fluorochrome	Clone	Supplier
Intravascular staining			
CD45.2	FITC	104 (RUO)	eBioscience, Hatfield, UK
Surface staining			
CD19	Brilliant Violet 510	6D5	BioLegend, CA, USA
CD3	Brilliant Violet 605	17A2	BioLegend, CA, USA
CD4	Alexa Fluor 700	GK1.5	BioLegend, CA, USA
CD8a	APC-eFluor780	53-6.7	eBioscience, Hatfield, UK
KLRG1	PE-Cyanine7	2F1	eBioscience, Hatfield, UK
CXCR3	PerCP-Cyanine5.5	CXCR3-173	eBioscience, Hatfield, UK
CX3CR1	Brilliant Violet 421	SA011F11	BioLegend, CA, USA
Intracellular staining			
IFN-γ	APC	XMG1.2	eBioscience, Hatfield, UK
TNF-α	AF488	MP6-XT22	eBioscience, Hatfield, UK

7.2 **Gating strategies**

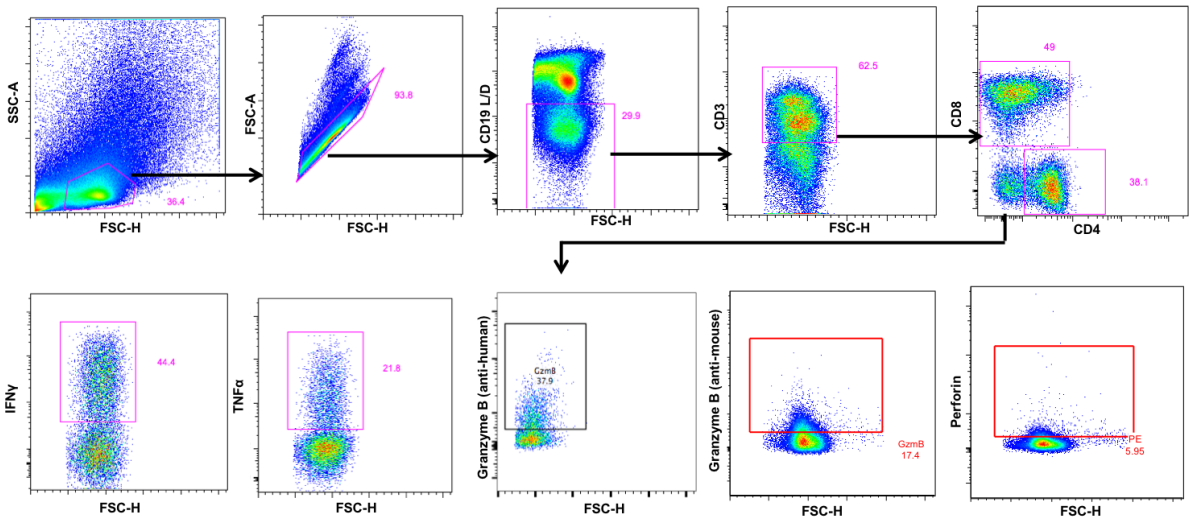

Figure 7-1 Gating strategy for the identification of T cells producing IFN-γ, TNF-α, granzyme B and perforin. Cells were analysed using effector panel (Table 7-1). Lymphocytes were selected followed by singlets and live cells (excluding $CD19^+$ cells at the same time). T cells were identified as $CD3^+$ before gating on $CD8^+$ and $CD4^+$ cells producing IFN-γ and TNF-α. $CD8^+$ T cells were also analysed for granzyme B and perforin production.

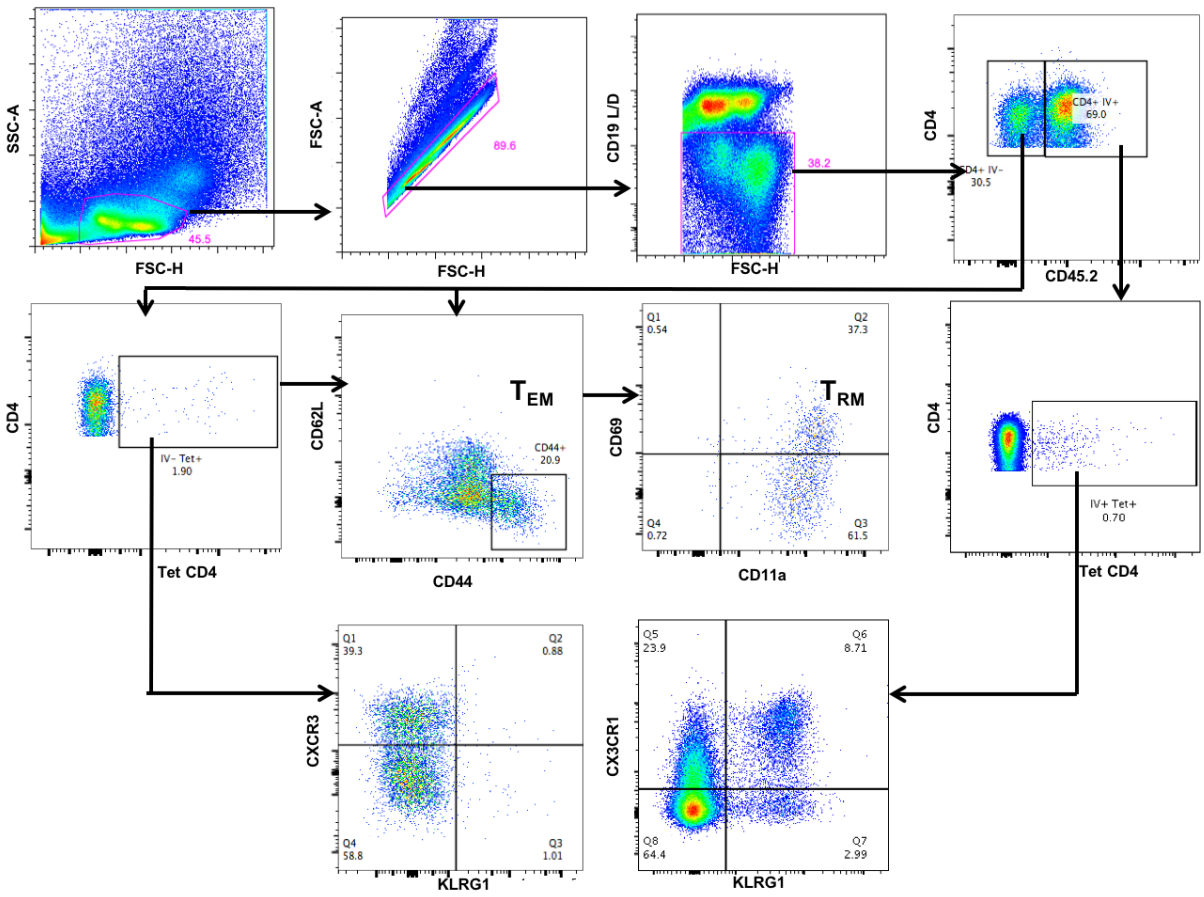

Figure 7-2 Gating strategy for the identification of lung-parenchymal CD4⁺ T cells expressing resident memory and lung-homing markers. Cells were analysed using lung-parenchymal CD4⁺ T_{RM} panel (Table 7-2). Lymphocytes were selected followed by singlets and live cells (excluding CD19⁺ cells at the same time). CD4⁺ T cells were divided to CD45.2- (IV-) and CD45.2+ (IV+) before gating on tetramer positive population. The antigen-specific cells were analysed on the expression of resident memory markers and lung homing phenotypes.

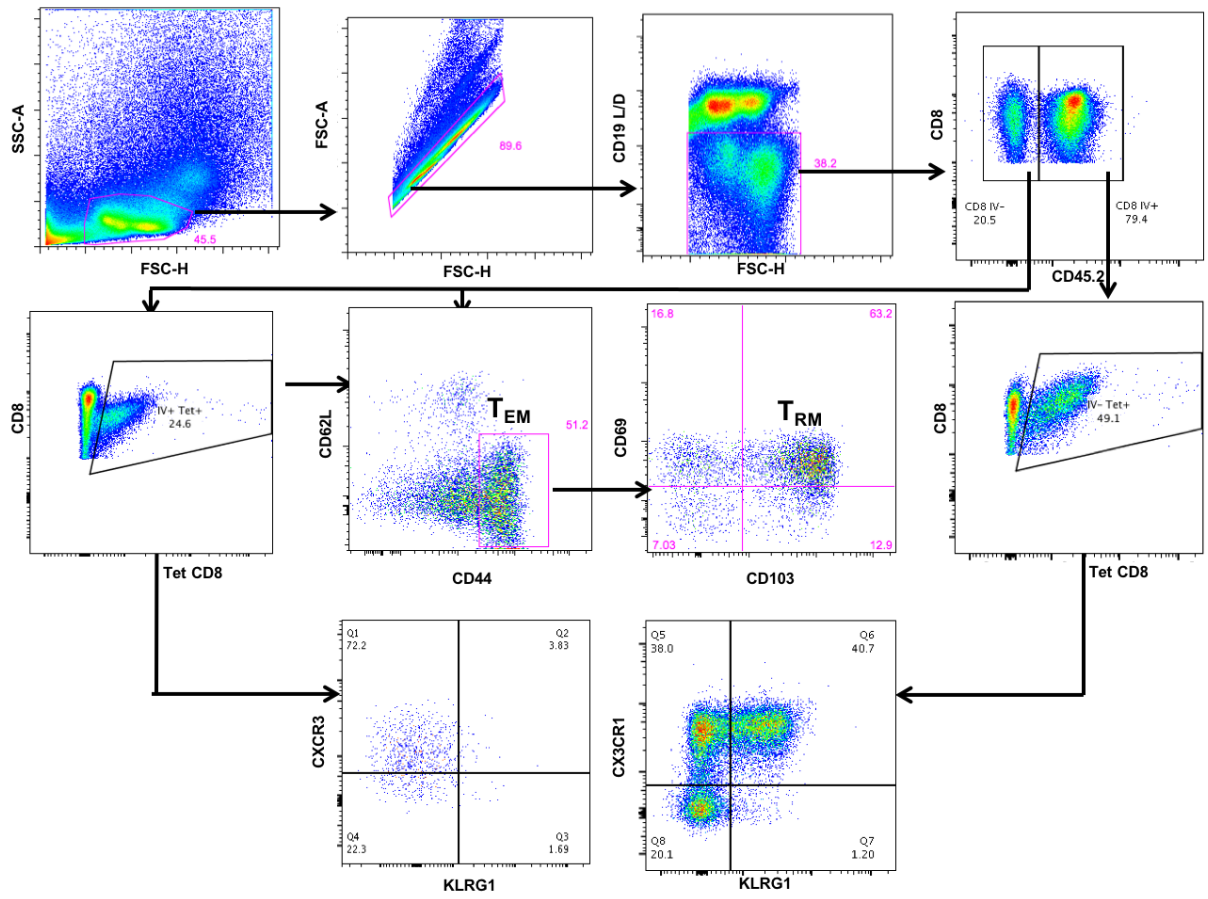

Figure 7-3 Gating strategy for the identification of lung-parenchymal CD8⁺ T cells expressing resident memory and lung-homing markers. Cells were analysed using lung-parenchymal CD8+ TRM panel (Table 7-3). Lymphocytes were selected on followed by singlets and live cells. CD8⁺ T cells were divided to CD45.2- (IV-) and CD45.2+ (IV+) before gating on tetramer positive population. The antigen-specific cells were analysed on the expression of resident memory markers and lung homing phenotypes.

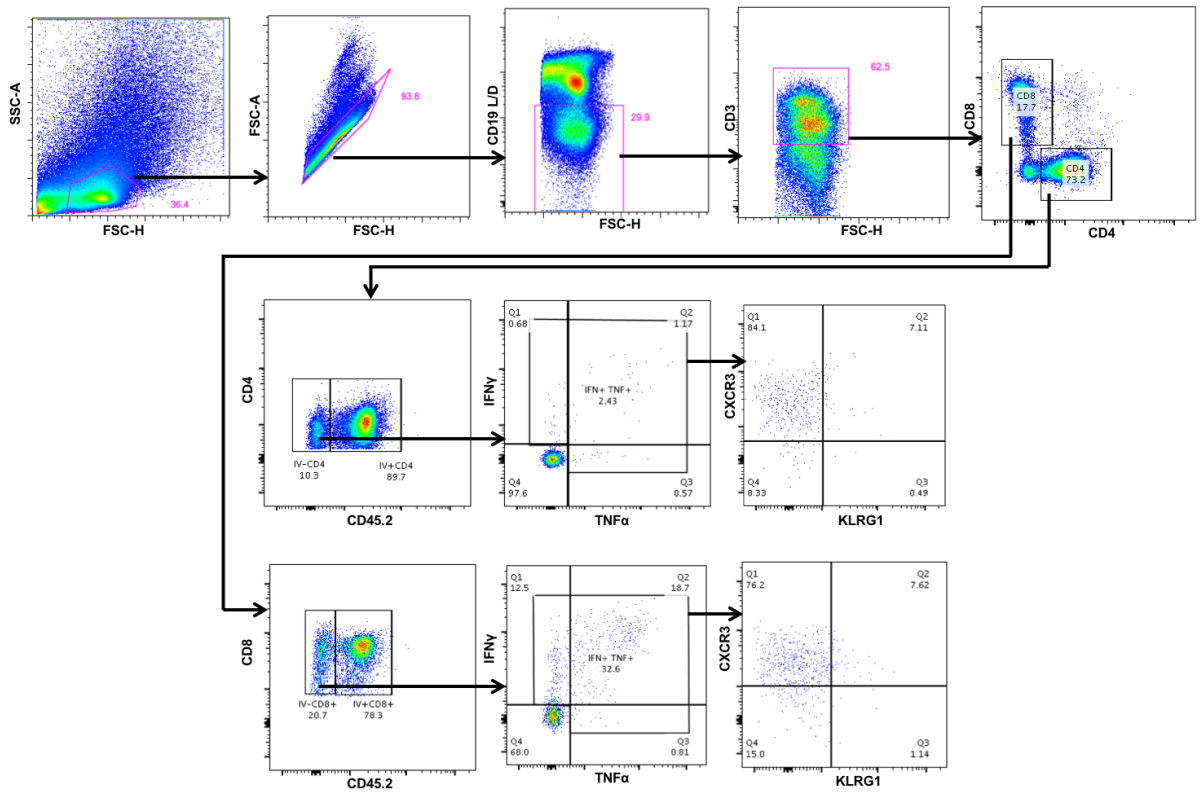

Figure 7-4 Gating strategy for the identification of cytokine producing lung-parenchymal T cells expressing lung-homing markers. Cells were analysed using effector lung parenchymal panel (Table 7-4). Lymphocytes were selected followed by singlets and live cells. T cells were identified as CD3+ before gating on CD8+ and CD4+ cells. CD45 negative population (IV-) was selected before gating on IFN-γ and TNF-α production. Cytokine producing cells were then analysed for the expression of the lung-homing markers.

Bibliography

1. WHO. Global tuberculosis report 2017. (2017).

2. WHO. The top 10 causes of death. 2015 [cited 2018 10/05/18]Available from: http://new.who.int/news-room/fact-sheets/detail/the-top-10-causes-of-death

3. Houben, R.M.G.J. & Dodd, P.J. The Global Burden of Latent Tuberculosis Infection: A Re-estimation Using Mathematical Modelling. *Plos Medicine* **13** (2016).

4. Uplekar, M. *et al.* WHO's new End TB Strategy. *Lancet* **385**, 1799-1801 (2015).

5. Tiberi, S. *et al.* Taking forward the Stop TB Partnership and World Health Organization Joint Theme for World TB Day March 24th 2018-"Wanted: Leaders for a TB-Free World. You can make history. End TB". *Int J Infect Dis* **68**, 122-124 (2018).

6. Migliori, G.B. *et al.* Combined Use of Delamanid and Bedaquiline to Treat Multidrug-Resistant and Extensively Drug-Resistant Tuberculosis: A Systematic Review. *International Journal of Molecular Sciences* **18** (2017).

7. Brigden, G., Hewison, C. & Varaine, F. New developments in the treatment of drug-resistant tuberculosis: clinical utility of bedaquiline and delamanid. *Infection and Drug Resistance* **8**, 367-378 (2015).

8. WHO. The End TB Strategy. 2015.

9. Mangtani, P. *et al.* Protection by BCG vaccine against tuberculosis: a systematic review of randomized controlled trials. *Clin Infect Dis* **58**, 470-480 (2014).

10. Corbett, E.L. *et al.* The growing burden of tuberculosis: global trends and interactions with the HIV epidemic. *Arch Intern Med* **163**, 1009-1021 (2003).

11. WHO. *Guidelines for treatment of tuberculosis*, 4th edn, 2010.

12. Metersky, M.L. & Schluger, N.W. New Guidelines for the Treatment of Drug-Susceptible Tuberculosis from the American Thoracic Society, Centers for

Disease Control and Prevention, and the Infectious Diseases Society of America: Now Comes the Hard Part (vol 194, pg 791, 2016). *Am J Resp Crit Care* **195**, 1540-1540 (2017).

13. Dheda, K. *et al.* Outcomes, infectiousness, and transmission dynamics of patients with extensively drug-resistant tuberculosis and home-discharged patients with programmatically incurable tuberculosis: a prospective cohort study. *Lancet Respir Med* **5**, 269-281 (2017).

14. Rodrigues, L.C., Diwan, V.K. & Wheeler, J.G. Protective effect of BCG against tuberculous meningitis and miliary tuberculosis: a meta-analysis. *Int J Epidemiol* **22**, 1154-1158 (1993).

15. Geldmacher, C. *et al.* Preferential infection and depletion of Mycobacterium tuberculosis-specific CD4 T cells after HIV-1 infection. *Journal of Experimental Medicine* **207**, 2869-2881 (2010).

16. Geldmacher, C. *et al.* Early depletion of Mycobacterium tuberculosis-specific T helper 1 cell responses after HIV-1 infection. *J Infect Dis* **198**, 1590-1598 (2008).

17. Geldmacher, C., Zumla, A. & Hoelscher, M. Interaction between HIV and Mycobacterium tuberculosis: HIV-1-induced CD4 T-cell depletion and the development of active tuberculosis. *Curr Opin HIV AIDS* **7**, 268-275 (2012).

18. Orme, I.M. The kinetics of emergence and loss of mediator T lymphocytes acquired in response to infection with Mycobacterium tuberculosis. *J Immunol* **138**, 293-298 (1987).

19. Caruso, A.M. *et al.* Mice deficient in CD4 T cells have only transiently diminished levels of IFN-gamma, yet succumb to tuberculosis. *Journal of Immunology* **162**, 5407-5416 (1999).

20. Mogues, T., Goodrich, M.E., Ryan, L., LaCourse, R. & North, R.J. The relative importance of T cell subsets in immunity and immunopathology of Airborne Mycobacterium tuberculosis infection in mice. *Journal of Experimental Medicine* **193**, 271-280 (2001).

21. Flynn, J.L. *et al.* An essential role for interferon gamma in resistance to Mycobacterium tuberculosis infection. *J Exp Med* **178**, 2249-2254 (1993).

22. Cooper, A.M. *et al.* Disseminated tuberculosis in interferon gamma gene-disrupted mice. *J Exp Med* **178**, 2243-2247 (1993).

23. Chan, J., Xing, Y., Magliozzo, R.S. & Bloom, B.R. Killing of virulent Mycobacterium tuberculosis by reactive nitrogen intermediates produced by activated murine macrophages. *J Exp Med* **175**, 1111-1122 (1992).

24. MacMicking, J.D., Taylor, G.A. & McKinney, J.D. Immune control of tuberculosis by IFN-gamma-inducible LRG-47. *Science* **302**, 654-659 (2003).

25. Gutierrez, M.G. *et al.* Autophagy is a defense mechanism inhibiting BCG and Mycobacterium tuberculosis survival in infected macrophages. *Cell* **119**, 753-766 (2004).

26. MacMicking, J.D. *et al.* Identification of nitric oxide synthase as a protective locus against tuberculosis. *Proc Natl Acad Sci U S A* **94**, 5243-5248 (1997).

27. Fabri, M. *et al.* Vitamin D is required for IFN-gamma-mediated antimicrobial activity of human macrophages. *Sci Transl Med* **3**, 104ra102 (2011).

28. Liu, P.T., Stenger, S., Tang, D.H. & Modlin, R.L. Cutting edge: Vitamin D-mediated human antimicrobial activity against Mycobacterium tuberculosis is dependent on the induction of cathelicidin. *Journal of Immunology* **179**, 2060-2063 (2007).

29. Zhang, S.Y. *et al.* Inborn errors of interferon (IFN)-mediated immunity in humans: insights into the respective roles of IFN-alpha/beta, IFN-gamma, and IFN-lambda in host defense. *Immunol Rev* **226**, 29-40 (2008).

30. Fletcher, H.A. *et al.* T-cell activation is an immune correlate of risk in BCG vaccinated infants. *Nat Commun* **7**, 11290 (2016).

31. Donovan, M.L., Schultz, T.E., Duke, T.J. & Blumenthal, A. Type I Interferons in the Pathogenesis of Tuberculosis: Molecular Drivers and Immunological Consequences. *Front Immunol* **8**, 1633 (2017).

32. Leal, I.S., Smedegard, B., Andersen, P. & Appelberg, R. Failure to induce enhanced protection against tuberculosis by increasing T-cell-dependent interferon-gamma generation. *Immunology* **104**, 157-161 (2001).

33. Mittrucker, H.W. *et al.* Poor correlation between BCG vaccination-induced T cell responses and protection against tuberculosis. *Proc Natl Acad Sci U S A* **104**, 12434-12439 (2007).

34. Vordermeier, H.M. *et al.* Correlation of ESAT-6-specific gamma interferon production with pathology in cattle following Mycobacterium bovis BCG vaccination against experimental bovine tuberculosis. *Infect Immun* **70**, 3026-3032 (2002).

35. Kagina, B.M. *et al.* Specific T cell frequency and cytokine expression profile do not correlate with protection against tuberculosis after bacillus Calmette-Guerin vaccination of newborns. *Am J Respir Crit Care Med* **182**, 1073-1079 (2010).

36. Hoft, D.F. *et al.* Investigation of the relationships between immune-mediated inhibition of mycobacterial growth and other potential surrogate markers of protective Mycobacterium tuberculosis immunity. *J Infect Dis* **186**, 1448-1457 (2002).

37. Fletcher, H.A. Correlates of immune protection from tuberculosis. *Curr Mol Med* **7**, 319-325 (2007).

38. Elias, D., Akuffo, H. & Britton, S. PPD induced in vitro interferon gamma production is not a reliable correlate of protection against Mycobacterium tuberculosis. *Trans R Soc Trop Med Hyg* **99**, 363-368 (2005).

39. Flynn, J.L. *et al.* Tumor necrosis factor-alpha is required in the protective immune response against Mycobacterium tuberculosis in mice. *Immunity* **2**, 561-572 (1995).

40. Mayer-Barber, K.D. *et al.* Cutting Edge: Caspase-1 Independent IL-1 beta Production Is Critical for Host Resistance to Mycobacterium tuberculosis and Does Not Require TLR Signaling In Vivo. *Journal of Immunology* **184**, 3326-3330 (2010).

41. Gonzalez-Juarrero, M. *et al.* Disruption of granulocyte macrophage-colony stimulating factor production in the lungs severely affects the ability of mice to control Mycobacterium tuberculosis infection. *J Leukocyte Biol* **77**, 914-922 (2005).

42. Ladel, C.H. *et al.* Lethal tuberculosis in interleukin-6-deficient mutant mice. *Infect Immun* **65**, 4843-4849 (1997).

43. Keane, J. *et al.* Tuberculosis associated with infliximab, a tumor necrosis factor alpha-neutralizing agent. *N Engl J Med* **345**, 1098-1104 (2001).

44. Chen, C.Y. *et al.* A critical role for CD8 T cells in a nonhuman primate model of tuberculosis. *PLoS Pathog* **5**, e1000392 (2009).

45. Woodworth, J.S., Wu, Y. & Behar, S.M. Mycobacterium tuberculosis-specific CD8+ T cells require perforin to kill target cells and provide protection in vivo. *J Immunol* **181**, 8595-8603 (2008).

46. Woodworth, J.S. & Behar, S.M. Mycobacterium tuberculosis-specific CD8+ T cells and their role in immunity. *Crit Rev Immunol* **26**, 317-352 (2006).

47. Caccamo, N. *et al.* Phenotypical and functional analysis of memory and effector human CD8 T cells specific for mycobacterial antigens. *J Immunol* **177**, 1780-1785 (2006).

48. Stenger, S. *et al.* An antimicrobial activity of cytolytic T cells mediated by granulysin. *Science* **282**, 121-125 (1998).

49. Sousa, A.O. *et al.* Relative contributions of distinct MHC class I-dependent cell populations in protection to tuberculosis infection in mice. *Proc Natl Acad Sci U S A* **97**, 4204-4208 (2000).

50. van Pinxteren, L.A.H., Cassidy, J.P., Smedegaard, B.H.C., Agger, E.M. & Andersen, P. Control of latent Mycobacterium tuberculosis infection is dependent on CD8 T cells. *European Journal of Immunology* **30**, 3689-3698 (2000).

51. Hernandez-Pando, R. *et al.* Persistence of DNA from Mycobacterium tuberculosis in superficially normal lung tissue during latent infection. *Lancet* **356**, 2133-2138 (2000).

52. Bellamy, R. *et al.* Tuberculosis and chronic hepatitis B virus infection in Africans and variation in the vitamin D receptor gene. *J Infect Dis* **179**, 721-724 (1999).

53. Bellamy, R. *et al.* Variations in the NRAMP1 gene and susceptibility to tuberculosis in West Africans. *N Engl J Med* **338**, 640-644 (1998).

54. Wilkinson, R.J. *et al.* Influence of vitamin D deficiency and vitamin D receptor polymorphisms on tuberculosis among Gujarati Asians in west London: a case-control study. *Lancet* **355**, 618-621 (2000).

55. Wilkinson, R.J. *et al.* Influence of polymorphism in the genes for the interleukin (IL)-1 receptor antagonist and IL-1beta on tuberculosis. *J Exp Med* **189**, 1863-1874 (1999).

56. Garcia, V.E. *et al.* IL-18 promotes type 1 cytokine production from NK cells and T cells in human intracellular infection. *J Immunol* **162**, 6114-6121 (1999).

57. Iho, S., Yamamoto, T., Takahashi, T. & Yamamoto, S. Oligodeoxynucleotides containing palindrome sequences with internal 5'-CpG-3' act directly on human NK and activated T cells to induce IFN-gamma production in vitro. *J Immunol* **163**, 3642-3652 (1999).

58. van Crevel, R., Ottenhoff, T.H. & van der Meer, J.W. Innate immunity to Mycobacterium tuberculosis. *Clin Microbiol Rev* **15**, 294-309 (2002).

59. Fletcher, H.A. & Schrager, L. TB vaccine development and the End TB Strategy: importance and current status. *Transactions of the Royal Society of Tropical Medicine and Hygiene* **110**, 212-218 (2016).

60. Sharma, A. *et al.* Estimating the future burden of multidrug-resistant and extensively drug-resistant tuberculosis in India, the Philippines, Russia, and South Africa: a mathematical modelling study. *Lancet Infect Dis* **17**, 707-715 (2017).

61. Mangtani, P. *et al.* Protection by BCG Vaccine Against Tuberculosis: A Systematic Review of Randomized Controlled Trials. *Clinical Infectious Diseases* **58**, 470-480 (2014).

62. Rodrigues, L.C. *et al.* Effect of BCG revaccination on incidence of tuberculosis in school-aged children in Brazil: the BCG-REVAC cluster-randomised trial. *Lancet* **366**, 1290-1295 (2005).

63. Norrby, M. *et al.* Safety and immunogenicity of the novel H4:IC31 tuberculosis vaccine candidate in BCG-vaccinated adults: Two phase I dose escalation trials. *Vaccine* **35**, 1652-1661 (2017).

64. Calmette, A. Preventive Vaccination Against Tuberculosis with BCG. *Proc R Soc Med* **24**, 1481-1490 (1931).

65. AERAS. Global Clinical Portfolio of TB Vaccine Candidates. 2018 [cited 2018 8/05/18]Available from: http://www.aeras.org/pages/global-portfolio

66. Andersen, P. & Kaufmann, S.H. Novel vaccination strategies against tuberculosis. *Cold Spring Harb Perspect Med* **4** (2014).

67. Arbues, A. *et al.* Construction, characterization and preclinical evaluation of MTBVAC, the first live-attenuated M. tuberculosis-based vaccine to enter clinical trials. *Vaccine* **31**, 4867-4873 (2013).

68. Nieuwenhuizen, N.E. *et al.* The Recombinant Bacille Calmette-Guerin Vaccine VPM1002: Ready for Clinical Efficacy Testing. *Front Immunol* **8**, 1147 (2017).

69. Aagaard, C. *et al.* Protection and polyfunctional T cells induced by Ag85B-TB10.4/IC31 against Mycobacterium tuberculosis is highly dependent on the antigen dose. *PLoS One* **4**, e5930 (2009).

70. Day, C.L. *et al.* Induction and regulation of T-cell immunity by the novel tuberculosis vaccine M72/AS01 in South African adults. *Am J Respir Crit Care Med* **188**, 492-502 (2013).

71. White, A.D. *et al.* Evaluation of the Immunogenicity of Mycobacterium bovis BCG Delivered by Aerosol to the Lungs of Macaques. *Clin Vaccine Immunol* **22**, 992-1003 (2015).

72. Sharpe, S. *et al.* Alternative BCG delivery strategies improve protection against Mycobacterium tuberculosis in non-human primates: Protection associated with mycobacterial antigen-specific CD4 effector memory T-cell populations. *Tuberculosis (Edinb)* **101**, 174-190 (2016).

73. Harris, S.A. *et al.* Development of a non-human primate BCG infection model for the evaluation of candidate tuberculosis vaccines. *Tuberculosis (Edinb)* **108**, 99-105 (2018).

74. Aguilo, N. *et al.* Pulmonary but Not Subcutaneous Delivery of BCG Vaccine Confers Protection to Tuberculosis-Susceptible Mice by an Interleukin 17-Dependent Mechanism. *J Infect Dis* **213**, 831-839 (2016).

75. Perdomo, C. *et al.* Mucosal BCG Vaccination Induces Protective Lung-Resident Memory T Cell Populations against Tuberculosis. *MBio* **7** (2016).

76. Tatsis, N. *et al.* Chimpanzee-origin adenovirus vectors as vaccine carriers. *Gene Ther* **13**, 421-429 (2006).

77. Ura, T., Okuda, K. & Shimada, M. Developments in Viral Vector-Based Vaccines. *Vaccines (Basel)* **2**, 624-641 (2014).

78. Ewer, K. *et al.* A Monovalent Chimpanzee Adenovirus Ebola Vaccine Boosted with MVA. *N Engl J Med* **374**, 1635-1646 (2016).

79. Sheehy, S.H. *et al.* Phase Ia clinical evaluation of the safety and immunogenicity of the Plasmodium falciparum blood-stage antigen AMA1 in ChAd63 and MVA vaccine vectors. *PLoS One* **7**, e31208 (2012).

80. Biswas, S. *et al.* Transgene optimization, immunogenicity and in vitro efficacy of viral vectored vaccines expressing two alleles of Plasmodium falciparum AMA1. *PLoS One* **6**, e20977 (2011).

81. Lambe, T. *et al.* Immunity against heterosubtypic influenza virus induced by adenovirus and MVA expressing nucleoprotein and matrix protein-1. *Sci Rep* **3**, 1443 (2013).

82. McShane, H. *et al.* Recombinant modified vaccinia virus Ankara expressing antigen 85A boosts BCG-primed and naturally acquired antimycobacterial immunity in humans. *Nat Med* **10**, 1240-1244 (2004).

83. Beverley, P.C. *et al.* A novel murine cytomegalovirus vaccine vector protects against Mycobacterium tuberculosis. *J Immunol* **193**, 2306-2316 (2014).

84. Dicks, M.D. *et al.* A novel chimpanzee adenovirus vector with low human seroprevalence: improved systems for vector derivation and comparative immunogenicity. *PLoS One* **7**, e40385 (2012).

85. Zhang, M., Dong, C. & Xiong, S. Heterologous boosting with recombinant VSV-846 in BCG-primed mice confers improved protection against Mycobacterium infection. *Hum Vaccin Immunother* **13**, 816-822 (2017).

86. Zhang, M., Dong, C. & Xiong, S. Vesicular Stomatitis Virus-Vectored Multi-Antigen Tuberculosis Vaccine Limits Bacterial Proliferation in Mice following a Single Intranasal Dose. *Front Cell Infect Microbiol* **7**, 34 (2017).

87. Churchyard, G.J. *et al.* The safety and immunogenicity of an adenovirus type 35-vectored TB vaccine in HIV-infected, BCG-vaccinated adults with CD4(+) T cell counts > 350 cells/mm(3). *Vaccine* **33**, 1890-1896 (2015).

88. Walsh, D.S. *et al.* Adenovirus type 35-vectored tuberculosis vaccine has an acceptable safety and tolerability profile in healthy, BCG-vaccinated, QuantiFERON (R)-TB Gold (+) Kenyan adults without evidence of tuberculosis. *Vaccine* **34**, 2430-2436 (2016).

89. Hu, Z. *et al.* Sendai Virus Mucosal Vaccination Establishes Lung-Resident Memory CD8 T Cell Immunity and Boosts BCG-Primed Protection against TB in Mice. *Mol Ther* **25**, 1222-1233 (2017).

90. Shakouri, M. *et al.* A novel dendritic cell-targeted lentiviral vector, encoding Ag85A-ESAT6 fusion gene of Mycobacterium tuberculosis, could elicit potent cell-mediated immune responses in mice. *Mol Immunol* **75**, 101-111 (2016).

91. Yang, E. *et al.* A lentiviral vector-based therapeutic vaccine encoding Ag85B-Rv3425 potently increases resistance to acute tuberculosis infection in mice. *Acta Biochim Biophys Sin (Shanghai)* **47**, 588-596 (2015).

92. Hansen, S.G. *et al.* Prevention of tuberculosis in rhesus macaques by a cytomegalovirus-based vaccine. *Nat Med* **24**, 130-143 (2018).

93. Basinski, A.J. *et al.* Evaluating the promise of recombinant transmissible vaccines. *Vaccine* **36**, 675-682 (2018).

94. Scriba, T.J. *et al.* Dose-finding study of the novel tuberculosis vaccine, MVA85A, in healthy BCG-vaccinated infants. *J Infect Dis* **203**, 1832-1843 (2011).

95. Tameris, M.D. *et al.* Safety and efficacy of MVA85A, a new tuberculosis vaccine, in infants previously vaccinated with BCG: a randomised, placebo-controlled phase 2b trial. *Lancet* **381**, 1021-1028 (2013).

96. Scriba, T.J. *et al.* Modified vaccinia Ankara-expressing Ag85A, a novel tuberculosis vaccine, is safe in adolescents and children, and induces polyfunctional CD4+ T cells. *Eur J Immunol* **40**, 279-290 (2010).

97. Abel, B. *et al.* The novel tuberculosis vaccine, AERAS-402, induces robust and polyfunctional CD4+ and CD8+ T cells in adults. *Am J Respir Crit Care Med* **181**, 1407-1417 (2010).

98. Stylianou, E. *et al.* Improvement of BCG protective efficacy with a novel chimpanzee adenovirus and a modified vaccinia Ankara virus both expressing Ag85A. *Vaccine* **33**, 6800-6808 (2015).

99. Reyes-Sandoval, A. *et al.* Prime-boost immunization with adenoviral and modified vaccinia virus Ankara vectors enhances the durability and polyfunctionality of protective malaria CD8+ T-cell responses. *Infect Immun* **78**, 145-153 (2010).

100. Dicks, M.D. *et al.* The relative magnitude of transgene-specific adaptive immune responses induced by human and chimpanzee adenovirus vectors differs between laboratory animals and a target species. *Vaccine* **33**, 1121-1128 (2015).

101. Lopez-Camacho, C. *et al.* Rational Zika vaccine design via the modulation of antigen membrane anchors in chimpanzee adenoviral vectors. *Nat Commun* **9**, 2441 (2018).

102. McShane, H. & Williams, A. A review of preclinical animal models utilised for TB vaccine evaluation in the context of recent human efficacy data. *Tuberculosis (Edinb)* **94**, 105-110 (2014).

103. Zhan, L., Tang, J., Sun, M. & Qin, C. Animal Models for Tuberculosis in Translational and Precision Medicine. *Front Microbiol* **8**, 717 (2017).

104. Cooper, A.M. Mouse model of tuberculosis. *Cold Spring Harb Perspect Med* **5**, a018556 (2014).

105. Green, A.M., Difazio, R. & Flynn, J.L. IFN-gamma from CD4 T cells is essential for host survival and enhances CD8 T cell function during Mycobacterium tuberculosis infection. *J Immunol* **190**, 270-277 (2013).

106. Sakai, S. *et al.* Cutting edge: control of Mycobacterium tuberculosis infection by a subset of lung parenchyma-homing CD4 T cells. *J Immunol* **192**, 2965-2969 (2014).

107. Adams, E.J. Diverse antigen presentation by the Group 1 CD1 molecule, CD1c. *Mol Immunol* **55**, 182-185 (2013).

108. Cooper, A.M., Magram, J., Ferrante, J. & Orme, I.M. Interleukin 12 (IL-12) is crucial to the development of protective immunity in mice intravenously infected with mycobacterium tuberculosis. *J Exp Med* **186**, 39-45 (1997).

109. Casanova, J.L. & Abel, L. Genetic dissection of immunity to mycobacteria: the human model. *Annu Rev Immunol* **20**, 581-620 (2002).

110. Chackerian, A.A. & Behar, S.M. Susceptibility to Mycobacterium tuberculosis: lessons from inbred strains of mice. *Tuberculosis (Edinb)* **83**, 279-285 (2003).

111. Marquis, J.F. *et al.* Fibrotic response as a distinguishing feature of resistance and susceptibility to pulmonary infection with Mycobacterium tuberculosis in mice. *Infect Immun* **76**, 78-88 (2008).

112. Mitsos, L.M. *et al.* Genetic control of susceptibility to infection with Mycobacterium tuberculosis in mice. *Genes Immun* **1**, 467-477 (2000).

113. Giannakaki, S. *et al.* Absence of human rhinovirus and respiratory syncytial virus from bronchoalveolar lavage and bronchial biopsies of selected patients with stable chronic obstructive pulmonary disease. *Respir Res* **17**, 11 (2016).

114. Teijaro, J.R. *et al.* Cutting edge: Tissue-retentive lung memory CD4 T cells mediate optimal protection to respiratory virus infection. *J Immunol* **187**, 5510-5514 (2011).

115. Anderson, K.G. *et al.* Intravascular staining for discrimination of vascular and tissue leukocytes. *Nat Protoc* **9**, 209-222 (2014).

116. Anderson, K.G. *et al.* Cutting edge: intravascular staining redefines lung CD8 T cell responses. *J Immunol* **189**, 2702-2706 (2012).

117. Turner, D.L. *et al.* Lung niches for the generation and maintenance of tissue-resident memory T cells. *Mucosal Immunol* **7**, 501-510 (2014).

118. Barletta, K.E. *et al.* Leukocyte compartments in the mouse lung: distinguishing between marginated, interstitial, and alveolar cells in response to injury. *J Immunol Methods* **375**, 100-110 (2012).

119. Patel, B.V., Tatham, K.C., Wilson, M.R., O'Dea, K.P. & Takata, M. In vivo compartmental analysis of leukocytes in mouse lungs. *Am J Physiol Lung Cell Mol Physiol* **309**, L639-652 (2015).

120. Moguche, A.O. *et al.* ICOS and Bcl6-dependent pathways maintain a CD4 T cell population with memory-like properties during tuberculosis. *J Exp Med* **212**, 715-728 (2015).

121. Stylianou, E. *et al.* Identification and Evaluation of Novel Protective Antigens for the Development of a Candidate TB Subunit Vaccine. *Infect Immun* (2018).

122. Laddy, D.J. *et al.* Toward Tuberculosis Vaccine Development: Recommendations for Nonhuman Primate Study Design. *Infection and Immunity* **86** (2018).

123. Foundation, B.M.G. Discovery & translational sciences: Strategy overview. 2018 [cited]Available from: https://www.gatesfoundation.org/What-We-Do/Global-Health/Discovery-and-Translational-Sciences

124. Sharpe, S.A., Smyth, D., McIntyre, A., Gleeson, F. & Dennis, M.J. Refinement and reduction through application of a quantitative score system for estimation of TB-induced disease burden using computed tomography. *Lab Anim*, 23677218757815 (2018).

125. Kaech, S.M., Wherry, E.J. & Ahmed, R. Effector and memory T-cell differentiation: Implications for vaccine development. *Nature Reviews Immunology* **2**, 251-262 (2002).

126. Pennock, N.D. *et al.* T cell responses: naive to memory and everything in between. *Adv Physiol Educ* **37**, 273-283 (2013).

127. Kotturi, M.F. *et al.* Human CD8(+) and CD4(+) T cell memory to lymphocytic choriomeningitis virus infection. *J Virol* **85**, 11770-11780 (2011).

128. Seder, R.A. & Ahmed, R. Similarities and differences in CD4+ and CD8+ effector and memory T cell generation. *Nat Immunol* **4**, 835-842 (2003).

129. Whitmire, J.K., Asano, M.S., Murali-Krishna, K., Suresh, M. & Ahmed, R. Long-term CD4 Th1 and Th2 memory following acute lymphocytic choriomeningitis virus infection. *J Virol* **72**, 8281-8288 (1998).

130. Vollers, S.S. & Stern, L.J. Class II major histocompatibility complex tetramer staining: progress, problems, and prospects. *Immunology* **123**, 305-313 (2008).

131. Sallusto, F., Lenig, D., Forster, R., Lipp, M. & Lanzavecchia, A. Two subsets of memory T lymphocytes with distinct homing potentials and effector functions. *Nature* **401**, 708-712 (1999).

132. Gebhardt, T. *et al.* Memory T cells in nonlymphoid tissue that provide enhanced local immunity during infection with herpes simplex virus. *Nat Immunol* **10**, 524-530 (2009).

133. Wakim, L.M., Woodward-Davis, A. & Bevan, M.J. Memory T cells persisting within the brain after local infection show functional adaptations to their tissue of residence. *Proc Natl Acad Sci U S A* **107**, 17872-17879 (2010).

134. Masopust, D. *et al.* Dynamic T cell migration program provides resident memory within intestinal epithelium. *J Exp Med* **207**, 553-564 (2010).

135. Jiang, X. *et al.* Skin infection generates non-migratory memory CD8+ T(RM) cells providing global skin immunity. *Nature* **483**, 227-231 (2012).

136. Shin, H. & Iwasaki, A. A vaccine strategy that protects against genital herpes by establishing local memory T cells. *Nature* **491**, 463-467 (2012).

137. Kaech, S.M., Wherry, E.J. & Ahmed, R. Effector and memory T-cell differentiation: implications for vaccine development. *Nat Rev Immunol* **2**, 251-262 (2002).

138. Morabito, K.M. *et al.* Intranasal administration of RSV antigen-expressing MCMV elicits robust tissue-resident effector and effector memory CD8+ T cells in the lung. *Mucosal Immunol* (2016).

139. Wakim, L.M., Gupta, N., Mintern, J.D. & Villadangos, J.A. Enhanced survival of lung tissue-resident memory CD8(+) T cells during infection with influenza virus due to selective expression of IFITM3. *Nat Immunol* **14**, 238-245 (2013).

140. Henao-Tamayo, M.I. *et al.* Phenotypic definition of effector and memory T-lymphocyte subsets in mice chronically infected with Mycobacterium tuberculosis. *Clin Vaccine Immunol* **17**, 618-625 (2010).

141. Schenkel, J.M. & Masopust, D. Tissue-resident memory T cells. *Immunity* **41**, 886-897 (2014).

142. Mackay, L.K. *et al.* Cutting edge: CD69 interference with sphingosine-1-phosphate receptor function regulates peripheral T cell retention. *J Immunol* **194**, 2059-2063 (2015).

143. Jeyanathan, M. *et al.* Murine airway luminal antituberculosis memory CD8 T cells by mucosal immunization are maintained via antigen-driven in situ proliferation, independent of peripheral T cell recruitment. *Am J Respir Crit Care Med* **181**, 862-872 (2010).

144. Lee, L.N. *et al.* CXCR6 is a marker for protective antigen-specific cells in the lungs after intranasal immunization against Mycobacterium tuberculosis. *Infect Immun* **79**, 3328-3337 (2011).

145. Woodworth, J.S. *et al.* Subunit vaccine H56/CAF01 induces a population of circulating CD4 T cells that traffic into the Mycobacterium tuberculosis-infected lung. *Mucosal Immunol* **10**, 555-564 (2017).

146. Wolf, A.J. *et al.* Initiation of the adaptive immune response to Mycobacterium tuberculosis depends on antigen production in the local lymph node, not the lungs. *J Exp Med* **205**, 105-115 (2008).

147. Walrath, E., Zukowski, L., Krywiak, A. & Silver, R.F. Resident Th1-like effector memory cells in pulmonary recall responses to Mycobacterium tuberculosis. *Am J Resp Cell Mol* **33**, 48-55 (2005).

148. Walrath, J.R. & Silver, R.F. The alpha 4 beta 1 Integrin in Localization of Mycobacterium tuberculosis-Specific T Helper Type 1 Cells to the Human Lung. *Am J Resp Cell Mol* **45**, 24-30 (2011).

149. Plotkin, S.A. Vaccines: correlates of vaccine-induced immunity. *Clin Infect Dis* **47**, 401-409 (2008).

150. Orme, I.M. Vaccines to prevent tuberculosis infection rather than disease: Physiological and immunological aspects. *Tuberculosis* **101**, 210-216 (2016).

151. Glatman-Freedman, A. & Casadevall, A. Serum therapy for tuberculosis revisited: reappraisal of the role of antibody-mediated immunity against Mycobacterium tuberculosis. *Clin Microbiol Rev* **11**, 514-532 (1998).

152. Torrado, E. *et al.* Differential and site specific impact of B cells in the protective immune response to Mycobacterium tuberculosis in the mouse. *PLoS One* **8**, e61681 (2013).

153. Kozakiewicz, L., Phuah, J., Flynn, J. & Chan, J. The role of B cells and humoral immunity in Mycobacterium tuberculosis infection. *Adv Exp Med Biol* **783**, 225-250 (2013).

154. Nimmerjahn, F. & Ravetch, J.V. Divergent immunoglobulin g subclass activity through selective Fc receptor binding. *Science* **310**, 1510-1512 (2005).

155. Sousa, A.O. *et al.* IgG subclass distribution of antibody responses to protein and polysaccharide mycobacterial antigens in leprosy and tuberculosis patients. *Clin Exp Immunol* **111**, 48-55 (1998).

156. Hussain, R., Shiratsuchi, H., Ellner, J.J. & Wallis, R.S. PPD-specific IgG1 antibody subclass upregulate tumour necrosis factor expression in PPD-stimulated monocytes: possible link with disease pathogenesis in tuberculosis. *Clin Exp Immunol* **119**, 449-455 (2000).

157. Gupta, S., Shende, N., Bhatia, A.S., Kumar, S. & Harinath, B.C. IgG subclass antibody response to mycobacterial serine protease at different stages of pulmonary tuberculosis. *Medical Science Monitor* **11**, Cr585-Cr588 (2005).

158. Rodriguez, A. *et al.* Role of IgA in the defense against respiratory infections IgA deficient mice exhibited increased susceptibility to intranasal infection with Mycobacterium bovis BCG. *Vaccine* **23**, 2565-2572 (2005).

159. Prados-Rosales, R. *et al.* Mycobacterial membrane vesicles administered systemically in mice induce a protective immune response to surface compartments of Mycobacterium tuberculosis. *MBio* **5**, e01921-01914 (2014).

160. Hamasur, B. *et al.* Mycobacterium tuberculosis arabinomannan-protein conjugates protect against tuberculosis. *Vaccine* **21**, 4081-4093 (2003).

161. Reljic, R. *et al.* Mucosal Vaccination against Tuberculosis Using Inert Bioparticles. *Infection and Immunity* **81**, 4071-4080 (2013).

162. Stylianou, E. *et al.* Mucosal delivery of antigen-coated nanoparticles to lungs confers protective immunity against tuberculosis infection in mice. *European Journal of Immunology* **44**, 440-449 (2014).

163. Jeyanathan, M. *et al.* AdHu5Ag85A Respiratory Mucosal Boost Immunization Enhances Protection against Pulmonary Tuberculosis in BCG-Primed Non-Human Primates. *PLoS One* **10**, e0135009 (2015).

164. Khera, A.K. *et al.* Role of B Cells in Mucosal Vaccine-Induced Protective CD8+ T Cell Immunity against Pulmonary Tuberculosis. *J Immunol* **195**, 2900-2907 (2015).

165. Cole, S.T. *et al.* Deciphering the biology of Mycobacterium tuberculosis from the complete genome sequence. *Nature* **393**, 537-544 (1998).

166. Coppola, M. *et al.* New Genome-Wide Algorithm Identifies Novel In-Vivo Expressed Mycobacterium Tuberculosis Antigens Inducing Human T-Cell Responses with Classical and Unconventional Cytokine Profiles. *Sci Rep* **6**, 37793 (2016).

167. Ernst, J.D. The immunological life cycle of tuberculosis. *Nat Rev Immunol* **12**, 581-591 (2012).

168. Davenne, T. & McShane, H. Why don't we have an effective tuberculosis vaccine yet? *Expert Rev Vaccines* **15**, 1009-1013 (2016).

169. Wilkins, M.R. *et al.* From proteins to proteomes: Large scale protein identification by two-dimensional electrophoresis and amino acid analysis. *Bio-Technol* **14**, 61-65 (1996).

170. Pandey, A. & Mann, M. Proteomics to study genes and genomes. *Nature* **405**, 837-846 (2000).

171. Potgieter, M.G. *et al.* Proteogenomic Analysis of Mycobacterium smegmatis Using High Resolution Mass Spectrometry. *Front Microbiol* **7** (2016).

172. Zheng, J. *et al.* Proteogenomic Analysis and Discovery of Immune Antigens in Mycobacterium vaccae. *Mol Cell Proteomics* **16**, 1578-1590 (2017).

173. Kelkar, D.S. *et al.* Proteogenomic analysis of Mycobacterium tuberculosis by high resolution mass spectrometry. *Mol Cell Proteomics* **10**, M111 011627 (2011).

174. Lewinsohn, D.A. *et al.* Comprehensive definition of human immunodominant CD8 antigens in tuberculosis. *NPJ Vaccines* **2** (2017).

175. Lewinsohn, D.A. *et al.* Immunodominant tuberculosis CD8 antigens preferentially restricted by HLA-B. *PLoS Pathog* **3**, 1240-1249 (2007).

176. Xiang, Z.H. *et al.* Immunogenicity and Protective Efficacy of a Fusion Protein Tuberculosis Vaccine Combining Five Esx Family Proteins. *Front Cell Infect Microbiol* **7**, 226 (2017).

177. Sayes, F. *et al.* Strong immunogenicity and cross-reactivity of Mycobacterium tuberculosis ESX-5 type VII secretion: encoded PE-PPE proteins predicts vaccine potential. *Cell Host Microbe* **11**, 352-363 (2012).

178. Brennan, M.J. The Enigmatic PE/PPE Multigene Family of Mycobacteria and Tuberculosis Vaccination. *Infect Immun* **85** (2017).

179. Ahmed, A., Das, A. & Mukhopadhyay, S. Immunoregulatory functions and expression patterns of PE/PPE family members: Roles in pathogenicity and impact on anti-tuberculosis vaccine and drug design. *IUBMB Life* **67**, 414-427 (2015).

180. Akhter, Y., Ehebauer, M.T., Mukhopadhyay, S. & Hasnain, S.E. The PE/PPE multigene family codes for virulence factors and is a possible source of mycobacterial antigenic variation: perhaps more? *Biochimie* **94**, 110-116 (2012).

181. Sayes, F. *et al.* CD4+ T Cells Recognizing PE/PPE Antigens Directly or via Cross Reactivity Are Protective against Pulmonary Mycobacterium tuberculosis Infection. *PLoS Pathog* **12**, e1005770 (2016).

182. Lewinsohn, D.M. *et al.* Human Mycobacterium tuberculosis CD8 T Cell Antigens/Epitopes Identified by a Proteomic Peptide Library. *PLoS One* **8**, e67016 (2013).

183. Skeiky, Y.A. *et al.* Differential immune responses and protective efficacy induced by components of a tuberculosis polyprotein vaccine, Mtb72F, delivered as naked DNA or recombinant protein. *J Immunol* **172**, 7618-7628 (2004).

184. Hebert, A.M. *et al.* DNA polymorphisms in the pepA and PPE18 genes among clinical strains of Mycobacterium tuberculosis: Implications for vaccine efficacy. *Infection and Immunity* **75**, 5798-5805 (2007).

185. Gillard, P. *et al.* Safety and immunogenicity of the M72/AS01E candidate tuberculosis vaccine in adults with tuberculosis: A phase II randomised study. *Tuberculosis (Edinb)* **100**, 118-127 (2016).

186. Bertholet, S. *et al.* A defined tuberculosis vaccine candidate boosts BCG and protects against multidrug-resistant Mycobacterium tuberculosis. *Sci Transl Med* **2**, 53ra74 (2010).

187. Penn-Nicholson, A. *et al.* Safety and immunogenicity of the novel tuberculosis vaccine ID93 + GLA-SE in BCG-vaccinated healthy adults in South Africa: a randomised, double-blind, placebo-controlled phase 1 trial. *Lancet Respir Med* **6**, 287-298 (2018).

188. Ondondo, B., Abdul-Jawad, S., Bridgeman, A. & Hanke, T. Characterization of T-cell responses to conserved regions of the HIV-1 proteome in BALB/c mice. *Clin Vaccine Immunol* **21**, 1565-1572 (2014).

189. McShane, H., Brookes, R., Gilbert, S.C. & Hill, A.V. Enhanced immunogenicity of CD4(+) t-cell responses and protective efficacy of a DNA-modified vaccinia

virus Ankara prime-boost vaccination regimen for murine tuberculosis. *Infect Immun* **69**, 681-686 (2001).

190. Serbina, N.V., Liu, C.C., Scanga, C.A. & Flynn, J.L. CD8+ CTL from lungs of Mycobacterium tuberculosis-infected mice express perforin in vivo and lyse infected macrophages. *J Immunol* **165**, 353-363 (2000).

191. Cooper, A.M., DSouza, C., Frank, A.A. & Orme, I.M. The course of Mycobacterium tuberculosis infection in the lungs of mice lacking expression of either perforin- or granzyme-mediated cytolytic mechanisms. *Infection and Immunity* **65**, 1317-1320 (1997).

192. Cho, S. *et al.* Antimicrobial activity of MHC class I-restricted CD8+ T cells in human tuberculosis. *Proc Natl Acad Sci U S A* **97**, 12210-12215 (2000).

193. Matloubian, M. *et al.* A role for perforin in downregulating T-cell responses during chronic viral infection. *J Virol* **73**, 2527-2536 (1999).

194. Lord, S.J., Rajotte, R.V., Korbutt, G.S. & Bleackley, R.C. Granzyme B: a natural born killer. *Immunological Reviews* **193**, 31-38 (2003).

195. Silva, B.D.S., Trentini, M.M., da Costa, A.C., Kipnis, A. & Junqueira-Kipnis, A.P. Different phenotypes of CD8+ T cells associated with bacterial load in active tuberculosis. *Immunol Lett* **160**, 23-32 (2014).

196. Krensky, A.M. & Clayberger, C. Biology and clinical relevance of granulysin. *Tissue Antigens* **73**, 193-198 (2009).

197. Grossman, W.J. *et al.* Differential expression of granzymes A and B in human cytotoxic lymphocyte subsets and T regulatory cells. *Blood* **104**, 2840-2848 (2004).

198. Loebbermann, J. *et al.* Regulatory T cells expressing granzyme B play a critical role in controlling lung inflammation during acute viral infection. *Mucosal Immunol* **5**, 161-172 (2012).

199. Cohnen, A. *et al.* Surface CD107a/LAMP-1 protects natural killer cells from degranulation-associated damage. *Blood* **122**, 1411-1418 (2013).

200. Betts, M.R. *et al.* Sensitive and viable identification of antigen-specific CD8+ T cells by a flow cytometric assay for degranulation. *J Immunol Methods* **281**, 65-78 (2003).

201. Chan, K.S. & Kaur, A. Flow cytometric detection of degranulation reveals phenotypic heterogeneity of degranulating CMV-specific CD8+ T lymphocytes in rhesus macaques. *J Immunol Methods* **325**, 20-34 (2007).

202. Zhang, Y. *et al.* Effects of the fusion design and immunization route on the immunogenicity of Ag85A-Mtb32 in adenoviral vectored tuberculosis vaccine. *Hum Vaccin Immunother* **11**, 1803-1813 (2015).

203. Whelan, K.T. *et al.* Safety and immunogenicity of boosting BCG vaccinated subjects with BCG: comparison with boosting with a new TB vaccine, MVA85A. *PLoS One* **4**, e5934 (2009).

204. Satti, I. *et al.* Safety and immunogenicity of a candidate tuberculosis vaccine MVA85A delivered by aerosol in BCG-vaccinated healthy adults: a phase 1, double-blind, randomised controlled trial. *Lancet Infect Dis* **14**, 939-946 (2014).

205. Ewer, K.J. *et al.* Protective CD8(+) T-cell immunity to human malaria induced by chimpanzee adenovirus-MVA immunisation. *Nature Communications* **4** (2013).

206. Rampling, T. *et al.* Safety and High Level Efficacy of the Combination Malaria Vaccine Regimen of RTS,S/AS01B With Chimpanzee Adenovirus 63 and Modified Vaccinia Ankara Vectored Vaccines Expressing ME-TRAP. *J Infect Dis* **214**, 772-781 (2016).

207. Jiang, H.B. *et al.* Decreased expression of perforin in CD8(+) T lymphocytes in patients with Mycobacterium tuberculosis infection and its potential value as a marker for efficacy of treatment. *Journal of Thoracic Disease* **9**, 1353-+ (2017).

208. Uranga, S., Marinova, D., Martin, C., Pardo, J. & Aguilo, N. Granzyme A Is Expressed in Mouse Lungs during Mycobacterium tuberculosis Infection but Does Not Contribute to Protection In Vivo. *Plos One* **11** (2016).

209. Andersson, J., Samarina, A., Fink, J., Rahman, S. & Grundstrom, S. Impaired expression of perforin and granulysin in CD8(+) T cells at the site of infection

in human chronic pulmonary tuberculosis. *Infection and Immunity* **75**, 5210-5222 (2007).

210. McElhaney, J.E. *et al.* Granzyme B: Correlates with protection and enhanced CTL response to influenza vaccination in older adults. *Vaccine* **27**, 2418-2425 (2009).

211. Pierantoni, A. *et al.* Mucosal delivery of a vectored RSV vaccine is safe and elicits protective immunity in rodents and nonhuman primates. *Molecular therapy. Methods & clinical development* **2**, 15018 (2015).

212. Prasad, T.S. *et al.* Proteomic analysis of purified protein derivative of Mycobacterium tuberculosis. *Clinical proteomics* **10**, 8 (2013).

213. Waag, D.M., McCluskie, M.J., Zhang, N. & Krieg, A.M. A CpG oligonucleotide can protect mice from a low aerosol challenge dose of Burkholderia mallei. *Infect Immun* **74**, 1944-1948 (2006).

214. Sharpe, S. *et al.* Ultra low dose aerosol challenge with Mycobacterium tuberculosis leads to divergent outcomes in rhesus and cynomolgus macaques. *Tuberculosis (Edinb)* **96**, 1-12 (2016).

215. Wakeham, J., Wang, J. & Xing, Z. Genetically determined disparate innate and adaptive cell-mediated immune responses to pulmonary Mycobacterium bovis BCG infection in C57BL/6 and BALB/c mice. *Infect Immun* **68**, 6946-6953 (2000).

216. Derrick, S.C., Kolibab, K., Yang, A. & Morris, S.L. Intranasal administration of Mycobacterium bovis BCG induces superior protection against aerosol infection with Mycobacterium tuberculosis in mice. *Clin Vaccine Immunol* **21**, 1443-1451 (2014).

217. Bull, N.C. *et al.* Induction and maintenance of a phenotypically heterogeneous lung tissue-resident CD4(+) T cell population following BCG immunisation. *Vaccine* (2018).

218. Weidinger, G., Ohlmann, M., Schlereth, B., Sutter, G. & Niewiesk, S. Vaccination with recombinant modified vaccinia virus Ankara protects against measles virus infection in the mouse and cotton rat model. *Vaccine* **19**, 2764-2768 (2001).

219. Lindenstrom, T., Knudsen, N.P., Agger, E.M. & Andersen, P. Control of chronic mycobacterium tuberculosis infection by CD4 KLRG1- IL-2-secreting central memory cells. *J Immunol* **190**, 6311-6319 (2013).

220. Jeyanathan, M. *et al.* CXCR3 Signaling Is Required for Restricted Homing of Parenteral Tuberculosis Vaccine-Induced T Cells to Both the Lung Parenchyma and Airway. *J Immunol* **199**, 2555-2569 (2017).

221. Andersen, P. & Urdahl, K.B. TB vaccines; promoting rapid and durable protection in the lung. *Curr Opin Immunol* **35**, 55-62 (2015).

222. Orme, I.M., Robinson, R.T. & Cooper, A.M. The balance between protective and pathogenic immune responses in the TB-infected lung. *Nat Immunol* **16**, 57-63 (2015).

223. Leung-Theung-Long, S. *et al.* A multi-antigenic MVA vaccine increases efficacy of combination chemotherapy against Mycobacterium tuberculosis. *PLoS One* **13**, e0196815 (2018).

224. Xin, Q. *et al.* Subunit vaccine consisting of multi-stage antigens has high protective efficacy against Mycobacterium tuberculosis infection in mice. *PLoS One* **8**, e72745 (2013).

225. Kaufmann, S.H., Weiner, J. & von Reyn, C.F. Novel approaches to tuberculosis vaccine development. *Int J Infect Dis* **56**, 263-267 (2017).

226. Demangel, C. *et al.* Cell envelope protein PPE68 contributes to Mycobacterium tuberculosis RD1 immunogenicity independently of a 10-kilodalton culture filtrate protein and ESAT-6. *Infect Immun* **72**, 2170-2176 (2004).

227. Dong, Z. *et al.* Primary application of PPE68 of Mycobacterium tuberculosis. *Hum Immunol* **75**, 428-432 (2014).

228. Meena, L.S. An overview to understand the role of PE_PGRS family proteins in Mycobacterium tuberculosis H37 Rv and their potential as new drug targets. *Biotechnol Appl Biochem* **62**, 145-153 (2015).

229. Pulido, P.A., Novoa-Aponte, L., Villamil, N. & Soto, C.Y. The DosR dormancy regulator of Mycobacterium tuberculosis stimulates the Na(+)/K (+) and Ca (2+) ATPase activities in plasma membrane vesicles of mycobacteria. *Curr Microbiol* **69**, 604-610 (2014).

230. Novoa-Aponte, L. & Soto Ospina, C.Y. Mycobacterium tuberculosis P-type ATPases: possible targets for drug or vaccine development. *Biomed Res Int* **2014**, 296986 (2014).

231. Farhana, A. *et al.* Mechanistic insights into a novel exporter-importer system of Mycobacterium tuberculosis unravel its role in trafficking of iron. *PLoS One* **3**, e2087 (2008).

232. Tiwari, B., Ramakrishnan, U.M. & Raghunand, T.R. The Mycobacterium tuberculosis protein pair PE9 (Rv1088)-PE10 (Rv1089) forms heterodimers and induces macrophage apoptosis through Toll-like receptor 4. *Cell Microbiol* **17**, 1653-1669 (2015).

233. Sampson, S.L. Mycobacterial PE/PPE Proteins at the Host-Pathogen Interface. *Clin Dev Immunol* (2011).

234. Brennan, M.J. & Delogu, G. The PE multigene family: a 'molecular mantra' for mycobacteria. *Trends Microbiol* **10**, 246-249 (2002).

235. Gey van Pittius, N.C. *et al.* Evolution and expansion of the Mycobacterium tuberculosis PE and PPE multigene families and their association with the duplication of the ESAT-6 (esx) gene cluster regions. *BMC Evol Biol* **6**, 95 (2006).

236. Goonetilleke, N.P. *et al.* Enhanced immunogenicity and protective efficacy against Mycobacterium tuberculosis of bacille Calmette-Guerin vaccine using mucosal administration and boosting with a recombinant modified vaccinia virus Ankara. *Journal of Immunology* **171**, 1602-1609 (2003).

237. Delogu, G. *et al.* PE_PGRS proteins are differentially expressed by Mycobacterium tuberculosis in host tissues. *Microbes Infect* **8**, 2061-2067 (2006).

238. Dheenadhayalan, V., Delogu, G., Sanguinetti, M., Fadda, G. & Brennan, M.J. Variable expression patterns of Mycobacterium tuberculosis PE(-)PGRS

genes: Evidence that PE(-)PGRS16 and PE(-)PGRS26 are inversely regulated in vivo. *J Bacteriol* **188**, 3721-3725 (2006).

239. Flores, J. & Espitia, C. Differential expression of PE and PE_PGRS genes in Mycobacterium tuberculosis strains. *Gene* **318**, 75-81 (2003).

240. Talarico, S. *et al.* Variation of the Mycobacterium tuberculosis PE_PGRS33 gene among clinical isolates. *J Clin Microbiol* **43**, 4954-4960 (2005).

241. Talarico, S. *et al.* Mycobacterium tuberculosis PE_PGRS16 and PE_PGRS26 genetic polymorphism among clinical isolates. *Tuberculosis* **88**, 283-294 (2008).

242. van Els, C.A. *et al.* Toward Understanding the Essence of Post-Translational Modifications for the Mycobacterium tuberculosis Immunoproteome. *Front Immunol* **5**, 361 (2014).

243. Prisic, S. *et al.* Extensive phosphorylation with overlapping specificity by Mycobacterium tuberculosis serine/threonine protein kinases. *Proc Natl Acad Sci U S A* **107**, 7521-7526 (2010).

244. Ates, L.S. *et al.* RD5-mediated lack of PE_PGRS and PPE-MPTR export in BCG vaccine strains results in strong reduction of antigenic repertoire but little impact on protection. *PLoS Pathog* **14**, e1007139 (2018).

245. Singh, P.P., Parra, M., Cadieux, N. & Brennan, M.J. A comparative study of host response to three Mycobacterium tuberculosis PE_PGRS proteins. *Microbiology* **154**, 3469-3479 (2008).

246. Skeiky, Y.A. *et al.* Protection of mice and guinea pigs against tuberculosis induced by immunization with a single Mycobacterium tuberculosis recombinant antigen, MTB41. *Vaccine* **23**, 3937-3945 (2005).

247. Romano, M. *et al.* Immunogenicity and protective efficacy of tuberculosis subunit vaccines expressing PPE44 (Rv2770c). *Vaccine* **26**, 6053-6063 (2008).

248. Saini, N.K. *et al.* Suppression of autophagy and antigen presentation by Mycobacterium tuberculosis PE_PGRS47. *Nat Microbiol* **1**, 16133 (2016).

249. Novoa-Aponte, L. *et al.* In silico identification and characterization of the ion transport specificity for P-type ATPases in the Mycobacterium tuberculosis complex. *BMC Struct Biol* **12**, 25 (2012).

250. Wang, X. *et al.* Protection against Mycobacterium tuberculosis infection offered by a new multistage subunit vaccine correlates with increased number of IFN-gamma+ IL-2+ CD4+ and IFN-gamma+ CD8+ T cells. *PLoS One* **10**, e0122560 (2015).

251. Ohta, Y. & Ichimura, K. Proliferation markers, proliferating cell nuclear antigen, Ki67, 5-bromo-2'-deoxyuridine, and cyclin D1 in mouse olfactory epithelium. *Ann Otol Rhinol Laryngol* **109**, 1046-1048 (2000).

252. Winking, H., Gerdes, J. & Traut, W. Expression of the proliferation marker Ki-67 during early mouse development. *Cytogenet Genome Res* **105**, 251-256 (2004).

253. Starborg, M., Gell, K., Brundell, E. & Hoog, C. The murine Ki-67 cell proliferation antigen accumulates in the nucleolar and heterochromatic regions of interphase cells and at the periphery of the mitotic chromosomes in a process essential for cell cycle progression. *J Cell Sci* **109 (Pt 1)**, 143-153 (1996).